P-08-13

Forsmark site investigation

Confirmatory hydraulic interference test and tracer test at drill site 2

Anna Lindquist, Calle Hjerne, Rune Nordqvist,
Johan Byegård, Ellen Walger, Jan-Erik Ludvigson, Eva Wass
Geosigma AB

September 2008

Svensk Kärnbränslehantering AB
Swedish Nuclear Fuel
and Waste Management Co
Box 250, SE-101 24 Stockholm
Tel +46 8 459 84 00

ISSN 1651-4416
SKB P-08-13

Forsmark site investigation

Confirmatory hydraulic interference test and tracer test at drill site 2

Anna Lindquist, Calle Hjerne, Rune Nordqvist,
Johan Byegård, Ellen Walger, Jan-Erik Ludvigson, Eva Wass
Geosigma AB

September 2008

Keywords: KFM02A, KFM02B, Tracer test, Dilution test, Sorption, Pumping test, Hydraulic interference test, Transport parameters, Hydrogeological model, ZFMA2, AP PF 400-07-013.

Abstract

A tracer test has been conducted between two packed-off sections in boreholes KFM02A (411.0–441.0 metres borehole length (mbl)) and KFM02B (408.5–434.0 mbl) within the Forsmark site investigation. The distance between the two sections is 46.4 m. A hydraulic interference test in combination with the tracer test was carried out by measuring the pressure in several boreholes surrounding the pumping borehole KFM02B.

The tracer injection and pumping sections intersect the major low-angle deformation Zone A2 and the aims of the tests were to verify transport parameters previously obtained using other methods and to, at least partly, verify the previously established hydrogeological model of the Forsmark investigation area.

The main tracer test was preceded by a pre-test using only a non-sorbing tracer. In the main tracer test, the non-sorbing tracer Uranine and three sorbing tracers, lithium (Li), cesium (Cs) and rubidium (Rb), were injected simultaneously. Both tests were evaluated with two different transport models (advection–dispersion and advection–dispersion with matrix diffusion).

The model where matrix diffusion was included was considered to provide the most reliable results. The results showed large dispersivity values and relatively low retardation for the sorbing tracers. The retardation factors were 1.1, 3.4 and 2.7 for Li, Cs and Rb, respectively. The longitudinal dispersivity was estimated at 50.4 m. A low retardation factor for Cs has also previously been determined by a SWIW-test in KFM02A.

Hydraulic responses to the pumping were detected in 25 out of 115 observation sections. The responses from the hydraulic interference test are on the whole in agreement with the hydrogeological model of the Forsmark area. The transmissivity of the pumping section in KFM02B was estimated at $3.0 \cdot 10^{-5}$ m^2/s.

Sammanfattning

Ett spårförsök har utförts mellan två isolerade sektioner i borrhålen KFM02A (411,0–441,0 mbl) och KFM02B (408,5–434,0 mbl) inom platsundersökningen i Forsmark. Avståndet mellan de båda sektionerna är 46,4 m. Kombinerat med detta genomfördes ett inteferenstest genom att trycket registrerades i ett stort antal borrhål omkring pumphålet KFM02B.

De båda sektionerna skär den stora flacka deformationszonen A2 och syftet med försöket var dels att verifiera transportparametrar som tidigare uppmätts på annat sätt samt att partiellt verifiera den tidigare upprättade hydrogeologiska modellen över Forsmarks undersökningsområde.

Spårförsöket utfördes dels i form av ett förförsök med ett icke sorberande spårämne, dels som ett huvudförsök med det icke sorberande spårämnet Uranin samt med litium (Li), cesium (Cs) och rubidium (Rb), vilka är sorberande i olika grad. Båda försöken utvärderades genom anpassning av två transportmodeller (advektion-dispersion och advektion-dispersion med matrisdiffusion) till uppmätta data. Dessutom beräknades transportparametrar.

Resultaten från modellen med matrisdiffusion som bedömdes vara mest pålitliga, visar på en förhållandevis stor dispersion och liten retardation av de sorberande spårämnena. Retardationsfaktorerna bestämdes till 1,1 för Li, 3,4 för Cs och 2,7 för Rb. Den longitudinella dispersiviteten bestämdes till 50,4 m. En låg retardationsfaktor för Cs har även tidigare bestämts genom SWIW-test i KFM02A.

Responser på pumpningen kunde ses i 25 sektioner av totalt 115 tryckregistrerade. Responserna från det hydrauliska interferenstestet är i huvudsak överensstämmande med den hydrogeologiska modellen över Forsmarks undersökningsområde. Transient utvärdering gjordes av både pumptestet och interferenstestet. Transmissiviteten för den pumpade sektionen i KFM02B bestämdes till $3{,}0 \cdot 10^{-5}$ m^2/s.

Contents

1 Introduction

This document reports the results from the interference test and tracer test in Zone A2 at drill site 2, which is one of the activities performed within the site investigation at Forsmark. A detailed map of drill site 2 and a map of the site investigation area in Forsmark are presented in Figure 1-1. The work was carried out in accordance with activity plan AP PF 400-07-013. In Table 1-1, the controlling documents for performing this activity are listed. The activity plan and the method descriptions are SKB's internal controlling documents. The obtained data from the activity are reported to the database Sicada, where they are traceable by the activity plan number.

The field work, which was performed during 9 weeks from March to May 2007, involved groundwater flow measurements in KFM02A by dilution measurements, pumping in KFM02B together with pressure registration in surrounding boreholes, a pre-test (tracer test) and the main tracer test.

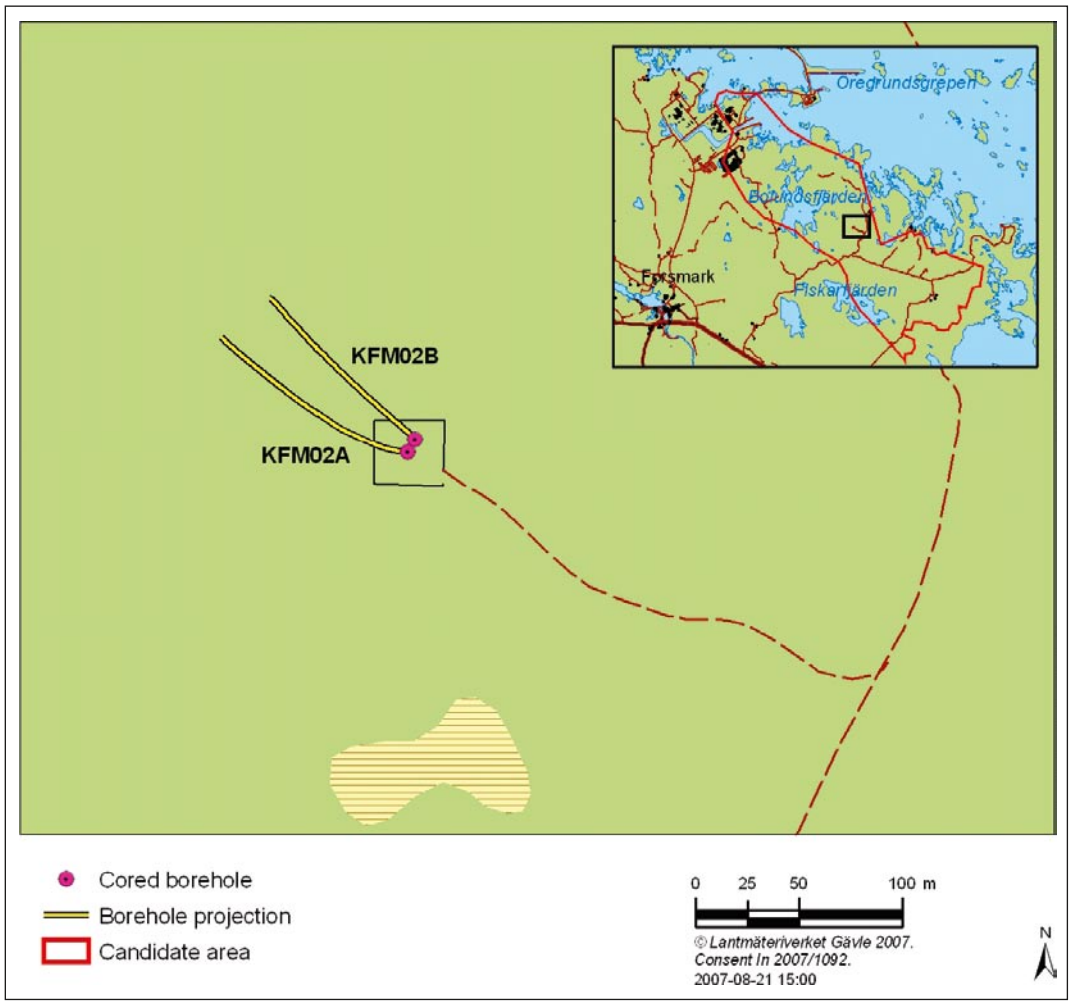

Figure 1-1. *Detailed map of KFM02A and KFM02B at DS 2.The small map shows a general overview of the Forsmark site investigation area.*

Table 1-1. Controlling documents for performance of the activity.

Activity plan	Number	Version
Interferenstest och spårförsök med sorberande spårämnen i zon A2 på borrplats 2	AP PF 400-07-013	1.0
Method documents	**Number**	**Version**
Metodbeskrivning för flerhålsspårförsök	SKB MD 530.006	1.0
Metodinstruktion för analys av injektions- och enhålspumptester	SKB MD 320.004	1.0
Metodbeskrivning för interferenstester	SKB MD 330.003	1.0
System för hydrologisk och meterologisk datainsamling. Vattenprovtagning och utspädningsmätning i observationshål.	SKB MD 368.010	1.0
Instruktion för rengöring av borrhålsutrustning och viss markbaserad utrustning).	MD 600.004	1.0

Pumping was conducted in a packed-off section in borehole KFM02B (408.5–434.0 metres borehole length below top of casing, TOC, (mbl)). Several boreholes and monitoring wells in soil surrounding the pumped borehole served as observation wells and the pressure was monitored using HMS (Hydro Monitoring System) or miniTroll loggers. After about 2 weeks of pumping, the tracer test begun by injecting four different tracers (Uranine, lithium, cesium and rubidium) in a packed-off section (411.0–442.0 mbl) of borehole KFM02A, the borehole collar of which is located 7.5 m from the borehole collar of KFM02B. The water in the injection section in KFM02A was circulated for mixing and samples were collected regularly to monitor the tracer concentrations in the section. Water samples from KFM02B were also taken and analysed for tracer breakthrough. A schematic view of the layout of the tracer test is shown in Figure 2-1.

KFM02A and KFM02B are both telescopic core-drilled boreholes drilled for the site investigation in the Forsmark area. The cleaning procedures of the equipment used for the tracer and pumping tests in the boreholes were performed according to level 1 in the cleaning instructions in MD 600.004 (Instruktion för rengöring av borrhålsutrustning och viss markbaserad utrustning).

Several other tests have previously been performed in KFM02A, such as single-hole injection tests /Källgården et al. 2004/, hydrochemical characterisation /Wacker et al. 2004/ and a SWIW-test /Gustafsson et al. 2005/. Section KFM02A:5 (411.0–442.0 mbl), which is the tracer injection section, is included in the monitoring program where groundwater flow measurements and water sampling are regularly carried out.

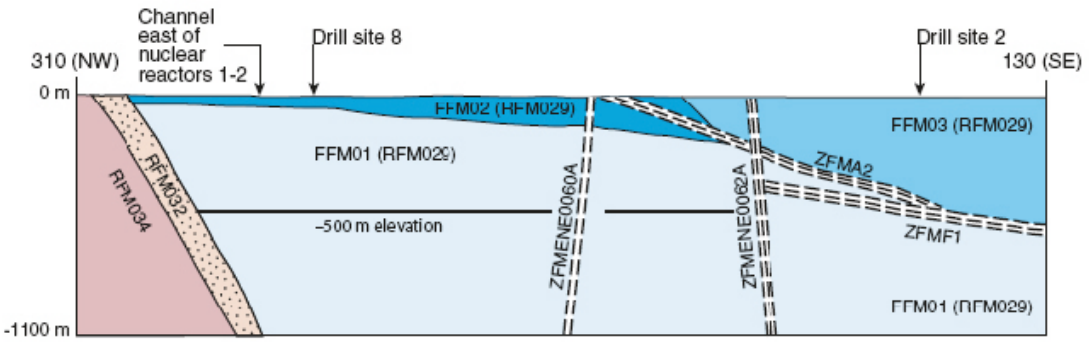

Figure 1-2. *Simplified profile in a NW-SE direction (310–130) that passes through drill sites 2 and 8. Only the high confidence deformation zones ZFMA2, ZFMF1, ZFMENE0060A and ZFMENE0062A are included in the profile /Olofsson et al. 2007/. FFM denotes fracture domain, whereas RFM denotes rock domain.*

KFM02B was originally drilled for the purpose of stress measurements /SKB 2006/. It was drilled in a NW direction to provide a favourable intersection angle with the deformation Zone A2 that dips gently to SSE /SKB 2005/. Other activities performed prior to the tracer test include BIPS logging, difference flow logging and geophysical logging.

The deformation zone that herein is abbreviated A2 is named ZFMA2 (model stage 2.2) or ZFMNE00A2 (model stage 2.1) in the site descriptive models for Forsmark /Olofsson et al. 2007, SKB 2006/, respectively. It is a gently dipping brittle deformation zone and it is described as a composite zone that consists of narrower, high-strain segments (sub-zones) that are inferred to diverge and converge in a complex pattern /Olofsson et al. 2007/. Already during the model stage 1.2 it was identified as a major structural feature steering both the hydrogeological and fracture properties at the site /SKB 2005/. It intersects many of the boreholes in the investigation area. The zone is considered to intersect KFM02A in the interval 417.0–441.0 mbl /Olofsson et al. 2007/. The sub-horizontal zone ZFMF1 also intersects KFM02A at borehole length 476.0–520.0 mbl /Olofsson et al. 2007/. Figure 1-2 shows a simplified profile of Zone A2 and a few other zones in Forsmark. The intersection of Zone A2 with KFM02B is not yet strictly defined, but the borehole interval 411.0–431.0 mbl (which lies within the pumped section) is interpreted as a possible deformation zone in the geological single-hole interpretation of KFM02B /Carlsten et al. 2007/.

2 Objectives and scope

The objectives of the combined interference test and tracer test were to partially verify the hydrogeological model over the Forsmark candidate area and to verify the transport characteristics that previously have been determined through laboratory tests of drill cores. The activity also gives a unique opportunity to directly compare transport parameters acquired from a single-hole tracer test (SWIW-test) that has been performed earlier in borehole KFM02A.

During the pumping, the withdrawal rate (constant flow rate) and the pressure response in KFM02B were registered. Pressure responses to the pumping in surrounding boreholes were monitored using HMS (Hydro Monitoring System). Tracers were injected into a packed-off section in KFM02A and the pumped water from KFM02B was analysed for tracer breakthrough. Water samples from KFM02A were also collected and analysed in order to monitor the tracer concentration in the injection section. The experimental data were used to estimate transport parameters.

The activity can be divided into two main parts, one part concerns the hydraulic parameters and the hydrogeological model (the pumping test and the interference test) and the second part addresses the transport characteristics (the tracer test). One of the aims is to combine the evaluation of these two parts of the activity as well as other investigations earlier performed in the area to make a combined interpretation of the results and to describe the characteristics of the area, especially Zone A2.

2.1 Borehole data

The reference point of the boreholes is always top of casing (ToC). The Swedish National coordinate system (RT90 2.5 gon V 0:-15) is used in the x-y-plane together with RHB70 in the z-direction. Northing and Easting refer to the top of the boreholes at top of casing. All section positions are given as length along the borehole (not vertical distance from ToC).

2.1.1 Injection and withdrawal boreholes

Technical data for the injection borehole KFM02A and the withdrawal borehole KFM02B are given in Table 2-1 and Appendix 1. In Table 2-2, some calculated data for the borehole sections are presented.

The distance between KFM02A and KFM02B is c 7.5 m at ground level and c 46 m between the tracer injection and the pumping sections.

Table 2-1. Selected technical data for boreholes KFM02A and KFM02B (from Sicada).

Borehole ID	Elevation of top of casing (ToC) (m.a.s.l.)	Borehole length from ToC (m)	Bh-diam. (below casing) (m)	Inclin. -top of bh (from horizontal plane) (°)	Dip-Direction -top of bh (°)	Northing (m)	Easting (m)
KFM02A	7.35	1,002.44	0.077	–85.38	275.76	6698712.50	1633182.86
KFM02B	7.62	573.87	0.076	–80.27	313.06	6698719.19	1633186.29

Table 2-2. Data on section volumes and transmissivity (T) for the borehole sections tested in KFM02A and KFM02B.

Bh ID	Secup (mbl)	Seclow (mbl)	Section length (m)	Section volume (ml)	T (transient eval.) (m^2/s)	T (PFL) (m^2/s)
KFM02A	411.0	442.0	31	60,780 [1)]	2.5·10–6 [2)]	2.9·10–6 [4)]
KFM02B	408.5	434.0	25.5	115,680	3.0·10–5 [3)]	3.6·10–5 [5)]

[1)] Including hoses and circulation equipment used in this test.

[2)] From PSS measurement (summation of TT measured in 5 m sections within the interval) /Källgården et al. 2004/.

[3)] From pumping test, transient evaluation /this report/.

[4)] From PFL measurement (summation of Tf from detected fractures within the interval) /Rouhiainen and Pöllänen, 2004/.

[5)] From PFL measurement (summation of Tf from detected fractures within the interval) /Väisäsvaara and Pöllänen, 2007/.

The transmissivity distributions according to PFL measurements in the intervals intersecting Zone A2 of boreholes KFM02A /Rouhiainen and Pöllänen 2004/ and KFM02B /Väisäsvaara and Pöllänen 2007/ are given in Figure 2-1, which also shows the test layout of the tracer test.

2.1.2 Interference test boreholes

The pressure was measured with increased sampling frequency in all boreholes within a radius of about 2 km from the pumping borehole KFM02B. The pressure changes were monitored in cored boreholes in rock, percussion boreholes in rock as well as in soil monitoring wells. Technical data and coordinates of the boreholes with a detectable response to the pumping in KFM02B are presented in Table A2-2 in Appendix 2. In Table A2-1 in Appendix 2, data for all of the investigated boreholes are presented, including boreholes where no response was detected.

Boreholes HFM14 and HFM25 that were intended, according to the activity plan, to be included in the interference test did not, for various reasons, provide any pressure data and were therefore excluded.

2.2 Tests performed

The tests performed within this activity comprise groundwater flow measurements (natural and stressed conditions), a preliminary tracer test (only with non-sorbing tracer), and a main tracer test (with both sorbing and non-sorbing tracers) combined with a hydraulic interference test, see Table 2-3. The boreholes and sections involved in the interference test and the tests performed within this sub-activity are presented in Section 2.2.1.

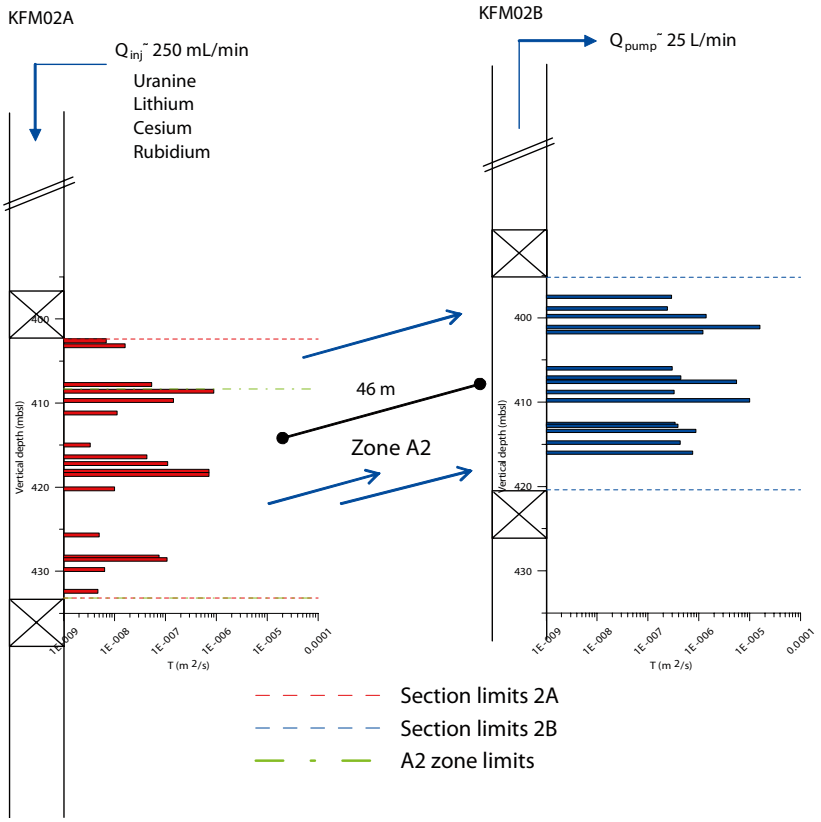

Figure 2-1. *Test layout of the tracer test together with transmissivity distribution in the sections of KFM02A and KFM02B intersecting Zone A2.*

Table 2-3. Tests performed within the activity

Test	Borehole	Secup (mbl)	Seclow (mbl)	Start date and time	Stop date and time
Gw flow measurement (natural gradient)	KFM02A	411.0	442.0	2007-03-15 10:42	2007-03-21 13:00
Gw flow measurement (stressed gradient)	KFM02A	411.0	442.0	2007-03-21 13:00	2007-03-23 14:21
Pre tracer test	KFM02A–2B			2007-03-27 10:30	2007-05-15 10:06
Main tracer test	KFM02A–2B			2007-04-04 13:45	2007-05-15 10:06
Pumping test	KFM02B	408.5	434.0	2007-03-21 13:00	2007-05-29 08:50
Interference test [1)]				2007-03-21 13:00	2007-06-03 10:00

[1)] The interference test is presented separately in Section 2.2.1.

2.2.1 Interference tests

The start and stop of pumping occurred on March, 21 at 13:00 and May 15 at 10:06, respectively. The overall data acquisition was continued until May 29 in the pumping borehole and until June 3 in the observation boreholes.

All borehole sections involved in the interference test in KFM02B are listed in Table A2-1 in Appendix 2 together with the start and stop times of the pumping and distances from the pumping section. The data extracted from HMS (Hydro Monitoring System) from the observation boreholes were selected to obtain sufficient data as well as adequate information about the hydraulic conditions prior to as well as after the interference test.

The test was performed according to the SKB internal documents presented in Table 1-1. However, no response matrix was prepared since only one major interference test was performed.

Interpreted points of application (mid-point of section), lengths of the borehole sections with a detected response during the interference test together with estimated transmissivities from previous investigations are presented in Table 2-4. The distances between the points of application in the pumping borehole and the observation borehole sections are shown in Table 2-5.

Table 2-4. Points of application and lengths of the observation sections with a detected response from the pumping in KFM02B as well as estimated transmissivities from previous investigations.

Bh ID	Test section (mbl)	Point of application (mbl below TOC)	Section length (m)	Transmissivity (m^2/s)
KFM02A:3	490.00–518.00	504.0	28.0	$2.1 \cdot 10^{-6}$ [1]
KFM02A:4	443.00–489.00	470.5	55.0	$3.9 \cdot 10^{-7}$ [1]
KFM02A:5	411.00–442.00	426.5	31.0	$2.5 \cdot 10^{-6}$ [1]
KFM02A:6	241.00–410.00	325.5	169.0	$1.3 \cdot 10^{-5}$ [1]
KFM02A:7	133.00–240.00	186.5	107.0	$5.1 \cdot 10^{-6}$ [1]
HFM32:1	98.00–202.65	150.5	105.0	$1.7 \cdot 10^{-5}$ [2]
HFM32:2	32.00–97.00	64.5	65.0	$1.7 \cdot 10^{-5}$ [2]
KFM05A:5	115.00–253.00	184.0	138.0	$5.3 \cdot 10^{-6}$ [3]
KFM05A:6	100.07–114.00	107.0	13.9	$1.2 \cdot 10^{-3}$ [3]
HFM16:1	68.00–132.50	100.0	64.0	$5.7 \cdot 10^{-5}$ [4]
HFM16:2	54.00–67.00	60.5	13.0	$3.5 \cdot 10^{-4}$ [4]
HFM16:3	12.02–53.00	32.5	41.0	$1.2 \cdot 10^{-4}$ [4]
KFM06B:1	51.00–100.33	75.5	49.0	$2.4 \cdot 10^{-4}$ [5]
KFM06B:2	27.00–50.00	38.5	23.0	$2.9 \cdot 10^{-4}$ [5]
KFM06B:3	6.33–26.00	15.5	21.0	$2.8 \cdot 10^{-6}$ [5]
KFM06A:6	247.00–340.00	293.5	93.0	$7.5 \cdot 10^{-5}$ [5]
KFM06A:7	151.00–246.00	198.5	95.0	$2.7 \cdot 10^{-5}$ [5]
KFM06A:8	100.40–150.00	125.2	49.6	$6.0 \cdot 10^{-5}$ [5]
HFM15:1	85.00–95.00	90.0	10.0	$1.0 \cdot 10^{-4}$ [6]
HFM15:2	6.00–84.00	45.0	78.0	$2.2 \cdot 10^{-4}$ [6]
HFM19:1	168.00–182.00	175.0	14.0	$2.7 \cdot 10^{-4}$ [7]
HFM19:2	104.00–167.00	135.5	63.0	$2.2 \cdot 10^{-5}$ [7]
HFM19:3	12.04–103.00	57.5	91.0	$4.0 \cdot 10^{-5}$ [7]
HFM13:1	159.00–173.00	166.0	14.0	$2.9 \cdot 10^{-4}$ [6]
HFM13:2	101.00–158.00	129.5	57.0	$2.1 \cdot 10^{-5}$ [6]

[1] /Källgården et al. 2004/.

[2] /Jönsson and Ludvigson, 2006/.

[3] /Gokall-Norman et al. 2005/.

[4] /Ludvigson et al. 2004a/.

[5] /Hjerne et al. 2005/.

[6] /Ludvigson et al. 2004b/.

[7] /Ludvigson et al. 2004c/.

Table 2-5. Calculated distances from the midpoint of the pumping section in KFM02B (408.5–434.0 mbl) to the observation sections with a detected response from the pumping in KFM02B.

Observation sections			Distance to KFM02B (m)
Borehole ID	Section (mbl)	Point of Application (mbl below TOC)	
KFM02A:3	490.00–518.00	504.0	97
KFM02A:4	443.00–489.00	470.5	66
KFM02A:5	411.00–442.00	426.5	47
KFM02A:6	241.00–410.00	325.5	104
KFM02A:7	133.00–240.00	186.5	237
HFM32:1	98.00–202.65	150.5	1047
HFM32:2	32.00–97.00	64.5	1080
KFM05A:5	115.00–253.00	184.0	1480
KFM05A:6	100.07–114.00	107.0	1525
HFM16:1	68.00–132.50	100.0	1205
HFM16:2	54.00–67.00	60.5	1219
HFM16:3	12.02–53.00	32.5	1225
KFM06B:1	51.00–100.33	75.5	1240
KFM06B:2	27.00–50.00	38.5	1247
KFM06B:3	6.33–26.00	15.5	1253
KFM06A:6	247.00–340.00	293.5	1336
KFM06A:7	151.00–246.00	198.5	1302
KFM06A:8	100.40–150.00	125.2	1282
HFM15:1	85.00–95.00	90.0	1605
HFM15:2	6.00–84.00	45.0	1584
HFM19:1	168.00–182.00	175.0	1711
HFM19:2	104.00–167.00	135.5	1692
HFM19:3	12.04–103.00	57.5	1659
HFM13:1	159.00–173.00	166.0	1717
HFM13:2	101.00–158.00	129.5	1715

3 Equipment

3.1 General

Borehole KFM02A and most of the surrounding boreholes where the pressure was measured during the interference test are permanently instrumented with 1–9 inflatable packers isolating 2–10 borehole sections in each borehole. In Figure 3-1 drawings of the instrumentation in core and percussion boreholes are presented.

All isolated borehole sections are connected to the HMS-system for pressure monitoring. In general, the sections planned to be used for tracer tests are equipped with three polyamide tubes. Two are used for injection, sampling and circulation in the borehole section and one is used for pressure monitoring.

The pressure monitoring is made by pressure transducers in standpipes connected to each section in the borehole (see Figure 3-1). All data are collected by means of pressure transducers connected to different types of data loggers. In order to calibrate registrations from the data loggers, manual levelling of all sections is made, normally once every month. The logger data are converted to water levels by means of a linear calibration equation. It is also necessary to subtract the air pressure since all transducers give the absolute pressure. The ground water levels are given in metres above sea level (m.a.s.l.).

Since the pressure in the boreholes are given in terms of groundwater levels by HMS, both terms “pressure” and “groundwater level” are used to explain the hydraulic conditions in the boreholes. Also the term (hydraulic) “head” is used synonymously to “groundwater level”.

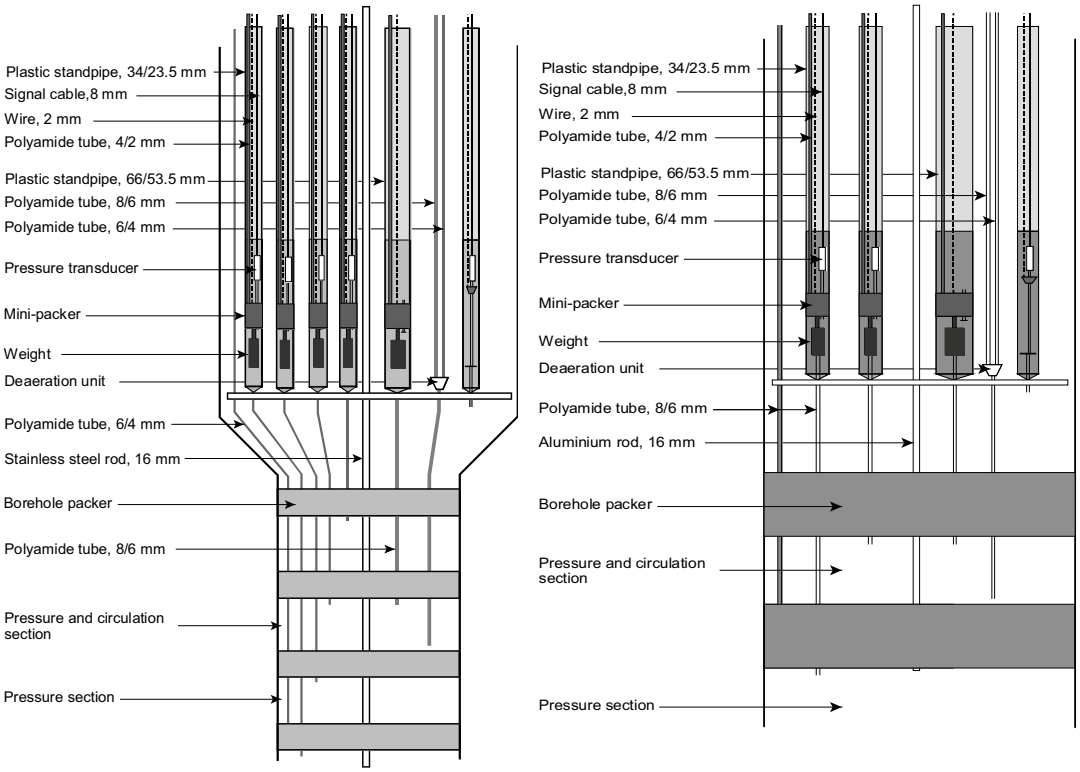

Figure 3-1. *Explanatory sketch of permanent instrumentation in core boreholes (left) and percussion boreholes (right) with circulation sections.*

3.2 Groundwater flow measurements

A schematic drawing of the dilution tracer test equipment is shown in Figure 3-2. The basic idea is to accomplish internal circulation in the borehole section. The circulation makes it possible to obtain a homogeneous tracer concentration in the borehole section and to sample the tracer concentration outside in order to monitor the dilution of the tracer with time.

Circulation is controlled by a down-hole pump with variable speed and is measured using a flow meter. Tracer injections are made with a peristaltic pump and sampling is performed by continuously extracting a small volume of water from the system through another peristaltic pump (constant leak) to a fractional sampler. The equipment and test procedure is described in detail in SKB MD 368.010, SKB internal document, see Table 1-1.

The tracer used was a fluorescent dye tracer, Uranine (Sodium Fluorescein), from Merck (purum quality).

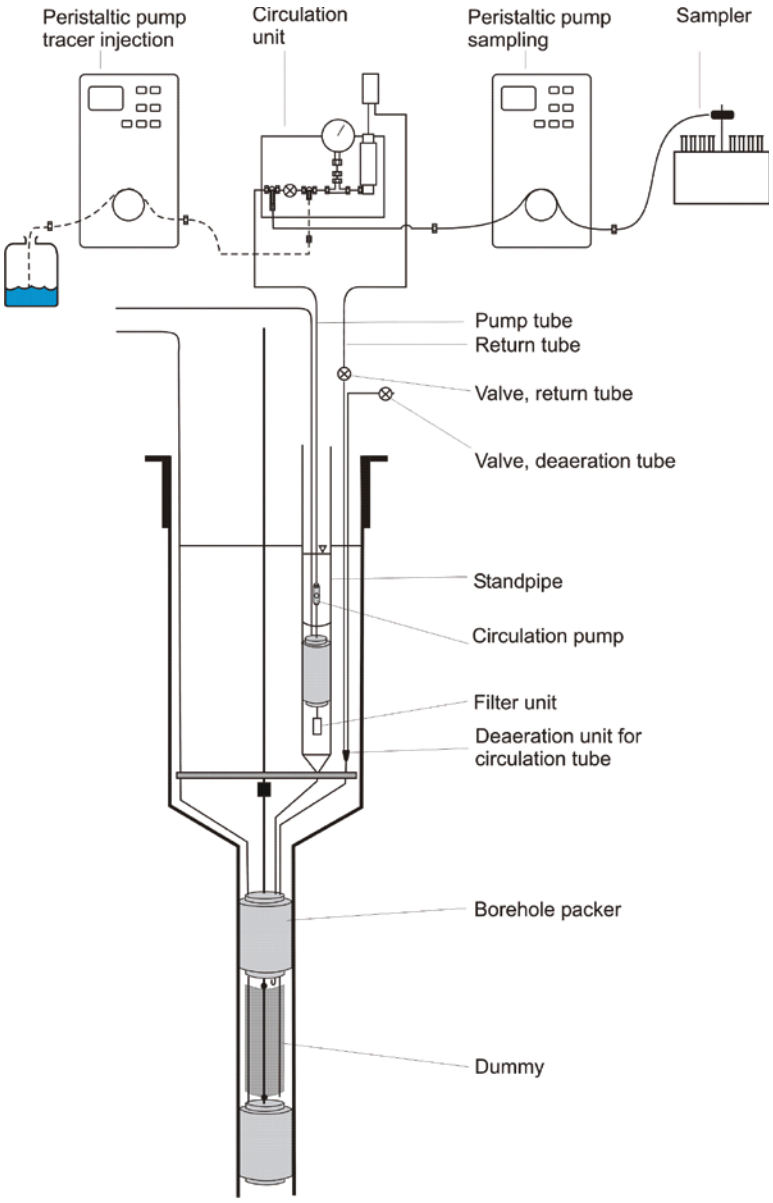

Figure 3-2. *Schematic drawing of the equipment used in tracer dilution measurements.*

3.3 Tracer tests

The same equipment that was used for the dilution measurements (with a few additions and modifications) was employed for sampling, injection and circulation in KFM02A during the tracer test. The tracers were mixed in a large (5 m^3) tank standing next to the borehole. The tracer solution in the tank was purged with nitrogen gas in order to remove oxygen. The injection of tracer was accomplished by a pump placed in the tracer tank and connected to the circulation loop through a hose. The injection pump was of the same type as the circulation pump in the borehole (instead of the peristaltic pump used for injection of tracer in the dilution measurement). Two sub-flows (HCO3- and Fe(II) solutions) and a flow meter attached to the data logger were connected to the injection-hose. An overview of the equipment used is shown in Figure 3-4.

Samples from the injection section were continuously collected in sampling tubes using a peristaltic pump extracting a small sample volume to a fractional sampler, see Figure 3-3. Every second tube was acid washed (12 ml) and used for analysis of lithium, cesium and rubidium, whereas every other second tube (19 ml) was reserved for analysis of Rhodamine WT and Uranine.

Samples were collected from the withdrawal borehole KFM02B using two different automatic samplers, see Figure 3-5. One of the samplers consists of 24 magnetic valves and a control unit allowing selection of time period between openings/samples and open time (to obtain the desired sample volume). Samples for analysis of metals (Li, Cs and Rb) were collected in 125 ml acid-washed plastic (HDPE) bottles. Samples for Uranine analysis were collected using the other sampler providing 500 ml samples. Also this sampler has 24 bottles and a portion of each sample was poured into 19 ml tubes kept for analyses and the rest was emptied and the bottles were re-used. The interval between samples was equal for both samplers.

All samples intended for analysis of Rhodamine WT and Uranine were buffered with c 1% Titrisol buffer solution (pH 9). Earlier experiences have shown that the buffer prevents decomposition of the dye.

Figure 3-3. *Peristaltic pump and fraction sampling equipment used at the injection hole KFM02A.*

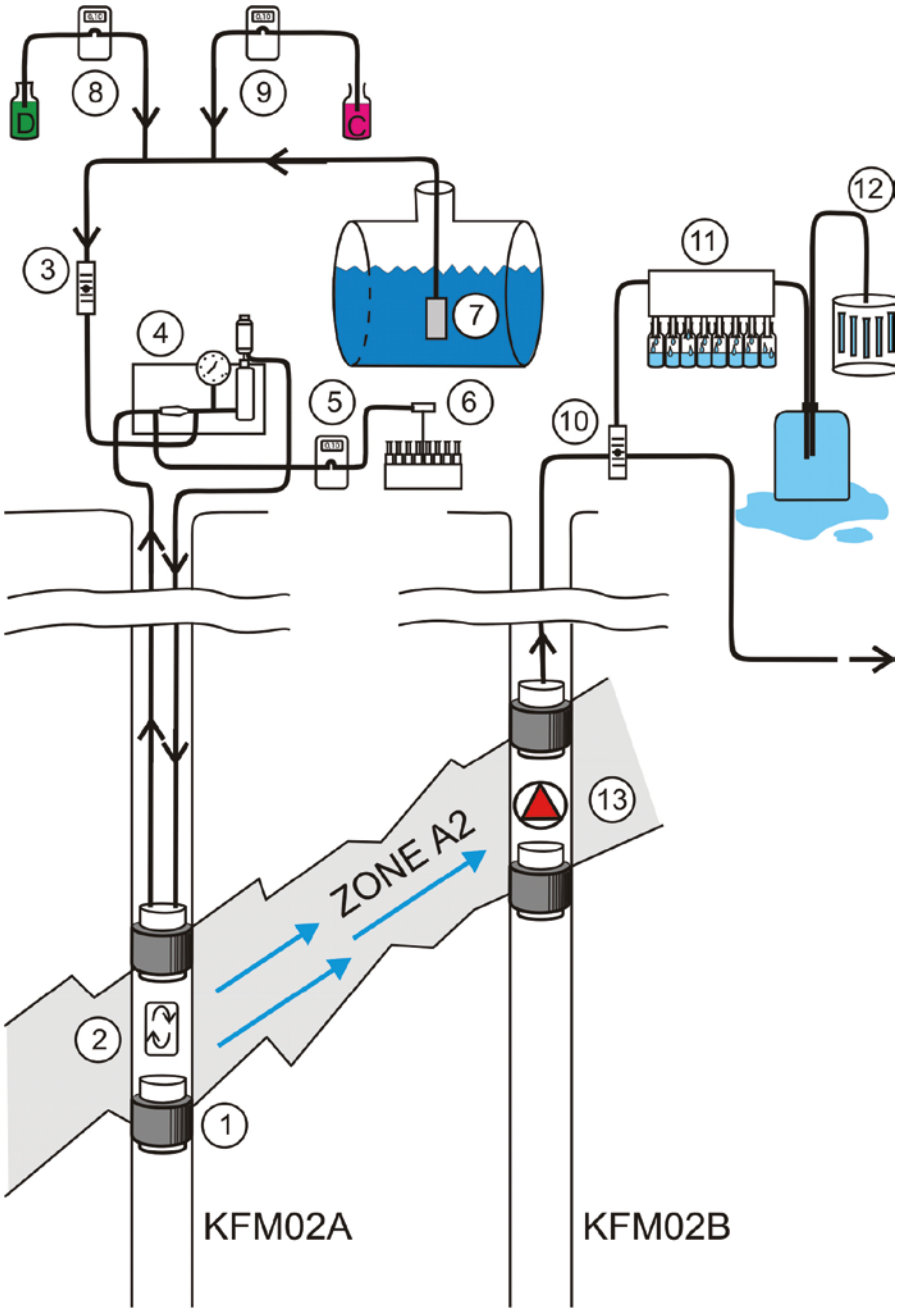

1. Packer
2. Circulation pump
3. Flow meter connected to logger
4. Circulation unit
5. Peristaltic pump for sample withdrawal
6. Fractional sampler
7. Tracer tank with injection pump
8. Peristaltic pump for sub flow D (Fe(II))
9. Peristaltic pump for sub-flow C (HCO_3^-)
10. Flow meter connected to logger
11. Automatic sampler
12. Fractional sampler
13. Pump

Figure 3-4. *Schematic overview of injection and sampling equipment used and tracer test layout.*

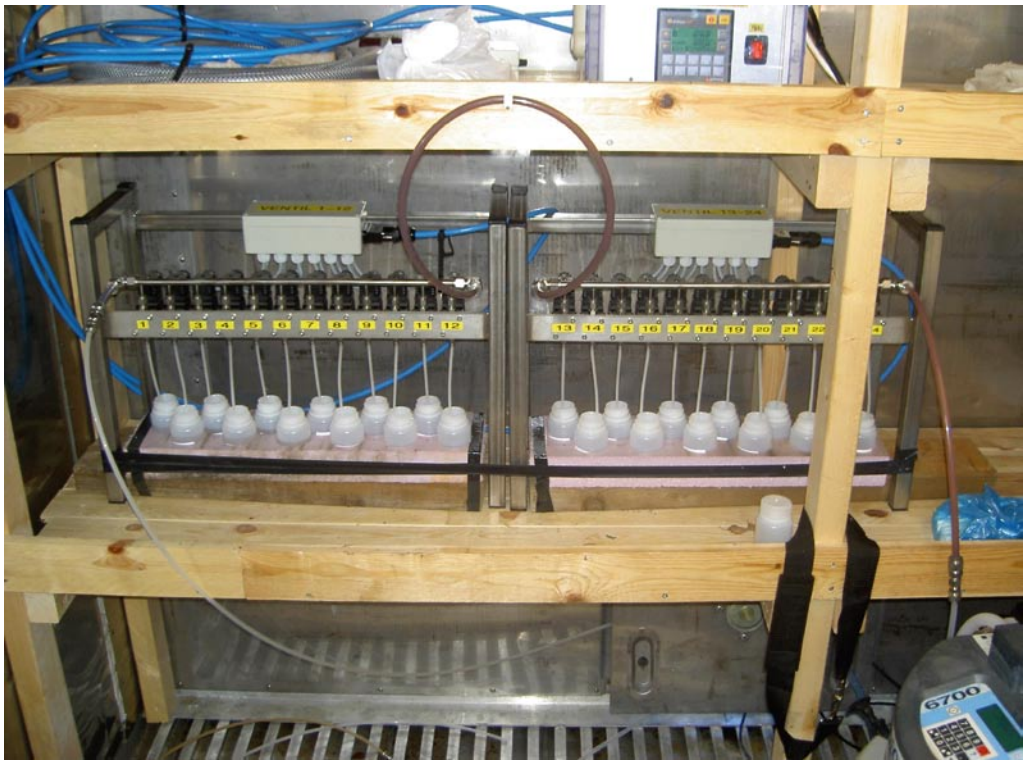

Figure 3-5. *The automatic sampling equipment (24 magnetic valves) used at the withdrawal hole KFM02B.*

3.3.1 Rationale for selection of sorbing tracers

Several general considerations have to be made for the selection of the sorbing tracer (preferably cations) in an in situ experiment of the present type:

- The injection concentration of the tracer should be high enough to allow detection in the withdrawal borehole where the dilution process often results in a concentration several orders of magnitudes lower than in the injection borehole.
- If the injection concentration is too high, some of the following problems may occur:
  - Full or partial saturation of the adsorption sites on the fracture walls leading to nonlinear adsorption giving lower retention compared to a realistic case of radionuclides dispersed in tracer concentrations.
  - Changes in water composition which may influence the competition for the cation exchange sorption sites.
  - Precipitation of less soluble compounds of the proposed cations, i.e. formation of e.g. carbonates, sulfates, fluorides and hydroxides.
  - Concentrations significantly higher than the natural salt content of the water may result in significantly increased density of injection solution and thus poor mixing with the natural groundwater.
- The retention should be low enough to enable tracer breakthrough within the time frame of a tracer experiment (weeks-month) and preferably high enough to permit distinguishing the breakthrough from a simultaneously injected non-sorbing tracer.

The best type of tracers, given the above considerations, is radioactive tracers; no background signal to overcome and a large dynamic range is in most cases available without making any significant concentration increase, cf. e.g. /Andersson et al. 2002/. However, it was in the present tracer experiment, for various practical reasons, not possible to use radioactive tracers. Instead, increased concentrations of naturally occurring cations were used.

From the commonly used types of sorbing tracers (alkali metals and alkaline earth metals, cf. e.g. /Andersson et al. 2002/), it is obvious that the alkaline earth metals (Mg^{2+}, Ca^{2+}, Sr^{2+} and Ba^{2+}) cannot be used due to their limited solubility as e.g. carbonates (Mg^{2+} and Ca^{2+}) and sulfates (Sr^{2+} and Ba^{2+}). An increase of the natural concentrations of these species with 1–2 orders of magnitudes is predicted to cause precipitation problems. Regarding the alkali metals (i.e. Li^{+}, Na^{+}, K^{+}, Rb^{+} and Cs^{+}), no compound with low solubility can be identified so there are no restrictions from this point of view. However, for Na+ being present in the groundwater at a natural concentration of 1,820 ppm (0.08 M) /Wacker et al. 2004/ it is obvious that an increase of the natural concentration in orders of magnitudes will lead to an increase of the density of the water. In addition, this will also make the solution approach the solubility limit of NaCl (~6 M). The ion K+ is present in the natural groundwater in a concentration of 21.4 ppm (5.5·10–4 M) /Wacker et al. 2004/, which also is comparatively high for the use of this cation as a tracer. The three best candidates are therefore Li^{+}, Rb^{+} and Cs^{+}, present in the natural concentrations of 57 ppb (8.2·10–6 M), 58 ppb (6.8·10–7 M) and 1.9 ppb (1.4·10–8 M), respectively /Wacker et al. 2004/.

Based on the considerations above and the results of the scoping calculation (see Section 4.2), the following strategy was outlined:

- Li^{+}, Rb^{+} and Cs^{+} should be used as sorbing tracers.
- Injection concentrations were, based on the scoping calculations, selected to be 8.0·10–2 M for Li+, 1.7·10–3 M for Rb^{+} and 2.9·10–4 M for Cs^{+}, i.e. a concentration increase with a factor 1·104, 2.5·103 and 2·104 for the different tracers, respectively.
- To avoid increasing the ionic strength and thereby minimize density changes, it was decided that the injection solutions should be prepared on a synthetic groundwater basis. A groundwater with the same composition as the natural groundwater should therefore be prepared, except that all of the natural Na^{+} concentration (0.08 M) should be changed to Li^{+}.

One should be aware of that this concept of significantly changing the water composition and increasing the tracer concentration may give retention characteristics that are not directly comparable to performance assessment cases, laboratory data and/or other in situ experiments. However, the objective of this work is more from a demonstration/confirmation perspective, i.e. to give a qualitative indication that tracer retardation can be obtained in situ.

In addition to the injection phase of the tracer experiment, this tracer experiment also involved a pre-test phase and a rinsing phase (after the injection phase in the sorbing tracer experiment). In order to obtain stable flow conditions during the experiment, a water injection at the same flow rate had to be performed during the other two phases. In order to minimize any changes in the groundwater composition, this should be performed using water with a salt matrix identical to the natural groundwater. This can be done using two alternative methods:

1. Pumping and storing natural groundwater in large tanks and inject directly from them.
2. Preparing a synthetic groundwater with the same composition as the natural groundwater.

A general disadvantage with sampling natural groundwater is that the pressure release combined with air contact may cause precipitation of e.g. iron and manganese hydroxides. On the other hand, preparation of synthetic groundwater is quite laborious. Nevertheless, since the execution of this experiment demanded preparation of synthetic groundwater for the injection phase, it was decided to also use synthetic groundwater for the other experimental phases.

For convenience, it was decided to prepare concentrated salt solutions in the laboratory and in the field subsequently dilute the concentrated solutions with tap water to obtain the correct water composition. For this reason, four different solutions had to be made:

- All major cations (except for Na and Li which are contained in solutions B, C and D) in their chloride form.
- All major anions (except Cl, which is contained in solutions A, C and D) in their Na/Li form.
- All carbonates in their Na/Li/H form.
- All redox-sensitive chemicals, Fe(II) and Mn(II).

Solutions A and B were mixed and diluted in a large tank at the experimental site. The reason that they were separated in their concentrated forms was to avoid precipitation of sulfates of the alkaline earth metals.

Solution C was never mixed into the large tank but was injected as a side flow during the injections. The reason for this was to avoid losses of CO^2 during the nitrogen purging of the injection solution; the purging was performed in order to significantly reduce the amount of dissolved oxygen in the water. For the same reason, injection of the solution containing redox-sensitive chemicals (solution D) was also done as a side flow.

The preparation of the synthetic groundwater and its detailed chemical composition is further described in Appendix 3.

3.3.2 Tracers used

In the pre-test, Rhodamine WT (50 ppm) was used as the non-sorbing tracer. In the main test, Uranine, lithium, cesium and rubidium at the concentrations presented in Table 3-1 were used. Lithium, cesium and rubidium were all added in the form of chloride salts. The discrepancy between the concentration suggested by the scoping calculations and the theoretical concentration presented in Table 3-1 is due to uncertainty in volume when filling the tank. The actual volume was measured by analysis of the concentrated Uranine (Rhodamine WT in the pre-test) solution added to the tank and the Uranine concentration after dilution in the tank. Since the volume showed to be somewhat larger than intended, the actual concentration of tracers are lower than suggested by the scoping calculations.

3.4 Pumping and interference test

The equipment in the pumping borehole, KFM02B, consisted primarily of the following parts:

- A submersible pump with a steel pipe to the ground surface and down to the measured section.
- Two hydraulically operated packers.
- Plastic hose and pipe for diverting the pumped water into the sea.
- Pressure transducer in the borehole.
- Flow meter at the surface.
- Data logger to sample data from the flow meter and the pressure transducer.
- Flow rate control valve at the surface.
- PC to visualize the data.

All of the observation sections included in the interference test are part of the SKB hydromonitoring system (HMS), where pressure is recorded continuously.

Table 3-1. Injection concentrations (C0) of the tracers.

Tracer	Conc. suggested by scoping (ppm)	Conc. heoretical (ppm)	Conc. Measured in tank (ppm)	Conc. Maximum-measured in KFM02A (ppm)	Comment
Rhodamine WT	50.0	50.0	45.0	46.7	Only used in the pre-test
Uranine	50.0	50.0	47.1	49.1	
Lithium	570	554	506	607[1)]	Since a part of the Li was added as a side injection-flow instead of being mixed in the tank, the total theoretical concentration and the concentration in the tank differs
Cesium	40.0	39.1	37.9	39.3	
Rubidium	150	147	139	146	

[1)] The high concentration of Li occurred when the injection pump stopped while the sub-flow pump with high Li-concentration continued.

3.4.1 Measurement sensors

Technical data for the measurement sensors together with corresponding data for the system are shown in Table 3-2.

3.5 Interpretation tools

Transient evaluation of the hydraulic responses in the pumping borehole KFM02B and sections in surrounding boreholes was made using the AQTESOLV software.

The models used for evaluation of the tracer test and calculation of transport parameters are described below.

Table 3-2. Technical data of measurement sensors used together with estimated data specifications of the test system for pumping tests (based on current laboratory and field experience).

Technical specification					
Parameter		**Unit**	**Sensor**	**Test system**	**Comments**
Absolute pressure	Output signal	mA	4–20		Depending on uncertainties of the sensor position
	Meas. range	kPa	0–1,500		
	Resolution	kPa	0.05		
	Accuracy	kPa	± 1.5*	± 10	
Flow (surface)	Output signal	mA	4–20		Passive Pumping tests
	Meas. range	l/min	1–150	5–c. 80	
	Resolution	l/min	0.1	0.1	
	Accuracy	% o.r.**	± 0.5	± 0.5	

*Includes hysteresis, linearity and repeatability.

**Maximum error in % of actual reading (% o.r.).

3.5.1 Transport models

Advection-dispersion model with sorption in a single pathway

This model is described by the standard governing equation for one-dimensional advection-dispersive transport with linear equilibrium sorption:

$$D_L \frac{\partial^2 C}{\partial x^2} - v \frac{\partial C}{\partial x} = R \frac{\partial C}{\partial t} \qquad (3\text{-}1)$$

where C is concentration [e.g. M/L^3], x is distance along transport path [L], t is time [T], v is the average water velocity [L/T] along the flow path, D_L is the longitudinal dispersion coefficient [L^2/T] and R is the retardation factor.

The following initial and boundary conditions are applied:

$$C(x,0) = 0 \qquad (3\text{-}2)$$

$$\frac{\partial C(\infty,t)}{\partial x} = 0 \qquad (3\text{-}3)$$

$$-D_L \frac{\partial C}{\partial x} + vC = vC_0 \qquad x = 0 \qquad (3\text{-}4)$$

where C_0 is the concentrations of the in-flowing water across the inlet boundary. The above boundary and initial conditions result in a solution for a constant injection of tracer. For a tracer pulse with constant concentration of limited duration (t_{inj}), the resulting tracer concentration may be calculated as:

$$C(x,t) = M(x,t) \qquad 0 < t \leq tinj \qquad (3\text{-}5)$$

$$C(x,t) = M(x,t) - M(x,\, t - tinj) \qquad t > tinj \qquad (3\text{-}6)$$

where $M(x,t)$ is the solution for a step-input injection with constant injection concentration. A more complex temporal variation in the tracer injection may be calculated in an analogous way by summation of a several such injection periods. A solution to the above equations, for a step input of constant concentration, is given by /Javandel et al. 1984/ as follows:

$$M(x,t) = \frac{1}{2} erfc\left[\frac{Rx - vt}{2(D_L Rt)^{1/2}}\right] + \left[\frac{v^2 t}{\pi D_L R}\right]^{1/2} \exp\left[-\frac{(Rx - vt)^2}{4 D_L Rt}\right] - \frac{1}{2}\left[1 + \frac{vx}{D_L} + \frac{v^2 t}{D_L R} + \right] \exp\left[\frac{vx}{D_L}\right] erfc\left[\frac{Rx + vt}{2(D_L Rt)^{1/2}}\right] \qquad (3\text{-}7)$$

where *erfc* is the complimetary error function.

The advection-dispersion model with sorption is herein referred to as the AD model.

The results from AD model evaluation are in this report presented using mean residence time, t_m $(= x/v)$, Peclet number, Pe $(=x/a_L)$ and retardation factor (R). Further, the proportionality factor, pf , which describes the fraction of the injected tracer mass that arrives at the sampling section, is obtained from the model fitting.

Advection-dispersion model in multiple pathways

This model is essentially the same as the preceding one (AD-1) except that tracer transport is assumed to occur in two, or more, separate pathways and mix in the pumping section. This is calculated by summing up the contribution from the different pathways as (for n pathways):

$$C(x,t) = \sum_{i=1}^{n} pf_i \cdot C_i(x,t) \tag{3-8}$$

where *Ci(x,t,)* represents the partial tracer breakthrough from each individual pathway and pf_i is a proportionality factor that describes the contribution from each pathway.

It may here be noted that the pf parameter also represents dilution effects in the pumping section as well as other proportional tracer losses. Thus, this parameter is often relevant to include also when applying the advection-dispersion model for a single pathway.

Advection-dispersion model with matrix diffusion (one pathway)

In this model, the governing equation for the AD model is extended by adding a term that represents diffusion of tracer into a hydraulically stagnant matrix:

$$R\frac{\partial C}{\partial t} = -v\frac{\partial C}{\partial x} + D_L\frac{\partial^2 C}{\partial x^2} + \frac{2D_e}{\delta}\frac{\partial C_p}{\partial y} \tag{3-9}$$

with the transport in the matrix given by:

$$\frac{\partial C_p}{\partial t} - \frac{D_e}{R_d n_p}\frac{\partial^2 C_p}{\partial y^2} = 0 \tag{3-10}$$

where n_p is the matrix porosity, D_e is the effective diffusion coefficient [L^2/T], δ is the fracture aperture [L] of the flowing fracture, $C_p\,(y)$ is the tracer concentration in the matrix, R_d is the matrix retardation factor and y is a spatial coordinate perpendicular to the direction of the flowing transport path. The matrix diffusion model used here is also presented by /Tang et al. 1981/ and /Moreno et al. 1985/. The model with advection-dispersion with sorption and matrix diffusion is herein referred to as the AD-MD model.

The boundary and initial conditions are:

$C(x,0) = 0$ (3-11)

$C(\infty,t) = 0$ (3-12)

$C(0,t) = C0$ (3-13)

$Cp(0,x,t) = C(x,t)$ (3-14)

$Cp(\infty,x,t) = 0$ (3-15)

$Cp(y,x,0) = 0$ (3-16)

When this matrix diffusion model is employed for interpretation of tracer breakthrough curves, all unknown parameters in Equations 3-8 and 3-9 cannot be evaluated independently. Instead, it is common to use a lumped parameter, A, which describes the effect of matrix diffusion. The parameter A may be written as:

$$A = \frac{\delta \cdot R}{2\sqrt{n_p D_e R_d}} \tag{3-17}$$

With this definition, the matrix diffusion effect increases with decreasing values of A.

3.5.2 Parameter estimation method

Estimated parameter values are obtained by non-linear least-squares regression. The basic non-linear least-squares regression minimises the sum of squared differences between the modelled (Y^M) and the observed (Y^O) variables and may be formulated as:

$$\min S = \mathbf{E_R}^T \mathbf{W} \mathbf{E} \mathbf{R} \tag{3-18}$$

where $\mathbf{E_R}$ is a vector of residuals ($\mathbf{Y^O} - \mathbf{Y^M}$) and $\mathbf{W}$ is a vector of reliability weights on observations.

The specific method for carrying out the regression employed in this study is often referred to as the Marquardt-Levenberg method. This method is a Newton-type optimisation algorithm that finds the parameter values that minimises the sum of squared errors between model and measurement values in an iterative manner. A basic Newton-type search algorithm used may be written as:

$$\mathbf{B}_{r+1} = \mathbf{B}_r + (\mathbf{X}_r^T \mathbf{W} \mathbf{X}_r)^{-1} \mathbf{X}_r^T (\mathbf{Y}^O - \mathbf{Y}_r^M) \tag{3-19}$$

where $\mathbf{B}$ is a vector of parameter estimates, X is a parameter sensitivity matrix, and the subscripts r and r+1 refer to the iteration number. The Marquardt-Levenberg method is an extension that enhances the convergence properties of the search algorithm by restricting the search direction.

Given an initial parameter estimate (B_r), the model variable vector (Y^M) and the sensitivity matrix (X) are calculated and a new vector of estimates (B_{r+1}) is obtained. Equation 3-18 is then repeated until a local optimal solution is found. The local minimum is defined by some convergence criterion, for example when parameter estimates are essentially identical between iterations. Finding a local minimum does not guarantee that the global minimum is found. When this appears to be a problem, several sets of initial estimates may be tried. When some knowledge about the parameters to be estimated and the physical system is already available, the initial estimates are often good enough for ensuring that a global minimum is found.

An important element of the above procedure is the matrix containing the parameter sensitivities. Parameter sensitivity is defined as the partial derivative of the dependent (simulated) variable with respect to a parameter. A sensitivity matrix contains one row for each observation and one column for each estimated parameter, as in the following example with three observations and two parameters.

$$\mathbf{X} = \begin{pmatrix} \frac{\partial y_1}{\partial b_1} & \frac{\partial y_1}{\partial b_2} \\ \frac{\partial y_2}{\partial b_1} & \frac{\partial y_2}{\partial b_2} \\ \frac{\partial y_3}{\partial b_1} & \frac{\partial y_3}{\partial b_2} \end{pmatrix} \tag{3-20}$$

Parameter sensitivities may be used to determine the precision of the estimated parameter values. Two diagnostic measures are given below regarding parameter uncertainty that may be obtained as a result of regression /Cooley 1979/.

The standard errors of parameter estimates are obtained by taking the square roots of the diagonals in the parameter covariance matrix, which is given by:

$$s^2(\mathbf{X}^T \mathbf{W} \mathbf{X})^{-1} \tag{3-21}$$

with s^2 being the error variance:

$$s^2 = \frac{\sum_{i=1}^{N} w_i \, (y_i^O - y_i^M)^2}{N - P} \tag{3-22}$$

where N is the number of measurements, P the number of parameters to be estimated and w_i the weight on observation i.

The linear correlation $r\,(p_1,p_2)$ between two parameters with values of p_1 and p_2, respectively, is given by:

$$r(p_1,p_2)=\frac{Cov(p_1,p_2)}{\sqrt{Var(p_1)Var(p_2)}} \qquad (3\text{-}23)$$

where the variance and covariance terms are elements of the $s^2\,(\mathbf{X}^T\mathbf{W}\mathbf{X})^{-1}$ matrix. The correlation is a measure of the inter-dependence between two parameter estimates, and correlation values range between –1 and 1. Values close to either –1 or 1 mean that a change in one parameter value may be compensated for by a similar change in another parameter value to maintain the same fit (sum of squares) between model and measurements. The standard errors and parameter correlation values are the main diagnostic measures used in this analysis when examining the parameter estimation results from evaluation of the tracer tests.

3.5.3 Handling of tracer injection data

Measured injection flows and tracer concentration in the injection section were used to calculate the tracer input function for the evaluation models. The input function was approximated by a large number of step input periods that were superimposed as described in Equation 3-6. Each injection period is given an input value that is proportional to the injected tracer mass/time. For periods when the injection pump malfunctioned, the previously determined (during pumping in KFM02B) natural flow through the injection section was used to calculate the tracer mass flow into the tested rock formation.

3.5.4 Other derived transport parameters

In accordance with the SKB method description for two-well tracer tests (SKB MD 530.006), some further transport parameters are derived, mainly based on the average residence time (t_m) determined from the model evaluation described above. The derived parameters are:

- fracture aperture (mass balance aperture),
- hydraulic fracture conductivity,
- flow porosity.

The fracture aperture, δ [L], is determined from:

$$\delta=\frac{Qt_m}{\pi(r^2-r_w^2)} \qquad (3\text{-}24)$$

where Q is the average pumping rate [L^3/T], r is the travel distance [L] and r_w is the borehole radius [L]. The hydraulic fracture conductivity, K_{fr} [L/T] is calculated using:

$$K_{fr}=\ln\left(\frac{r}{r_w}\right)\frac{\left(r^2-r_w^2\right)}{2t_m\Delta h} \qquad (3\text{-}25)$$

where Δh is the head difference [L] between the injection and pumping sections. The flow porosity, ε_f is determined from:

$$\varepsilon_f=\frac{K}{K_{fr}} \qquad (3\text{-}26)$$

where K is the hydraulic conductivity of the packed-off section determined from a steady-state evaluation of the interference test /Moye 1967/.

4 Execution

4.1 General

The activity included planning and preparations, execution of field work and analyses and interpretation of data.

4.2 Scoping calculations

In order to optimize the test in terms of tracer injection method, injection times, pumping rates, tracers, etc, some scoping calculations were performed during the planning stage. It is important to keep in mind that the drilling of KFM02B was completed shortly before the execution of the test and only limited data from KFM02B were available during the scoping calculations. Hence, some assumption had to be made about KFM02B based on data from KFM02A.

4.2.1 Injection method

Two main tracer injection methods were considered, with and without additional pressure in the injection section. The intention was that the selected injection method should provide low dilution between KFM02A and KFM02B and a temporally well-defined injection period.

Injection without additional pressure is done by replacing the ambient water in the injection interval with a tracer solution. The tracer will then be injected simply by dilution caused from withdrawal in the pumping well. The dilution from KFM02A to KFM02B with this method depends on the induced flow rate in KFM02A while pumping in KFM02B. No such measurement had been performed at the time of the scoping calculations and therefore some assumptions had to be made. The groundwater flow was assumed to be radially converging while pumping in KFM02B. Furthermore, the flow was assumed to converge/diverge to some extent around the injection section. With these assumptions a dilution of c 2,000 times is expected if the distance is c 50 m between the sections. The scoping calculations also indicated that the concentration decrease in the injection section would be rather slow with tracer injection without applying additional pressure.

If tracer injection with additional pressure is used, the dilution between the injection and pumping sections would be equal to the ratio of the flow rates if the recovery is 100%, i.e. if the injection rate is 100 times lower than the pumping rate the dilution would be 100 times. Hence, a much smaller dilution is possible to achieve with this method compared to the one described above. Another benefit of this method is that the injection period is rather distinct, i.e. the concentration increases and decreases rather rapidly at the start and stop of the injection, according to the scoping calculations. A disadvantage with injection with this method is that water without tracer has to be injected both before and after the period of tracer injection in order to maintain stable hydraulic conditions during the test.

The recommended methodology was to inject tracer with an additional pressure due to the lower dilution and the more distinct injection period compared to the tracer injection without applying additional pressure.

4.2.2 Pumping flow rate

The duration of the test was originally planned to be 4-6 weeks. In order to ensure a tracer breakthrough in KFM02B, a high flow rate in the section was preferable. On the other hand, the flow rate should be constrained so that the total expected drawdown in KFM02B not exceeds 50 m. The transmissivity, T, of the chosen section of KFM02B was c $2 \cdot 10^{-5}$ m^2/s. An approximation of T according to Equation 4-1 then results in a maximum flow rate of c 60 l/min.

$$T \approx \frac{Q}{s} \tag{4-1}$$

where T is the transmissivity (m^2/s), Q is the flow rate (m^3/s) and s is the drawdown (m).

However, because flow rate changes during the test should be avoided, some safety margin is preferable. In addition, at these relatively high flow rates the friction losses in the pipe string are significant.

As mentioned above, the pumping flow rate has significance for the residence time of the tracer. The residence time for a radially converging flow field may be estimated according to Equation 4-2 (SKB MD 530.006):

$$t_m = \frac{\delta \pi (r^2 - r_w^2)}{Q} \tag{4-2}$$

where t_m is mean residence time (s), δ is fracture aperture (m), r is travel distance (m), r_w is borehole radius (m) and Q is mean pumping rate (m^3/s).

Equation 4-2 requires an assumption of the fracture aperture since no data of this was available during the scoping calculations. According to the cubic law and the transmissivities reported from the borehole sections the fracture aperture (one equivalent fracture) would be in the range of 0.2 – 0.3 mm. However, from experience it is commonly known that the cubic law underestimates the fracture aperture considerably. In Table 4-1 the mean residence time is calculated depending on the pumping flow rate and the fracture aperture. Since there is considerable uncertainty about the fracture aperture, there was an obvious risk that the residence time would be rather large, especially for low flow rates.

The recommendation about pumping flow rate was therefore to maximize the flow rate. However, the flow rate has to be adjusted to the chosen equipment and the expected friction losses in the pipe string. After these considerations, the recommended initial pumping flow rate was 20 l/min.

Table 4-1. Mean residence time (h) with different pumping flow rates and fracture apertures. The distance between the sections is assumed to be 50 m.

Mean residence time [h]		Pumping flow rate [l/min]				
		5	10	20	40	60
Fracture aperture [mm]	1	26	13	7	3	2
	5	131	65	33	16	11
	10	262	131	65	33	22
	20	524	262	131	65	44

4.2.3 Tracers

A prerequisite for the main tracer test was that non-sorbing as well as sorbing tracers should be used. An overview of possible tracers resulted in that some tracers could be rejected early in the process as described in Section 3.3.1. Radioactive tracers were not suitable to use in these boreholes due to safety aspects. Natural Mg^{2+}, Ca^{2+}, Sr^{2+} and Ba^{2+} are often close to their solubility maximum so that they might precipitate if the concentration is increased. Na^{+} has high natural background values and a very high concentration would be necessary to detect a breakthrough. Injection of NH_4^{+} would lead to a decrease in pH which would be unsuitable for interpretation of the results.

Given these considerations and prevailing background concentrations, the list of possible tracers included:

- Dye tracers (Uranine and Rhodamine WT).
- Metal complexes (Ho-DTPA and Tb-DTPA).
- Stabile isotopes (Sr-84 and Ba-130).
- Ions (Cs^{+}, Rb^{+}, Li^{+}, K^{+} and I^{-}).

A number of simulations where performed with the AD model in a single pathway, described in Section 3.5, in order to investigate the applicability of the tracers listed above. Since there is uncertainty about residence time, dispersivity and sorption, several combinations of these parameters were simulated. Different injection schedules with regard to time and flow rate were also simulated. Because of the various uncertainties in the scoping simulations, it is only reasonable to discuss if a tracer is likely to be suitable or not in the test. In these scoping calculations, numerous simulated breakthrough curves were produced that will not be shown in this report. However, one example is presented in Figure 4-1.

Previously, a SWIW test was performed in Zone A2 in KFM02A that resulted in a relatively low retardation factor for Cs, (R=11) /Gustafsson et al. 2005/, which also is the lowest reported retardation factor for all SWIW tests performed within the site investigation programmes in Forsmark and Oskarshamn. Hence, the sorption in the tracer test was expected to be rather low.

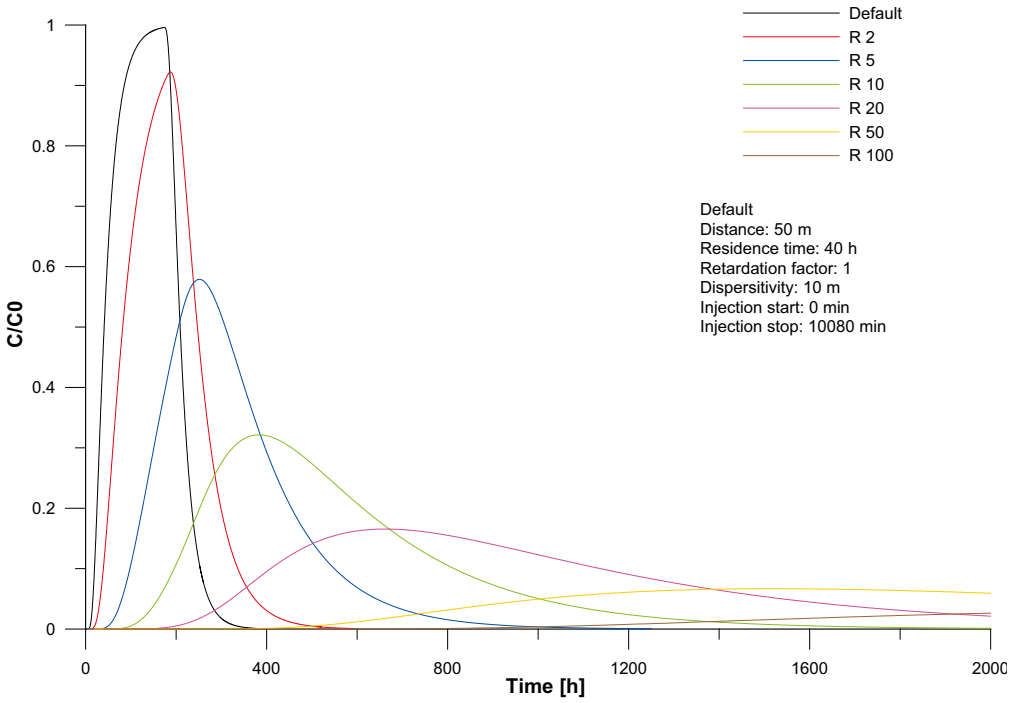

Figure 4-1. *Example of simulated breakthrough curves. The injection has a duration of one week with constant concentration. All curves assume a dispersivity of 10 m and a residence time of 40 h. The retardation factor varies from 1 to 100 in the example.*

The simulations indicated that Sr-84 and Ba-130 would be very costly to use in order to detect a breakthrough curve. The use of K^+ would require such high concentrations in the injection hole that there would be a clear risk that the transport would be affected by a significant difference in density between the injection water and the formation water. Sr-84, Ba-130 and K^+ were therefore excluded from the recommended tracers to be used.

For the main test, Li^+, Rb^+ and Cs^+ were suggested as sorbing tracers. The suggested non-sorbing tracer was Uranine if the background concentration was low during the pre-test. Otherwise Ho-DTPA or Tb-DTPA could be used instead.

The simulations also showed that reasonable injection concentrations of Uranine, RdWT, Ho-DTPA, Tb-DTPA, Li^+, Rb^+ and Cs^+ that would provide significant breakthrough in KFM02B may be attainable.

If large quantities or high concentrations of Rb^+ and Cs^+ are used, the sorption sites in the fractures may become limited so that an assumption of a linear sorption isotherm would no longer be valid. However, the concentrations and amounts of Cs^+ and Rb^+ should not be too low since the concentration in the pumping section may be too low compared with the background level. Hence, the recommended total concentrations and amounts of Cs^+ and Rb^+ constitute a trade-off between the risk of non-linear sorption and the risk of too low concentration in the pumping section. Based on experience from a cation exchange experiment in TRUE–1 /Winberg et al. 2000/ and the scoping simulations, the recommended total amounts and concentrations of Rb^+ and Cs^+ were 4 moles and $2 \cdot 10^{-3}$ M, respectively, which also were used in the experiment.

Based on the scoping simulations, an injection period of one week was recommended since the highest concentration in the breakthrough is less dependent on the dispersivity when the injection period is longer.

Because of uncertainty about the residence time and therefore how long time the experiment should be to meet the objectives of the test, it was recommended to perform a short pre-test with RdWT. This would also be an opportunity to test the equipment prior to the main test.

4.3 Preparations

The preparation activities involved calibrations, preparation of synthetic groundwater and tracer solutions. The following sections (Section 4.3.1–4.3.2) describe the various preparations in detail.

In addition, the groundwater flow measurements and the pre-test can be regarded as preparations. However, they are treated as separate tests in this report and will therefore be presented in Section 4.4 instead.

4.3.1 Calibration and functionality checks

Functionality checks of the equipment were performed before starting the measurements. An equipment check was carried out at the Geosigma engineering workshop in Uppsala as well as at the site as a simple and fast test to establish the operating status of sensors and other equipment. In addition, calibration constants were implemented and checked. To check the function of the pressure sensor, the air pressure was recorded and found to be as expected. Submerged in water, the pressure coincided well with the total head of water, while lowering.

The flow meter for the injection flow was approximately calibrated prior to the test (only two calibration points). After the measurements a more accurate calibration was made using more calibration points, especially in the range used during the test. The logged values were then re-calculated.

The peristaltic pumps used for injection of HCO_3^- – and Fe(II) solutions were calibrated before the test and they were also checked after the test.

4.3.2 Preparation of synthetic groundwater and tracer solutions

To maintain the current natural chemistry in the borehole, all the water injected into KFM02A (including the tracer solutions) consisted of synthetic groundwater. This synthetic groundwater was prepared to have the same water composition as earlier analyses of water samples from KFM02A:5 have shown /Wacker et al. 2004/. If the chemistry is considerably altered it may affect sorption mechanisms and thereby lead to non-representative results. The reason for using synthetic groundwater is further described in Section 3.3.1.

A portion of the synthetic groundwater was added as sub-flows and the rest was mixed in the large tracer injection tank. The preparation of the synthetic groundwater and the tracer solutions together with its chemical composition and amounts of salts added is further described in Appendix 3.

4.4 Execution of field work

The field work was performed during nine weeks from March to May 2007. Table 4-2 lists the major field work events. Pumping was conducted in a packed-off section in borehole KFM02B (408.5–434.0 mbl). After about 2 weeks of pumping the tracer test started by injecting four different tracers (Uranine, Li, Cs and Rb) into a packed-off section (411.0–442.0 mbl) of the permanently instrumented borehole KFM02A, which is located near KFM02B. The water in the injection interval in KFM02A was circulated for mixing and samples were continuously collected to monitor the tracer concentrations. Water samples from KFM02B were also taken and analysed for tracer breakthrough.

To optimize the design of the tracer test (to choose an appropriate withdrawal rate and concentrations of tracers), preparations consisting of scoping calculations, dilution measurements (to monitor the groundwater flow during both natural and stressed conditions) and a pre-test were performed. The pre-test resembled the main test but only one tracer (Rhodamine WT) was used. The pre-test resulted in tracer breakthrough and indicated that the flow rate could be increased before performing the main tracer test.

The tracer test was performed as a weak dipole (1/100), meaning that the injection flow rate (KFM02A) was 1/100 of the withdrawal rate (KFM02B). The dipole was maintained during the whole test period by injection of synthetic groundwater after the tracer injections.

The interference test was performed by pumping in KFM02B and at the same time monitoring pressure responses in observation sections in surrounding boreholes. All boreholes monitored for potential responses are part of HMS (Hydro Monitoring System). A total of 115 observation sections were included in the interference test.

Water samples (SKB Class 3) were taken at three occasions during the eight weeks pumping period. The tap water used for the synthetic groundwater was also sampled.

4.4.1 Groundwater flow measurements

The groundwater flow measurement in KFM02A was performed before the start of the tracer test. The time periods for the measurements are presented in Table 4-2. The period with natural gradient was 146 hours, and the corresponding time during the period with stressed gradient (during pumping) was 49 hours.

The pumping in KFM02B started at 13:00 on March 21 and the flow rate was kept at 19.8 l/min after an initial period of regulation to obtain a steady flow rate. The pumping is described in detail in Section 4.3.2

The groundwater flow measurement was made by injecting a slug of tracer (Uranine, 500 mg/l) in the selected borehole section and allowing the natural groundwater flow to dilute the tracer. The tracer was injected during a time period equivalent to the time it takes to circulate one section volume. The injection/circulation flow ratio was set to 1/1,000, implying that the initial concentration in the borehole section would be about 0.5 mg/l. The tracer solution was continuously circulated and sampled using the equipment described in Section 3.2.

The samples were analysed for dye tracer content at the Geosigma Laboratory using a Jasco FP 777 Spectrofluorometer.

Table 4-2. Overview of field work events.

Activity	Borehole	Date
Dilution mesurements, natural conditions	KFM02A	2007-03-15 10:42 – 2007-03-21 13:00
Start pumping (pressure registration by HMS)	KFM02B	2007-03-21 13:00
Dilution mesurements, stressed conditions	KFM02A	2007-03-21 13:00 – 2007-03-23 14:21
Injcection of Rhodamine WT	KFM02A	2007-03-27 10:30 – 2007-04-03 10:51
Performance of pre-test	KFM02A and KFM02B	2007-03-27 10:30 – 2007-05-15 10:06
Flow rate increased from 20 l/min to 25 l/min	KFM02B	2007-04-03 13:15
Injection of tracers (Uranine, Li, Cs, Rb) for the main tracer test	KFM02A	2007-04-04 13:45 – 2007-04-13 01:15
Performance of main tracer test	KFM02A and KFM02B	2007-04-04 13:45 – 2007-05-15 10:06
Injection of synthetic groundwater (rinsing) to maintain the 1/100 dipole	KFM02A	2007-04-03 16:03 – 2007-04-04 13:41 2007-04-13 09:50 – 2007-05-15 10:00
Stop pumping	KFM02B	2007-05-15 10:06

4.4.2 Pumping and interference test

The pumping was performed as a constant flow rate pumping test with a flow rate of 19.8 l/min during the pre-test. Before the main tracer test started, the flow rate was increased and then kept at 24.8 l/min due to a somewhat lower tracer recovery than expected in the pre-test. The pumping was followed by a pressure recovery period. The data logger sampled data at a suitable frequency determined by the operator, see Table 4-3. The pressure interference was recorded in a total of 115 sections in 31 observation boreholes, both core- and percussion-drilled boreholes, all part of the HMS (Hydro Monitoring System).

Approximate sampling intervals for flow rate and pressure in the pumping borehole KFM02B are presented in Table 4-3. During the first hours of pumping the sampling frequency was adjusted manually and Table 4-3 shows only the changes of frequency intervals. The interval was shortened during certain periods, for example when the withdrawal rate was increased.

After the stop of pumping the sampling frequency was automatically changed in accordance with Table 4-3.

The observation sections are either fitted with permanently installed equipment or with removable miniTroll transducers equipped with an attached logger for measuring pressure in the different sections. The miniTroll transducers recorded a pressure value with the standard frequency of one reading every two hours. In addition, logging was done whenever there was a pressure change of at least 0.1 m since the last logging. The permanent installations were set to automatically measure once every 5 minutes and store a value every 30 minutes as well as at a pressure change of 0.01 m. During the first 24 hours in connection with pump start or stop, the logging frequency was further increased.

4.4.3 Tracer tests

Prior to the main tracer test a pre-test was performed. The injection of synthetic groundwater with tracer (50 ppm Rhodamine WT) started after 6 days of pumping in KFM02B. The performance of the test (including the injection procedure) was similar to the main tracer test and is further described below. After the injection of tracer, the pumping rate was increased to 24.8 l/min and synthetic groundwater was injected at 250 ml/min to maintain the 1/100 dipole until the injection of tracers for the main test started (also 250 ml/min). Sampling and analyses for RdWT was continued also during the main tracer test to get data for the whole breakthrough curve from the pre-test.

Table 4-3. Standard sampling intervals used for pressure registration during the pumping test.

Time interval (s) from start/stop of pumping	Sampling interval (s)
1–300	1
301–600	10
601–30,600	60
> 3,600	300
> 3,600 [1)]	600

[1)] The 600 s sampling interval was used during recovery instead of the 300 s interval.

The tracer injections were performed as c one week continuous injections with a small excess pressure created by the injection flow. However, during the initial time period tracer was injected through an "exchange" procedure, i.e. water was also withdrawn from the section during the tracer injection in order to quickly exchange the ambient water with synthetic, tracer labelled water. The withdrawal from the section and the injection rate were balanced to keep a net injection flow rate at 1/100 of the flow in KFM02B. For practical reasons it was difficult to achieve the desired net inflow during the "exchange" procedure as can be seen in Table 4-4, where injection rates and times are presented. This "exchange" procedure continued for a time equal to the time required for circulation of one section volume, i.e. 1.5–2 hours. After the initial exchange, the tracer injection continued for about a week and after that synthetic groundwater was injected at the same rate to maintain the 1/100 dipole.

For practical reasons, the injection flow was not stable during the entire continuous injection, which means the rates in Table 4-4 are only approximate mean values. The actual flow was measured using a flow meter connected to the logger, and these are the flow data that should be considered for the evaluation. The injection pump stopped at a few occasions during the test and the dates and times for the stops are presented in Table 5-11 (pre-test) and Table 5-12 (main tracer test) in Section 5.4. The concentrations of the tracers are presented in Table 3-1 in Section 3.3.2.

A simple and reasonable assumption is that the amount of tracer that leaves the injection section (and into the transport path) is proportional to the tracer concentration in the injection section. Samples were continuously withdrawn from the injection section to monitor the tracer injection versus time. Samples were also continuously collected from KFM02B and analysed for tracer breakthrough.

Table 4-4. Injection rates and times.

	Unit	Pre-test	Main tracer test
Circulation rate	(l/h)	22	28
Net inflow during "exchange"	(ml/min)	**160**	**225**
Rate in during "exchange"	(ml/min)	300	485
Rate out during "exchange"	(ml/min)	140	260
Injection rate during continuous injection	(ml/min)	200	250
"Exchange" duration time	(min)	117	92
Total injection time	(min)	10,101	12,930

The samples were analysed for dye tracer content at the Geosigma Laboratory using a Jasco FP 777 Spectrofluorometer. The samples to be analysed for metals (Li, Cs and Rb) were sent to ALS Scandinavia laboratory in Luleå for analysis (using ICP-AES and ICP-SFMS).

The samples were withdrawn more often during the beginning of the test period. During most of the test, a sample was retrieved every hour and every two hours from KFM02A in the pre-test and main tracer test, respectively, and from KFM02B every three hours. The exact sampling frequency is presented in Table 4-5.

4.4.4 Water sampling

Water samples submitted for analyses according to SKB class 3 were taken during the pumping test. Three samples were collected, one immediately after pumping start, one after about three weeks of pumping and one at the end of the pumping, one day before the pumping was stopped. A fourth sample was taken from the tap water that was used to prepare the synthetic groundwater. Table 4-6 presents the date and time when the samples were taken together with the SKB sample number.

Table 4-5. Sampling frequency during the tracer tests.

Pre-test			Main tracer test		
Time after injection start	Sample interval (min) KFM02A	KFM02B	Time after injection start	Sample interval (min) KFM02A	KFM02B
During “exchange”	10		During “exchange”	5	
After ”exchange”	60		< 2 h	30	
			> 19 h	120	
0–2h		10			
2–4h		20	0–20 h		30
4–24 h		30	20–47 h		60
>24 h		180	> 47 h		180

Table 4-6. SKB class 3 water samples taken during the pumping test in KFM02B.

Bh ID	Date and time of sample	Pumped section (mbl)	Pumped volume ($m^{3)}$	Sample type	Sample ID no	Remarks
KFM02B	2007–03–21 13:05	408.5–434.0	0.1	WC080	12730	
KFM02B	2007–04–10 13:34	408.5–434.0	621	WC080	12754	
KFM02B	2007–05–14 11:20	408.5–434.0	1832	WC080	12755	
	2007–05–14 12:51			WC109	12756	Tap water

4.5 Data handling

Data were downloaded from the logger (Campbell CR 5,000) to a laptop with the program PC9,000 and were already in the logger transformed to engineering units. All files (*.DAT) were comma–separated when copied to the computer.

The results from the laboratory analyses were compiled in an Excel-file together with sample date for further processing, plotting and calculations.

4.6 Analysis and interpretation

4.6.1 Groundwater flow measurements

In the dilution method, a tracer is introduced and homogeneously distributed into a borehole test section. The tracer is subsequently diluted by the ambient groundwater flowing through the borehole test section. The dilution of the tracer is proportional to the water flow through the borehole section and the groundwater flow is calculated from the rate with which the tracer concentration decreases with time, Figure 4-2.

Flow rates were calculated from the decay of tracer concentration versus time through dilution with natural unlabelled groundwater, cf. /Gustafsson 2002/. The so-called "dilution curves" were plotted as the natural logarithm of concentration versus time. Theoretically, a straight-line relationship exists between the natural logarithm of the relative tracer concentration (c/c_0, where c_0 is the initial concentration) and time, t (s):

$$\ln (c/c_0) = -(Q_{bh}/V) \cdot \Delta t \qquad (4\text{-}3)$$

where Q_{bh} (m^3/s) is the groundwater flow rate through the borehole section and V (m^3) is the volume of the borehole section. By plotting ln (c/c_0) or ln c versus t, and by knowing the borehole volume V, Q_{bh} may then be obtained from the straight-line slope.

The sampling procedure with a constant flow of 4–10 ml/h also creates a dilution of tracer. The sampling flow rate is therefore subtracted from the value obtained from Equation 4-3.

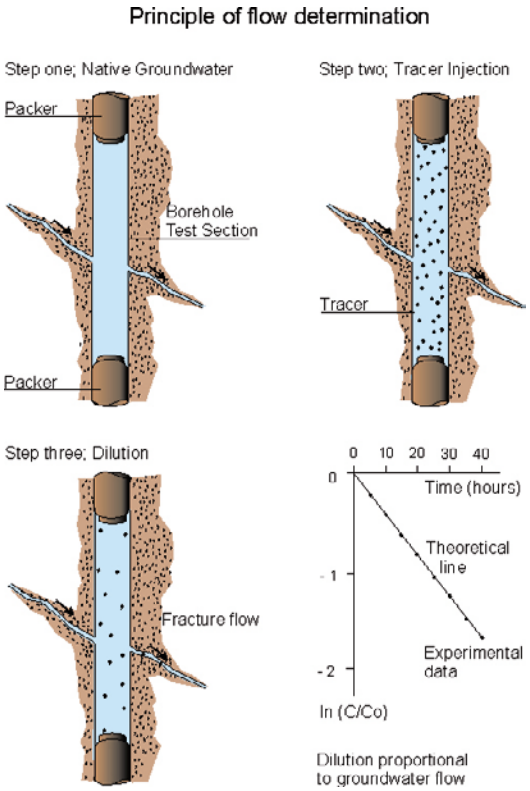

Figure 4-2. *General principles of dilution and flow determination.*

4.6.2 Pumping- and interference test

Qualitative and quantitative analyses have been carried out in accordance with the methodology descriptions for interference tests, SKB MD 330.003, and are reported in Section 5.3 below. Methods for constant-flow rate tests in an equivalent porous medium were used for the analysis and interpretation of the tests.

The main objective of the interference test was to document how different fracture zones are connected hydraulically, to quantify their hydraulic properties and to clarify whether there are any major hydraulic boundaries in the area. Quantitative evaluation of observation sections with a clear response to the pumping was also included. A total of 18 sections were analysed with regard to transmissivity and storativity. Other borehole sections included in the interference tests were only qualitatively analysed, mainly by means of the response analysis reported in Section 5.3.2 below. The borehole sections involved in the interference test that showed none or a very weak and/or uncertain response are not included in the response analyses but some of the sections with possible but very weak response are discussed in Appendix 6.

Data from all available observation sections were used in the primary qualitative analyses. The qualitative analysis of the responses on the interference test in KFM02B was primarily based on time versus pressure diagrams together with response diagrams. Linear diagrams of pressure versus time for all test sections are presented in Appendix 6. For the 18 observation sections where unambiguous transient evaluation was possible the dominating flow regimes (pseudo-linear, pseudo-radial and pseudo-spherical flow, respectively) and possible outer boundary conditions were identified. In particular, pseudo-radial flow is reflected by a constant (horizontal) derivative in the diagrams, whereas no-flow and constant-head boundaries are characterized by a rapid increase and decrease of the derivative, respectively.

Varying values were applied for the filter coefficient (step length) in the calculation of the pressure derivative in order to investigate the effect of this coefficient on the derivative. It is desirable to achieve maximum smoothing of the derivative without altering the original shape of the data series.

In addition, the response in the pumping borehole KFM02B was evaluated as a single-hole pumping test according to the methods described in /Almén et al. 1986/.

The quantitative transient analysis was performed by a special version of the test analysis software AQTESOLV that enables both visual and automatic type curve matching. The transient evaluation was carried out as an iterative process of type curve matching and automatic non-linear regression. The quantitative, transient interpretation of the hydraulic parameters (transmissivity and storativity) is normally based on the identified pseudo-radial flow regime during the tests in log-log and lin-log data diagrams. For the single-hole pumping test in KFM02B the storativity was calculated using an empirical regression relationship between storativity and transmissivity /Rhén et al. 1997/:

$$S = 0.0007 \cdot T^{0.5} \qquad (4\text{-}4)$$

where S is the storativity (–) and T is transmissivity (m^2/s).

First, the transmissivity and skin factor were obtained by type curve matching on the data curve using a fixed storativity value of 10–6 according to the instruction SKB MD 320.004. From the transmissivity value obtained, the storativity was then calculated according to Equation 4-4 and the type curve matching was repeated. In most cases the change of storativity does not significantly alter the calculated transmissivity by the new type curve matching. Instead, the estimated skin factor, which is strongly correlated to the storativity using the effective borehole radius concept, is altered correspondingly.

4.6.3 Tracer test

The concentration in the borehole at a certain time is reflected in the sample a short time later, since there is a delay caused by the transport time through the hoses from the section to the sample bottle/tube. Hence, the elapsed time must be corrected for the water residence time in the hoses. This can be done when the volume of the hoses and the flow rate is known. The corrected elapsed time was calculated for both KFM02A and KFM02B before plotting concentrations against elapsed time and evaluating the data. The elapsed time is always referred to as the time since injection start.

Since the injection flow was not constant (and hence not the concentration in KFM02A either) a function of normalized mass flux against elapsed time had to be created as an input function for the model analysis. When normalising the mass flux it is also possible to plot the data from all tracers in the same scale. The data from the breakthrough curves were also calculated and presented as normalized mass flux. The procedure for calculating the normalized mass flux is further described in Appendix 4.

The total mass of tracer recovered was then calculated by integration of the breakthrough curves for mass flux in KFM02B. Comparing the calculated total injected mass in KFM02A (M_A) with the total mass detected in KFM02B (M_B) gives the mass recovery.

$$Recovery\ (\%) = \frac{M_B}{M_A} \cdot 100 \qquad (4\text{-}5)$$

Assumptions

- Complete mixing is assumed in the section in KFM02A.
- The groundwater flow that was measured in KFM02A during pumping is expected to be proportional to the withdrawal rate. Hence, when the withdrawal rate was increased by 20% from (19.8 l/min to 24.8 l/min) the induced groundwater flow in KFM02A is assumed to increase from 15 ml/min to 18 ml/min.
- During the stop of the injection pump, the flow out of the injection section in KFM02A into the rock formation, is assumed to equal the measured groundwater flow in the section.
- The recovery of tracers was calculated assuming a constant withdrawal rate in KFM02B (or for Rhodamine WT in the pre-test, two different constant flow rates).

Modelling

The tracer breakthrough curves were evaluated using the one-dimensional transport models described in Section 3.5. Estimation of model parameters was accomplished by employing non-linear regression as outlined in Section 3.5.

Estimation parameters comprise tracer residence time (for non-sorbing tracers), Peclet number and a fracture retardation factor for sorbing tracers. For the matrix diffusion model, a composite matrix diffusion parameter (Equation 3-16) was estimated as well.

As a possible additional estimation parameter, a proportionality factor (*pf*) may be used. The parameter *pf* is simply a multiplying factor for the simulated tracer breakthrough curve. Alternatively, this parameter may be set a fixed value. With the assumptions made for calculation of normalised mass flux for injection and sampling, as described above, the value of *pf* is 1.0 at 100% tracer recovery.

Breakthrough curves for sorbing data may be estimated simultaneously with non-sorbing tracers or, alternatively, a sequential approach may be employed.

Estimation parameters comprise tracer residence time (for non-sorbing tracers), Peclet number and a fracture retardation factor for sorbing tracers. For the matrix diffusion model, a composite matrix diffusion parameter (Equation 3-16) was estimated as well.

As a possible additional estimation parameter, a proportionality factor (*pf*) may be used. The parameter *pf* is simply a multiplying factor for the simulated tracer breakthrough curve. Alternatively, this parameter may be set a fixed value. With the assumptions made for calculation of normalised mass flux for injection and sampling, as described above, the value of *pf* is 1.0 at 100% tracer recovery.

Breakthrough curves for sorbing data may be estimated simultaneously with non-sorbing tracers or, alternatively, a sequential approach may be employed.

4.7 Nonconformities

- The injection pump stopped at several occasions and the reason for this is not clear.
- There was a power failure at one occasion. Only the automatic equipment sampling the pumped water from KFM02B was affected. Since it occurred at the end of the test when the temporal changes in concentration were very small, the samples had no effect on the evaluation of the experimental data.
- The peristaltic pump used for the carbonate solution (solution C) gave c 20% more at the check after the end of the tracer test than it did at the calibration prior to the test. This means that for part of the test, the carbonate concentration was somewhat higher than intended.
- Two of the boreholes that, in the Activity Plan, were intended to be included in the interference test did not, for various reasons, provide any pressure data and were therefore excluded. These boreholes are HFM14 and HFM25.
- The head responses in several of the investigated boreholes were disturbed by a separate pumping in borehole KFM08D starting 2007-03-17 12:10 and ending 2007-03-23 22:34. The flow rate during this pumping was about 72 l/min.

5 Results

Original data from the reported activity are stored in the primary database Sicada. Data are traceable in Sicada by the Activity Plan number (AP PF 400–07–013). Only data in databases are accepted for further interpretation and modelling. The data presented in this report are regarded as copies of the original data. Data in the databases may be revised, if needed. However, such revision of the database will not necessarily result in a revision of this report, although the normal procedure is that major data revisions entail a revision of P-reports. Minor data revisions are normally presented as supplements, available at www.skb.se.

5.1 Nomenclature and symbols

The nomenclature and symbols used for the results of the single-hole and interference test are according to the Instruction for analysis of single-hole injection- and pumping tests (SKB MD 320.004) and the method description for interference tests (SKB MD 330.003), respectively (both are SKB internal controlling documents). The same applies for nomenclature and symbols used for the results from groundwater flow measurements and tracer tests which are carried out according to the method descriptions SKB MD 368.010 and SKB MD 530.006, respectively (SKB internal controlling documents). Additional symbols used are explained in the text.

Since the pressure in the boreholes are given in terms of groundwater levels by HMS, both the terms “pressure” and “groundwater level” are used to explain the hydraulic conditions in the boreholes. Also, the term (hydraulic) “head” is used synonymously to “groundwater level”.

5.2 Groundwater flow measurements

The results obtained are presented in Table 5-1 including measured groundwater flow rates together with transmissivity and volume for the section. In Figure 5-1, the tracer dilution curve in KFM02A is shown. The flow rate is calculated from the slope of the straight-line fit. A clear and immediate influence of the pumping in KFM02B can be observed.

In Appendix 5, the groundwater level during the entire test period is shown; see also Table 4-2 for actual measurement periods.

Table 5-1. Measured groundwater flow in KFM02A:5.

Borehole section	Borehole length (mbl)	Transmissivity (m^2/s)	Volume (l)	Measured flow (ml/min) Natural gradient	Measured flow (ml/min) Stressed gradient
KFM02A:5	411–442	2.5 E–6*	60.78	0.65	15.0

* From PSS measurements, transient evaluation, /Källgården et al. 2004/.

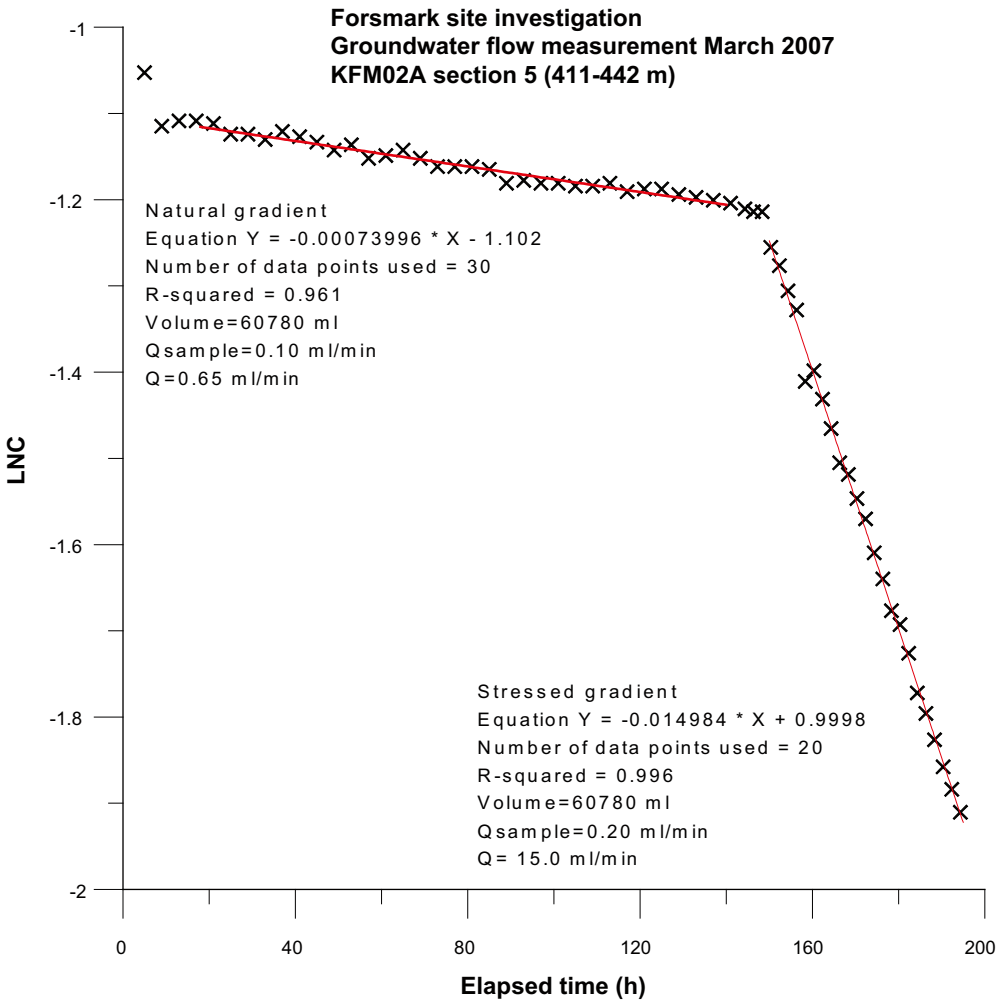

Figure 5-1. *The tracer dilution graph (logarithm of concentration versus time) for borehole KFM02A, Section 5, including straight-line fits during both natural and pumped conditions.*

5.3 Pumping test and interference test

All observation rock boreholes included in the interference test and their approximate distances to the pumping borehole KFM02B are marked in Figure 5-2. The flow rate and pressure in the pumping borehole are shown in Figure 5-3. Linear diagrams of groundwater level versus time in all responding observation boreholes from the pumping in KFM02B are presented in Figures A6-2 through A6-13 in Appendix 6. There were also 56 monitoring wells in soil within the 2 km radius in 26 of which pressure registration was performed during the time of the test. None of the soil boreholes showed any responses to the pumping. Observation boreholes HFM14 and HFM25, originally intended to be included in the interference test, did not provide any pressure data and are therefore excluded.

Visual inspection of the pressure responses in the observation sections indicates that significant responses were registered in c 22% of the 115 observation sections included in the interference test (Figures A6-2 through A6-13 in Appendix 6). 90 of the sections were apparently unaffected during the interference test, but 9 of them were uncertain and it cannot be decided whether they were affected or not. The drawdown (sp) at the end of the flow period together with the estimated response lag times (dtL) in all observation sections with a detected response are shown in Tables 5-7 and 5-8. The response time is here defined as the lag time after start of pumping until a drawdown response of 0.1 m was observed in the actual observation section. In addition, the corresponding response times were also determined at a drawdown response of 0.01 m.

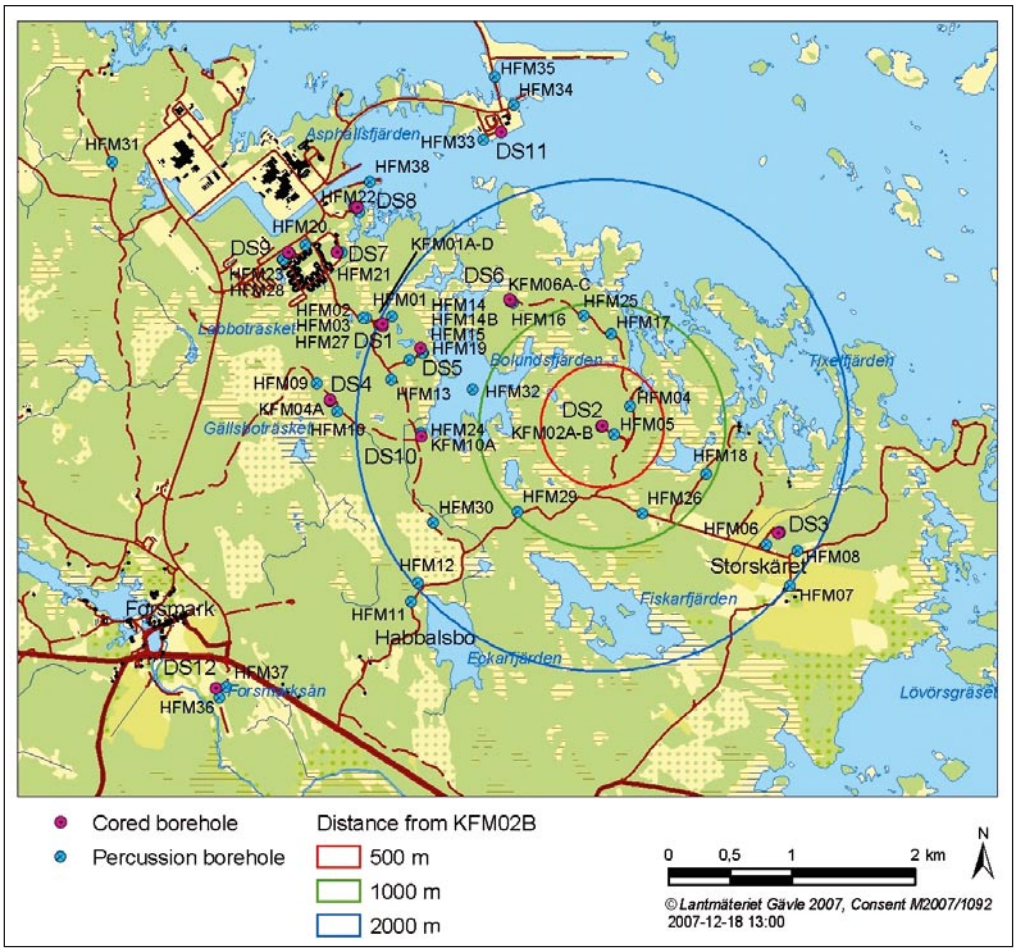

Figure 5-2. *Locations of percussion boreholes and drill sites in the Forsmark investigation area.*

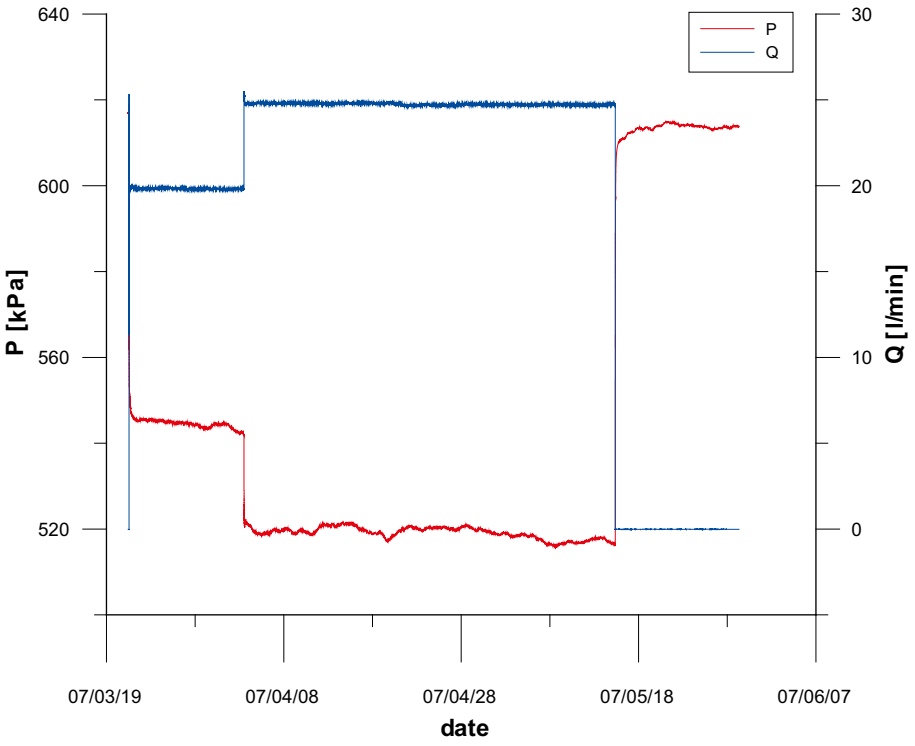

Figure 5-3. *Linear plot of flow rate (Q) and pressure (P) versus time in the pumping borehole KFM02B.*

Figure 5-3 below shows the pressure and the flow rate in KFM02B during the pumping test. Standard transient evaluation of responses was made for the pumping section and the observation sections in which pressure interference was detected. In Appendix 6 general test data and comments on the tests are presented, whereas the test diagrams are exposed in Appendix 7.

All pressure data from the observation boreholes presented in this report have been corrected for atmospheric pressure changes by subtracting the latter pressure from the measured (absolute) pressure. Corrections for the natural decreasing head trend has also been done in the observation sections as discussed below. No other corrections of the measured drawdown due to e.g. precipitation, tidal effects etc have been made.

During the interference test approximately 50 mm of total precipitation (of which c 20 mm during the flow period) was reported at two stations in the vicinity of the boreholes included in the test, see Figure A7-81. The rain that fell just before stop of pumping and during the recovery period may in some boreholes have influenced the pressure in the observation boreholes. In Figure A7-81, the air pressure together with the sea-water level during the interference test period, as recorded from a station in the vicinity of the investigation area, are also included.

There are strong indications of a natural trend of decreasing groundwater levels during the entire interference test period. At the end of the recovery period, the levels in many observation sections had not returned to those prevailing prior to start of pumping. In some boreholes the decreasing natural trend continued at the end of the recovery period. An example of this effect can be observed in Figure 5-4 (also named Figure A6-3 in Appendix 6).

When a natural trend was observed, the head data were corrected prior to the transient analysis. Corrected head and drawdown data for the natural trend are presented together with the test diagrams in Appendix 7. The correction procedure is displayed in Appendix 8. The natural trend is generally different in each observation section.

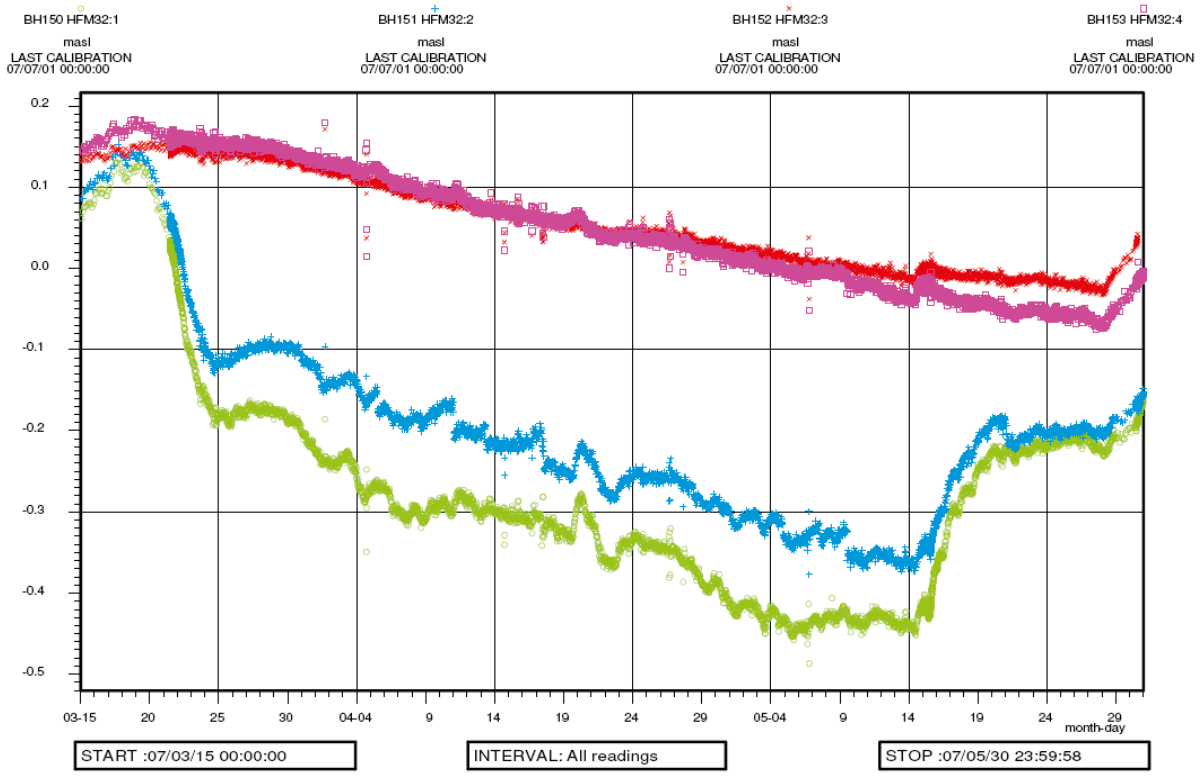

Figure 5-4. *Linear plot of observed head versus time in observation borehole HFM32 during pumping in KFM02B illustrating the natural decreasing head trend and the oscillating behaviour of the head.*

In several of the observation sections included in the interference test, the head was displaying an oscillating behaviour. This is believed to be naturally caused by so called tidal fluctuations or earth tides in combination with changes of the sea water level. These phenomena have, to some extent, been investigated previously in /Ludvigson et al. 2004d/. This effect will not be further commented on in this report.

In the transient evaluation of the responses in the pumping borehole and responding observation sections, the models described in /Hantush and Jacob 1955/, /Theis 1935/ and /Moench 1985/ respectively were used. The tests were analysed as variable flow rate tests with the transient evaluation.

The head responses in several of the investigated boreholes are disturbed by a separate pumping in borehole KFM08D starting 2007-03-17 12:10 and ending 2007-03-23 22:34. The flow rate during this pumping was about 72 l/min.

5.3.1 Summary of the results of the interference test

A compilation of measured test data from the pumping in KFM02B and the observation boreholes are shown in Tables 5-2 and 5-3 respectively. In Tables 5-4 and 5-5, calculated hydraulic parameters for the pumping borehole and the responding observation sections are presented. The evaluation of the pumping test in KFM02B is also presented in the Test Summary Sheet in Table 5-6.

Table 5-2. Summary of test data from the pumping borehole during the interference test performed in KFM02B in the Forsmark area.

Pumping borehole ID	Section (mbl)	Test type[1)]	pi (m)	pp (m)	pF (m)	Qp (m^3/s)	Qm (m^3/s)	Vp (m^3)
KFM02B	408.5–434.0	1B	616.80	516.10	613.73	4.12·10–4	3.93·10–4	1.87·103

[1)] 1B: Pumping test-submersible pump, 2: Interference test (observation borehole during pumping in another borehole).

p_i = Pressure in measuring section before start of flow.

p_p = Pressure in measuring section before flow stop.

p_F = Pressure in measuring section at end of recovery.

Q_p = Flow in test section immediately before stop of flow.

Q_m = Arithmetical mean flow during perturbation phase.

V_p = Total water volume injected/pumped during perturbation phase.

Table 5-3. Summary of test data from the observation sections involved in the interference tests performed in KFM02B in the Forsmark area.

Pumping borehole ID	Borehole ID	Section (mbl)	Test type[1)]	h_i (m)	h_p (m)	h_F (m)	h_i Corrected (m)	h_p Corrected (m)	h_F Corrected (m)
KFM02B	KFM02A:3	490.00–518.00	2	0.20	–0.61	–0.03	0.20	–0.41	0.24
KFM02B	KFM02A:4	443.00–489.00	2	0.23	–1.30	–0.02	0.23	–1.25	0.05
KFM02B	KFM02A:5	411.00–442.00	2	0.28	–6.68	–0.04	0.28	–6.63	0.11
KFM02B	KFM02A:6	241.00–410.00	2	1.27	–0.30	0.97	1.27	–0.10	1.24
KFM02B	KFM02A:7	133.00–240.00	2	0.94	0.40	0.58	0.94	0.70	0.98
KFM02B	HFM32:1	98.00–202.65	2	0.03	–0.42	–0.17	0.03	–0.29	0.00
KFM02B	HFM32:2	32.00–97.00	2	0.05	–0.34	–0.15	0.05	–0.19	0.05
KFM02B	KFM05A:5	115.00–253.00	2	0.37	0.13	0.31	1.12	0.68	1.09
KFM02B	KFM05A:6	100.07–114.00	2	0.51	0.27	0.49	0.37	0.23	0.45
KFM02B	HFM16:1	68.00–132.50	2	0.86	0.31	0.63	0.86	0.48	0.86
KFM02B	HFM16:2	54.00–67.00	2	0.88	0.36	0.68	0.88	0.51	0.88
KFM02B	HFM16:3	12.02–53.00	2	0.88	0.35	0.65	0.88	0.50	0.85
KFM02B	KFM06B:1	51.00–100.33	2	0.90	0.37	0.70	0.90	0.50	0.88
KFM02B	KFM06B:2	27.00–50.00	2	0.95	0.40	0.70	0.95	0.57	0.93
KFM02B	KFM06B:3	6.33–26.00	2	1.12	0.48	0.82	1.12	0.68	1.09
KFM02B	KFM06A:6	247.00–340.00	2	0.44	0.14	0.36	0.51	0.39	0.62
KFM02B	KFM06A:7	151.00–246.00	2	0.18	–0.06	0.10	0.44	0.20	0.38
KFM02B	KFM06A:8	100.40–150.00	2	0.36	0.16	0.29	0.18	0.01	0.12
KFM02B	HFM15:1	85.00–95.00	2	0.83	0.63	0.83	1.50	1.48	1.70
KFM02B	HFM15:2	6.00–84.00	2	0.92	0.68	0.90	0.83	0.75	0.97
KFM02B	HFM19:1	168.00–182.00	2	0.28	0.14	0.35	0.92	0.83	1.05
KFM02B	HFM19:2	104.00–167.00	2	0.76	0.63	0.79	0.28	0.24	0.44
KFM02B	HFM19:3	12.04–103.00	2	0.97	0.80	0.97	0.76	0.73	0.93
KFM02B	HFM13:1	159.00–173.00	2	0.41	0.26	0.42	0.36	0.23	0.29
KFM02B	HFM13:2	101.00–158.00	2	1.50	1.31	1.48	0.41	0.37	0.57

[1)] 1B: Pumping test-submersible pump, 2: Interference test (observation borehole during pumping in another borehole).

h_i = Level above reference level in measuring section before start of flow.

h_p = Level above reference level in measuring section before flow stop.

h_F = Level above reference level in measuring section at end of recovery.

Table 5-4. Summary of calculated hydraulic parameters from the single–hole test in KFM02B in the Forsmark area.

Pumping borehole ID	Section (mbl)	Test type	Q/s (m^2/s)	TM (m^2/s)	TT (m^2/s)	ζ (–)	C (m^3/Pa)	S* (–)
KFM02B	408.5–434.0	1B	$4.01 \cdot 10^{-5}$	$4.35 \cdot 10^{-5}$	$2.98 \cdot 10^{-5}$	–5.31	–	$2.98 \cdot 10^{-6}$

Table 5-5. Summary of calculated hydraulic parameters from the interference test between KFM02B and observation boreholes in the Forsmark area.

Pumping borehole ID	Observation borehole ID	Section (mbl)	Test type	To (m^2/s)	So (–)	To/So (m^2/s)	K'/b' (s–1)
KFM02B	KFM02A:3	490.00–518.00	2	2.69E–04	1.46E–04	1.84E+00	2.22E–10
KFM02B	KFM02A:4	443.00–489.00	2	4.29E–05	3.10E–05	1.39E+00	2.23E–09
KFM02B	KFM02A:5	411.00–442.00	2	2.48E–05	1.66E–06	1.49E+01	1.08E–10
KFM02B	KFM02A:6	241.00–410.00	2	9.60E–05	1.22E–04	7.84E–01	2.22E–10
KFM02B	KFM02A:7	133.00–240.00	2	4.66E–04	6.49E–04	7.19E–01	3.68E–10
KFM02B	HFM32:1	98.00–202.65	2	5.36E–04	1.31E–05	4.08E+01	1.83E–12
KFM02B	HFM32:2	32.00–97.00	2	7.72E–04	1.76E–05	4.39E+01	5.79E–19
KFM02B	KFM05A:5	115.00–253.00	2	1.09E–03	6.40E–05	1.70E+01	–
KFM02B	KFM05A:6	100.07–114.00	2	4.22E–04	3.75E–04	1.12E+00	–
KFM02B	HFM16:1	68.00–132.50	2	2.45E–04	9.20E–06	2.66E+01	1.23E–11
KFM02B	HFM16:2	54.00–67.00	2	1.99E–04	9.59E–06	2.08E+01	2.04E–11
KFM02B	HFM16:3	12.02–53.00	2	2.23E–04	1.02E–05	2.17E+01	1.73E–11
KFM02B	KFM06B:1	51.00–100.33	2	2.36E–04	8.61E–06	2.74E+01	1.17E–11
KFM02B	KFM06B:2	27.00–50.00	2	2.66E–04	8.65E–06	3.08E+01	9.66E–12
KFM02B	KFM06B:3	6.33–26.00	2	3.71E–04	1.04E–05	3.56E+01	9.44E–13
KFM02B	KFM06A:6	247.00–340.00	2	1.64E–04	8.40E–06	1.96E+01	4.84E–11
KFM02B	KFM06A:7	151.00–246.00	2	1.39E–04	8.27E–06	1.68E+01	8.02E–11
KFM02B	KFM06A:8	100.40–150.00	2	1.37E–04	7.81E–06	1.75E+01	1.08E–10
KFM02B	HFM15:1	85.00–95.00	2	–	–	–	–
KFM02B	HFM15:2	6.00–84.00	2	–	–	–	–
KFM02B	HFM19:1	168.00–182.00	2	–	–	–	–
KFM02B	HFM19:2	104.00–167.00	2	–	–	–	–
KFM02B	HFM19:3	12.04–103.00	2	–	–	–	–
KFM02B	HFM13:1	159.00–173.00	2	–	–	–	–
KFM02B	HFM13:2	101.00–158.00	2	–	–	–	–

$Q/_s$ = specific flow for the pumping/injection borehole.

T_M = steady state transmissivity from Moye´s equation.

T_T = transmissivity from transient evaluation of single–hole test.

T_o = transmissivity from transient evaluation of interference test.

S_o = storativity from transient evaluation of interference test.

T_o/S_o = hydraulic diffusivity (m^2/s).

K'/b' = leakage coefficient from transient evaluation of interference test.

S* = assumed/calculated storativity from estimation of the skin factor.

C = wellbore storage coefficient.

ζ = skin factor.

Table 5-6. Test Summary Sheet – Pumping test in KFM02B

Test Summary Sheet – Pumping section KFM02B: 408.5–434.0 mbl			
Project:	PLU	Test type:	1B
Area:	Forsmark	Test no:	1
Borehole ID:	KFM02B	Test start:	2007-03-21 13:00
Test section (mbl):	408.5–434.0	Responsible for test performance:	GEOSIGMA AB
Section diameter, 2·rw (m):	0.152	Responsible for test evaluation:	GEOSIGMA AB J-E Ludvigson

Linear plot pressure – Entire test period

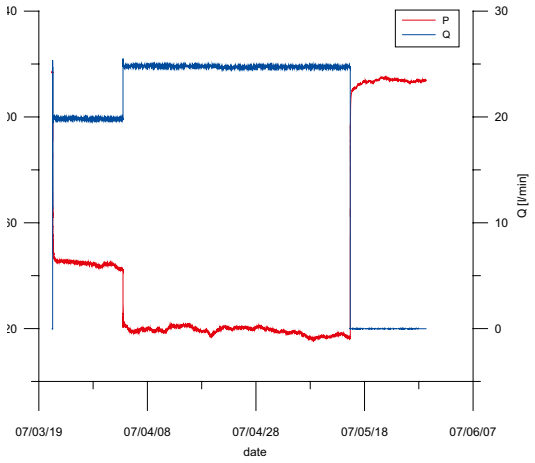

Flow period		**Recovery period**	
Indata		**Indata**	
p_0 (kPa)			
p_i (kPa)	616.80		
p_p(kPa)	516.10	pF (kPa)	613.73
Q_p (m^3/s)	$4.12 \cdot 10^{-4}$		
tp (s)	4737960	tF (s)	1205040
S*	$2.98 \cdot 10^{-6}$	S*	$3.39 \cdot 10^{-6}$
EC_w (mS/m)			
Te_w(gr C)			
Derivative fact.	0.2	Derivative fact.	0.2
Results		**Results**	
Q/s (m^2/s)	$4.01 \cdot 10^{-5}$		

Log-Log plot incl. derivate – Flow period

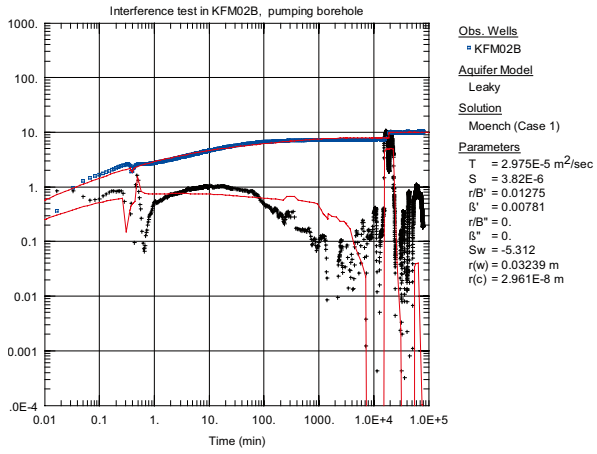

T_{Moye}(m^2/s)	**$4.35 \cdot 10^{-5}$**		
Flow regime:	PLF–>PRF–>PSF	Flow regime:	PLF–>PRF–>PSF
t_1 (s)	180	dt_{e1} (s)	120
t_2 (s)	1800	dt_{e2} (s)	2400
T_w (m^2/s)	$2.98 \cdot 10^{-5}$	T_w (m^2/s)	$2.31 \cdot 10^{-5}$
S_w (–)		S_w (–)	
K_{sw} (m/s)		K_{sw} (m/s)	
S_{sw} (1/m)		S_{sw} (1/m)	
C (m^3/Pa)	–	C (m^3/Pa)	–
CD (–)		CD (–)	
ξ (–)	–5.31	ξ (–)	–5.68
T_{GRF} (m^2/s)		T_{GRF} (m^2/s)	
S_{GRF} (–)		S_{GRF} (–)	
D_{GRF} (–)		D_{GRF} (–)	

Log-Log plot incl. derivative – Recovery period

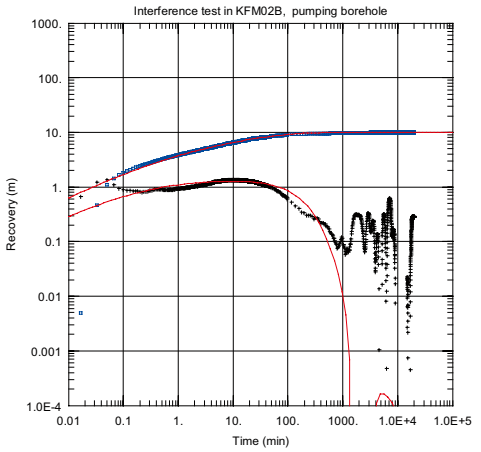

Interpreted formation and well parameters.

Flow regime:	PLF–>PRF –>PSF	C (m^3/Pa)	
t1 (s)	180	CD (–)	
t2 (s)	1800	ξ (–)	–5.31
TT (m^2/s)	2.98·10–5		
S (–)			
Ks (m/s)			
Ss (1/m)			

Comments: After initial pseudo-linear flow, pseudo-radial flow occurred between c 3–30 min during the flow period and c 2–40 min during the recovery period. A transition to pseudo-spherical (leaky) flow occurred by the end during both the flow- and recovery period. The flow rate was increased after c 19,000 min during the flow period. Transient evaluation was based on variable flow rate. The agreement in evaluated parameter values between the flow and recovery period is good. The parameter values from the flow period are selected as the most representative.

5.3.2 Response analysis and estimation of the hydraulic diffusivity of the response sections

A response analysis according to the method description for interference tests was made. All obtained results from evaluated responses are included in the response analysis. However, since only one interference test was performed, no response matrix was made. The response lag times (dtL) in the observation sections during pumping in KFM02B are shown in Table 5-7 and Table 5-8. The lag times were derived from the corrected drawdown curves in the observation borehole sections at actual drawdowns of 0.01 m and 0.1 m, respectively.

Because of disturbances, e.g. oscillating head or hydraulic responses to other activities in the area, see for instance Figure 5-4, it was sometimes difficult to determine the exact time for the occurrence of a specific drawdown. It was possible, however, to make approximate estimates from the drawdown curves. For the sections where a drawdown of 0.1 m was not achieved, only the lag time derived from the 0.01 m drawdown is presented.

In Tables 5-7 and 5-8 all sections with detected responses are included. The normalized response time with respect to the distance to the pumping borehole (dt_L/r_s^2/) was calculated. This time is inversely related to the hydraulic diffusivity (T/S) of the formation. The inverse of (dt_L/r_s^2/) was also calculated since it is more closely related to the hydraulic diffusivity. In addition, the normalized drawdown with respect to the flow rate was calculated and is presented in Table 5-9.

Figure 5-5a and 5-5b show response diagrams of the responding observation sections. The figures are based on lag times of 0.1 m and 0.01 m, respectively. In the response diagrams, observation sections represented by data points in the upper left corner generally indicate a better connectivity with the pumping borehole section and a higher hydraulic diffusivity than sections represented by data points in the bottom right corner in the diagram.

The following parameters are used in Tables 5-7 – 5-10 as well as in Figures 5-5 – 5-7:

$dt_{L\,[s=0.1\ m]}$ = time after start of pumping (s) at a drawdown s=0.1 m in the observation section. Drawdown data corrected for the natural decreasing head trend are used.

$dt_{L\,[s=0.1\ m]} / r_s^2$ = normalized response time with respect to the distance r_s (s/m^2).

$dt_{L\ [s=0.01\ m]}$ = time after start of pumping (s) at a drawdown s=0.01 m in the observation section. Drawdown data corrected for the natural decreasing head trend are used.

dtL [s=0.01 m] / rs2 = normalized response time with respect to the distance rs (s/m^2).

r_s = 3D-distance between the hydraulic point of application (hydr. p.a.) in the pumping borehole and observation borehole (m).

s_p = drawdown at stop of pumping in the actual observation borehole/section (m).

s_{p_corr} = drawdown at stop of pumping in the actual observation borehole/section (m). Drawdown data corrected for the natural decreasing head trend are used.

Q_p = pumping flow rate by the end of the flow period (m^3/s).

s_p/Q_p = normalized drawdown with respect to the pumping flow rate (s/m^2).

s_{p_corr}/Q_p = normalized drawdown with respect to the pumping flow rate (s/m^2). Drawdown data corrected for the natural decreasing head trend are used.

Table 5-7. Calculated response lag times for a drawdown of 0.1 m and normalized response lag times for the responding observation sections included in the interference tests.

Pumping borehole	Observation borehole	Section (mbl)	dt_L[s=0.1 m] (s)	r_s (m)	dt_L[s=0.1 m]/r_s^2 (s/m^2)	r_s^2/dt_L[s=0.1 m (m^2/s)
KFM02B	KFM02A:3	490.00–518.00	4,200	97	0.45	2.24
KFM02B	KFM02A:4	443.00–489.00	570	66	0.13	7.64
KFM02B	KFM02A:5	411.00–442.00	18	47	0.01	122.72
KFM02B	KFM02A:6	241.00–410.00	6,000	104	0.55	1.80
KFM02B	KFM02A:7	133.00–240.00	180,000	237	3.20	0.31
KFM02B	HFM32:1	98.00–202.65	84,000	1,047	0.08	13.05
KFM02B	HFM32:2	32.00–97.00	135,000	1,080	0.12	8.64
KFM02B	KFM05A:5	115.00–253.00	3,000,000	1,480	1.37	0.73
KFM02B	KFM05A:6	100.07–114.00	3,300,000	1,525	1.42	0.70
KFM02B	HFM16:1	68.00–132.50	60,000	1,205	0.04	24.20
KFM02B	HFM16:2	54.00–67.00	63,000	1,219	0.04	23.59
KFM02B	HFM16:3	12.02–53.00	66,000	1,225	0.04	22.74
KFM02B	KFM06B:1	51.00–100.33	60,000	1,240	0.04	25.63
KFM02B	KFM06B:2	27.00–50.00	63,000	1,247	0.04	24.68
KFM02B	KFM06B:3	6.33–26.00	79,500	1,253	0.05	19.75
KFM02B	KFM06A:6	247.00–340.00	72,000	1,336	0.04	24.79
KFM02B	KFM06A:7	151.00–246.00	78,000	1,302	0.05	21.73
KFM02B	KFM06A:8	100.40–150.00	81,000	1,282	0.05	20.29
KFM02B	HFM15:1	85.00–95.00	3,840,000	1,605	1.49	0.67
KFM02B	HFM15:2	6.00–84.00	3,360,000	1,584	1.34	0.75
KFM02B	HFM19:1	168.00–182.00	–	1,711	–	–
KFM02B	HFM19:2	104.00–167.00	–	1,692	–	–
KFM02B	HFM19:3	12.04–103.00	–	1,659	–	–
KFM02B	HFM13:1	159.00–173.00	–	1,717	–	–
KFM02B	HFM13:2	101.00–158.00	–	1,715	–	–

Table 5-8. Calculated response lag times for a drawdown of 0.01 m and normalized response lag times for the responding observation sections included in the interference tests.

Pumping borehole	Observation borehole	Section (mbl)	dt_L[s=0.01 m] (s)	r_s (m)	dt_L[s=0.01 m]/r_s^2 (s/m^2)	r_s^2/dt_L[s=0.01 m] (m^2/s)
KFM02B	KFM02A:3	490.00–518.00	300	97	0.03	31.36
KFM02B	KFM02A:4	443.00–489.00	18	66	0.00	242.00
KFM02B	KFM02A:5	411.00–442.00	9	47	0.00	245.44
KFM02B	KFM02A:6	241.00–410.00	1,200	104	0.11	9.01
KFM02B	KFM02A:7	133.00–240.00	30,000	237	0.53	1.87
KFM02B	HFM32:1	98.00–202.65	12,000	1,047	0.01	91.35
KFM02B	HFM32:2	32.00–97.00	27000	1,080	0.02	43.20
KFM02B	KFM05A:5	115.00–253.00	660,000	1,480	0.30	3.32
KFM02B	KFM05A:6	100.07–114.00	780,000	1,525	0.34	2.98
KFM02B	HFM16:1	68.00–132.50	9,000	1,205	0.01	161.34
KFM02B	HFM16:2	54.00–67.00	9,000	1,219	0.01	165.11
KFM02B	HFM16:3	12.02–53.00	10,500	1,225	0.01	142.92
KFM02B	KFM06B:1	51.00–100.33	6,000	1,240	0.00	256.27
KFM02B	KFM06B:2	27.00–50.00	9,000	1,247	0.01	172.78
KFM02B	KFM06B:3	6.33–26.00	13,800	1,253	0.01	113.77
KFM02B	KFM06A:6	247.00–340.00	9,600	1,336	0.01	185.93
KFM02B	KFM06A:7	151.00–246.00	10,800	1,302	0.01	156.96
KFM02B	KFM06A:8	100.40–150.00	9,000	1,282	0.01	182.61
KFM02B	HFM15:1	85.00–95.00	1,500,000	1,605	0.58	1.72
KFM02B	HFM15:2	6.00–84.00	900,000	1,584	0.36	2.79
KFM02B	HFM19:1	168.00–182.00	3,240,000	1,711	1.11	0.90
KFM02B	HFM19:2	104.00–167.00	3,000,000	1,692	1.05	0.95
KFM02B	HFM19:3	12.04–103.00	3,120,000	1,659	1.13	0.88
KFM02B	HFM13:1	159.00–173.00	30,00,000	1,717	1.02	0.98
KFM02B	HFM13:2	101.00–158.00	33,00,000	1,715	1.12	0.89

Table 5-9. Drawdown and normalized drawdown for the responding observation sections included in the interference test.

Pumping borehole	Flow rate Q_p (m^3/s)	Observation borehole	Section (mbl)	s_p (m)	s_{p_corr} (m)	s_p/Q_p (s/m^2)	s_{p_corr}/Q_p (s/m^2)
KFM02B	4.12E–04	KFM02A:3	490.00–518.00	0.81	0.61	1.96E+03	1.48E+03
KFM02B	4.12E–04	KFM02A:4	443.00–489.00	1.53	1.48	3.71E+03	3.59E+03
KFM02B	4.12E–04	KFM02A:5	411.00–442.00	6.96	6.91	1.69E+04	1.68E+04
KFM02B	4.12E–04	KFM02A:6	241.00–410.00	1.57	1.37	3.80E+03	3.31E+03
KFM02B	4.12E–04	KFM02A:7	133.00–240.00	0.54	0.24	1.31E+03	5.82E+02
KFM02B	4.12E–04	HFM32:1	98.00–202.65	0.45	0.32	1.09E+03	7.77E+02
KFM02B	4.12E–04	HFM32:2	32.00–97.00	0.39	0.24	9.57E+02	5.93E+02
KFM02B	4.12E–04	KFM05A:5	115.00–253.00	0.24	0.14	5.93E+02	3.50E+02
KFM02B	4.12E–04	KFM05A:6	100.07–114.00	0.25	0.13	5.95E+02	3.04E+02
KFM02B	4.12E–04	HFM16:1	68.00–132.50	0.55	0.38	1.33E+03	9.17E+02
KFM02B	4.12E–04	HFM16:2	54.00–67.00	0.52	0.37	1.25E+03	8.88E+02
KFM02B	4.12E–04	HFM16:3	12.02–53.00	0.53	0.38	1.30E+03	9.31E+02
KFM02B	4.12E–04	KFM06B:1	51.00–100.33	0.53	0.40	1.30E+03	9.80E+02
KFM02B	4.12E–04	KFM06B:2	27.00–50.00	0.55	0.38	1.34E+03	9.31E+02
KFM02B	4.12E–04	KFM06B:3	6.33–26.00	0.64	0.44	1.54E+03	1.06E+03
KFM02B	4.12E–04	KFM06A:6	247.00–340.00	0.30	0.24	7.31E+02	5.85E+02
KFM02B	4.12E–04	KFM06A:7	151.00–246.00	0.24	0.17	5.88E+02	4.18E+02
KFM02B	4.12E–04	KFM06A:8	100.40–150.00	0.21	0.14	5.00E+02	3.30E+02
KFM02B	4.12E–04	HFM15:1	85.00–95.00	0.20	0.08	4.83E+02	1.92E+02
KFM02B	4.12E–04	HFM15:2	6.00–84.00	0.24	0.09	5.79E+02	2.16E+02
KFM02B	4.12E–04	HFM19:1	168.00–182.00	0.14	0.04	3.41E+02	9.85E+01
KFM02B	4.12E–04	HFM19:2	104.00–167.00	0.13	0.03	3.18E+02	7.52E+01
KFM02B	4.12E–04	HFM19:3	12.04–103.00	0.18	0.05	4.33E+02	1.18E+02
KFM02B	4.12E–04	HFM13:1	159.00–173.00	0.15	0.04	3.57E+02	9.00E+01
KFM02B	4.12E–04	HFM13:2	101.00–158.00	0.19	0.02	4.58E+02	4.61E+01

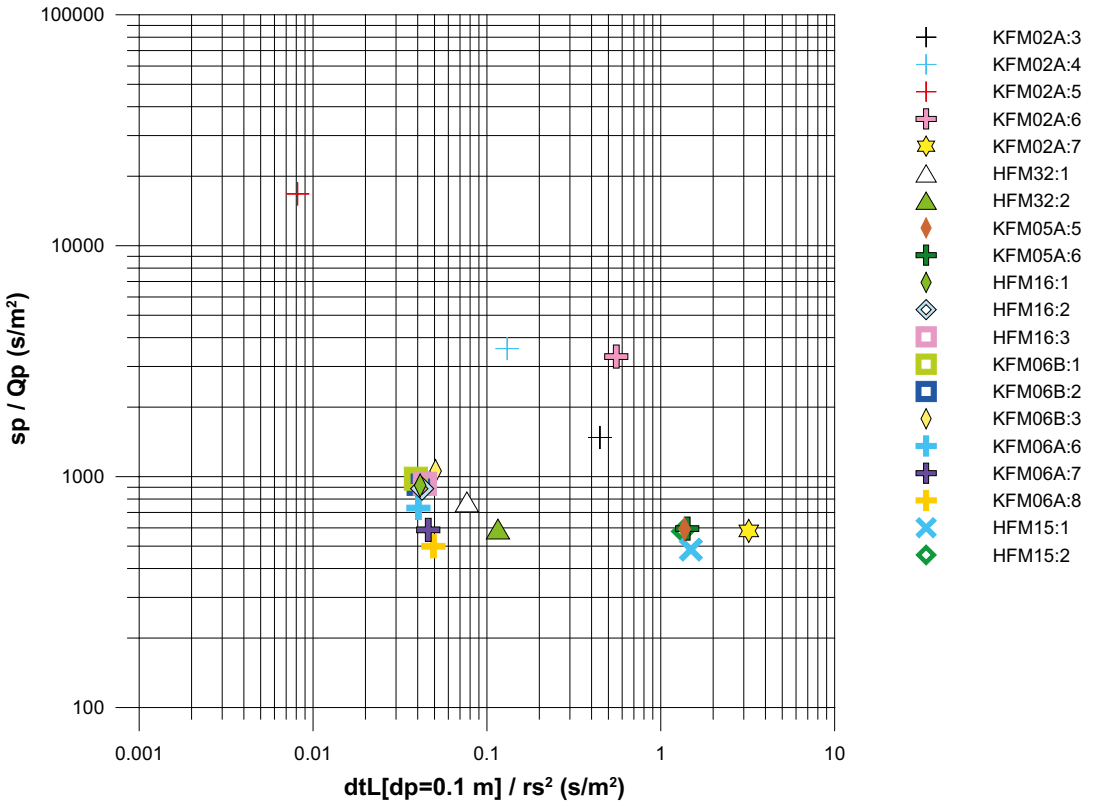

Figure 5-5a. *Response diagram showing the responses in the presumed responding observation sections during pumping in KFM02B. Lag time based on a drawdown of 0.1 m.*

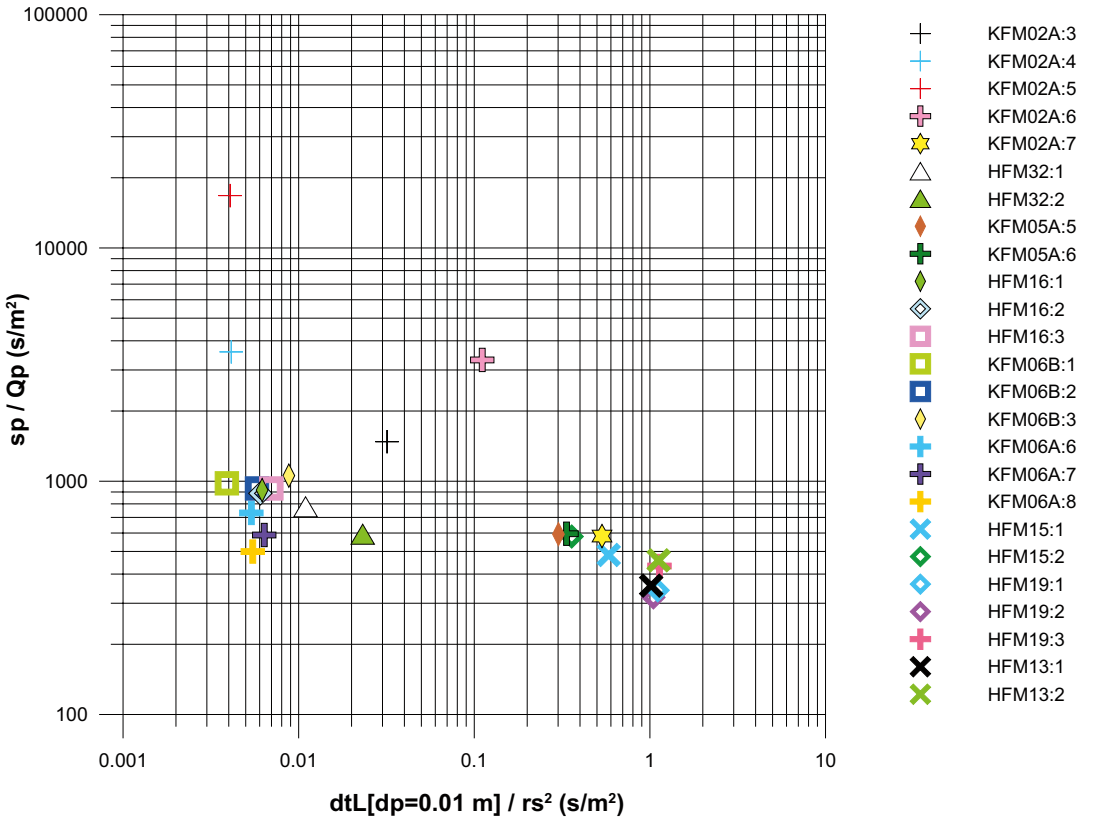

Figure 5-5b. *Response diagram showing the responses in the presumed responding observation sections during pumping in KFM02B. Lag time based on a drawdown of 0.01 m.*

Table 5-10. Estimated response lag times and hydraulic diffusivity for the observation sections from the interference test in KFM02B at Forsmark.

Pumping borehole	Observation borehole	Section (mbl)	dtL[s=0.01 m] (s)	rs (m)	T/S (m^2/s)	To /So (m^2/s)
KFM02B	KFM02A:3	490.00–518.00	300	97	0.81	1.84
KFM02B	KFM02A:4	443.00–489.00	18	66	4.85	1.39
KFM02B	KFM02A:5	411.00–442.00	9	47	4.66	14.93
KFM02B	KFM02A:6	241.00–410.00	1,200	104	0.27	0.78
KFM02B	KFM02A:7	133.00–240.00	30,000	237	0.09	0.72
KFM02B	HFM32:1	98.00–202.65	12,000	1,047	3.81	40.85
KFM02B	HFM32:2	32.00–97.00	27,000	1,080	2.08	43.94
KFM02B	KFM05A:5	115.00–253.00	660,000	1,480	0.35	17.02
KFM02B	KFM05A:6	100.07–114.00	780,000	1,525	0.33	1.12
KFM02B	HFM16:1	68.00–132.50	9,000	1,205	6.42	26.62
KFM02B	HFM16:2	54.00–67.00	9,000	1,219	6.57	20.78
KFM02B	HFM16:3	12.02–53.00	10,500	1,225	5.83	21.73
KFM02B	KFM06B:1	51.00–100.33	6,000	1,240	9.59	27.38
KFM02B	KFM06B:2	27.00–50.00	9,000	1,247	6.88	30.80
KFM02B	KFM06B:3	6.33–26.00	13,800	1,253	4.85	35.64
KFM02B	KFM06A:6	247.00–340.00	9,600	1,336	7.48	19.56
KFM02B	KFM06A:7	151.00–246.00	10,800	1,302	6.43	16.78
KFM02B	KFM06A:8	100.40–150.00	9,000	1,282	7.27	17.54
KFM02B	HFM15:1	85.00–95.00	1,500,000	1,605	0.23	–
KFM02B	HFM15:2	6.00–84.00	900,000	1,584	0.32	–
KFM02B	HFM19:1	168.00–182.00	3,240,000	1,711	0.15	–
KFM02B	HFM19:2	104.00–167.00	3,000,000	1,692	0.15	–
KFM02B	HFM19:3	12.04–103.00	3,120,000	1,659	0.14	–
KFM02B	HFM13:1	159.00–173.00	3,000,000	1,717	0.16	–
KFM02B	HFM13:2	101.00–158.00	3,300,000	1,715	0.15	–

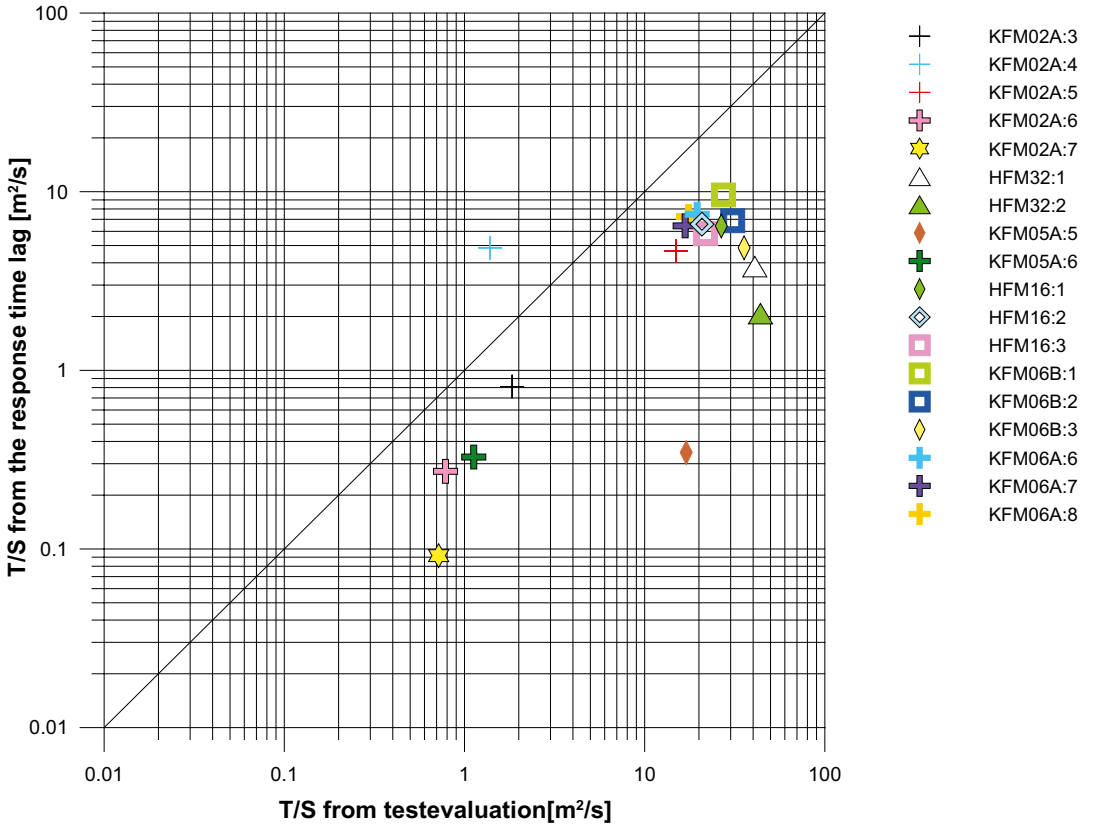

Figure 5-6. *Comparison of estimated hydraulic diffusivity, of observation sections from the interference tests in KFM02B at Forsmark.*

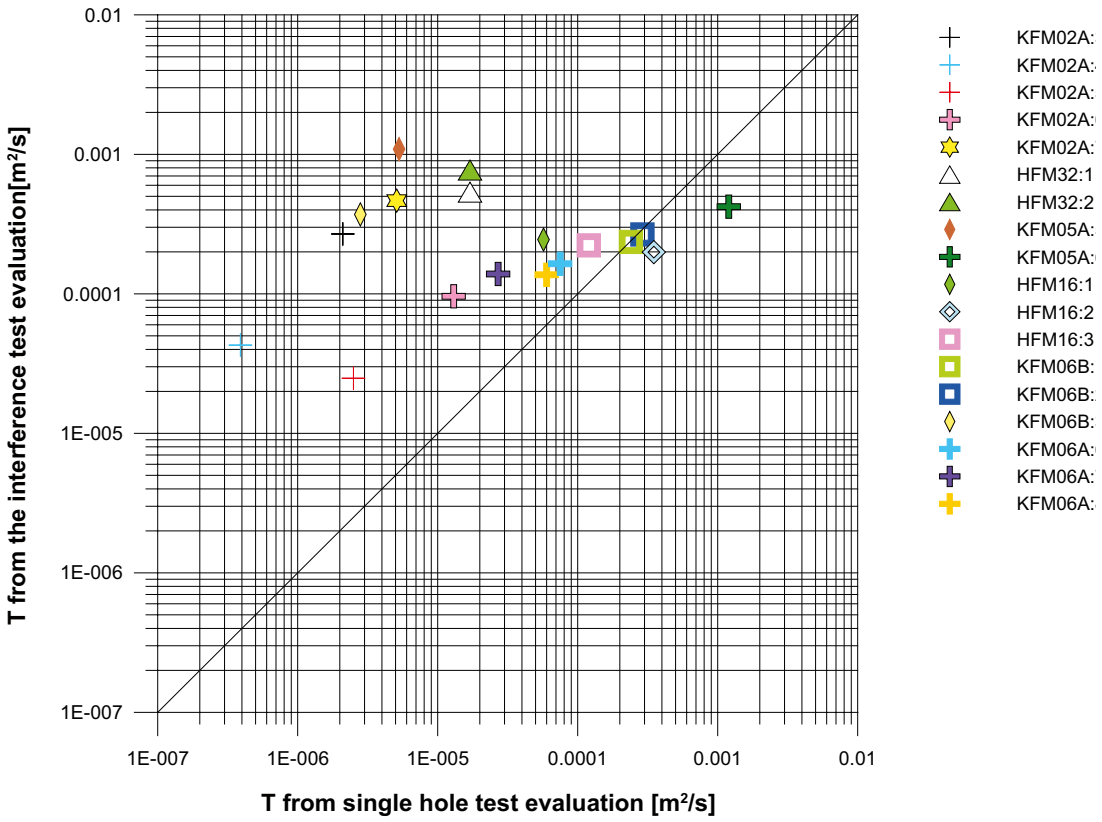

Figure 5-7. *Comparison of estimated transmissivity of observation sections from the interference test in KFM02B and previous single hole tests at Forsmark.*

The (normalized) response lag time for many of the observation sections included in the interference test, where a response was detected, must be considered as rough estimates. The main reason for this is, as mentioned above, the difficulty to make an estimate of this parameter due to the oscillating pressure and other disturbances.

The response diagrams in Figures 5-5a and 5-5b can be used to group observation sections by the strength of their responses and so the observation sections with the most distinct responses can be identified. Figure 5-5b indicates that the largest drawdown was found in section KFM02A:5 and the weakest response in section HFM19:2. The most delayed response occurred in section HFM19:3.

Some of the sections in the upper left part of Figure 5-5a and b are likely to represent sections with more or less direct responses along fracture zones between borehole KFM02B and the observations sections. Sections 3, 4, 5 and 6 in KFM02A are the sections that stand out as responding most strongly. These sections and also the observation sections in boreholes HFM32, HFM16, KFM06B, KFM05A and KFM06A show responses that are distinct enough to be characterized as potential zone responses (i.e. dominated by an adjacent zone). However, it is not certain that the zone penetrates the borehole sections directly; the sections may also be hydraulically connected to the zone via interconnecting fractures since the responses are influenced by a larger volume of rock in a long-term interference test. The observation sections in boreholes HFM13, HFM15, HFM19 and section 7 in KFM02A show weak and delayed responses and may thus be secondary (indirect) responses from the pumping in KFM02B, cf. Figure 5-5b.

The hydraulic diffusivity of observation sections can be estimated from the response lag time in the section according to Streltsova (1988):

$$T/S = r_s^2 / [4 \cdot dt_L \cdot (1+dt_L/t_p) \cdot ln(1+t_p/dt_L)] \qquad (5\text{-}1)$$

The lag times were estimated from the corrected drawdown curves as the time after start of pumping when a drawdown of 0.01 m was observed in the borehole section. The estimated lag times based on the corrected drawdown in the selected sections are shown in Table 5-10 together with the corresponding hydraulic diffusivity T/S of the sections. For comparison, the ratio of the estimated transmissivity and storativity, To/So, from the transient evaluation of the responses in these sections during the interference tests are also presented. The observation boreholes HFM13, HFM15 and HFM19 are excluded from the table since no unambiguous transient evaluation was possible in these sections.

Table 5-10 and Figure 5-6 show that there is a fair agreement between the estimated hydraulic diffusivity of the sections based on the response lag times and from the results of the transient evaluation, respectively, also at long distances from the pumping borehole. The results from the response lag time are in general, however, somewhat lower than the results from the transient evaluation.

In Figure 5-7 the discrepancies (further discussed below) between the estimated transmissivities from the interference tests and the results of the previous single-hole tests in these sections are shown. It can be noted that the interference test generally provides higher transmissivity values than the single-hole tests. This fact is assumed to be due to the inherent differences between single-hole tests and interference tests regarding test scale, duration of pumping and investigated volume of rock. Several of the deviating sections are located adjacent to a section which penetrates an interpreted zone.

5.4 Tracer tests

5.4.1 Tracer injection

The water and tracer injection procedure generally worked well. However the injection pump stopped at a few occasions both during the pre-test and the main tracer test. The times of the pump stops are presented in Table 5-11 and Figure 5-8 for the pre-test and in Table 5-12 and Figure 5-9 for the main tracer test. The pump stops are well documented and could be taken into account in the evaluation of the test. A problem was identified during the injection of the tracers when brown precipitate, presumably iron(III)-hydroxides, was observed after the inlet of the side flow of the HCO_3^--solution (Figure 3-4). The precipitation was suspected to have caused some of the pump stops during the experiment.

Several explanations for the observed precipitation may be possible. One possibility is that the injected solutions were not de-aerated enough to prevent oxidation of the Fe(II). Furthermore, occasional deviations in the flow rate of the various side flows could have caused local super-saturation of iron hydroxides.

Figure 5-10 shows the injection flow rate together with the pressure and withdrawal rate in KFM02B during the entire tracer test period (pre-test, main tracer test and rinsing).

The total volume of injected tracer solution was measured in two ways in the main tracer test. Firstly, the volume of tracer in the tank was determined by measuring the dilution of the concentrated Uranine solution added to the tank and calculating the total volume. The volume of tracer solution remaining after injection was then measured by pumping it into 25 l vessels. Secondly, the injection flow was logged by a flow meter and the total injected volume was calculated from these readings. The volumes injected during the tests are shown in Table 5-13. The total injected volume measured by the flow meter was used in all calculations and regarded as the more accurate volume. The difference in volume by the two different methods is 5%. In the pre-test the tracer volume injected was only measured by the flow meter.

Table 5-11. Injection pump stops and other major events during the pre-test.

	Date and time	Elapsed time (h)	Duration of stop (min)	Number in Figure 5-18	Comment
Injection start (tracer)	**2007-03-27 10:30**	**0**			
Injection stop (tracer)	**2007-04-03 10:51**	**168.35**			
Stop inj. Pump	2007-03-28 06:00	19.50	170	1	
Start inj. Pump	2007-03-28 08:50	22.33			
Stop inj. Pump	**2007-04-03 10:51**	**168.35**	312	2	
Withdrawal rate increase	2007-04-03 13:20	170.83			
Start inj. pump (water)	2007-04-03 16:03	173.55			Rinsing by water starts
Stop inj. pump (water)	2007-04-04 13:41	195.18	4	3	
Start inj.pump (main tracer test)	2007-04-04 13:45	195.20			The main tracer test injection starts

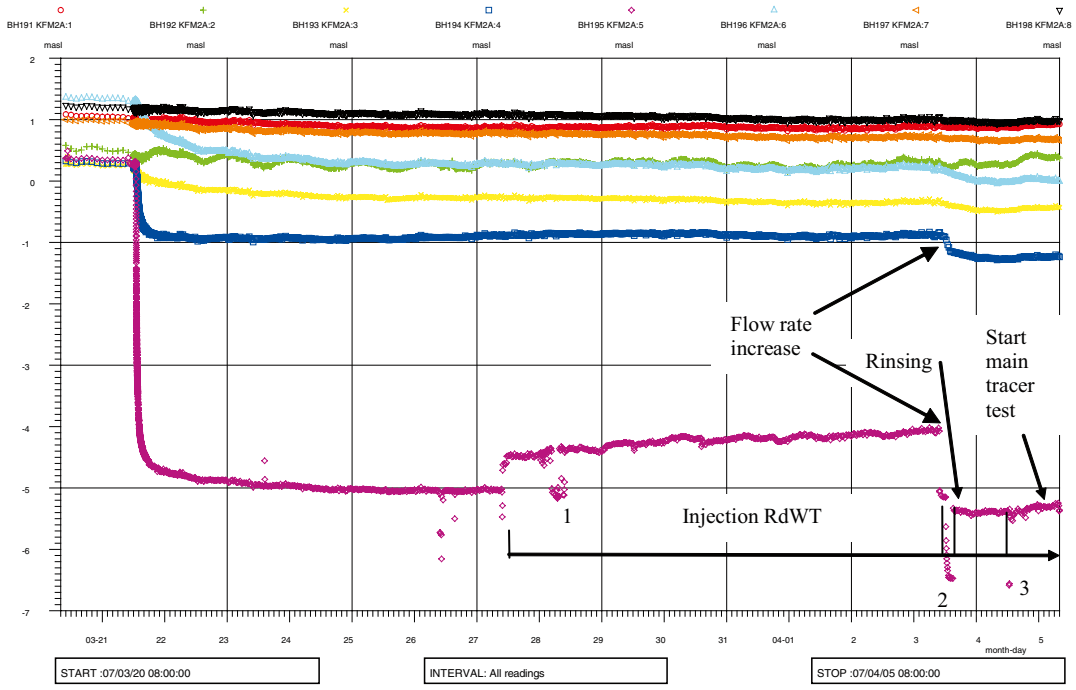

Figure 5-8. *Groundwater levels in KFM02A:5 (purple colour) and the other seven sections in KFM02A during the pre-test. The numbers refer to stops of the injection pump (also presented in Table 5-11).*

Table 5-12. Injection pump stops during the main tracer test.

	Date and time	Elapsed time (h)	Duration of stop (min)	Number in Figure 5-19	Comment
Injection start (tracer)	**2007-04-04 13:45**	**0**			
Injection stop (tracer)	**2007-04-13 01:15**	**203.50**			
Stop inj. pump	2007-04-06 06:00	40.25	325	1	
Start inj. pump	2007-04-06 11:25	45.67			
Stop inj. pump	2007-04-08 22:00	104.25	960	2	
Start inj. pump	2007-04-09 14:00	120.25			
Stop inj. pump	**2007-04-13 01:15**	**203.50**	515	3	End of tracer injection
Start inj. pump (water)	2007-04-13 09:50	212.08			Rinsing by water starts
Stop inj. pump (water)	2007-04-13 17:10	219.42	1090	4	
Start inj. pump (water)	2007-04-14 11:20	237.58			
Stop inj. pump (water)	2007-04-27 00:10	538.42	777	5	
Start inj. pump (water)	2007-04-27 13:07	551.37			
Stop inj. pump (water)	2007-04-27 14:41	552.93	11	6	
Start inj. pump (water)	2007-04-27 14:52	553.12			
Stop inj. pump (water)	2007-05-15 10:00	980.25			End of tracer test

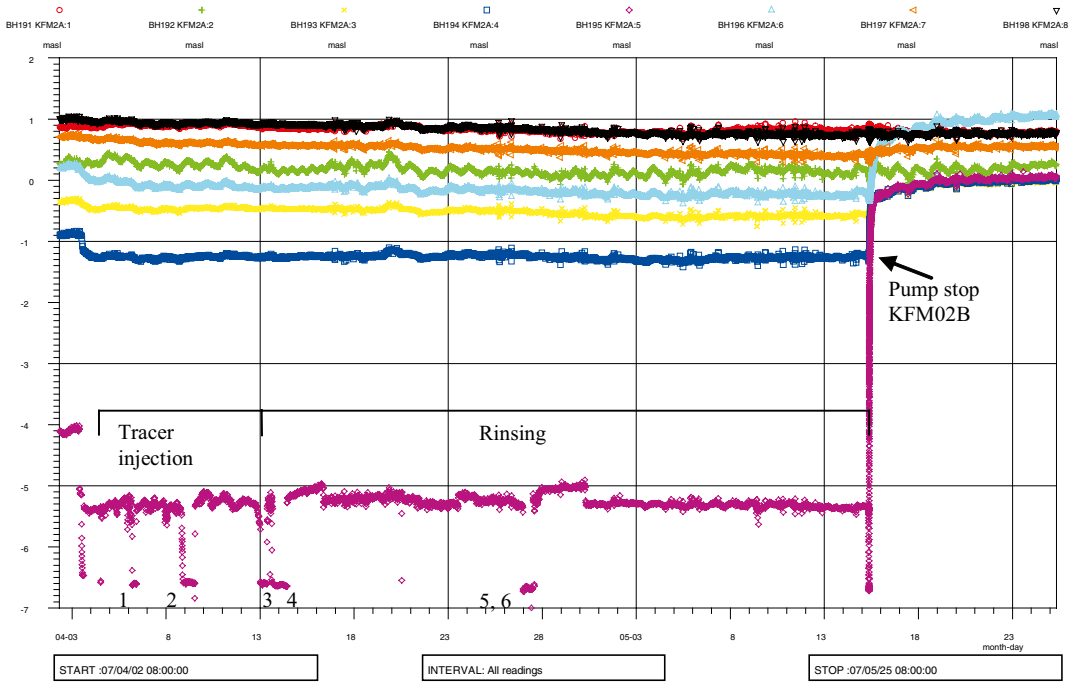

Figure 5-9. *Groundwater levels in KFM02A:5 (purple colour) and the other seven sections in KFM02A during the main tracer test. The numbers refer to stops of the injection pump (also presented in Table 5-12).*

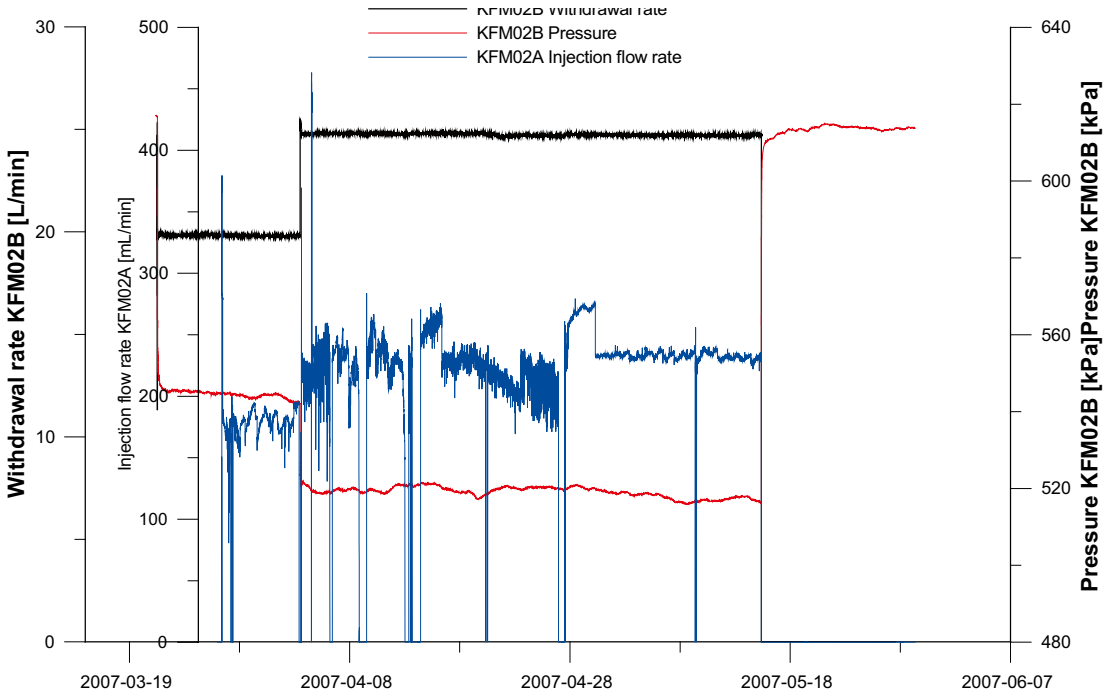

Figure 5-10. *Injection flow rate together with withdrawal rate and pressure response in KFM02B.*

Table 5-13. Volume of tracer solution injected.

	Measured in tank (l)	By flow meter (l)
Main tracer test	2,662	2,531
Pre-test	-	1,787

5.4.2 Tracer breakthrough

Tracer breakthrough was obtained for all tracers in both the pre-test and in the main tracer test. The time for first arrival is c 11 h for Uranine and Li, 50 h for Cs and 26 h for Rubidium. In the pre-test, the time for first arrival of Rhodamine WT was 16 h (pumping rate 19.8 l/min) which corresponds to 12.5 h in transformed time (pumping rate 24.8 l/min), see further discussion below.

Pre-test

In Figure 5-11 the normalized mass flux in the injection and the withdrawal sections are plotted against transformed time since injection start. The pumping flow rate in KFM02B was increased in the middle of the test period from 19.8 l/min to 24.8 l/min. In order to facilitate the comparison between the main test and the pre-test, the time of the pre-test was transformed so that the volume pumped per time unit (i.e. pumping flow rate) was constant (24.8 l/ transformed minute) throughout the pre-test. The consequence for the breakthrough curve is that the first part is somewhat compressed since one real hour is longer than one transformed hour for this period. Since the time is affected by this transformation, so is also the normalized mass flux as plotted on the y-axis in Figure 5-11.

Main tracer test

The normalized mass fluxes for all tracers out of the injection section KFM02A:5 are plotted against time since injection in Figure 5-13 and the breakthrough curves are shown in Figure 5-12. In Appendix 9, the corresponding curves are also presented for each tracer separately. Unfortunately, the injection pump stopped at several occasions, both during the period of tracer injection and during the rinsing. The stops during the tracer injection are reflected as dips in Figure 5-13 and as two notches in the Uranine and lithium breakthrough curves in Figure 5-12. The stops during times of rinsing are not as distinct. However, the stops are taken into consideration when evaluating the data and they should have no effect on the interpreted results.

The total mass injected of each tracer and their mass recovery at pump stop are shown in Table 5-14.

When the sampling in KFM02B ended, the concentration of Uranine was still not down to its background value which explains why the recovery does not reach 100 %.

The fact that the calculated mass recovery for lithium is higher than for Uranine is further discussed in Section 6.2.

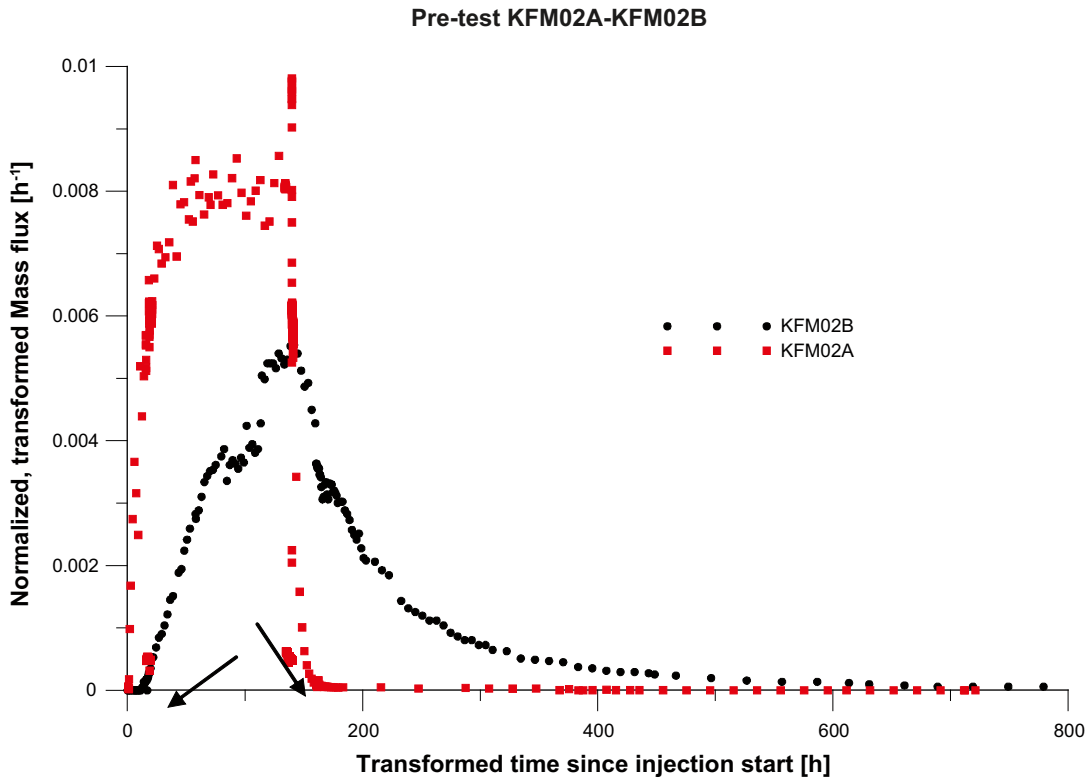

Figure 5-11. *Tracer (Rhodamine WT) breakthrough in KFM02B and injection in KFM02A:5 from the pre-test. Normalized transformed mass flux against transformed elapsed time. The arrows indicate injection pump stops.*

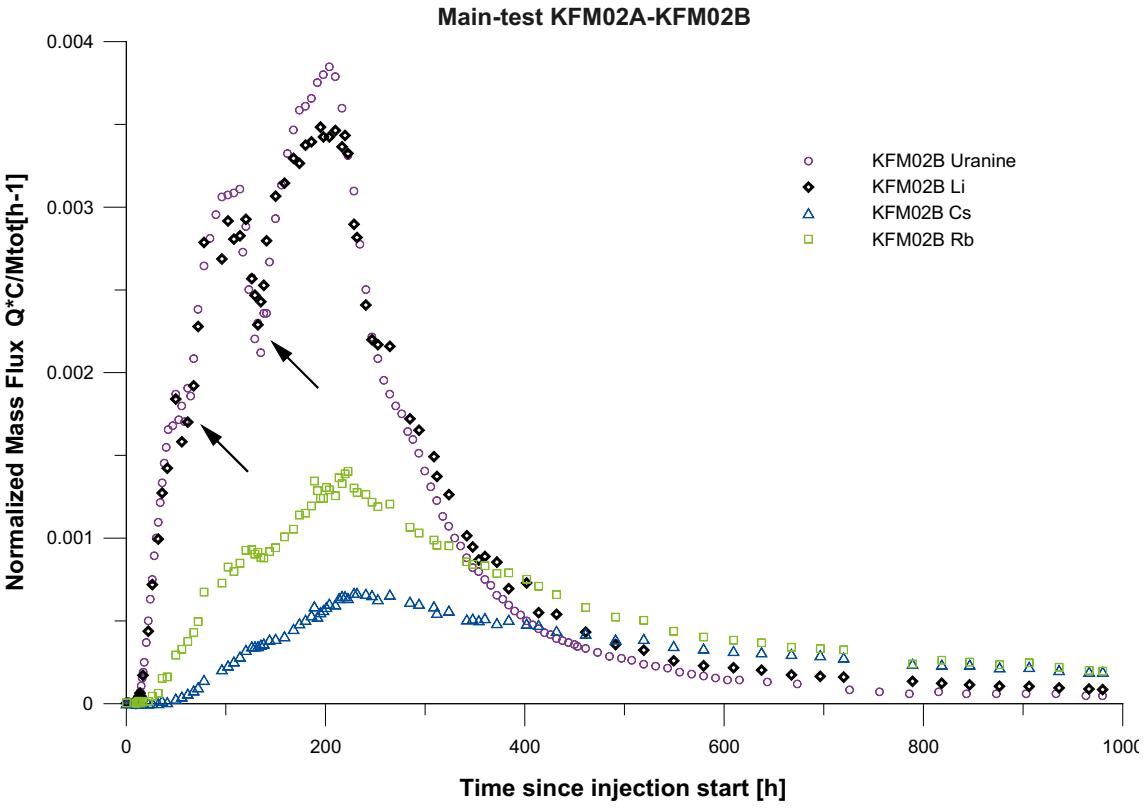

Figure 5-12. *Tracer breakthrough in KFM02B from injection in KFM02A:5 from the main tracer test. Normalized mass flux against elapsed time. The arrows indicate notches caused by injection pump stops.*

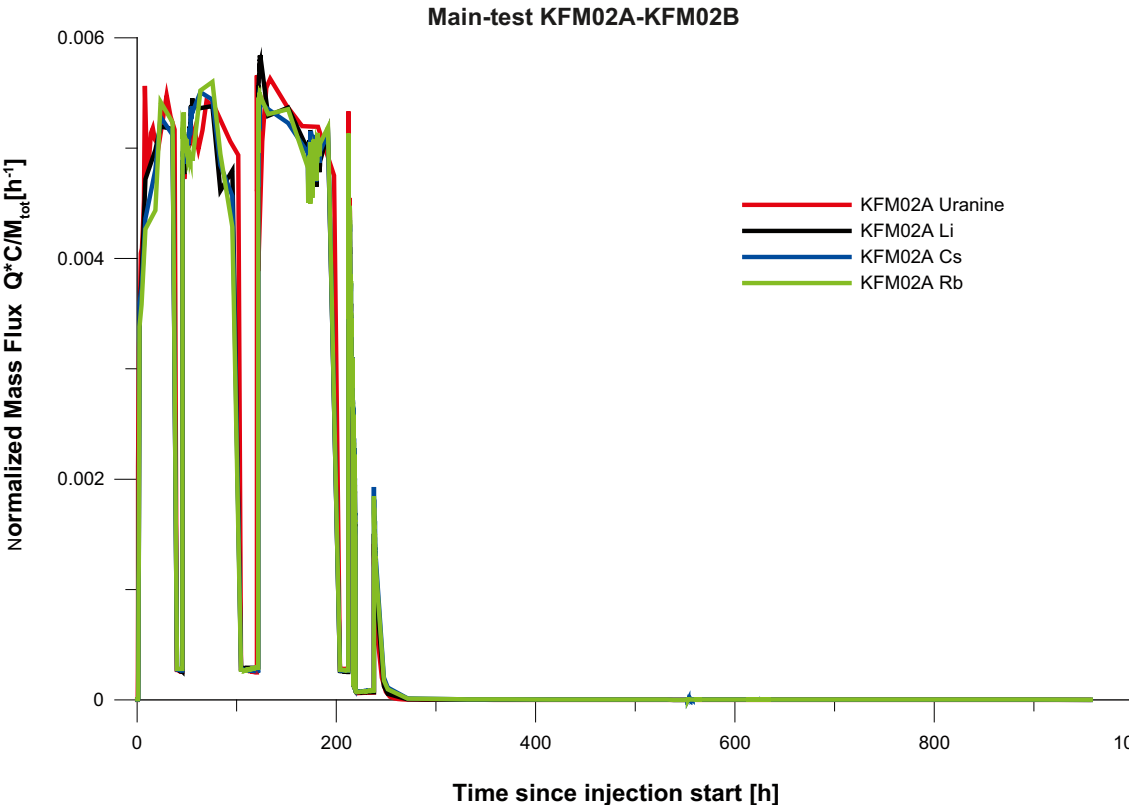

Figure 5-13. *Tracer injection in KFM02A:5. Normailized mass flux from the injection section against elapsed time.*

Table 5-14. Total injected mass and mass recovery of the different tracers at pump stop (980 hours after injection start).

	Total injected mass (g)	Recovery (%)
Rhodamine WT [1)]	75.8	85
Uranine	125.4	90
Lithium	1,501	96
Cesium	104.9	37
Rubidium	385.1	77

[1)] Time since the injection for Rhodamine WT is 125 h longer than for the other tracers.

5.4.3 Model results and evaluated parameters

The models used in the evaluation of the tracer tests are presented in Section 3.5. The simulation procedure was to choose suitable starting values, then to run the selected model and finally examine the results mainly by considering the reasonableness, standard errors and correlation of the parameters as well as visual inspection of the model fit. The model used first was the AD model for a single pathway. After that, further simulations were tried with multiple pathways and finally the AD-MD model.

The results from the model simulations are presented below in Figures 5-14 to 5-21, where estimated parameter values also are presented. The transport parameters that are extracted from the models are the proportionality factor (*pf*), longitudinal dispersivity in terms of Peclet number (*Pe*), mean residence time (t_m), retardation factor for the fracture (*R*) and the lumped matrix diffusion parameter (*A*). For further description of the parameters see Section 3.5.

The data used in the simulations are normalized mass flux (h^{-1}) and time (h). By using these units, the value of *pf* directly indicates the recovery in the simulation as *pf* = 1 implies 100% recovery in the simulation.

Generally, the AD and AD-MD models were both useful in the evaluation. However, the AD model with multiple pathways was difficult to use since it did not converge to reasonable values. Hence, results presented below are only from the AD and AD-MD models with one pathway.

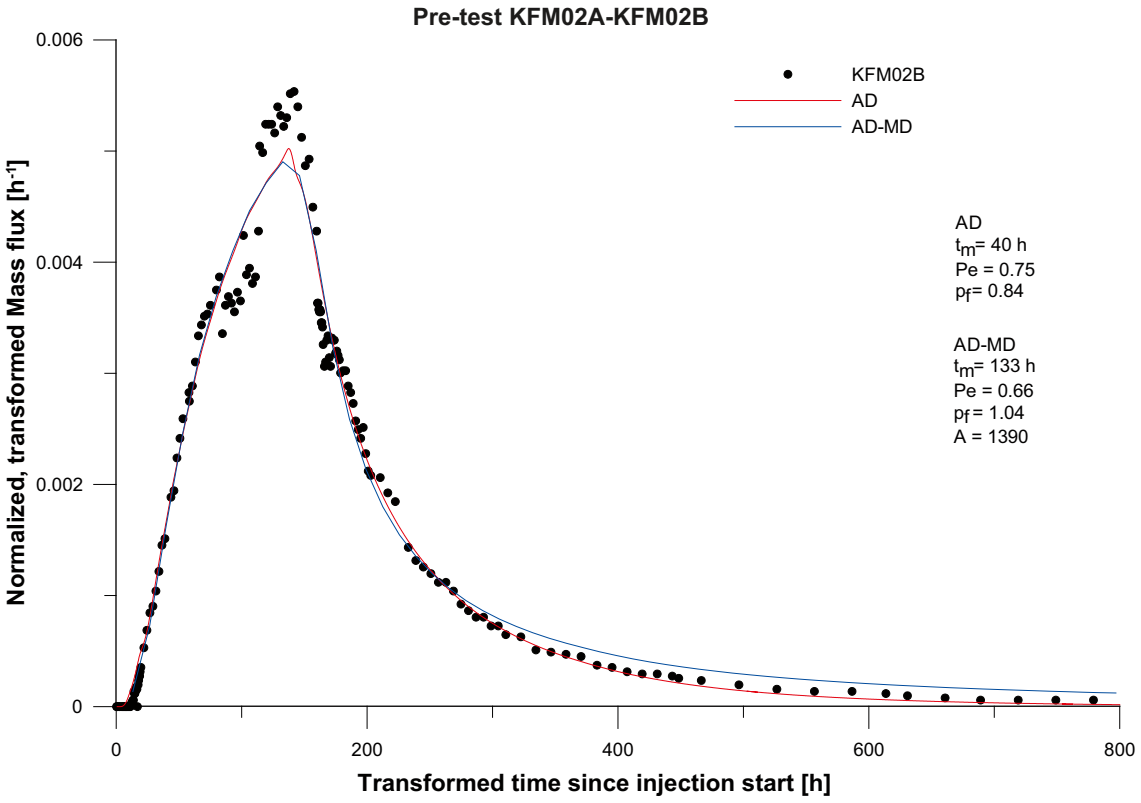

Figure 5-14. *Linear plot of model fits using the AD and AD-MD models to experimental data for the pre-test (Rhodamine WT). Note the transformed units on the axes.*

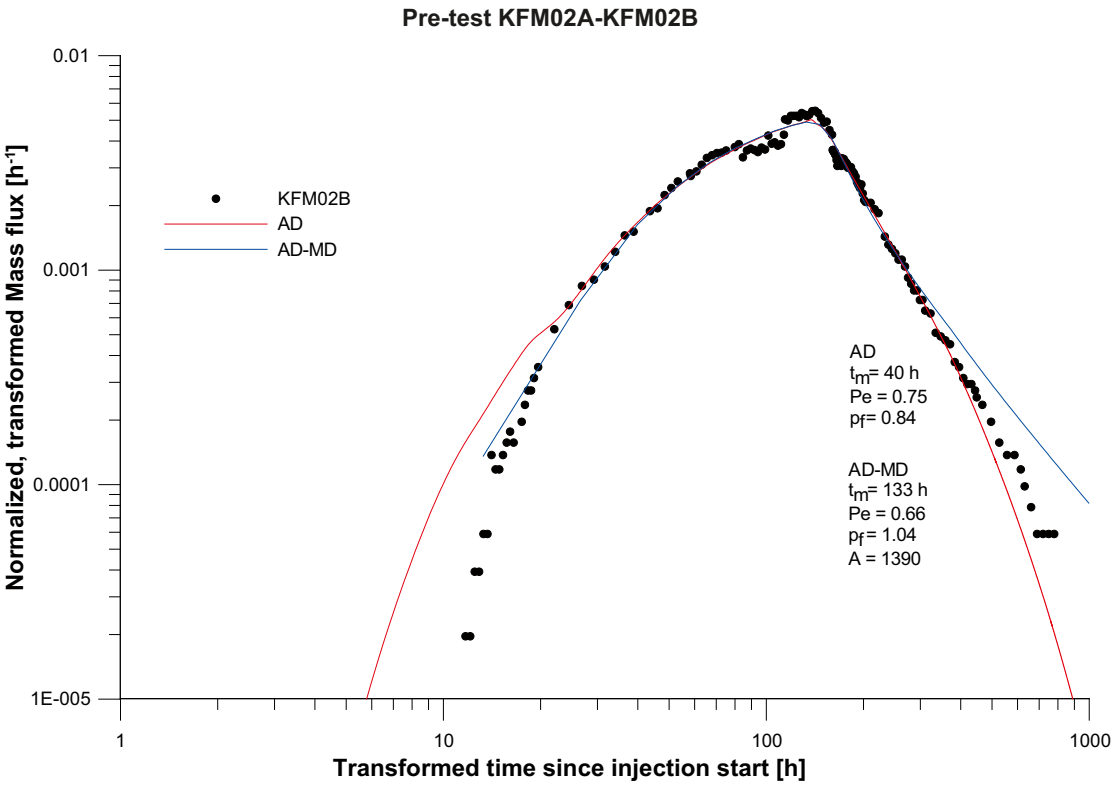

Figure 5-15. *Logarithmic plot of model fits using the AD and AD-MD models to experimental data for the pre-test (Rhodamine WT). Note the transformed units on the axes.*

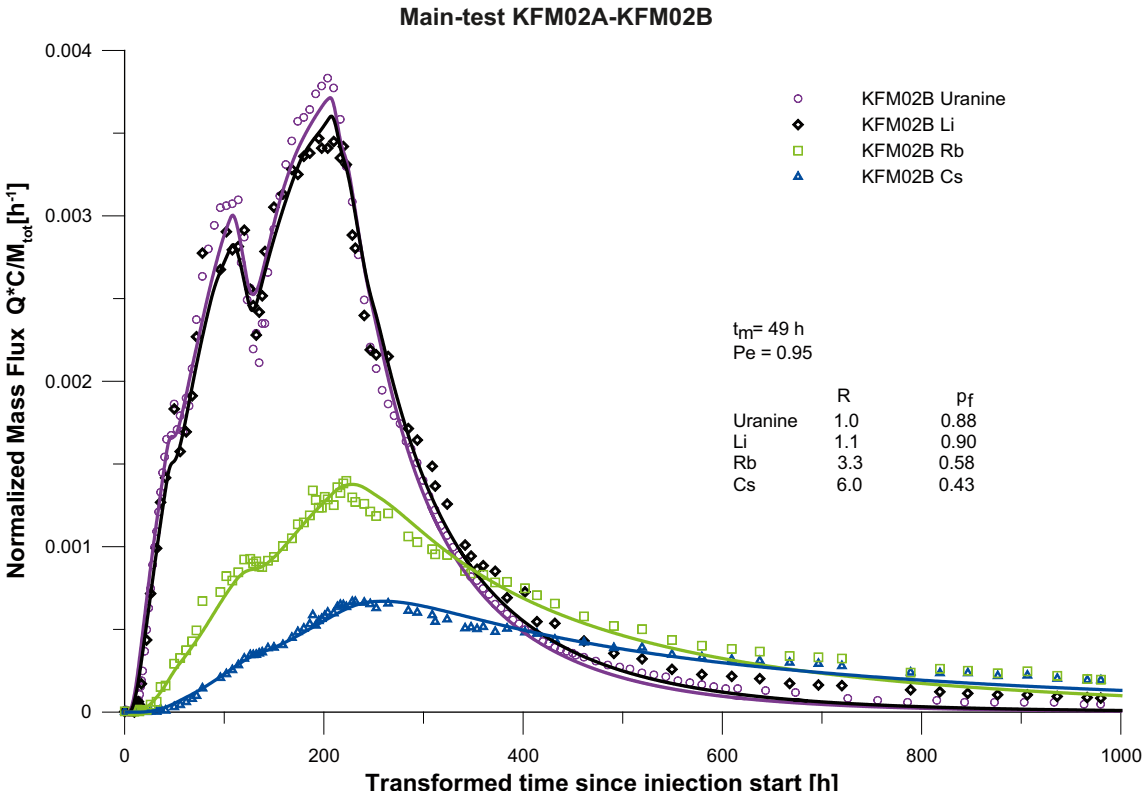

Figure 5-16. *Linear plot of model fit using the AD model to experimental data for the main test. t_m and Pe were evaluated by using only Uranine and fixed during simulation of Li, Rb and Cs.*

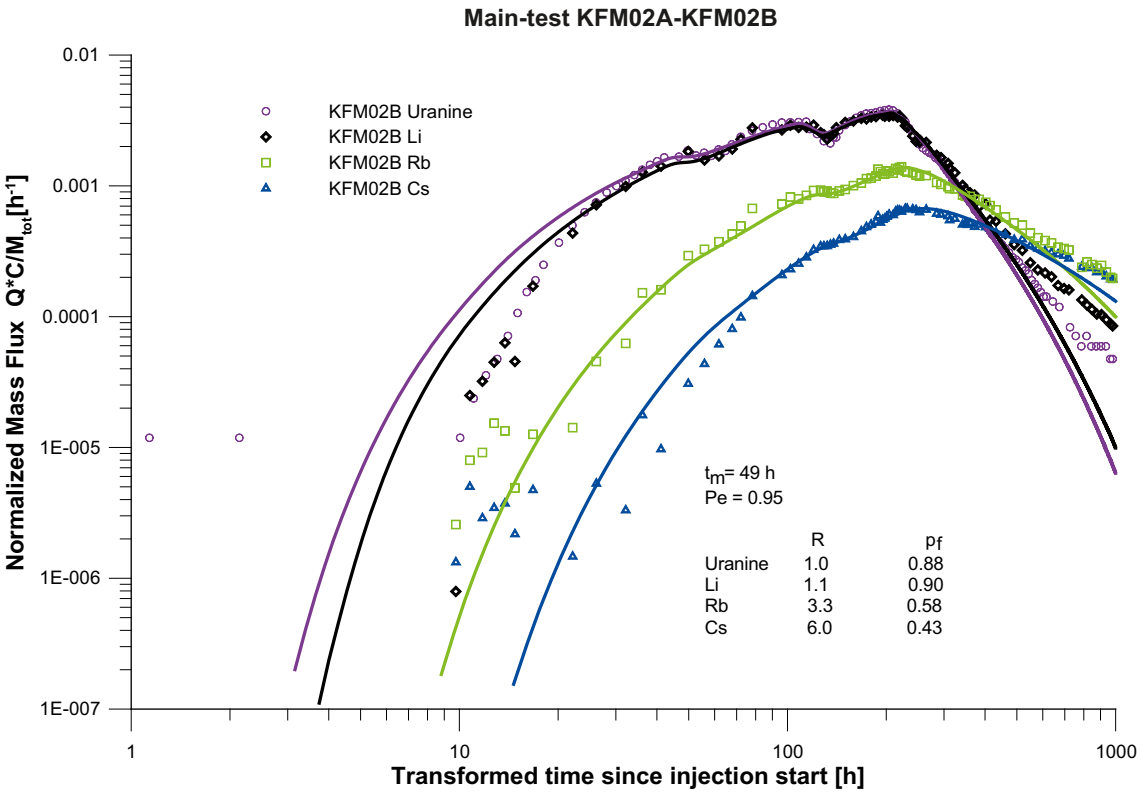

Figure 5-17. *Logarithmic plot of model fit using the AD model to experimental data for the main test. t_m and Pe were evaluated by using only Uranine and fixed during simulation of Li, Rb and Cs.*

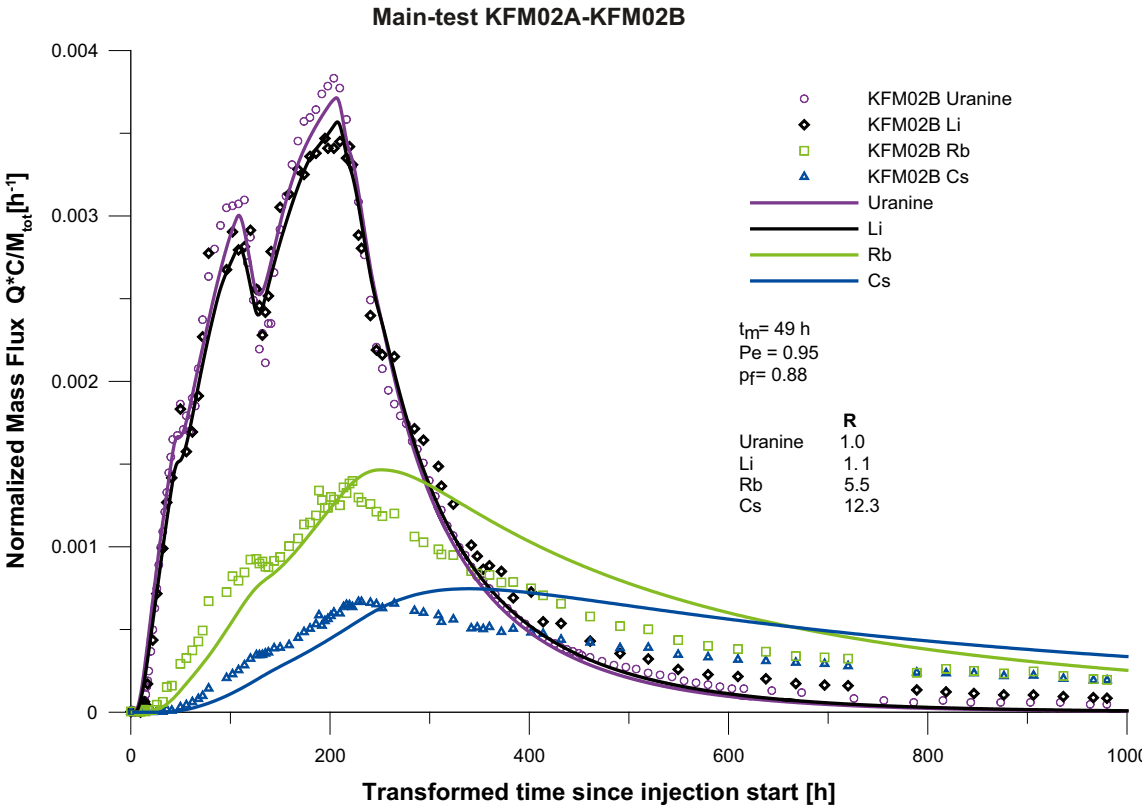

Figure 5-18. *Linear plot of model fit using the AD model to experimental data for the main test. t_m, Pe and pf were evaluated by using only Uranine and fixed during simulation of Li, Rb and Cs.*

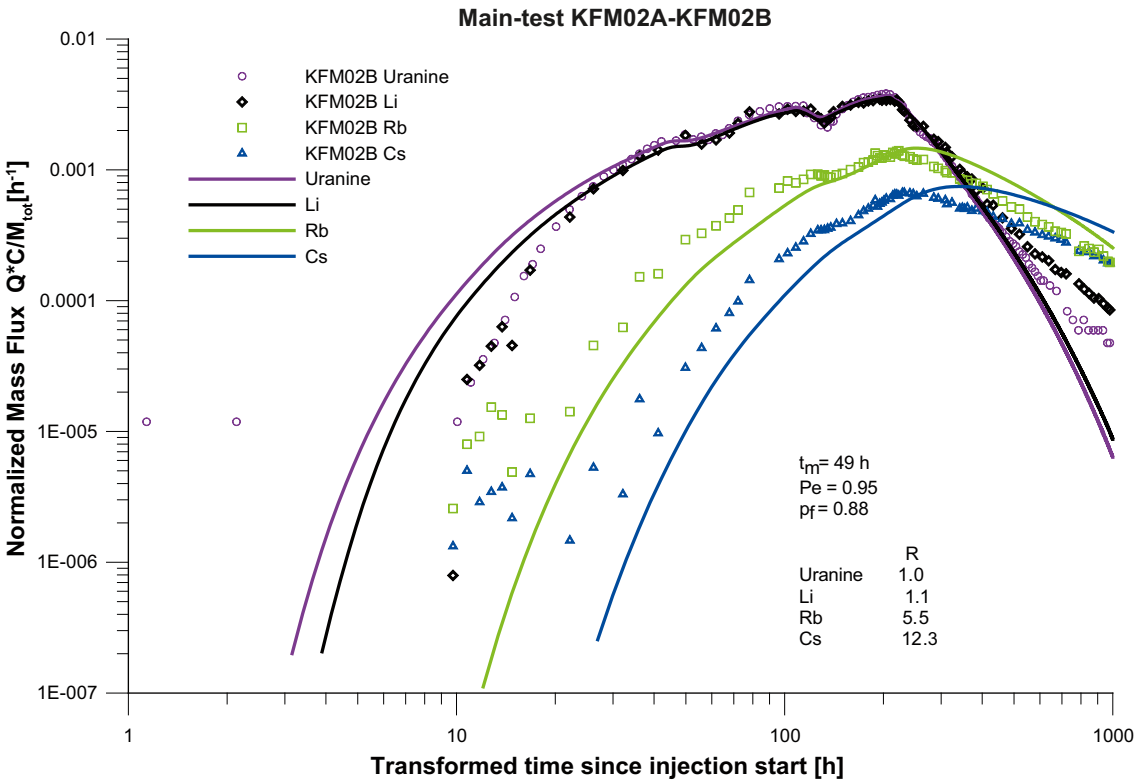

Figure 5-19. *Logarithmic plot of model fit using the AD model to experimental data for the main test. t_m, Pe and pf were evaluated by using only Uranine and fixed during simulation of Li, Rb and Cs.*

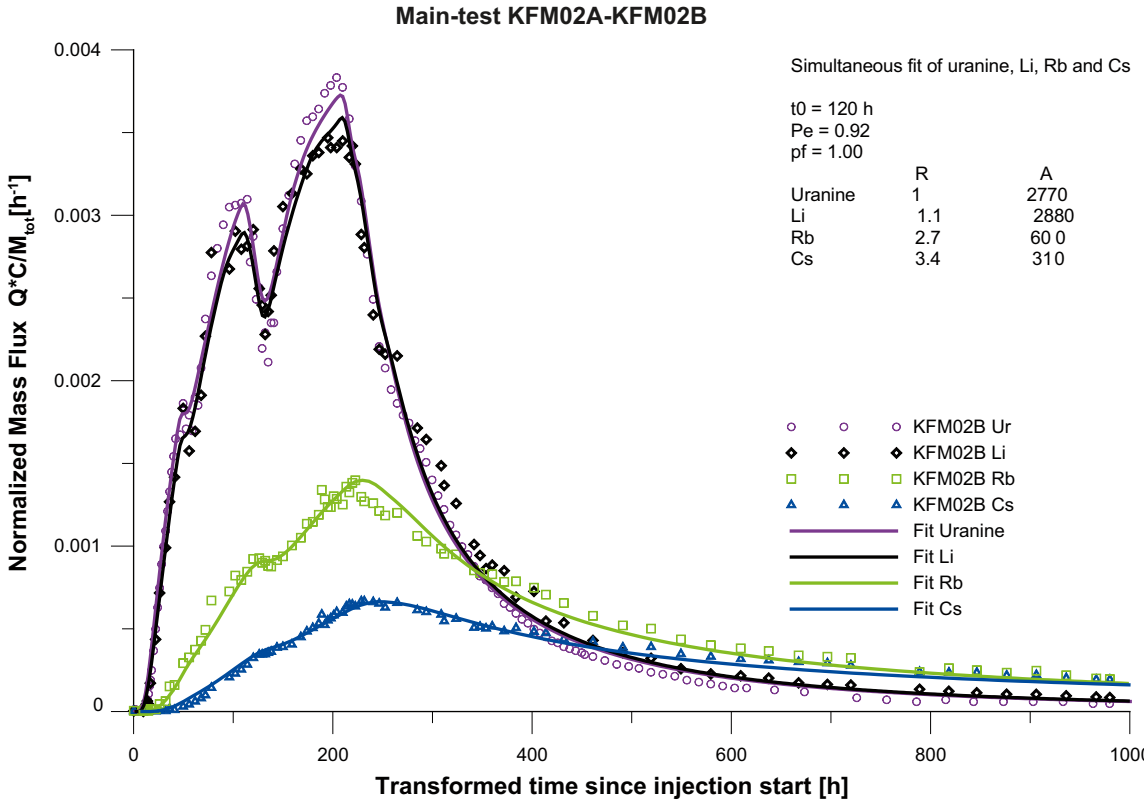

Figure 5-20. *Linear plot of model fit using the AD-MD model to experimental data for the main test. All tracers were simulated simultaneously with the restriction of t_m, Pe and pf equal for all tracers and R set to 1 for Uranine.*

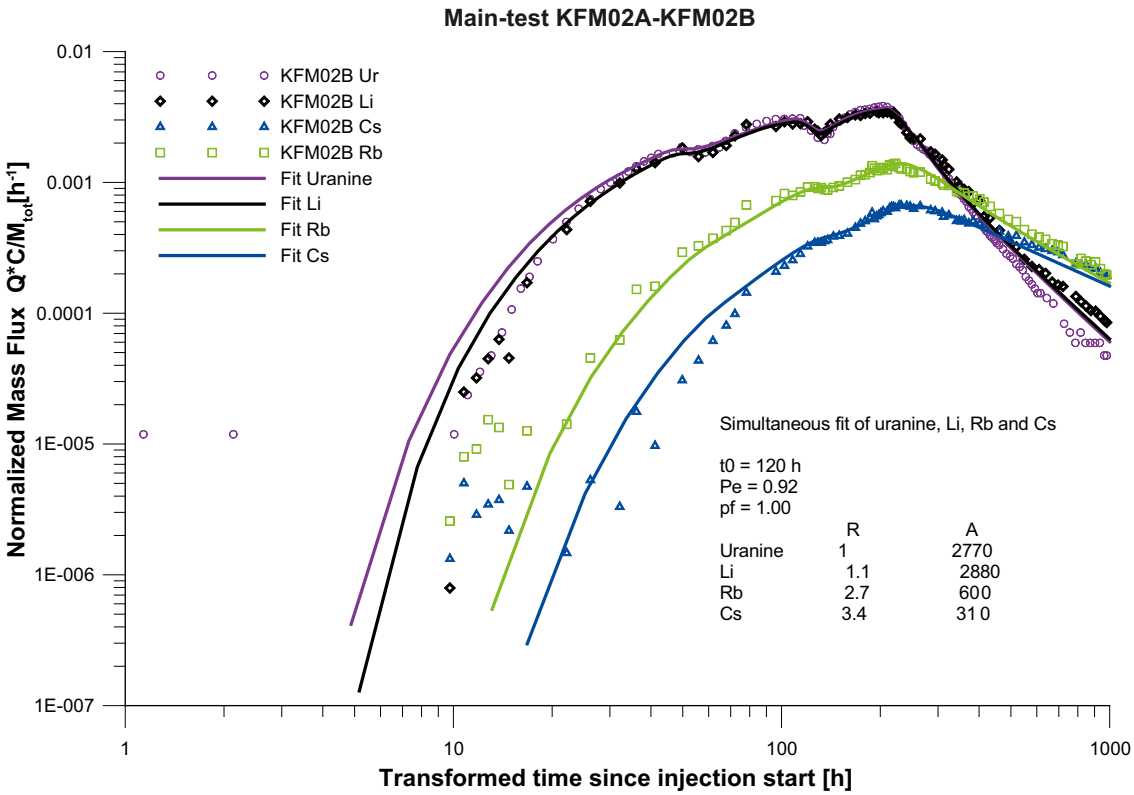

Figure 5-21. *Logarithmic plot of model fit using the AD-MD model to experimental data for the main test. All tracers were simulated simultaneously with the restriction of t_m, Pe and pf equal for all tracers and R set to 1 for Uranine.*

Pre-test

As described in Section 5.4.2, the data from the pre-test were transformed in order to facilitate simulations and a comparison to the main test. The simulations of the pre-test are presented in Figure 5-14 and 5-15. As may be seen in these figures, the fits of the models are rather good although the maximum values are not quite matched by the models. Furthermore, the tail of the breakthrough curve is rather high for the AD-MD model while it is too low in the AD model.

When considering the parameters extracted from the models it is evident that the recovery is rather high, 84% with the AD model and 104% with the AD-MD model. This is expected since the recovery as determined by mass flux calculations at the time of pump stop was 85% for the pre-test. Further, it is obvious that the Peclet number is low for both models. Finally, the mean residence time, t_m, is quite different in the two models as the AD model indicates 40 h while AD-MD indicates 133 h. These observations are further discussed below.

Main test

The main test included several tracers and the parameter estimation may be performed for one tracer at a time or several tracers simultaneously. Both ways were tested in the simulations.

First, the AD model was used only for Uranine, which is assumed to be non-sorbing and R was therefore fixed to 1.0. The mean residence time and Peclet number from that simulation were then fixed and used in simulations of the other tracers, one at a time. In these later simulations, only R and pf were free parameters. As shown in Figure 5-16 and 5-17, the model fits the data quite well although the tails are low in the simulations, especially for Uranine and Li. The proportionality factors, pf, show that the recoveries according to the simulations at infinite time are different for the tracers (Uranine 88%, Li 90%, Rb 58%, Cs 43%).

Simultaneous estimation, of for example Uranine and Cs, was also performed with t_m, *Pe* and *pf* as free parameters (and *R* in the case of Cs). The results from these simulations did not differ much from the results presented in Figure 5-16 and 5-17 and are therefore not presented in this report.

In order to examine the effect on the breakthrough curves if the recovery was assumed to be the same for all tracers at infinite time, the AD model was used but with *pf* fixed instead. Also in this case, Uranine was simulated first and its evaluated parameters (t_m, *Pe* and *pf*) were later fixed in simulations of Li, Rb and Cs. The results from these simulations are shown in Figure 5-18 and 5-19. It is evident in these figures that the restriction of *pf* causes the fits of Rb and Cs to be rather poor.

Simulations with the AD-MD model gave a different result than the AD model. It was not possible to achieve fits that converged for the sorbing tracers if Uranine had been simulated first and t_m, *Pe* and *pf* from that simulation were fixed. Hence, Uranine, Li, Rb and Cs were all simulated simultaneously when using the AD-MD model. In these simulations, all tracers were forced to have the same t_m, *Pe* and *pf* while *R* and *A* were fitted individually for each tracer (except that *R* for Uranine was set to 1). The result from this is presented in Figure 5-20 and 5-21. The figures show that the AD-MD model fits the data quite well for all tracers. Furthermore, *pf* is 1.0 suggesting a recovery of 100% at infinite time for all of the tracers. *R* is higher for Rb and Cs while A is lower compared to Uranine which is expected. The Peclet number is rather low which is consistent with simulations with the AD model as well as simulations of the pre-test. Another consistency with the pre-test is that the mean residence time with the AD-MD model is significantly longer than with the AD model.

Transport parameters

A number of other transport parameters may be derived from the modelling results. The simulation with the AD-MD model of the main test presented in Figures 5-20 and 5-21 was considered to provide the most reliable result and is therefore used for the following calculations. The background data from the modelling used to calculate additional transport parameters are presented in Table 5-15 together with the corresponding parameters evaluated from the pre-test. Fracture conductivity (K_{fr}), equivalent fracture aperture (δ) and flow porosity (εf) were calculated according to SKB's methods description (SKB MD 530.006). These calculated parameters are presented in Table 5-17.

In order to calculate the additional transport parameters the mean head difference, Δh [m], between injection– and pumping section has to be determined. The mean head differences were determined from head readings (pressure registrations) in both boreholes just before pump stop. The head difference, Δh, is shown together with the distance between the two borehole sections in Table 5-16.

The additional transport parameters were not calculated for the pre-test since the mean residence time, t_m, is a transformed time unit corresponding to flow rate 24.8 l/min and the groundwater levels used to calculate the head difference, Δh, correspond to the drawdown caused by the lower flow rate (19.8 l/min). In addition, Rhodamine WT might be weakly sorbing.

It may also be possible to use the estimated values of parameter *A* for further analysis. If one assumes that the non-sorbing and sorbing tracers "experience" the same matrix porosity and other formation properties (tortuosity, constrictivity) and that diffusivity values in water (D_w) are independently known, then the matrix retardation factor (R_d) for the sorbing tracer may be obtained from:

$$R_{d2} = R_2^{\,2}\left(\frac{A_1}{A_2}\right)^2\left(\frac{D_{w1}}{D_{w2}}\right) \qquad (5\text{-}2)$$

where indices 1 and 2 refer to the non-sorbing and sorbing tracer, respectively. An example using the estimated values for Uranine and Cs in Table 5-15 and assuming that the diffusivity in water is about 5 times higher for Cesium than for Uranine (see for example /Ohlsson and Neretnieks, 1995/), then the matrix retardation factor for Cs would be about 31.

Table 5-15. Evaluated transport parameters from the AD-MD model.

	tm (h)	pf	R	A	Pe
Rhodamine WT [1)]	133	1.04	1.0 [3)]	1390	0.66
Uranine			1.0 [3)]	2770	0.92 [2)]
Lithium			1.1	2880	
Cesium	120 [2)]	1.00 [2)]	3.4	310	
Rubidium			2.7	600	

[1)] From the pre-test.

[2)] Restricted to be the same for all four tracers in the main test.

[3)] Assumed to be non-sorbing.

Table 5-16. Background data for calculations of transport parameters.

	Distance (m)	Mean head difference, Δh (m)
Main test	46.4	2.63

Table 5-17. Calculated transport parameters.

	Fracture conductivity, K_{fr} (m/s)	Equivalent fracture aperture, δ (m)	Flow porosity, ε_f (-)
Main test	$6.7 \cdot 10^{-3}$	$2.6 \cdot 10^{-2}$	$2.5 \cdot 10^{-4}$

5.5 Water sampling

The water samples taken at three occasions during the long pumping period indicate only small differences in the chemical composition. These differences are so small that they are considered not to have any effect on the results. In Table 5-18 the concentrations of some of the main constituents are shown.

Table 5-18. Results of some chemical constituents in the SKB class 3 water samples taken during the pumping test in KFM02B.

Date and time of sample	Sample ID no	Na^+ (mg/l)	K^+ (mg/l)	Ca^{2+} (mg/l)	Cl^- (mg/l)
2007-03-21 13:05	12,730	20,400	38.70	957.0	53,000
2007-04-10 13:34	12,754	19,600	24.90	12,300	54,800
2007-05-14 11:20	12,755	18,900	26.70	12,600	55,200

6 Summary and discussion

The results from the tracer tests show a high dispersion (Pe ≈ 1). The mean residence time, tm, was estimated at 120 h with the AD-MD model and 49 h using the AD-model. The result evaluated with the AD-MD model is considered to be the most representative. The reasons for the different solutions and the choice of representative t_m are further discussed in Section 6.3. The retardation factors for the sorbing tracers Li, Cs and Rb were estimated at 1.1, 2.7 and 3.4 respectively.

Generally, the results from the tracer test and the interference test verify the geohydraulic model for the actual sub-area of the Forsmark site investigation area. Details and exceptions are discussed in Section 6.5.3.

6.1 Equipment and procedures

The performance of this tracer test included a rather complicated chain of methods and procedures in order to maintain and control both chemical and hydraulic boundary conditions. Synthetic water was manufactured in large quantities and three different chemical solutions were added simultaneously and with constant flow rates to maintain a steady flow field. Overall this worked rather well. The major technical problem was a number of stops of the main injection pump creating a somewhat varying injection curve. This is considered not to have any significant impact on the results and evaluation of the test.

6.2 Tracer test

The result that the calculated mass recovery for lithium is higher than for Uranine is not very likely. The recovery calculation for Li is complicated by the fact that Li was also added in one of the sub-flows, which makes the determination of the total injected mass more uncertain for Li than for the other tracers. Also, the background concentration is somewhat more uncertain for lithium than for Uranine. The calculation of recovery is sensitive to the background concentration since the concentrations at the "tail" of the breakthrough curve are approaching the background concentration.

During planning and design of the tracer test, the risk of saturating sorption sites was considered. The test was designed to avoid saturation of sorption sites, and the scoping calculations implied that the sorption sites should not be saturated using the present concentrations of the sorbing tracers. However, it may still be possible that some part of the flow-path might be partly saturated. If this is the case, it is not likely that this should have any effect on the results.

As shown in Figure 5-12, the maximum concentrations of all four tracers appear to occur almost at the same time. Intuitively it would seem logical that the maximum concentration for the non-sorbing tracer should occur earlier than for the sorbing tracers. However, Figure 5-12 gives a somewhat illusory impression because of the timing of the injection duration and the tracer travel times between the borehole sections. Figure 6-1 shows a simulation of the breakthrough curves with the parameters obtained from the real modelling, but with the injection performed as a shorter pulse of one hour. Then it is clear that the maximum concentrations occur at different times.

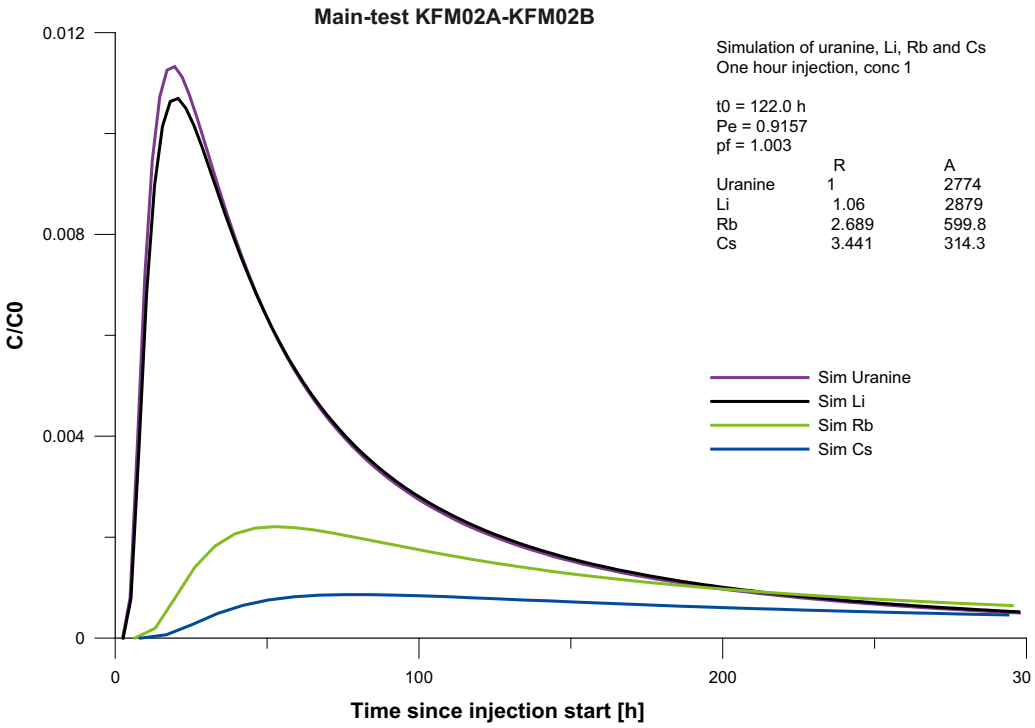

Figure 6-1. *Lin- lin plot of simulation using the AD-MD model assuming a shorter injection time (1h) and the transport parameters (t0, Pe, pf, R and A) obtained from modelling with fit to experimental data.*

6.3 Model simulations

The main test and the pre-test were consistent regarding the non-sorbing tracer in the simulations. This was expected since the two tests were performed with basically the same set-up. The small differences that still can be observed may, for example, depend on the difference in pumping flow rate during the two tests.

In order to obtain well fitted simulations of the main test with the AD model, the recovery of the tracers at infinite time must be different among the tracers. To explain this result, the tracers with lower recovery must, for example, be affected by irreversible sorption, other flow paths not leading to the pumping section, degradation or some other effect causing the tracers to not reach the pumping hole. Such effects are, however, not likely in this system whereas the rather straight-forward and simple explanation would be that advection, dispersion and sorption alone may not simulate the tracer transport correctly in this test. Instead, some other effect, such as diffusion, may play a significant role. The AD-MD model provides simulations that fit well to the data for all tracers used, in the main test as well as in the pre-test, which would suggest that the diffusion is not an insignificant effect in this experiment.

The dispersivity in the simulations was consistently high (i.e. low Peclet number). A rather high dispersivity may be expected due to several reasons. The system is made up of a number of flowing fractures (see Figure 2-1) which may have different mean transport times and therefore causing the breakthrough curve to spread (i.e. to increase the dispersivity). Theoretically, this system might therefore be possible to simulate with several flow paths and in this way obtain a lower dispersivity in the individual flow paths than for the entire system. However, as pointed out above, it was difficult to achieve converging solutions if more than one flow path were considered. This is not unexpected, because well fitted simulations were obtained with only one flow path. Hence, adding another separate flow path may not improve the fit. Another reason for a high dispersivity may be related to the fact that the transmissivity of the injection section is lower than in the pumping section by a factor of c 10. Hence, the 1/100 dipole in terms of flow rates was in fact larger in terms of hydraulic head which may have caused the tracers to spread more around the injection section than under homogenous conditions. However, to investigate whether this effect might contribute to a higher dispersivity, further simulations of the test in a 2D-geometry would be necessary.

One striking difference between the simulations with the AD and the AD-MD models is the significantly shorter mean residence time in the AD simulations than in the AD-MD simulations. This may partly be an effect of that the tail of the AD fit is significantly lower than corresponding fit for the AD-MD model, causing the centre of the fit to be earlier for AD than for AD-MD. However, the differences in the mean residence time may also depend on the slightly different boundary conditions for the tracer inlet that are used in the two models (see Section 3.5); this difference may become important at high dispersivity values /Andersson et al. 1993/. The effect of dispersivity in the two models may be illustrated with some simple simulations as shown in Figure 6-2. The simulations in the figure are based on a one hour step injection with concentration 1.0, mean residence time of 100 h, no sorption and full recovery. As shown in Figure 6-2, the difference between the AD and AD-MD models is rather moderate for high Peclet numbers (5 and 10) but quite large for Peclet number 1, suggesting that the two models result in different solutions for high dispersivities.

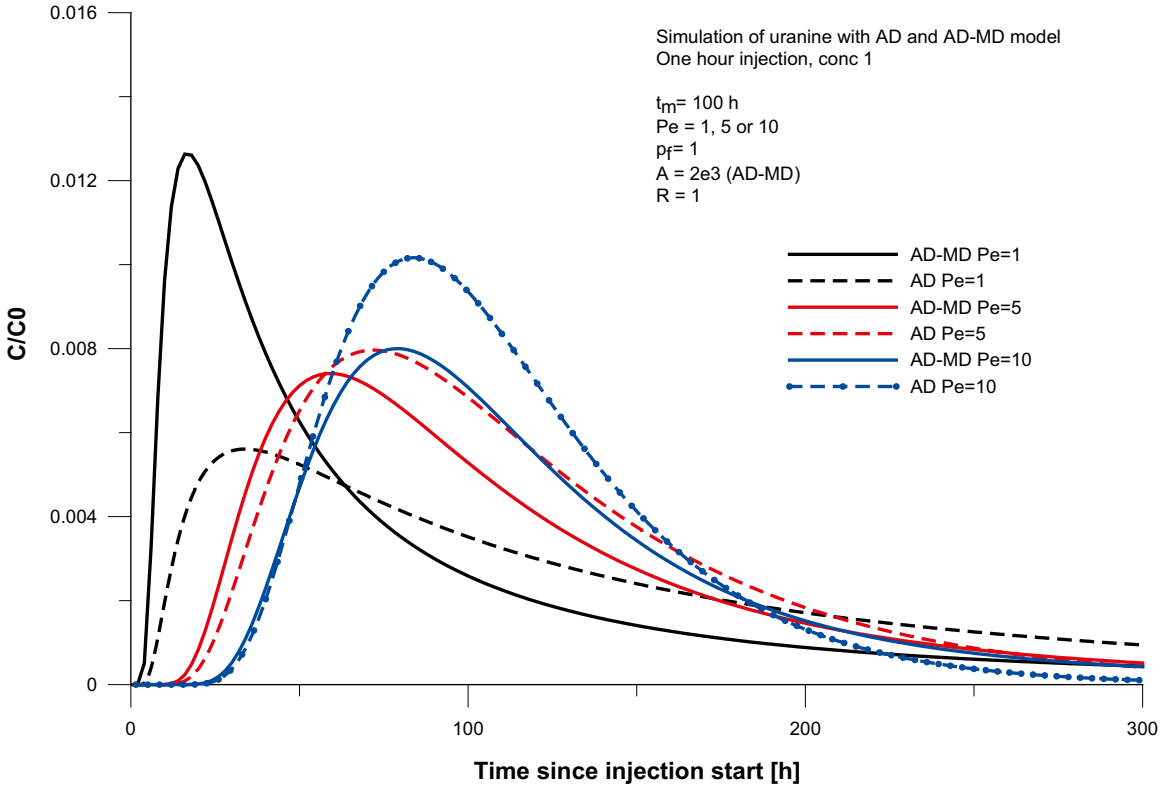

Figure 6-2. *Linear plot of simulation using the AD (dashed lines) and AD-MD (solid lines) models with one hour step injection and 100 h mean residence time and various dispersivity.*

6.4 Transport parameters

The estimated value of R for Cs indicates a moderately sorbing tracer. The results from the tracer experiment are fairly consistent with results from Single-Well Injection-Withdrawal (SWIW) tests with Cs performed in section 414.7–417.7 mbl in KFM02A /Gustafsson et al. 2005/ where the retardation factor was estimated at R=11. This is the lowest retardation factor obtained for Cs in all SWIW-tests conducted within the Forsmark and the Oskarshamn site investigations. Significantly higher R-values have been reported from other tracer tests using similar transport models (advection-dispersion and linear sorption). For example, /Gustafsson and Nordqvist 2005/, reported R = 90, /Winberg et al. 2000/, reported R = 69, whereas R = 140 was reported by /Andersson et al. 1999/. Also, /Gustafsson et al. 2005/ reported a retardation factor of R = 73 in a SWIW-test in KFM03A (643.5–644.5 mbl) at Forsmark.

According to /Ogata and Banks 1961/ and /Zuber 1974/, the dispersion in a radially converging flow field can be calculated with good approximation by equations valid for one-dimensional flow. Although a linear flow model (constant velocity) is used for a converging flow field, it can be demonstrated that breakthrough curves and parameter estimates are similar for Peclet numbers of about 10 and higher. The estimated Peclet numbers from this tracer test is lower, about 1. This might introduce additional uncertainties in the estimation of other transport parameters.

6.4.1 Fracture minerals and geology

Investigations of fracture minerals in KFM02A showed that many of the open fractures, which according to PFL– and PSS measurements are dominating in the investigated section of KFM02A (411.0–441.0 mbl), do not have a visible mineral coating or filling, see Table 6-1. The majority of the fractures are fresh or slightly altered. The rock type in the interval is granite to granodiorite (metamorphic, medium-grained) /Carlsten et. al. 2004/. The same investigation of fracture minerals was made in KFM02B in the tested interval (408.5–434.0 mbl). This borehole interval also contains many fractures without a visible mineral coating or filling, see Table 6-2. The pre-dominant fracture minerals in the interval are chlorite and calcite and the fractures coated by these minerals are also fresh or slightly altered. The major part of the interval is dominated by pegmatitic granite, but continues downwards across the contact to the medium-grained metagranite-granodiorite /Carlsten et al. 2007/. When considering all fractures in the intervals in each of the two borehole sections, only c 50% have visible fracture minerals or coatings. It is very unusual that such a large part of the fractures lack visible mineral fillings. In Figure 6-3, the fracture frequency and their mineral coating in two different boreholes (KFM02A and KFM10A) intersecting Zone A2 are compared, and it is clear that the frequency of fractures with no mineral coating is much larger in KFM02A.

The lack of visible fracture coatings and minerals may be one explanation for the moderate sorption effects observed in the tracer test.

Table 6-1. Occurrence of fracture minerals in the hydraulically dominating fractures in borehole interval 411.0–442.0 mbl in KFM02A (Data from Sicada).

T tot = 2.9·10–6 m^2/s (Summation of T_f from detected fractures measured by difference flow-logging (PFL) /Rouhiainen P and Pöllänen J/).

Length to fracture (PFL) (mbl)	Length to fracture (geology) (mbl)	Tf (PFL) (m^2/s)	% of section transmissivity (%)	Fracture mineral	Fracture interpretation	Aperture (mm)	Surface	Rock alteration
417.3	417.3	9.0·10–7	30.8	No	open	1.0	Rough	Fresh
427.2	427.2	7.1·10–7	24.4	No	open	1.0	Rough	Fresh
418.4	418.3	1.4·10–7	4.9	No	open	1.0	Smooth	Fresh
	418.5			No	open	1.0	Smooth	Fresh
425.9	425.9	1.1·10–7	3.8	Chlorite/ calcite	open	1.0	Rough	Slightly altered
426.8	426.8	7.2·10–7	24.4	Chlorite/ calcite	sealed	0.0	Rough	Fresh
437.3	437.4	1.1·10–7	3.7	No	sealed	0.0	Rough	Slightly altered
416.5	416.5	5.3·10–8	1.8	No	open	2.5	Smooth	Slightly altered
425.1	425.1	4.3·10–8	1.5	Clay Minerals	open	3.0	Rough	Moderately altered
	425.1			Clay Minerals	open	3.0	Rough	Moderately altered
Total		2.8·10–6	95.3					

Table 6-2. Occurrence of fracture minerals in the hydraulically dominating fractures in borehole interval 408.5–434.0 mbl in KFM02B (Data from Sicada).

T tot = 3.9·10–5 m^2/s (Summation of Tf from detected fractures measured by difference flow-logging (PFL) /Väisäsvaara J and Pöllänen J/)

Length to fracture (PFL) (mbl)	Length to fractur (geology) (mbl)	Tf (PFL) (m^2/s)	% of section transmissivity (%)	Fracture mineral	Fracture Interpretation	Apertur (mm)	Surface	Rock alteration
414.5	414.5	$1.6\cdot10^{-5}$	44.8	No	Open	0.5	Rough	Fresh
423.3	423.2	$1.0\cdot10^{-5}$	28.0	Chlorite	Open	2.0	Rough	Fresh
421.1	421.1	$5.5\cdot10^{-6}$	15.4	Chlorite	Open	1.0	Rough	Slightly Altered
413.1	413.1	$1.4\cdot10^{-6}$	3.9	No	Open	0.5	Rough	Fresh
	413.1			No	Open	0.5	Rough	Fresh
415.1	415.2	$1.2\cdot10^{-6}$	3.4	Chlorite	Open	0.5	Smooth	Slightly Altered
426.9	426.9	$8.7\cdot10^{-7}$	2.4	Chlorite	Open	2.0	Smooth	Slightly Altered
	426.9			Chlorite	Open	0.5	Smooth	Slightly Altered
	426.9			Chlorite	Open	0.5	Rough	Slightly Altered
429.6	429.6	$7.6\cdot10^{-7}$	2.1	no	Open	0.5	Smooth	Fresh
	429.6			no	Open	0.5	Rough	Fresh
	429.6			no	Open	1.0	Rough	Fresh
	429.6			no	Open	1.0	Rough	Fresh
	429.6			calcite	Open	1.0	Smooth	Fresh
	429.6			no	Open	2.0	Rough	Fresh
Total		$3.6\cdot10^{-5}$	92.8					

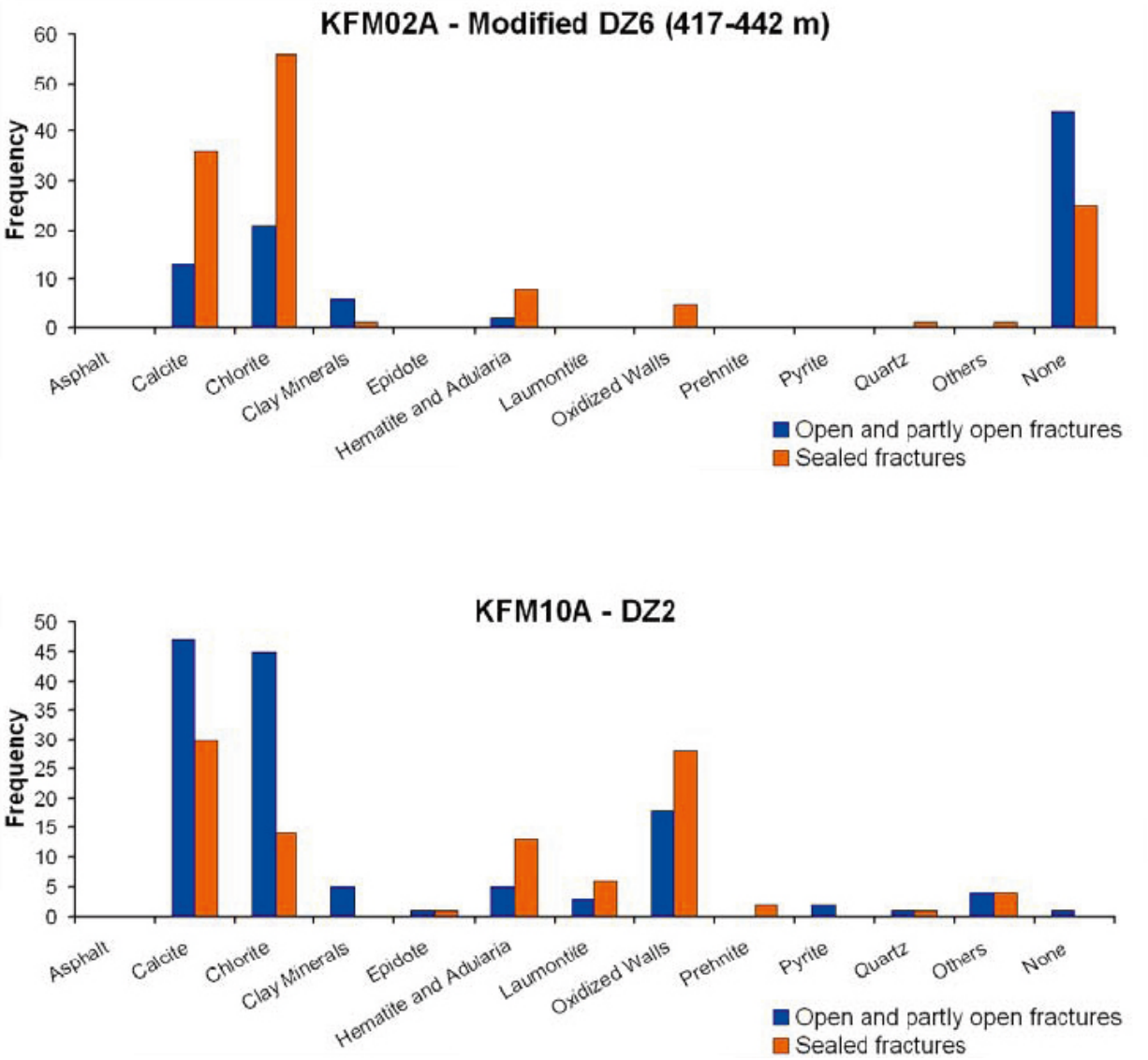

Figure 6-3. *Fracture frequency in two boreholes intersecting Zone A2. Note the many fractures lacking mineral coatings in KFM02A. Picture taken from /Stephens et al. 2007/.*

6.5 Geohydraulic conditions

6.5.1 Comparision of different hydraulic tests

The estimated transmissivity for the pumping section in KFM02B from transient evaluation ($T = 3.0 \cdot 10^{-5}$ m^2/s) is in good agreement with that ($T=4.5 \cdot 10^{-5}$ m^2/s) from the previous difference flow logging in this borehole, /Väisäsvaara and Pöllänen 2007/. However, the estimated transmissivities from several observation sections, primarily sections 3, 4 and 5 in KFM02A, are significantly higher than the T-values obtained from single-hole tests from previous investigations /Rouhiainen and Pöllänen 2004/ and /Källgården et al. 2004/, cf. Figure 5-7. This is assumed to be due to the fact that the calculated T-values from the interference tests represent a larger volume of rock than the single-hole tests since the pumping duration is a much longer, resulting in a larger radius of influence. Furthermore, during interference tests the more transmissive hydraulic units dominate and the less transmissive rock is disguised by units of higher transmissivities. Hence, a T-value from a section measured by PSS cannot directly be compared with the corresponding T-value obtained from an interference test.

The single-hole tests performed in the injection section of KFM02A (411.0–442.0 mbl) give a transmissivity of $2 \cdot 10^{-6}$ m^2/s /Källgården et al. 2004/. The radius of influence, r_i, was not calculated in that report, but it can be calculated according to Appendix 10. A majority of the intervals tested have a radius of influence < 46 m (see Table 6-3), which is the distance to KFM02B at the actual depth. Only the hydraulically dominating interval 426.0–431.0 mbl has a radius of influence > 46 m. This indicates that only the rock volume very close to the borehole is represented by this T-value. However, the interference test evaluation of KFM02A:5 indicates a transmissivity of $2.5 \cdot 10^{-5}$ m_2/s, which is in accordance with the pumping test in KFM02B ($T=3.0 \cdot 10^{-5}$ m_2/s).

The pumping borehole is assumed to be located in Zone A2 with quite high transmissivity and boreholes in, close to, or with connections to the zone may result in transmissivity values representative for the zone rather than for the rock volume close to the borehole that is investigated in single-hole tests. On the other hand, the estimated transmissivity of observation sections may sometimes be overestimated from the interference test due to poor hydraulic connection to the pumping borehole, cf Figure 5-7. Transmissivity and storativity can probably be separated individually only for observation sections having a good hydraulic connection to the pumping borehole. In other cases, only the hydraulic diffusivity T/S may be estimated.

6.5.2 Flow regimes

The hydraulic single-hole tests interpretation in KFM02A also included an evaluation of flow regimes /Källgården et al. 2004/. The flow regimes were mainly interpreted as pseudo-radial flow regime (PRF) and in some cases the pseudo-radial flow showed a transition to pseudo-spherical flow (PSF) or an apparent no-flow boundary (NFB). The pumping test in KFM02B (408.5–434.0 mbl) also indicates a PRF transitioning to a PSF, thus the results are consistent. The scoping calculations and the models used assume a radial flow distribution around the pumping borehole. The transient evaluations of the injection tests in KFM02A and of the pumping test in KFM02B indicate that this assumption is reasonable.

Table 6-3. Data from injection tests with PSS in KFM02A (411.0–442.0 mbl) and calculated radius of influence (r_i) and r_i -index.

Secup (mbl)	Seclow (mbl)	Flow regime [1] (flow period)	Flow regime [1] (recovery period)	$T_R=T_T=T_f$ [2] (m^2/s)	S -	t1 (s)	t2 (s)	r_i (m)	r_i –index [3] -
411.0	416.0	PRF	PRF->PSF	4.58E–08	1.00E–06	60	1200	11.12	0
416.0	421.0	PRF->PSF	PSF	9.15E–07	1.00E–06	100	300	24.85	–1
421.0	426.0	PRF->NFB?	PSS	2.30E–07	1.00E–06	50	400	14.39	1
426.0	431.0	PRF	PSS	1.15E–06	1.00E–06	100	1200	55.72	0
431.0	436.0	PRF?	WBS->PSS	3.56E–09	1.00E–06	100	1000	2.83	0
436.0	441.0	PRF	PSS	1.06E–07	1.00E–06	30	1000	15.44	0

[1] The acronyms in the column “Flow regime are as follow: wellbore starage (WBS), pseudo-linear flow (PLF), pseudoradial flow (PRF), pseudo-spherical flow (PSF), pseudo-stationary flow (PSS) and apparent no-flow boundary (NFB).

[2] T_R=Representative Transmissivity from the measured section

T_T=Representative Transmissivity from transient evaluation.

T_f=Representative Transmissivity from flow period.

[3] The r_i -index is defined in Appendix 10.

6.5.3 The hydrogeological model

The hydrogeolocical model describes the different fracture domains and deformation zones in the candidate area. The interpretation is based on the many borehole investigations performed in the area. Already during model version 1.2 at Forsmark, significant spatial variability in the fracture pattern was observed. The gently dipping deformation zone ZFMA2 (here denoted Zone A2) was identified as a major structural feature steering both the hydrogeological and fracture properties at the site /SKB 2005a/. Zone A2 is in the hydrological model described as a major structural feature steering both the hydrogeological and fracture properties at the site and it intersects many of the boreholes in the investigation area /Olofsson et al. 2007/. Its position (a simplified profile) together with some of the other deformation zones is shown in Figure 6-4.

Zone A2 is considered to intersect KFM02A in the interval 417.0–441.0 mbl /Olofsson et al. 2007/. The sub-horizontal zone ZFMF1 also intersects KFM02A at borehole length 476.0–520.0 mbl /Olofsson et al. 2007/.

This tracer test and interference test pumping was performed in a section of KFM02B believed to intersect zone A2. The aim was to test whether borehole sections that are interpreted to intersect A2, or other deformation zones that have contact with Zone A2, show more distinct responses than boreholes that are thought to have no contact with these structures.

The results from the interference test are generally in accordance with what was expected from the hydrogeological model. All sections that are responding to the pumping are located in the west-north-west to north-west direction of KFM02B. No responses are seen in for example HFM04, HFM05, HFM17, HFM25 or HFM26 although they are among the boreholes closest to KFM02B (see Figure 6-5).

In Figure 6-5, the sections in the boreholes closest to the pumping hole are marked with different colours indicating whether they are interpreted as intersecting Zone A2 or not, and whether they showed responses in the interference test or not. Where there is more than one dot, each dot represents a section. Only the order of sections is correct, not the length scale.

Out of the 115 observation sections included in the interference test, 90 sections did not respond at all to pumping in KFM02B or responded very weakly. Of the remaining 25 sections, 18 showed distinct responses. Four observation sections stand out as responding most strongly. These sections, section 3, 4, 5, and 6 in KFM02A, together with 14 other sections (observation sections in boreholes HFM32, HFM16, KFM06B, KFM05A and KFM06A) and section KFM02A:7 show responses that are distinct enough to be characterized as potential zone responses, i.e. dominated by an adjacent zone. For three of the responding boreholes (HFM13, HFM15 and HFM19), the responses were too small and/or disturbed to be analysed. In borehole KFM01C, HFM01 and KFM10A a small interference could neither be confirmed nor excluded.

Table 6-4 shows a classification of connectivity together with the intersecting zone or fracture domain.

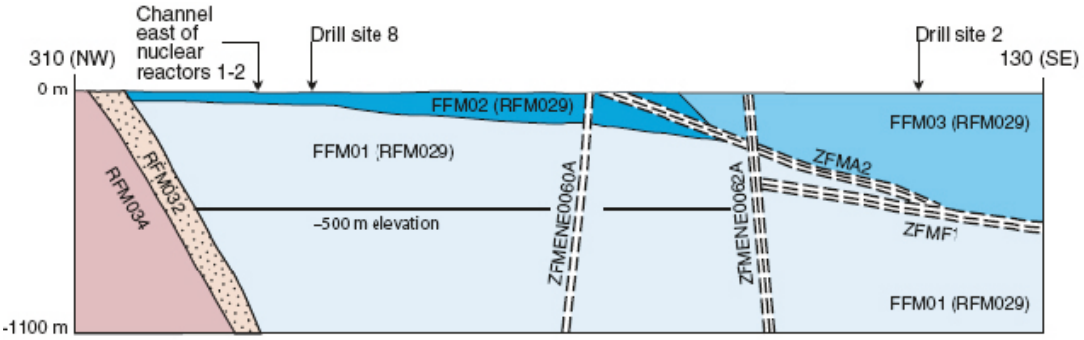

Figure 6-4. *Simplified profile in a NW-SE direction (310–130) that passes through drill sites 2 and 8. Only the high confidence deformation zones ZFMA2, ZFMF1, ZFMENE0060A and ZFMENE0062A are included in the profile /Olofsson et al. 2007/. FFM denotes fracture domain, whereas RFM denotes rock domain.*

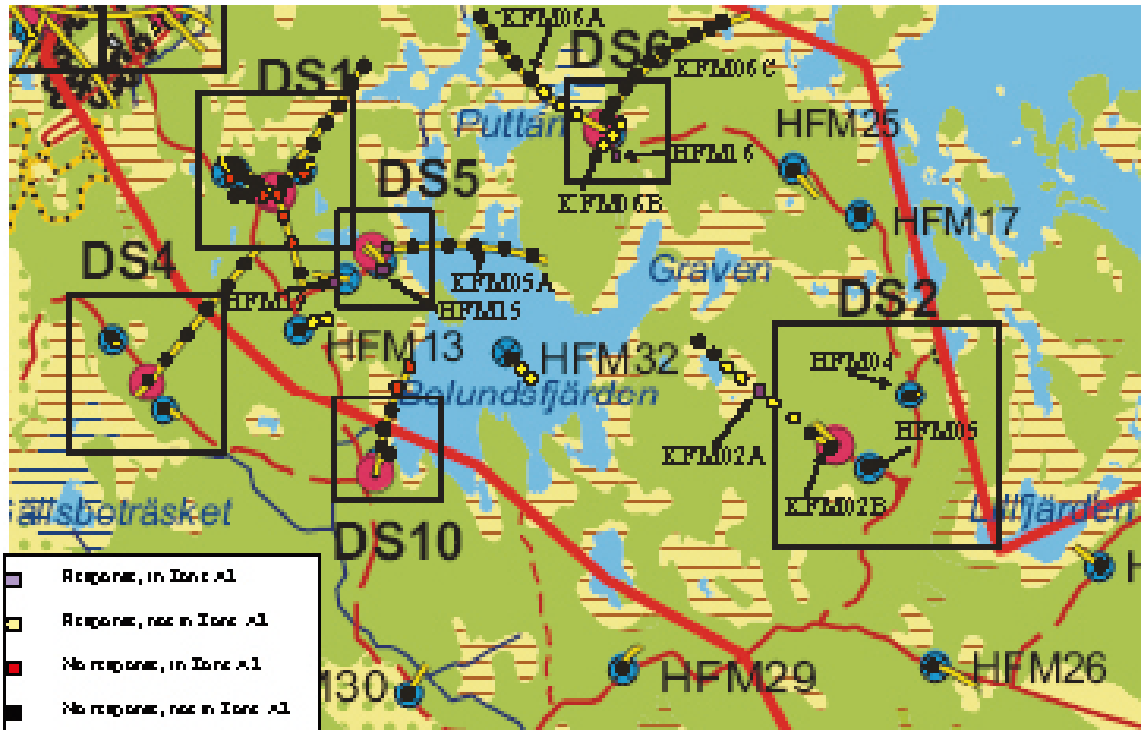

Figure 6-5. *Map of boreholes near KFM02B. The coloured dots indicate response/no response as well as intersection with Zone A2 or not. Where there is more than one dot, each dot represents a section in the borehole. The large red dots represent core-drilled boreholes and the large blue dots percussion-drilled boreholes.*

No responses are noted in the boreholes at drill site 1 or 4, which may be a result of that they are simply too far away from the pumping borehole. Responses are seen in the upper parts of KFM06A and KFM06B although they are not interpreted as Zone A2. However, the responses may be explained by a hydraulic connection between A2 and ZFMA8, ZFMENE0060A, ZFMENE0060B or ZFMB7, which intersect these borehole sections, and also by connection of near-surface fracture networks in the area around HFM16. Also in two sections of HFM13, a response to the pumping is noted. Zone ZFMENE0401 is interpreted to intersect these sections. Two sections of HFM32 are also showing response during the interference test. Although KFM10A is thought to intersect Zone A2 at c 450–500 mbl, no clear responses are noted in these two sections. A small response may be visible in the data from this borehole, but this has not been verified (see Section 1.1.11 in Appendix 6). The section in KFM02A responding most strongly is the injection section KFM02A:5, as expected. Also the adjacent sections KFM02A:4 and KFM02:6 show distinct responses. Zone F1, which is connected to A2, intersects KFM02 in section 3 and 4 and in section 6 where the vuggy granite occurs /Stephens et al. 2007/. Hence, rather strong responses were observed as expected in these sections. Section KFM02A:7 shows a much weaker and slower response which indicates that the hydraulic connection between ZFM1189 and A2 is rather poor.

Table 6-4. Responding sections in the interference test.

Borehole	Section	Bh-length (mbl)	Zone or fracture domain *	Connectivity **
KFM02A	3	490–518	F1	2
	4	443–489	F1	3
	5	411–441	A2	3
	6	241–410	1189	2
	7	133–240	A3	1
KFM05A	5	115–253	– (FFM02)	1
	6	100.07–114	A2	1
KFM06A	6	247–340	NE060A/B7	3
	7	151–246	NE060B	3
	8	100.40–150	– (FFM02)	3
KFM06B	1	51–100	A8	3
	2	27–50	– (FFM02)	3
	3	4.61–26	– (FFM02)	3
HFM15	1	85–95	A2	1
	2	6–84	– (FFM02)	1
HFM16	1	68–132	– (FFM02)	3
	2	54–67	A8	3
	3	12.02–53	A8	3
HFM13	1	159–173	NE0401A	1
	2	101–158	–	1
HFM19	1	168–182	A2	1
	2	104–167	A2	1
	3	12.04–103	– (FFM03)	
HFM32	1	98–203	– (FFM03)	3
	2	32–97	– (FFM03)	2

* /Olofsson et al. 2007/ and /Follin et al. 2008/.

** 0 = no, 1= low, 2 = medium, 3 = high.

When examining the response diagram (Figure 5-5), some groups can be distinguished. This is also illustrated on the map in Figure 6-5. All sections of the four boreholes HFM13, HFM15, HFM19 and KFM05A show slow responses and are observed at the right-hand side of Figure 5-5. HFM16, KFM06A and KFM06B, on the other hand, demonstrate quick responses. Four of the sections in KFM02A stand out and show both relatively strong and fast responses. However, one section in KFM02A displays both slow and weak responses. The two responding sections in HFM32 can be interpreted as yet another group with response time somewhere between the previously mentioned groups.

The groups identified can be geographically separated (Figure 6-5 and Figure 6-6) with one exception, section KFM02A:7. It is difficult to determine whether the differences are due to different characteristics of the zone in the different directions or if it is a matter of distance since the boreholes at or near drill site 6 are somewhat closer to KFM02B (Table 2-5).

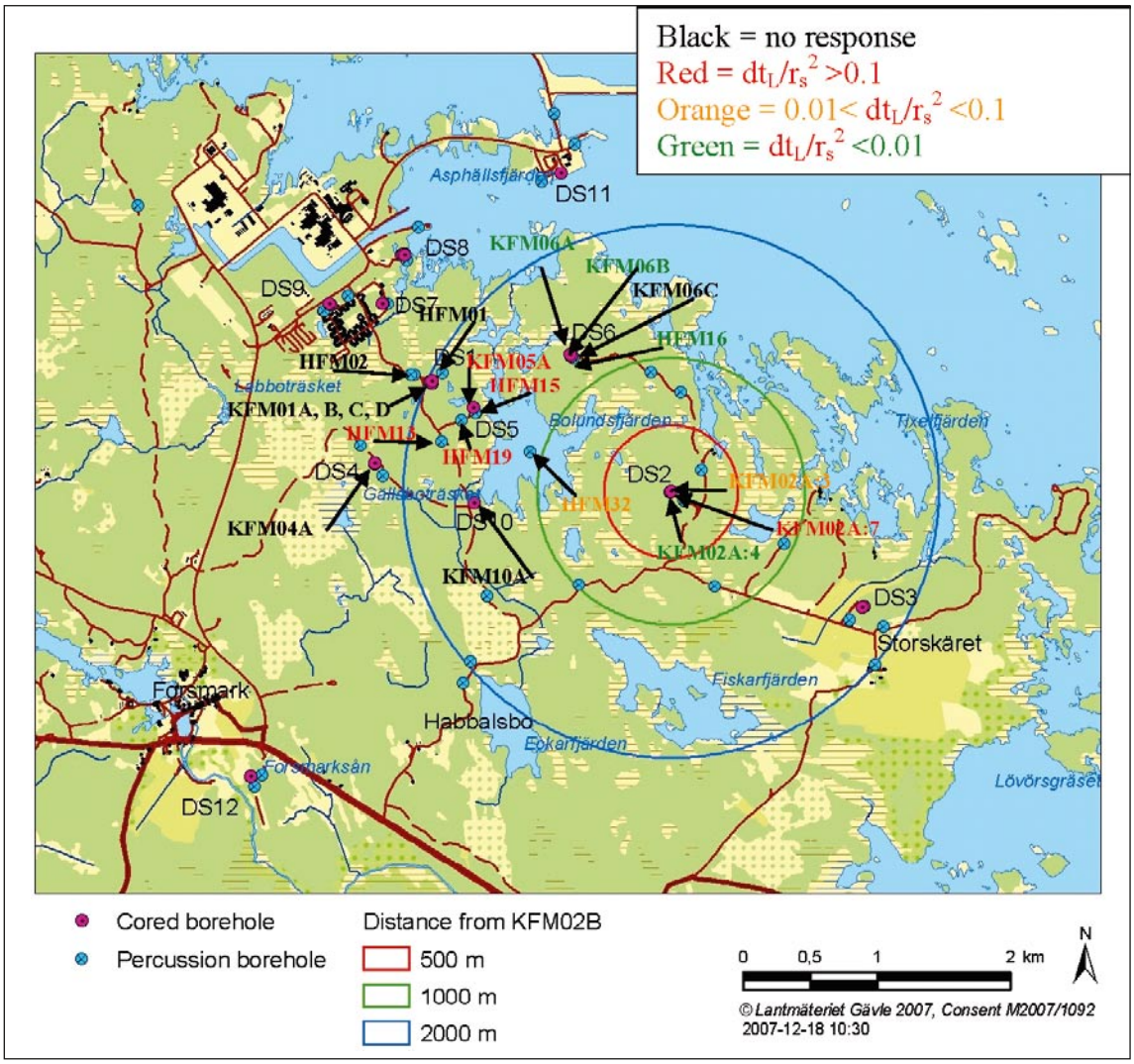

Figure 6-6. *Responses from interference test with pumping in KFM02B. The different colours represent different normalized response time with respect to the distance to the pumping section, dt_L/r_s^2 [s/m²]. Time lag is based on a drawdown of 0.01 m.*

7 References

Almén K-E, Andersson J-E, Carlsson L, Hansson K, Larsson N-Å, 1986. Hydraulic testing in crystalline rock. A comparative study of single-hole test methods. Technical Report 86-27, Svensk Kärnbränslehantering AB.

Andersson P, Andersson J-E, Gustafsson E, Nordqvist R, Voss C, 1993. Site characterization in fractured crystalline rock-A critical Rewiew of Geohydraulic Measurement Methods, SKI Technical report 93:23, Swedish nuclear power inspectorate.

Andersson P, Wass E, Byegård J, Johansson H, Skarnemark G, 1999. Äspö Hard Rock Laboratory. True 1st stage tracer programme. Tracer test with sorbing tracers. Experimental description and preliminary evaluation. SKB IPR-99-15, Svensk Kärnbränslehantering AB.

Andersson P, Byegård J, Winberg A, 2002. Final report of the TRUE Block Scale project 2. Tracer tests in the block scale. SKB TR-02-14, Svensk Kärnbränslehantering AB.

Carlsten S, Döse C, Gustafsson J, Petersson J, Samuelsson E, Stephens M, Thunehed H, 2007. Forsmark site investigation. Geological single-hole interpretation of KFM02B. SKB P-07-107, Svensk Kärnbränslehantering AB.

Carlsten S, Petersson J, Stephens M, Mattsson H, Gustafsson J, 2004. Forsmark site investigation. Geologocal single-hole interpretation of KFM02A and HFM04-05 (DS2). SKB P-04-117 (revised October 2006), Svensk Kärnbränslehantering AB.

Cooley R L, 1979. A method of estimating parameters and assessing reliability for models of steady ground water flow. 2. Applications of statistical analysis. Water Resources Research, 15: 318-324.

Cooper H H Jr, Jacob C E, 1946. A generalized graphical method for evaluating formation constants and summarizing well-field history. Trans. Am. Geophys. Union, vol 27.

Follin S, Hartley L, Joyce S, Marsic N, Martin D, 2008. Hydrogeology Forsmark. Site-descriptive modelling Forsmark stage 2.3. SKB R-08-23 (in prep), Svensk Kärnbränslehantering AB.

Gokall-Norman K, Ludvigson J-E, Hjerne C, 2005. Forsmark site investigation. Single-hole injection tests in borehole KFM05A. SKB P-05-56, Svensk Kärnbränslehantering AB.

Gustafsson E, 2002. Bestämning av grundvattenglödet med utspädningsteknik – Modifiering av utrustning och kompletterande mätningar. SKB R-02-31, Svensk Kärnbränslehantering AB.

Gustafsson E, Nordqvist R, Thur P, 2005. Forsmark site investigation. Groundwater flow measurements in boreholes KFM01A, KFM02A, KFM03A, KFM03B and SWIW tests in KFM02A, KFM03A. SKB P-05-77, Svensk Kärnbränslehantering AB.

Gustafsson E, Nordqvist R, 2005. Oskarshamn site investigation. Groundwater flow measurements and SWIW-tests in boreholes KLX02 and KSH02. SKB P-05-28, Svensk Kärnbränslehantering AB.

Hantush M S, Jacob C E, 1955. Nonsteady radial flow in an infinite leaky aquifer. Am. Geophys. Union Trans., v. 36, no 1, pp. 95–100.

Hjerne C, Ludvigson J-E, Lindquist A, 2005. Forsmark site investigation. Single-hole injection tests in borehole KFM06A and KFM06B. SKB P-05-165, Svensk Kärnbränslehantering AB.

Javandel I, Doughty C, Tsang C F, 1984. Groundwater transport: Handbook of mathematical models. American Geophysical Union, Washington, D.C.

Jönsson S, Ludvigson J-E, 2006. Forsmark site investigation. Pumping tests and flow logging – Boreholes HFM24, HFM32. SKB P-06-96, Svensk Kärnbränslehantering AB.

Källgården J, Ludvigson J-E, Jönsson J, 2004. Forsmark site investigation. Single-hole injection tests in borehole KFM02A. SKB P-04-100, Svensk Kärnbränslehantering AB.

Ludvigson J-E, Jönsson S, Hjerne C, 2004a. Forsmark site investigation. Pumpingtests and flow logging – Boreholes KFM06A (0–100 m) and HFM16. SKB P-04-65, Svensk Kärnbränslehantering AB.

Ludvigson J-E, Jönsson S, Jönsson J, 2004b. Forsmark site investigation. Pumping tests and flow logging – Boreholes HFM13, HFM14 and HFM15. SKB P-04-71, Svensk Kärnbränslehantering AB.

Ludvigson J-E, Källgården J, Hjerne C, 2004c. Forsmark site investigation. Pumping tests and flow logging – Boreholes HFM17, HFM18 and HFM19. SKB P-04-72, Svensk Kärnbränslehantering AB.

Ludvigson J-E, Jönsson S, Levén J, 2004d. Forsmark site investigation. Hydraulic evaluation of pumping activities prior to hydro-geochemical sampling in borehole KFM03A – Comparison with results from difference flow logging. SKB P-04-96, Svensk Kärnbränslehantering AB.

Moench A F, 1985. Transient flow to a large-diameter well in an aquifer with storative semiconfining layers. Water Resources Research, vol. 21, no. 8, pp. 1121–1131.

Moreno L, Neretnieks I, Klockars C-E, 1983. Evaluation of some tracer tests in the granitic rock at Finnsjön. SKB TR 83-38, Svensk Kärnbränslehantering AB.

Moye D G, 1967. Diamond drilling for foundation exploration. Civ. Eng. Trans. 7th. Inst. Eng. Australia.

Ogata A, Banks R, 1961. A solution to the differential equation of longitudinal dispersion in porous media. U.S. Geol. Surv. Prof. Paper 411-A, Washington.

Ohlsson Y, Neretnieks I, 1995. Literature survey of matrix diffusion theory and of experiments and data including natural analogues. SKB TR 95-12, Svensk Kärnbränslehantering AB.

Olofsson I, Simeonov A, Stephens M, Follin S, Nilsson A-C, Röshoff K, Lindberg U, Lanaro F, Fredriksson A, Persson L, 2007. Site descriptive modelling Forsmark, stage 2.2. SKB R-07-15, Svensk Kärnbränslehantering AB.

Rhen I (ed), Gustafson G, Stanfors R, Wikberg P, 1997. Äspö HRL – Geoscientific evaluation 1997/5. Models based on site characterization 1986–1995. SKB TR 97-06, Svensk Kärnbränslehantering AB.

Rouhiainen P, Pöllänen J, 2004. Forsmark site investigation. Difference flow logging in borehole KFM02A. SKB P-04-188, Svensk kärnbränslehantering AB.

SKB, 2006. Site descriptive modelling Forsmark, stage 2.1. SKB R-06-38, Svensk Kärnbränslehantering AB.

SKB, 2005. Preliminary site description Forsmark area-version 1.2. SKB R-05-18, Svensk Kärnbränslehantering AB.

Streltsova T D, 1988. Well testing in heterogeneous formations. Exxon Monograph. John Wiley and sons.

Stephens M, Fox A, La Pointe P, Simeonov A, Isaksson H, Hermanson J, Öhman J, 2007. Geology Forsmark. Site descriptive modelling Forsmark stage 2.2. SKB R-07-45, Svensk Kärnbränslehantering AB.

Tang G H, Frind E O, Sudicky E A, 1981. Contaminant transport in fractured porous media. An analytical solution for a single fracture. Water Resources Research, Vol 17, 555.

Theis C V, 1935. The relation between lowering of the piezometric surface and the rate and duration of discharge of a well using groundwater storage, Am. Geophys. Union Trans., vol. 16, pp. 519–524.

Väisäsvaara J, Pöllänen J, 2007. Forsmark site investigation. Difference flow logging in borehole KFM02B. SKB P-07-83, Svensk Kärnbränslehantering AB.

Wacker P, Bergelin A, Nilsson A-C, 2004. Forsmark site investigation. Hydrochemical characterisation in KFM02A. Results from three investigated borehole sections; 106.5–126.5, 413.5-433.5 and 509.0-516.1 m. SKB P-04-70, Svensk Kärnbränslehantering AB.

Winberg A, Andersson P, Hermansson J, Byegård J, Cvetkovic V, Birgersson L, 2000. Äspö Hard Rock Laboratory. Final report of the first stage of the tracer retention understanding experiment. SKB TR-00-07, Svensk Kärnbränslehantering AB.

Zuber A, 1974. Theoretical possibilities of the two-well pulse method. Isotope Techniques in Groundwater Hydrology 1974, Proc. Symp., Vienna 1974, IAEA,Vienna.

Technical data of boreholes KFM02A and KFM02B

Technical data

Borehole KFM02A

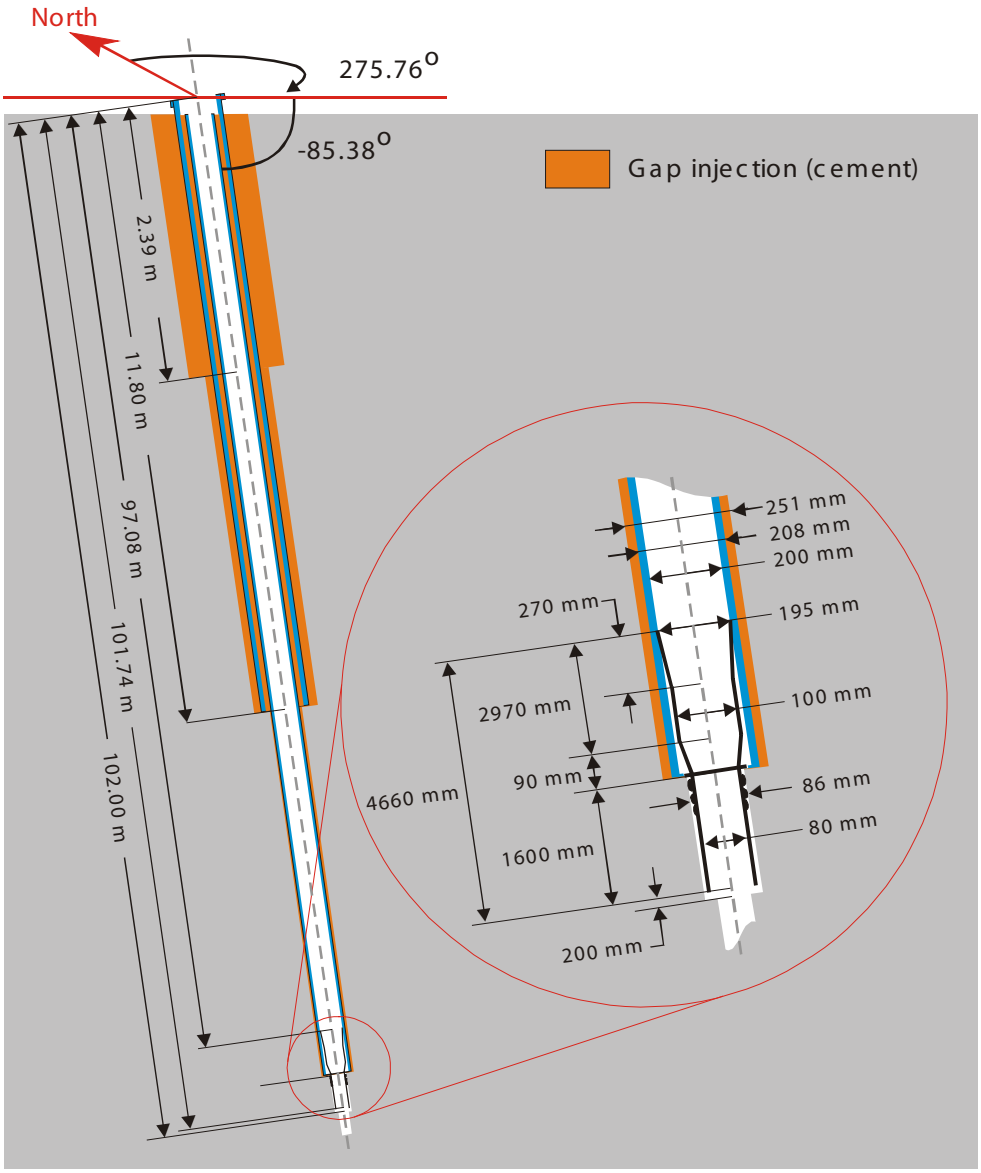

Drilling reference point		
Northing:	6698712.50	(m), RT90 2,5 gon V 0:-15
Easting:	1633182.86	(m), RT90 2,5 gon V 0:-15
Elevation:	7.35	(m), RHB 70
Drilling period		
Drilling start date:	2003-01-08	
Drilling stop date:	2003-03-12	
Borehole		
Lenght:	1002.44 m	

Technical data
Borehole KFM02B

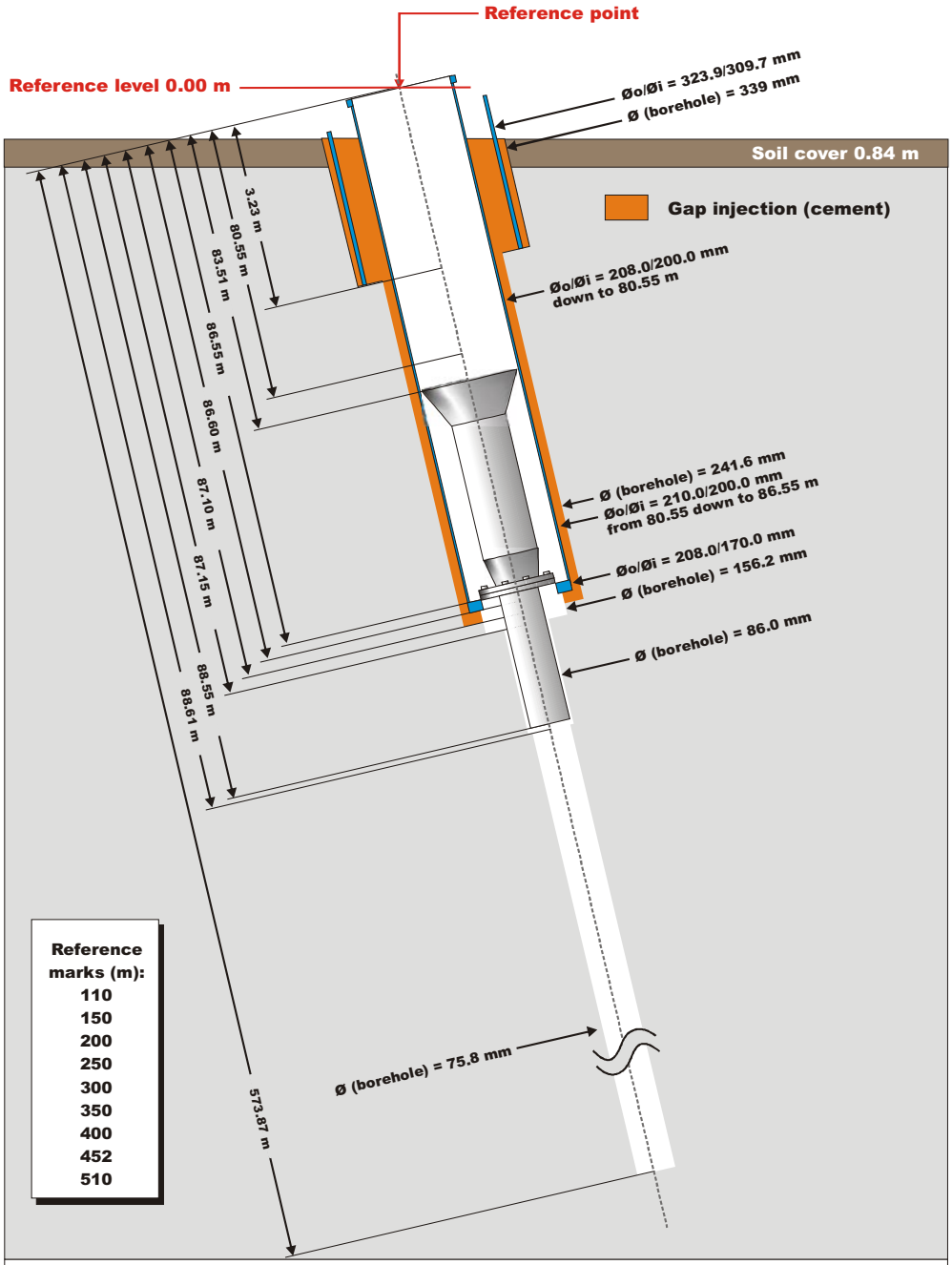

Drilling reference point

Northing:	6698719.19 (m),	RT90 2,5 gon V 0:-15
Easting:	1633186.29 (m),	RT90 2,5 gon V 0:-15
Elevation:	7.62 (m),	RHB 70

Orientation

Bearing (degrees):	313.06 ^{o}
Inclination (degrees):	-80.27 ^{o}

Borehole

Length:	573.87 m

Percussion drilling period

Drilling start date: 2006-01-18
Drilling stop date: 2006-01-30

Core drilling period

Drilling start date: 2006-06-08
Drilling stop date: 2007-02-13

2007-05-28

Appendix 2

Borehole data for interference test boreholes

The column “Test section” in Table A2-1 reports the length of the test sections. In sections “Above packers” and in “Open boreholes” the length of the open intervals are shown. Hence, the casing length is not included in the test section. The casing length of each borehole that showed any response in the interference test can be found in Table A2-2.

Table A2-1. Data for all observation sections involved in the interference test in KFM02B.

Bh ID	Test section (m)	Test type[1]	Test config.	Distance to KFM02B @ 421.25 m (m)	Test start date and time (YYYY-MM-DD hh:mm)	Test stop date and time (YYYY-MM-DD hh:mm)
KFM02B	408.5–434.0	1B	Between packers		2007-03-21 13:00	2007-05-15 10:06
KFM02A:1	889.00–1002.44	2	Below packer	526	2007-03-21 13:00	2007-05-15 10:06
KFM02A:2	519.00–888.00	2	Between packers	287	2007-03-21 13:00	2007-05-15 10:06
KFM02A:3	490.00–518.00	2	Between packers	97	2007-03-21 13:00	2007-05-15 10:06
KFM02A:4	443.00–489.00	2	Between packers	66	2007-03-21 13:00	2007-05-15 10:06
KFM02A:5	411.00–442.00	2	Between packers	47	2007-03-21 13:00	2007-05-15 10:06
KFM02A:6	241.00–410.00	2	Between packers	104	2007-03-21 13:00	2007-05-15 10:06
KFM02A:7	133.00–240.00	2	Between packers	237	2007-03-21 13:00	2007-05-15 10:06
KFM02A:8	100.14–132.00	2	Above packer	307	2007-03-21 13:00	2007-05-15 10:06
HFM05	11.87–200.10	2	Open borehole	303	2007-03-21 13:00	2007-05-15 10:06
HFM04:1	66.90–221.70	2	Below packer	415	2007-03-21 13:00	2007-05-15 10:06
HFM04:2	57.90–65.90	2	Between packers	466	2007-03-21 13:00	2007-05-15 10:06
HFM04:3	12.12–56.90	2	Above packer	486	2007-03-21 13:00	2007-05-15 10:06
HFM17	8.00–210.65	2	Open borehole	778	2007-03-21 13:00	2007-05-15 10:06
HFM29	9.03–199.70	2	Open borehole	986	2007-03-21 13:00	2007-05-15 10:06
HFM18:1	42.00–180.65	2	Below packer	997	2007-03-21 13:00	2007-05-15 10:06
HFM18:2	28.00–41.00	2	Between packers	1,058	2007-03-21 13:00	2007-05-15 10:06
HFM18:3	9.00–27.00	2	Above packer	1,071	2007-03-21 13:00	2007-05-15 10:06
HFM26	12.03–202.70	2	Open borehole	963	2007-03-21 13:00	2007-05-15 10:06
HFM32:1	98.00–202.65	2	Below packer	1,047	2007-03-21 13:00	2007-05-15 10:06
HFM32:2	32.00–97.00	2	Between packers	1,080	2007-03-21 13:00	2007-05-15 10:06

Bh ID	Test section (m)	Test type[1]	Test config.	Distance to KFM02B @ 421.25 m (m)	Test start date and time (YYYY-MM-DD hh:mm)	Test stop date and time (YYYY-MM-DD hh:mm)
HFM32:3	26.00–31.00	2	Between packers	1,095	2007-03-21 13:00	2007-05-15 10:06
HFM32:4	6.03–25.00	2	Above packer	1,100	2007-03-21 13:00	2007-05-15 10:06
KFM05A:1	699.00–1,002.71	2	Below packer	1,157	2007-03-21 13:00	2007-05-15 10:06
KFM05A:2	490.00–698.00	2	Between packers	1,261	2007-03-21 13:00	2007-05-15 10:06
KFM05A:3	273.00–489.00	2	Between packers	1,369	2007-03-21 13:00	2007-05-15 10:06
KFM05A:4	254.00–272.00	2	Between packers	1,435	2007-03-21 13:00	2007-05-15 10:06
KFM05A:5	115.00–253.00	2	Between packers	1,480	2007-03-21 13:00	2007-05-15 10:06
KFM05A:6	100.07–114.00	2	Above packer	1,525	2007-03-21 13:00	2007-05-15 10:06
HFM16:1	68.00–132.50	2	Below packer	1,205	2007-03-21 13:00	2007-05-15 10:06
HFM16:2	54.00–67.00	2	Between packers	1,219	2007-03-21 13:00	2007-05-15 10:06
HFM16:3	12.02–53.00	2	Above packer	1,225	2007-03-21 13:00	2007-05-15 10:06
KFM06B:1	51.00–100.33	2	Below packer	1,240	2007-03-21 13:00	2007-05-15 10:06
KFM06B:2	27.00–50.00	2	Between packers	1,247	2007-03-21 13:00	2007-05-15 10:06
KFM06B:3	6.33–26.00	2	Above packer	1,253	2007-03-21 13:00	2007-05-15 10:06
KFM06A:1	827.00–1,000.64	2	Below packer	1,711	2007-03-21 13:00	2007-05-15 10:06
KFM06A:2	749.00–826.00	2	Between packers	1,618	2007-03-21 13:00	2007-05-15 10:06
KFM06A:3	738.00–748.00	2	Between packers	1,587	2007-03-21 13:00	2007-05-15 10:06
KFM06A:4	363.00–737.00	2	Between packers	1,464	2007-03-21 13:00	2007-05-15 10:06
KFM06A:5	341.00–362.00	2	Between packers	1,360	2007-03-21 13:00	2007-05-15 10:06
KFM06A:6	247.00–340.00	2	Between packers	1,336	2007-03-21 13:00	2007-05-15 10:06
KFM06A:7	151.00–246.00	2	Between packers	1,302	2007-03-21 13:00	2007-05-15 10:06
KFM06A:8	100.40–150.00	2	Above packer	1,282	2007-03-21 13:00	2007-05-15 10:06
KFM06C:1	873.00–1,000.91	2	Below packer	1,395	2007-03-21 13:00	2007-05-15 10:06
KFM06C:2	667.00–872.00	2	Between packers	1,355	2007-03-21 13:00	2007-05-15 10:06
KFM06C:3	647.00–666.00	2	Between packers	1,333	2007-03-21 13:00	2007-05-15 10:06
KFM06C:4	541.00–646.00	2	Between packers	1,323	2007-03-21 13:00	2007-05-15 10:06
KFM06C:5	531.00–540.00	2	Between packers	1,315	2007-03-21 13:00	2007-05-15 10:06
KFM06C:6	402.00–530.00	2	Between packers	1,304	2007-03-21 13:00	2007-05-15 10:06

Bh ID	Test section (m)	Test type[1]	Test config.	Distance to KFM02B @ 421.25 m (m)	Test start date and time (YYYY-MM-DD hh:mm)	Test stop date and time (YYYY-MM-DD hh:mm)
KFM06C:7	351.00–401.00	2	Between packers	1,291	2007-03-21 13:00	2007-05-15 10:06
KFM06C:8	281.00–350.00	2	Between packers	1,284	2007-03-21 13:00	2007-05-15 10:06
KFM06C:9	187.00–280.00	2	Between packers	1,275	2007-03-21 13:00	2007-05-15 10:06
KFM06C:10	100.12–186.00	2	Above packer	1,268	2007-03-21 13:00	2007-05-15 10:06
KFM10A:1	441.00–500.16	2	Below packer	1,342	2007-03-21 13:00	2007-05-15 10:06
KFM10A:2	430.00–440.00	2	Between packers	1,352	2007-03-21 13:00	2007-05-15 10:06
KFM10A:3	353.00–429.00	2	Between packers	1,364	2007-03-21 13:00	2007-05-15 10:06
KFM10A:4	153.00–352.00	2	Between packers	1,404	2007-03-21 13:00	2007-05-15 10:06
KFM10A:5	60.39–152.00	2	Above packer	1,448	2007-03-21 13:00	2007-05-15 10:06
HFM24:1	66.00–151.35	2	Below packer	1,412	2007-03-21 13:00	2007-05-15 10:06
HFM24:2	36.00–65.00	2	Between packers	1,446	2007-03-21 13:00	2007-05-15 10:06
HFM24:3	18.03–35.00	2	Above packer	1,461	2007-03-21 13:00	2007-05-15 10:06
HFM30:1	177.00 –200.75	2	Below packer	1,494	2007-03-21 13:00	2007-05-15 10:06
HFM30:2	74.00–176.00	2	Between packers	1,530	2007-03-21 13:00	2007-05-15 10:06
HFM30:3	61.00–73.00	2	Between packers	1,566	2007-03-21 13:00	2007-05-15 10:06
HFM30:4	18.03–60.00	2	Above packer	1,533	2007-03-21 13:00	2007-05-15 10:06
HFM15:1	85.00–95.00	2	Below packer	1,605	2007-03-21 13:00	2007-05-15 10:06
HFM15:2	6.00–84.00	2	Above packer	1,584	2007-03-21 13:00	2007-05-15 10:06
HFM19:1	168.00–182.00	2	Below packer	1,711	2007-03-21 13:00	2007-05-15 10:06
HFM19:2	104.00–167.00	2	Between packers	1,692	2007-03-21 13:00	2007-05-15 10:06
HFM19:3	12.04–103.00	2	Above packer	1,659	2007-03-21 13:00	2007-05-15 10:06
HFM13:1	159.00–173.00	2	Below packer	1,717	2007-03-21 13:00	2007-05-15 10:06
HFM13:2	101.00–158.00	2	Between packers	1,715	2007-03-21 13:00	2007-05-15 10:06
HFM13:3	14.90–100.00	2	Above packer	1,712	2007-03-21 13:00	2007-05-15 10:06
KFM01C:1	238.00–450.05	2	Below packer	1,764	2007-03-21 13:00	2007-05-15 10:06
KFM01C:2	59.00–237.00	2	Between packers	1,856	2007-03-21 13:00	2007-05-15 10:06
KFM01C:3	11.96–58.00	2	Above packer	1,916	2007-03-21 13:00	2007-05-15 10:06
KFM03A:1	969.50–994.50	2	Below packer	1,762	2007-03-21 13:00	2007-05-15 10:06

Bh ID	Test section (m)	Test type[1]	Test config.	Distance to KFM02B @ 421.25 m (m)	Test start date and time (YYYY-MM-DD hh:mm)	Test stop date and time (YYYY-MM-DD hh:mm)
KFM03A:2	820.50–968.50	2	Between packers	1,747	2007-03-21 13:00	2007-05-15 10:06
KFM03A:3	651.00–819.50	2	Between packers	1,728	2007-03-21 13:00	2007-05-15 10:06
KFM03A:4	633.50–650.00	2	Between packers	1,723	2007-03-21 13:00	2007-05-15 10:06
KFM03A:5	472.50–632.50	2	Between packers	1,723	2007-03-21 13:00	2007-05-15 10:06
KFM03A:6	402.50–471.50	2	Between packers	1,728	2007-03-21 13:00	2007-05-15 10:06
KFM03A:7	351.50–401.50	2	Between packers	1,734	2007-03-21 13:00	2007-05-15 10:06
KFM03A:8	11.96–350.50	2	Above packer	1,761	2007-03-21 13:00	2007-05-15 10:06
KFM03B:1	52.00–101.54	2	Below packer	1,774	2007-03-21 13:00	2007-05-15 10:06
KFM03B:2	5.00–51.00	2	Above packer	1,788	2007-03-21 13:00	2007-05-15 10:06
HFM01:1	46.50–200.20	2	Below packer	1,869	2007-03-21 13:00	2007-05-15 10:06
HFM01:2	33.50–45.50	2	Between packers	1,887	2007-03-21 13:00	2007-05-15 10:06
HFM01:3	31.93–32.50	2	Above packer	1,889	2007-03-21 13:00	2007-05-15 10:06
KFM01D:1	439.00–800.24	2	Below packer	1,872	2007-03-21 13:00	2007-05-15 10:06
KFM01D:2	429.00–438.00	2	Between packers	1,869	2007-03-21 13:00	2007-05-15 10:06
KFM01D:3	322.00–428.00	2	Between packers	1,872	2007-03-21 13:00	2007-05-15 10:06
KFM01D:4	311.00–321.00	2	Between packers	1,878	2007-03-21 13:00	2007-05-15 10:06
KFM01D:5	253.00–310.00	2	Between packers	1,882	2007-03-21 13:00	2007-05-15 10:06
KFM01D:6	154.00–252.00	2	Between packers	1,894	2007-03-21 13:00	2007-05-15 10:06
KFM01D:7	89.51–153.00	2	Above packer	1,910	2007-03-21 13:00	2007-05-15 10:06
KFM04A:1	496.00–1,001.42	2	Below packer	1,962	2007-03-21 13:00	2007-05-15 10:06
KFM04A:2	391.00–495.00	2	Between packers	2,040	2007-03-21 13:00	2007-05-15 10:06
KFM04A:3	246.00–390.00	2	Between packers	2,078	2007-03-21 13:00	2007-05-15 10:06
KFM04A:4	230.00–245.00	2	Between packers	2,106	2007-03-21 13:00	2007-05-15 10:06
KFM04A:5	186.00–229.00	2	Between packers	2,117	2007-03-21 13:00	2007-05-15 10:06
KFM04A:6	164.00–185.00	2	Between packers	2,129	2007-03-21 13:00	2007-05-15 10:06
KFM04A:7	106.95–163.00	2	Above packer	2,144	2007-03-21 13:00	2007-05-15 10:06
KFM01A:1	431.00–10,0149	2	Below packer	2,021	2007-03-21 13:00	2007-05-15 10:06
KFM01A:2	374.00–430.00	2	Between packers	1,944	2007-03-21 13:00	2007-05-15 10:06

Bh ID	Test section (m)	Test type[1]	Test config.	Distance to KFM02B @ 421.25 m (m)	Test start date and time (YYYY-MM-DD hh:mm)	Test stop date and time (YYYY-MM-DD hh:mm)
KFM01A:3	205.00–373.00	2	Between packers	1,933	2007-03-21 13:00	2007-05-15 10:06
KFM01A:4	131.00–204.00	2	Between packers	1,930	2007-03-21 13:00	2007-05-15 10:06
KFM01A:5	109.00–130.00	2	Between packers	1,932	2007-03-21 13:00	2007-05-15 10:06
KFM01A:6	100.48–108.00	2	Above packer	1,933	2007-03-21 13:00	2007-05-15 10:06
KFM01B:1	142.00–500.52	2	Below packer	1,983	2007-03-21 13:00	2007-05-15 10:06
KFM01B:2	101.00–141.00	2	Between packers	1,955	2007-03-21 13:00	2007-05-15 10:06
KFM01B:3	15.53–100.00	2	Above packer	1,953	2007-03-21 13:00	2007-05-15 10:06
HFM08:1	117.00–143.50	2	Below packer	1,984	2007-03-21 13:00	2007-05-15 10:06
HFM08:2	18.00–116.00	2	Above packer	1,984	2007-03-21 13:00	2007-05-15 10:06
HFM12:1	57.50–209.55	2	Below packer	2,066	2007-03-21 13:00	2007-05-15 10:06
HFM12:2	14.90–56.50	2	Above packer	2,014	2007-03-21 13:00	2007-05-15 10:06
SFM0005	2.21–3.21	2	Open borehole		2007-03-21 13:00	2007-05-15 10:06
SFM0004	5.02–6.02	2	Open borehole		2007-03-21 13:00	2007-05-15 10:06
SFM0073	3.50–4.50	2	Open borehole		2007-03-21 13:00	2007-05-15 10:06
SFM0028	7.00–8.00	2	Open borehole		2007-03-21 13:00	2007-05-15 10:06
SFM0106	3.00–4.00	2	Open borehole		2007-03-21 13:00	2007-05-15 10:06
SFM0081	4.85–5.25	2	Open borehole		2007-03-21 13:00	2007-05-15 10:06
SFM0040	1.50–2.50	2	Open borehole		2007-03-21 13:00	2007-05-15 10:06
SFM0021	2.00–3.00	2	Open borehole		2007-03-21 13:00	2007-05-15 10:06
SFM0068	0.80–1.80	2	Open borehole		2007-03-21 13:00	2007-05-15 10:06
SFM0022	5.30–5.80	2	Open borehole		2007-03-21 13:00	2007-05-15 10:06
SFM0105	2.00–3.00	2	Open borehole		2007-03-21 13:00	2007-05-15 10:06
SFM0062	3.25–3.65	2	Open borehole		2007-03-21 13:00	2007-05-15 10:06
SFM0084	3.70–4.10	2	Open borehole		2007-03-21 13:00	2007-05-15 10:06
SFM0033	3.00–4.00	2	Open borehole		2007-03-21 13:00	2007-05-15 10:06
SFM0080	8.62–9.62	2	Open borehole		2007-03-21 13:00	2007-05-15 10:06
SFM0019	4.50–5.50	2	Open borehole		2007-03-21 13:00	2007-05-15 10:06
SFM0030	4.00–5.00	2	Open borehole		2007-03-21 13:00	2007-05-15 10:06

Bh ID	Test section (m)	Test type[1]	Test config.	Distance to KFM02B @ 421.25 m (m)	Test start date and time (YYYY-MM-DD hh:mm)	Test stop date and time (YYYY-MM-DD hh:mm)
SFM0069	1.00–2.00	2	Open borehole		2007-03-21 13:00	2007-05-15 10:06
SFM0058	2.85–3.85	2	Open borehole		2007-03-21 13:00	2007-05-15 10:06
SFM0006	3.21–4.21	2	Open borehole		2007-03-21 13:00	2007-05-15 10:06
SFM0008	5.14–6.14	2	Open borehole		2007-03-21 13:00	2007-05-15 10:06
SFM0034	2.00–3.00	2	Open borehole		2007-03-21 13:00	2007-05-15 10:06
SFM0039	1.10–2.10	2	Open borehole		2007-03-21 13:00	2007-05-15 10:06
SFM0003	8.98–10.98	2	Open borehole		2007-03-21 13:00	2007-05-15 10:06
SFM0036	1.99–2.99	2	Open borehole		2007-03-21 13:00	2007-05-15 10:06
SFM0091	1.90–2.30	2	Open borehole		2007-03-21 13:00	2007-05-15 10:06

[1)] 1B: Pumping test-submersible pump, 2: Interference test

Table A2-2. Pertinent technical data of the pumping borehole and the observation boreholes with a detected response from the pumping in KFM02B. (From Sicada).

Borehole data							
Bh ID	**Elevation of top of casing (ToC) (m.a.s.l.)**	**Borehole interval from ToC (m)**	**Casing/ Bh-diam. (m)**	**Inclinationtop of bh (from horizontal plane) (°)**	**Dip-direction-top of borehole (from local N)(°)**	**Remarks**	**Drilling finished Date (YYYY–MM–DD)**
KFM02A	7.353	0.00–2.39	0.44	–85.385	275.764	Borehole	2003-03-12
”		2.39–11.80	0.358			Borehole	
”		11.80–100.35	0.251			Borehole	
”		100.35–100.42	0.164			Borehole	
”		100.42–102.00	0.086			Borehole	
”		102.00–1002.44	0.077			Borehole	
”		0.00–100.14	0.2			Casing ID	
”		0.10–11.80	0.265			Casing ID	
HFM32	0.974	0.00–6.03	0.175	–86.057	116.146	Borehole	2006-01-14
		6.03–106.60	0.139			Borehole	
		106.60–169.65	0.136			Borehole	
		169.65–202.65	0.132			Borehole	
		0.00–5.94	0.16			Casing ID	
		5.94–6.03	0.143			Casing ID	
KFM05A	5.528	0.00–12.25	0.34	–59.804	80.897	Borehole	2004-05-05
”		12.25–100.30	0.244			Borehole	
”		100.30–100.35	0.164			Borehole	
”		100.35–110.10	0.086			Borehole	
”		110.10–1,002.71	0.077			Borehole	
”		0.00–100.02	0.2			Casing ID	
”		0.00–12.25	0.31			Casing ID	
”		0.19–12.25	0.309			Casing ID	
”		100.02–100.07	0.17			Casing ID	
HFM16	3.21	0.00–12.02	0.195	–84.218	327.957	Borehole	2003-11-11
”		12.02–82.00	0.14			Borehole	
”		82.00–132.50	0.139			Borehole	
”		0.00–12.02	0.16			Casing ID	
KFM06B	4.13	0.00–3.88	0.116	–83.52	296.96	Borehole	2003-06-08
”		3.88–4.61	0.101			Borehole	
”		4.61–6.33	0.086			Borehole	
		6.33–54.65	0.077			Borehole	
		54.65–56.40	0.084			Borehole	
”		56.40–100.33	0.077			Borehole	
”		0.00–6.33	0.078			Casing ID	
KFM06A	4.1	0.00–2.12	0.415	–60.25	300.92	Borehole	2004-09-21
”		2.12–12.30	0.333			Borehole	
”		12.30–100.59	0.243			Borehole	
”		100.59–100.64	0.164			Borehole	
”		100.64–102.19	0.086			Borehole	
”		102.19–1,000.64	0.077			Borehole	
”		0.00–100.35	0.2			Casing ID	

Borehole data							
Bh ID	**Elevation of top of casing (ToC) (m.a.s.l.)**	**Borehole interval from ToC (m)**	**Casing/ Bh-diam. (m)**	**Inclinationtop of bh (from horizontal plane) (°)**	**Dip-direction-top of borehole (from local N)(°)**	**Remarks**	**Drilling finished Date (YYYY–MM–DD)**
”		0.19–2.12	0.392			Casing ID	
”		0.19–12.30	0.310			Casing ID	
”		100.35–100.40	0.17			Casing ID	
HFM15	3.878	0.00–6.00	0.176	–43.7	314.305	Borehole	2003-10-15
”		6.00–99.50	0.139			Borehole	
”		0.00–6.00	0.16			Casing ID	
HFM19	3.656	0.00–12.04	0.18	–58.103	280.915	Borehole	2003-12-18
”		12.04–185.20	0.137			Borehole	
”		0.00–12.04	0.16			Casing ID	
HFM13	5.687	0.00–4.40	0.235	–58.845	51.194	Borehole	2003-10-02
”		4.40–14.90	0.189			Borehole	
”		14.90–101.00	0.138			Borehole	
”		101.00–152.35	0.137			Borehole	
”		152.35–175.60	0.135			Borehole	
”		0.00–14.90	0.16			Casing ID	

Table A2-3. Coordinates of the observation boreholes with a detected response from the pumping in KFM02B. (From Sicada).

Borehole data		
Bh ID	**Northing (m)**	**Easting (m)**
KFM02B	6.698,719.19	1.633,186.29
HFM32	6.699,015.036	1.632,137.068
KFM05A	6.699,344.850	1.631,710.804
HFM16	6.699,721.098	1.632,466.182
KFM06B	6.699,732.240	1.632,446.410
KFM06A	6.699,732.880	1.632,442.510
HFM15	6.699,312.444	1.631,733.081
HFM19	6.699,257.585	1.631,626.925
HFM13	6.699,093.678	1.631,474.404

Appendix 3

Preparation of synthetic groundwater and tracer solutions

The synthetic groundwater was prepared at the Geosigma laboratory in Uppsala. The water was prepared by weighing and adding salts to 25 L cans with tap water from Forsmark. To calculate the addition of salts needed to achieve the same concentrations of the main constituents as the water in the fracture of current interest, results from earlier sampling in KFM02A /Wacker et al. 2004/ and from the tap water in Forsmark were used. The different salts were weighed and stored in bottles and cans for transport to Forsmark where they were mixed with the rest of the tap water in the large tanks. In table A3-1 the chemical composition of the tap water and groundwater from KFM02A:5 are presented together with the theoretical chemical composition of the prepared synthetic groundwater. The analysis of the tap water was made years ago, hence a new sample was taken from the tap to control the chemical composition. However, the calculation of the amounts of chemicals needed was based on the old tap water sample result.

Two different synthetic groundwater solutions were prepared. One of them, the "clean synthetic groundwater" was used as rinsing water and was injected (at the same rate) after the injection of tracers to keep the pressure constant and maintain the 1/100 dipole. Also a portion of the "clean synthetic groundwater" was mixed with Rhodamine WT and used as tracer solution in the pre-test. The other solution was used as tracer solution in the main tracer test. Two different groundwater solutions had to be prepared since three of the tracers (Li, Cs and Rb) were added as chloride salts. Hence, the composition of the synthetic groundwater used in the pre-test and for rinsing was different from the synthetic groundwater used in the main tracer test. In the synthetic groundwater used in the main tracer test many of the sodium salts were exchanged for lithium salts. Table A3-2 shows the chemicals and the amounts used to prepare the synthetic groundwater.

Each synthetic groundwater was prepared as four different concentrated solutions which were then mixed together in the large tank in Forsmark (A and B) or injected as sub flows (C and D). Solutions A and B were mixed at concentrations 50 times higher than in the final solution, in 25 L cans at the laboratory in Uppsala and were then mixed with water in the 5 m^3 tank at the drill site. Solutions C and D were mixed in higher concentrations and then injected as sub flows at a lower, proper rate to achieve the desired concentration in the tracer solution/synthetic groundwater. Table A3-3 shows the concentrations and flow rates used for the sub flows during the different phases of the experiment.

Table A3-1. Chemical composition of groundwater, synthetic groundwater and tap water used for preparing synthetic groundwater.

	Results from analyses			Theoretical composition of Prepared solutions	
	Tap water First analysis	KFM02A [1]	Tap water Second analysis (control sample)	Pre-test and rinsing	Main tracer test
Na(mg/l)	23.4	1,820	28.4	1,828	9.87
K(mg/l)	1.05	21.4	1.46	20.8	20.8
Ca(mg/l)	29.9	1,140	32.7	1,131	1131
Mg(mg/l)	1.9	198	1.9	199	199
Mn(mg/l)	–	1.81	–	1.81	1.81
Si(mg/l)	1.59	7.8	2.14	6.0	6.0
Sr(mg/l)	< 0.037	11.2	0.041	11.2	11.2
Ba(µg/l)	–	0.0856	–	0.0857	0.0857
HCO_3(mg/l)	71.1	93	77.7	91.0	90.9
Cl(mg/l)	6.4	5,380	8.1	5,076	5,186
SO_4(mg/l)	64.1	434	73.9	377	379
SO_4_S(mg/l)	20.9	136	25.8		
Br(mg/l)	< 0.039	25.8	< 0.2	25.8	26.3
F(mg/l)	< 0.2	< 0.2	–	0.20	0.20
NH_4 (N) (mg/l)	–	1.88	–	1.88	1.88
Fe(mg/l)	–	0.736	–		
Fe_{TOT}(mg/l)	–	0.747	–		
Fe(II) (mg/l)	–	0.727	–	0.748	0.748
Li(mg/l)	< 0.004	0.057	< 0.004	0.054	554 [2]
Rb(µg/l)	–	58.3	–	58.3	146,760 [2]
Cs(µg/l)	–	1.9	–	1.9	39,108 [2]
pH(pH)	7.88	7.37	8.03		
COND(mS/m)	28.2	1,640	32.7		

[1] /Wacker et al. 2004/.

[2] Used as tracers and added in excess amounts.

Table A3-2. Chemicals added to the tap water for preparation of synthetic groundwater.

Solution	Chemical	Amount added to tap water Main tracer test (mg/l)	Amount added to tap water Pre test and rinsing (mg/l)	Comment
A	LiCl	2907.1	0.331	
	NaCl	0	4031.3	
	KCl	39.68	39.68	
	RbCl	207.6	0.083	
	CsCl	49.54	0.002	
	$MgCl_2 * 6H_2O$	1663.8	1663.8	
	$CaCl_2 * 2H_2O$	4148.4	4148.4	
	$SrCl_2 * 6H_2O$	34.16	34.16	
	$BaCl_2*2H_2O$	0.067	0.067	
	NH_4Cl	5.578	5.578	
B	NaF	–	0.442	
	NaBr	–	33.23	
	Na_2SO_4r	–	556.2	
	LiF	0.267	–	
	LiBr	28.63	–	
	Li_2SO_4	432.8	–	
	HCl (100%)	15.63	15.63	HCl 37% was used and weight recalculated
	Na_2S	0.024	0.024	
	$Na_2Si_3O_7$	51.91	51.91	
Sub-flows				
C	$NaHCO_3$	–	125.29	
	Li_2CO_3	110.0	–	
	HCl (100%)	54.30	–	HCl 37% was used and weight recalculated
D	$FeSO_4*7H_2O$	3.726	3.726	
	$MnCl_2$	4.144	4.144	

Table A3-3. Sub flows added to the synthetic groundwater.

		Pre test (Q_{pump} = 19.8 L/min) (Q_{inj} ≈ 200 ml/min)		Main tracer test (Q_{pump} = 24.8 L/min) (Q_{inj} ≈ 250 ml/min)		Rinsing (Q_{pump}= 24.8 L/min) (Q_{inj} ≈ 250 ml/min)	
Solution	**Chemical**	**Concentration in solution (g/l)**	**Subinjection flow (ml/min)**	**Concentration in solution (g/l)**	**Subinjection flow (ml/min)**	**Concentration in solution (g/l)**	**Subinjection flow (ml/min)**
C	$NaHCO_3$	62.65	0.400	–	1.250	62.65	0.500
	Li_2CO_3	–		22.01		–	
	HCl (100%)	–		10.86		–	
D	$FeSO_4 * 7H_2O$	3.726	0.200	3.726	0.250	3.726	0.250
	$MnCl_2$	4.144		4.144		4.144	

Appendix 4

Calculation of normalized mass flux

Injection borehole (KFM02A)

After the mass flux was calculated, it was integrated to calculate the total injected mass of each tracer and finally the mass flux function was normalized by dividing it by the total injected mass of each tracer, respectively.

First, the representative injection flow (Q_t) for the concentration measured at time t was calculated according to Equation A4-1 and Figure A4-1.

$$Q_t = \frac{\sum_{-\Delta t_1/2}^{\Delta t 2/2} dQ_{inj} \times dt}{\frac{\Delta t_1}{2} + \frac{\Delta t_2}{2}} \qquad \text{(A4-1)}$$

where Q_t is the representative injection flow at the time t, Δt_1 is the time to the previous measured concentration point and Δt_2 is the time to the next measured concentration point.

The mass flux (m_t) from KFM02A into the fracture at time, t, was then calculated by multiplying the measured concentration (c_t) by the representative injection flow rate at that time (Q_t).

$$m_t = Q_t \times c_t \qquad \text{(A4-2)}$$

The total mass of the different tracers injected (M_{tot}) were calculated by numerical integration of the calculated mass flux assuming that the mass flux calculated in one point is constant until the next measured point according to Equation A4-3 and Figure A4-2.

$$M_{tot} = \sum \Delta M_t = \sum \left(m_t \times \Delta t_2 \right) \qquad \text{(A4-3)}$$

Finally the mass flux was divided by the total injected mass (for each tracer respectively) and plotted against elapsed time to calculate the function of normalized mass flux used in the model tool.

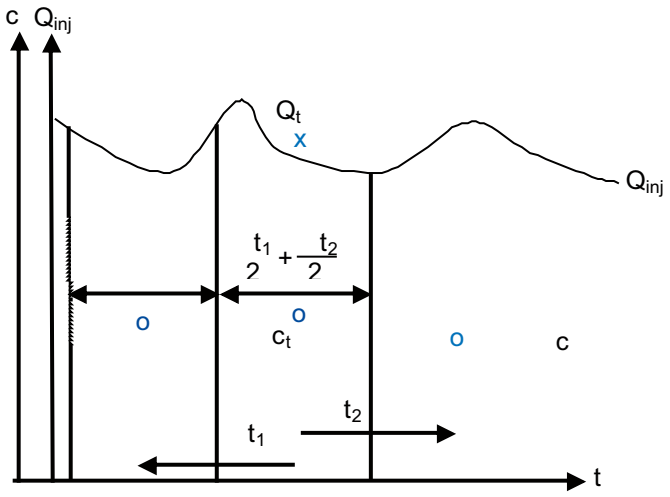

Figure A4-1. *Principle of calculation of a representative flow rate at time t.*

During some time periods, the increase/decrease of tracer concentration between two measured points was big and the time between samples analysed was long. When this occurred, the concentration between two points was calculated by linear interpolation to prevent a major over- or under estimation of mass flux. The flow rate was logged and stored in the logger every five minutes.

Withdrawal borehole (KFM02B)

The breakthrough curve from KFM02B was also transformed into mass flux against elapsed time. This calculation was much easier since the withdrawal rate was constant (no integration needed). The mass flux from KFM02B was calculated by multiplying the concentration measured at each time by the withdrawal rate.

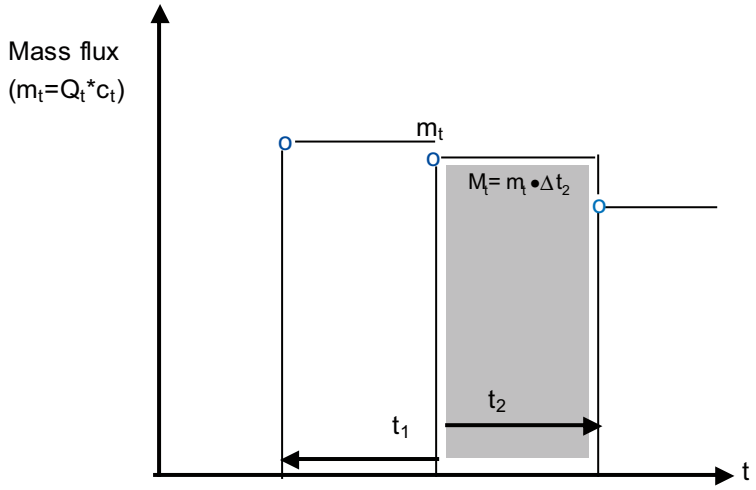

Figure A4-2. *Principle for calculation of total injected mass.*

Appendix 5

Groundwater levels (m.a.s.l)

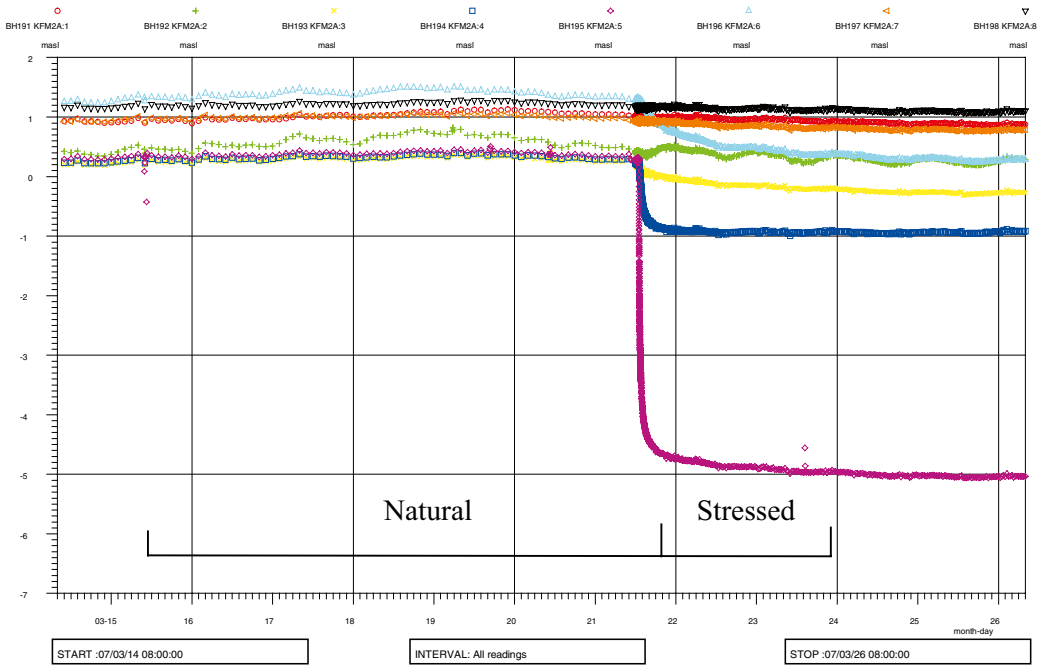

Figure A5-1. *Groundwater levels in KFM02A during the groundwater flow measurements. Measured section: KFM02A:5 (purple).*

Appendix 6

Transient evaluation of responses in the pumping section and in the observation sections

Standard transient evaluation was made for the pumping borehole KFM02B and all observation sections in which pressure interference was detected. However, in some boreholes the response was very small and the transient evaluation was considered to be too uncertain and thus no evaluated parameters are presented. Before the analysis, the observed drawdown and recovery curves were corrected for the estimated natural head trend during the rest period. A certain linear correction was applied to each section, based on the linear head-time diagrams presented below.

Abbreviations of flow regimes and hydraulic boundaries that may appear in the text are as follows:

WBS = Wellbore storage
PRF = Pseudo-radial flow regime
PLF = Pseudo-linear flow regime
PSF = Pseudo-spherical (leaky) flow regime
PSS = Pseudo-stationary flow regime
NFB = No-flow boundary
CHB = Constant-head boundary

In this appendix metres above sea level in the coordinate system RHB 70 is used frequently. This is shortened to m.a.s.l in text and tables.

Pumping borehole KFM02B: 408.5–434.0 m

General test data for the pumping test in KFM02B are presented in Table A6-1.

Table A6-1. General test data for the pumping test in KFM02B: 408.5–434.0 mbl.

General test data			
Pumping borehole	KFM02B		
Test type[1)]	Constant Rate withdrawal and recovery test		
Test section (open borehole/packed-off section):	open borehole		
Test No	1		
Field crew	GEOSIGMA AB		
Test equipment system			
General comment	Interference test		
	Nomen-clature	Unit	Value
Borehole length	L	m	573.87
Casing length	L_c	m	86.60
Test section- secup	Secup	mbl	408.5
Test section- seclow	Seclow	mbl	434.0
Test section length	L_w	m	25.5
Test section diameter[2)]	$2 \cdot r_w$	mm	76
Test start (start of pressure registration)		yymmdd hh:mm	070321 10:47:15
Packer expanded		yymmdd hh:mm:ss	
Start of flow period		yymmdd hh:mm:ss	070321 13:00:02
Stop of flow period		yymmdd hh:mm:ss	070515 10:06:05
Test stop (stop of pressure registration)		yymmdd hh:mm	070529 07:50:08
Total flow time	t_p	min	78966
Total recovery time	t_F	min	20084

Pressure data			
Relative pressure in test section before start of flow period	p_i	kPa	616.80
Relative pressure in test section before stop of flow period	p_p	kPa	516.10
Relative pressure in test section at stop of recovery period	p_F	kPa	613.73
Pressure change during flow period ($p_i - p_p$)	dp_p	kPa	100.70

Flow data			
Flow rate from test section just before stop of flow period	Q_p	m^3/s	$4.12 \cdot 10^{-4}$
Mean (arithmetic) flow rate during flow period	Q_m	m^3/s	$3.93 \cdot 10^{-4}$
Total volume discharged during flow period	V_p	m^3	$1.87 \cdot 10^{3}$

Manual groundwater level measurements in KFM02B			**GW level**	
Date YYYY-MM-DD	**Time tt:mm**	**Time (min)**	**(m b. ToC)**	**(m.a.s.l.)**
2007-03-20	15:30	15:30	6.71	1.01
2007-03-21	10:26	10:26	6.72	1.00

[1)] Constant Head injection and recovery or Constant Rate withdrawal and recovery

[2)] Nominal diameter

Comments on the test

The test was performed as a constant-flow rate pumping test. The average flow rate was c 23.6 l/min and the duration of the flow period was c 55 days. During the first 13 days of the pumping the flow rate was c 19.8 l/min. After that the flow rate was increased to c 24.7 l/min, which also was the final flow rate. The final drawdown in KFM02B was approximately 10 m. The pressure recovery was measured for almost 14 days. Overviews of the flow rate and pressure responses in KFM02B are presented in Figure A6-1. The pressure responses in log-log and lin-log diagrams during the flow period are presented in Figures A7-2 and A7-3 in Appendix 7. In Figures A7-4 and A7-5, log-log and lin-log diagrams of the recovery period are shown.

Interpreted flow regimes

After initial pseudo-linear flow, pseudo-radial flow occurred between c 3-30 min during the flow period and c 2-40 min during the recovery period, followed by a transition to pseudo-spherical flow during both the flow and recovery period.

Interpreted parameters

Transient evaluation was based on variable flow rate. The agreement in evaluated parameter values between the flow and recovery period is good. The parameter values from the flow period are selected as the most representative.

Transient, quantitative interpretation of the flow period is shown in log-log and lin-log diagrams in Figures A7-2 and A7-3 and of the recovery period in Figures A7-4 and A7-5, all in Appendix 7. The results from the transient evaluation of the single-hole pumping test in KFM02B are summarized in Table 5-4 and in the Test Summary Sheet, Table 5-6 in the main report.

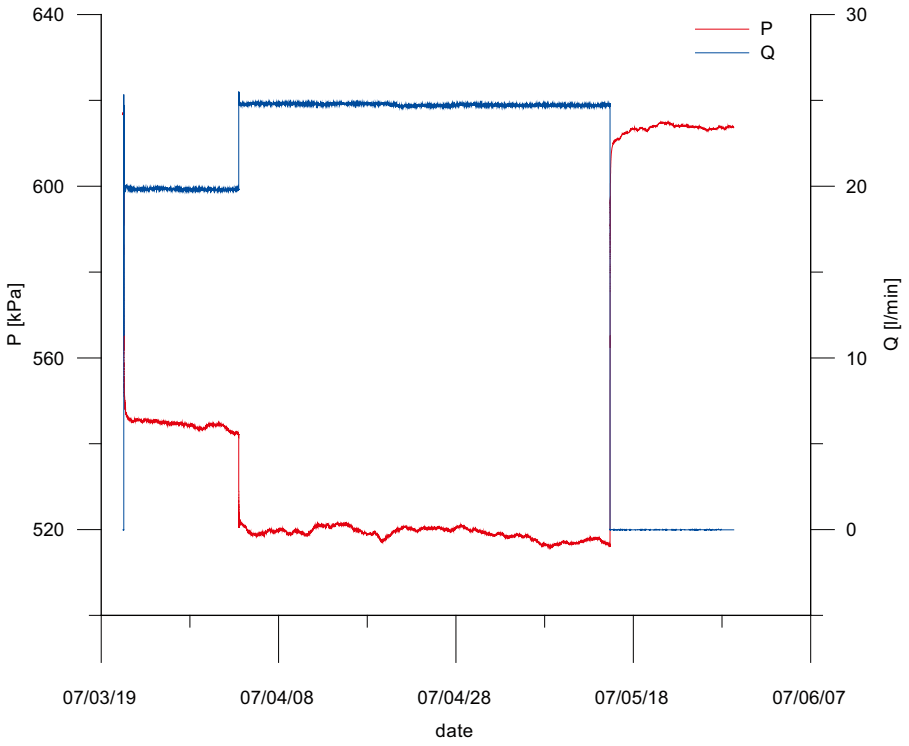

Figure A6-1. *Linear plot of flow rate (Q) and pressure (p) versus time in the pumping borehole KFM02B during the interference test in KFM02B.*

Observation borehole KFM02A

In Figure A6-2 an overview of the observed head versus time in the sections in observation borehole KFM02A is shown. Clear responses were observed in sections 3, 4, 5, 6 and 7. These sections are presented below. No responses from the pumping in KFM02B can be detected in sections 1 or 8 and thus no analysis is performed in these sections. In section 2, a weak response can not be confirmed but neither excluded. No further evaluation is made of this section.

There is an overall decreasing trend in the water levels which is not related to the pumping in KFM02B. The borehole is also disturbed by the pumping in borehole KFM08D, see Section 5.3 in the main report. The slightly increased head in section 2 which can be observed in connection to stop of pumping in KFM02B (2007-05-15) is probably due to precipitation.

Observation section KFM02A:3 490.00–518.00 m

In Figure A6-2 an overview of the observed head responses in observation borehole KFM02A is shown. General test data from the observation section KFM02A:3 are presented in Table A6-2. Table A6-2. General test data from the observation section KFM02A:3 during pumping in KFM02B.

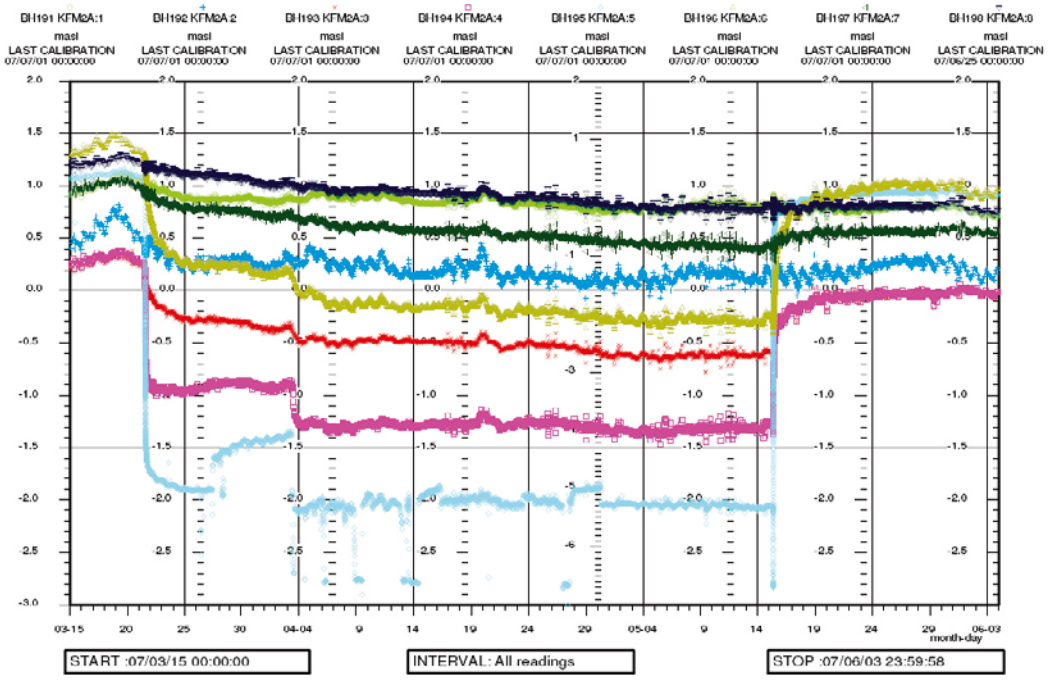

Figure A6-2. *Linear plot of observed head versus time in sections 1-8 in observation borehole KFM02A during pumping in KFM02B.*

Table A6-2. General test data from the observation section KFM02A:3 during pumping in KFM02B.

Pressure data	Nomenclature	Unit	Value	Corrected Value[1)]
Hydraulic head in test section before start of flow period	h_i	m.a.s.l.	0.20	0.20
Hydraulic head in test section before stop of flow period	h_p	m.a.s.l.	–0.61	–0.41
Hydraulic head in test section at stop of recovery period	h_F	m.a.s.l.	–0.03	0.24
Hydraulic head change during flow period (h_i–h_p)	dh_p	m	0.81	0.61

[1)] Head corrected for the natural decreasing head trend.

Comments on the test

A clear response to the pumping in KFM02B is indicated in this section. The corrected drawdown during the flow period was c 0.6 m. A (corrected) drawdown of 0.1 m was reached approximately 70 minutes (c 1.2 hours) after start of pumping in KFM02B. There was a corrected recovery of c 0.6 m during the recovery period, lasting for approximately 19 days. The sudden pressure decrease due to the increased pumping rate, observed in the pumping borehole KFM02B on 2007-04-03, can clearly be seen in this section.

Due to the natural decreasing pressure trend during the interference test, the head in this section was corrected for the natural trend before the analysis. A linear correction was applied based on the linear head diagrams presented above. A linear plot of the corrected and uncorrected head versus time is presented in Figure A7-6 in Appendix 7.

Interpreted flow regimes and calculated parameters

During both the flow and recovery period a pseudo-radial flow occurred. During the flow period a transition to pseudo-spherical flow is indicated at the end of the period. The change in flow rate occurred after c 19,000 min during the flow period. The transient evaluation was based on variable flow rate.

The agreement in evaluated parameter values between the flow and recovery period is good. The parameter values from the flow period are selected as the most representative.

Transient interpretation of the flow and recovery period is shown in log-log diagrams in Figure A7-7 and A7-8, Appendix 7. The results from the transient evaluation are summarized in Table 5-5 in the main report.

Observation section KFM02A:4 443.00–489.00 m

In Figure A6-2 an overview of the observed head responses in observation borehole KFM02A is shown. General test data from the observation section KFM02A:4 are presented in Table A6-3.

Comments on the test

A clear response to the pumping is indicated in this section. The corrected drawdown during the flow period was c 1.5 m. A (corrected) drawdown of 0.1 m was reached approximately 10 minutes after start of pumping in KFM02B. There was a corrected recovery of c 1.3 m during the recovery period lasting for approximately 19 days. The sudden pressure decrease due to the increased pumping rate, observed in the pumping borehole KFM02B on 2007-04-03, can clearly be clearly seen in this section.

Table A6-3. General test data from observation section KFM02A:4 during pumping in KFM02B.

Pressure data	Nomenclature	Unit	Value	Corrected Value[1)]
Hydraulic head in test section before start of flow period	h_i	m.a.s.l.	0.23	0.23
Hydraulic head in test section before stop of flow period	h_p	m.a.s.l.	–1.30	–1.25
Hydraulic head in test section at stop of recovery period	h_F	m.a.s.l.	–0.02	0.05
Hydraulic head change during flow period (h_i–h_p)	dh_p	m	1.53	1.48

[1)] Head corrected for the natural decreasing head trend.

Due to the natural decreasing pressure trend during the interference test, the head in this section was corrected for the natural trend before the analysis. A linear correction was applied based on the linear head diagrams presented above. A linear plot of the corrected and uncorrected head versus time is presented in Figure A7-9 in Appendix 7.

Interpreted flow regimes and calculated parameters

During both the flow and the recovery period a short period of pseudo-radial flow occurred followed by a transition to pseudo-spherical (leaky) flow. A change in flow rate occurred after c 19,000 min during the flow period. The responses during the flow and recovery periods are similar except the increase of drawdown due to the change in flow rate at the end of the period. Transient evaluation was based on variable flow rate. The parameter values from the flow period are selected as the most representative.

Transient interpretation of the flow and recovery periods is shown in log-log diagrams in Figures A7-10 and A7-11, Appendix 7. The results from the transient evaluation are summarized in Table 5-5 in the main report.

Observation section KFM02A:5 411.00–442.00 m

In Figure A6-2 an overview of the observed head responses in observation borehole KFM02A is shown. General test data from the observation section KFM02A:5 are presented in Table A6-4.

Comments on the test

A clear response to the pumping in KFM02B is indicated in this section. The corrected drawdown during the flow period was c 6.9 m. A (corrected) drawdown of 0.1 m was reached approximately 0.3 minutes after start of pumping in KFM02B. There was a corrected recovery of c 6.9 m during the recovery period lasting for approximately 19 days. The sudden pressure decrease, due to the increased pumping rate, that was observed 2007-04-03 in the pumping borehole KFM02B can be clearly seen in this section. This section was used for tracer injection during the pumping, hence it is somewhat disturbed hydraulically.

Due to the natural decreasing pressure trend during the interference tests, the heads in this section were corrected before the analysis. A linear correction was applied based on the linear head diagrams presented above. A linear plot of the corrected and uncorrected head versus time is presented in Figure A7-12 in Appendix 7.

Table A6-4. General test data from observation section KFM02A:5 during pumping in KFM02B.

Pressure data	Nomenclature	Unit	Value	Corrected Value[1)]
Hydraulic head in test section before start of flow period	h_i	m.a.s.l.	0.28	0.28
Hydraulic head in test section before stop of flow period	h_p	m.a.s.l.	–6.68	–6.63
Hydraulic head in test section at stop of recovery period	h_F	m.a.s.l.	–0.04	0.11
Hydraulic head change during flow period (h_i–h_p)	dh_p	m	6.96	6.91

[1)] Head corrected for the natural decreasing head trend.

Interpreted flow regimes and calculated parameters

During both the flow and the recovery period, a transition to a short period of pseudo-radial flow occurred followed by a transition to a period of pseudo-spherical (leaky) flow. The change in flow rate occurred after c 19,000 min during the flow period. The responses during the flow and recovery period are very similar. Transient evaluation was based on variable flow rate. The end of the flow period is disturbed by the tracer injection in this section, hence only the first 10,000 minutes are used for evaluation.

The agreement in evaluated parameter values between the flow and recovery periods is good. The parameter values from the flow period are selected as the most representative.

Transient interpretation of the flow and recovery period is shown in log-log diagrams in Figures A7-13 to A7-14, Appendix 7. The results from the transient evaluation are summarized in Table 5-5 in the main report.

Observation section KFM02A:6 241.00–410.00 m

In Figure A6-2 an overview of the observed head responses in observation borehole KFM02A is shown. General test data from the observation section KFM02A:6 are presented in Table A6-5.

Comments on the test

A clear response to the pumping in KFM02B is indicated in this section. The corrected drawdown during the flow period was c 1.4 m. A (corrected) drawdown of 0.1 m was reached approximately 100 minutes (c 1.7 h) after start of pumping in KFM02B. There was a corrected recovery of c 1.3 m during the recovery period lasting for approximately 19 days. The sudden pressure decrease, due to the increased pumping rate, that was observed in the pumping borehole KFM02B on 2007-04-03 can be clearly seen in this section.

Due to the natural decreasing pressure trend during the interference test, the heads in this section were corrected before the analysis. A linear correction was applied based on the linear head diagrams presented above. A linear plot of the corrected and uncorrected head versus time is presented in Figure A7-15 in Appendix 7.

Interpreted flow regimes and calculated parameters

During both the flow and the recovery period, a transition to pseudo-radial flow occurred followed by a transition to pseudo-spherical flow at the end of the period. A change in flow rate occurred after c 19,000 min during the flow period. The responses during the flow and recovery periods are similar. Transient evaluation was based on variable flow rate. The agreement in evaluated parameter values between the flow and the recovery period is good. The parameter values from the flow period are selected as the most representative.

Transient interpretation of the flow and recovery period is shown in log-log diagrams in Figures A7-16 and A7-17, Appendix 7. The results from the transient evaluation are summarized in Table 5-5 in the main report.

Table A6-5. General test data from observation section KFM02A:6 during pumping in KFM02B.

Pressure data	Nomenclature	Unit	Value	Corrected Value[1)]
Hydraulic head in test section before start of flow period	h_i	m.a.s.l.	1.27	1.27
Hydraulic head in test section before stop of flow period	h_p	m.a.s.l.	–0.30	–0.10
Hydraulic head in test section at stop of recovery period	h_F	m.a.s.l.	0.97	1.24
Hydraulic head change during flow period (h_i–h_p)	dh_p	m	1.57	1.37

[1)] Head corrected for the natural decreasing head trend.

Observation section KFM02A:7 133.00–240.00 m

In Figure A6-2 an overview of the observed head responses in observation borehole KFM02A is shown. General test data from the observation section KFM02A:7 are presented in Table A6-6.

Comments on the test

A small response to the pumping is indicated in this section. The corrected drawdown during the flow period was c 0.2 m. A (corrected) drawdown of 0.1 m was reached approximately 3,000 minutes (c 50 hours) after start of pumping in KFM02B. There was a corrected recovery of c 0.3 m during the recovery period lasting for approximately 19 days.

Due to the natural decreasing pressure trend during the interference test, the head in this section was corrected before the analysis. A linear correction was applied based on the linear head diagrams presented above. A linear plot of the corrected and uncorrected head versus time is presented in Figure A7-18 in Appendix 7.

Interpreted flow regimes and calculated parameters

The flow period is characterised by a pseudo-radial flow followed by a transition to pseudo-spherical flow by the end. A change in the flow rate occurred after c 19,000 min during the flow period. During the recovery period a transition to pseudo-radial flow occurred. Transient evaluation was based on variable flow rate.

The agreement in evaluated parameter values between the flow and recovery period is good. The parameter values from the flow period are selected as the most representative.

Transient interpretation of the flow and recovery period is shown in log-log diagrams in Figures A7-19 and A7-20, Appendix 7. The results from the transient evaluation are summarized in Table 5-5 in the main report.

Observation borehole HFM32

In Figure A6-3 an overview of the observed head responses in observation borehole HFM32 is shown. Clear responses were observed in sections 1 and 2. These sections are presented below. No certain responses from the pumping in KFM02B can be detected in sections 3 or 4 and thus no transient analysis is performed in these sections.

There is an overall decreasing trend in the water levels which is not related to the pumping in KFM02B. The borehole is also disturbed by the pumping in borehole KFM08D, see Section 5.3 in the main report. The short period of increased head in sections 3 and 4 which can be observed in connection to stop of the pumping in KFM02B (2007-05-15) is probably due to precipitation.

Table A6-6. General test data from observation section KFM02A:7 during pumping in KFM02B.

Pressure data	Nomenclature	Unit	Value	Corrected Value[1)]
Hydraulic head in test section before start of flow period	h_i	m.a.s.l.	0.94	0.94
Hydraulic head in test section before stop of flow period	h_p	m.a.s.l.	0.40	0.70
Hydraulic head in test section at stop of recovery period	h_F	m.a.s.l.	0.58	0.98
Hydraulic head change during flow period (h_i–h_p)	dh_p	m	0.54	0.24

[1)] Head corrected for the natural decreasing head trend.

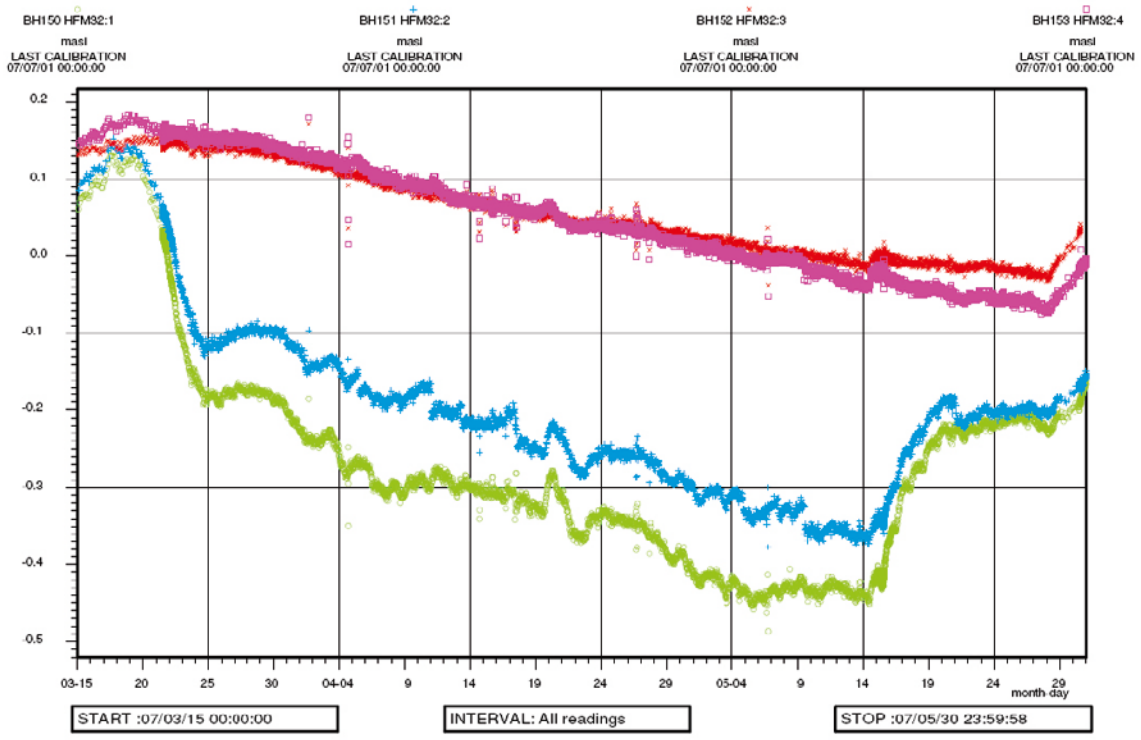

Figure A6-3. *Linear plot of observed head versus time in observation borehole HFM32 during pumping in KFM02B.*

Observation section HFM32:1 98.00–202.65 m

In Figure A6-3 an overview of the observed head responses in observation borehole HFM32 is shown. General test data from the observation section HFM32:1 are presented in Table A6-7.

Comments on the test

A clear response to the pumping in KFM02B is indicated in this section. The corrected drawdown during the flow period was c 0.3 m. A (corrected) drawdown of 0.1 m was reached approximately 1,400 minutes (c 23 hours) after start of pumping in KFM02B. There was a corrected recovery of c 0.3 m during the recovery period lasting for approximately 19 days.

The response is disturbed by the overall decreasing trend in the water levels that starts before the start of the pumping in KFM02B and which is not related to the pumping. There were also some precipitation shortly before the end of the pumping which may have disturbed the evaluation for the recovery period. The heads in this section were corrected for the natural trend before the analysis. A linear correction was applied based on the linear drawdown diagrams presented above. A linear plot of the corrected and uncorrected head versus time is presented in Figure A7-21 in Appendix 7.

Table A6-7. General test data from observation section HFM32:1 during pumping in KFM02B.

Pressure data	Nomenclature	Unit	Value	Corrected Value[1)]
Hydraulic head in test section before start of flow period	h_i	m.a.s.l.	0.03	0.03
Hydraulic head in test section before stop of flow period	h_p	m.a.s.l.	–0.42	–0.29
Hydraulic head in test section at stop of recovery period	h_F	m.a.s.l.	–0.17	0.00
Hydraulic head change during flow period (h_i–h_p)	dh_p	m	0.45	0.32

[1)] Head corrected for the natural decreasing head trend.

Interpreted flow regimes and calculated parameters

During the flow period, pseudo-radial flow occurred transitioning to pseudo-spherical (leaky) flow at the end of the period. A change in flow rate occurred after c 19,000 min during the flow period. During the recovery period, slightly leaky flow was observed. The responses during the flow and recovery period are rather similar. Transient evaluation was based on variable flow rate.

The agreement in evaluated parameter values between the flow and recovery period is good. The parameter values from the flow period are selected as the most representative.

Transient interpretation of the flow and recovery periods is shown in log-log diagrams in Figures A7-22 to A7-23, Appendix 7. The results from the transient evaluation are summarized in Table 5-5 in the main report.

Observation section HFM32:2 32.00–97.00 m

In Figure A6-3 an overview of the observed head responses in observation borehole HFM32 is shown. General test data from the observation section HFM32:2 are presented in Table A6-8.

Comments on the test

A clear response to the pumping in KFM02B is indicated in this section. The corrected drawdown during the flow period was c 0.2 m. A (corrected) drawdown of 0.1 m was reached approximately 2,050 minutes (c 34 hours) after start of pumping in KFM02B. There was a corrected recovery of c 0.2 m during the recovery period lasting for approximately 19 days.

The response is disturbed by the overall decreasing trend in the water levels that commences before the start of the pumping in KFM02B and that is not related to the pumping. There were also some precipitations shortly before stop of pumping which may have disturbed the evaluation recovery period. The head in this section was corrected for the natural trend before the analysis. A linear correction was applied based on the linear drawdown diagrams presented above. A linear plot of the corrected and uncorrected head versus time is presented in Figure A7-24 in Appendix 7.

Interpreted flow regimes and calculated parameters

During both the flow and recovery period, dominating pseudo-radial flow occurred. A change in flow rate occurred after c 19,000 min during the flow period. The responses during the flow and recovery period are similar. Transient evaluation was based on variable flow rate.

The agreement in evaluated parameter values between the flow and recovery period is good. The parameter values from the flow period are selected as the most representative.

Transient, quantitative interpretation of the flow and recovery period is shown in log-log diagrams in Figures A7-25 and A7-26, Appendix 7. The results from the transient evaluation are summarized in Table 5-5 in the main report.

Table A6-8. General test data from observation section HFM32:2 during pumping in KFM02B.

Pressure data	Nomenclature	Unit	Value	Corrected Value[1)]
Hydraulic head in test section before start of flow period	h_i	m.a.s.l.	0.05	0.05
Hydraulic head in test section before stop of flow period	h_p	m.a.s.l.	–0.34	–0.19
Hydraulic head in test section at stop of recovery period	h_F	m.a.s.l.	0.15	0.05
Hydraulic head change during flow period (h_i–h_p)	dh_p	m	0.39	0.24

[1)] Head corrected for the natural decreasing head trend.

Observation borehole KFM05A

In Figure A6-4 an overview of the observed head responses in observation borehole KFM05A is shown. Clear responses were observed in sections 5 and 6. These sections are presented below. No certain responses from the pumping in KFM05A can be detected in sections 1, 2, 3 or 4 and thus no transient analysis is performed for these sections.

There is an overall decreasing trend in the water levels that is not related to the pumping in KFM02B. The borehole is also disturbed by the pumping in borehole KFM08D, see Section 5.3 in the main report.

Observation section KFM05A:5 115.00–253.00 m

In Figure A6-4 an overview of the observed head responses in observation borehole KFM05A is shown. General test data from the observation section KFM05A:5 are presented in Table A6-9.

Comments on the test

A small response is indicated in this section due to pumping in KFM02B. The beginning of the response during the flow period is disturbed by the pumping activities in KFM08D, see above. A corrected drawdown during the flow period of c 0.15 m was registered. A (corrected) drawdown of 0.1 m was reached approximately 50,000 minutes (c 833 hours) after start of pumping in KFM02B. There was a corrected recovery of c 0.2 m during the recovery period of approximately 19 days. Substantial precipitation around the 29th of May caused a peak in the head values. This results in higher corrected head values at the stop of recovery than before the start of flow period.

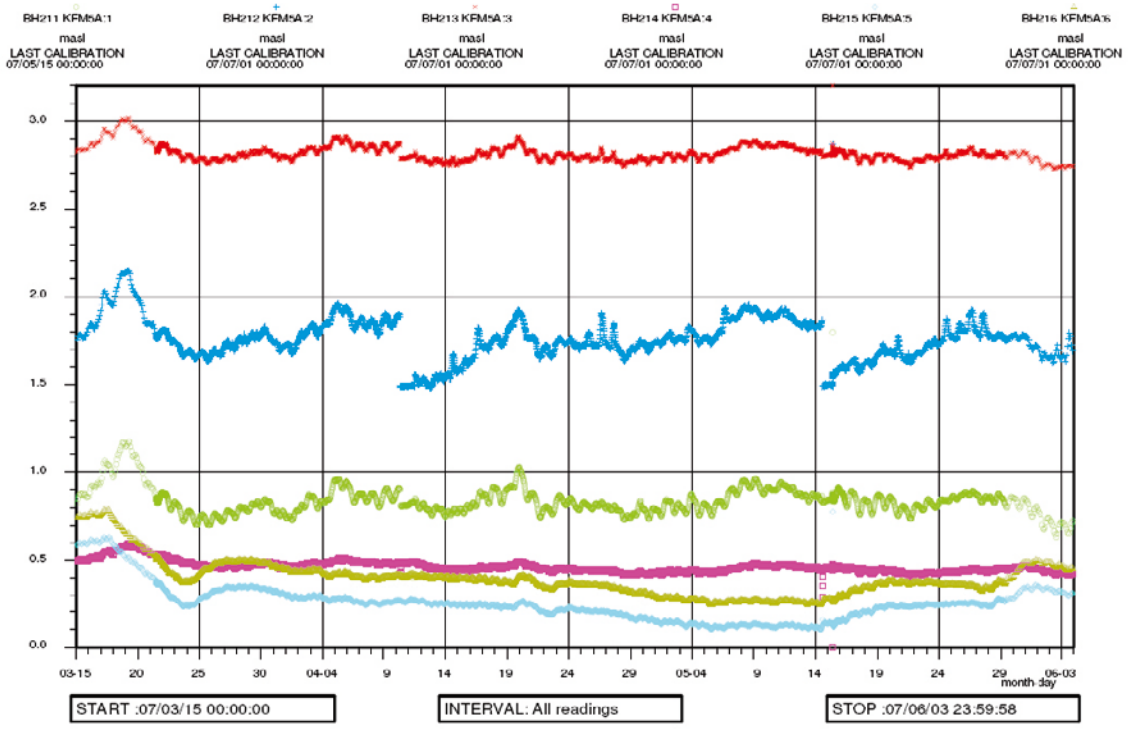

Figure A6-4. *Linear plot of observed head versus time in the observation sections in KFM05A during pumping in KFM02B.*

Table A6-9. General test data from observation section KFM05A:5 during pumping in KFM02B.

Pressure data	Nomenclature	Unit	Value	Corrected Value[1)]
Hydraulic head in test section before start of flow period	h_i	m.a.s.l	0.37	0.37
Hydraulic head in test section before stop of flow period	h_p	m.a.s.l	0.13	0.23
Hydraulic head in test section at stop of recovery period	h_F	m.a.s.l	0.31	0.45
Hydraulic head change during flow period (h_i–h_p)	dh_p	m	0.24	0.14

[1)] Head corrected for the naturally decreasing head trend.

The response is disturbed by the overall decreasing trend in the water level that began before start of pumping in KFM02B and which is not related to the pumping. There was also some precipitation shortly before stop of pumping that may have disturbed the evaluation of the recovery period. The heads in this section were corrected for the natural trend before the transient analysis. A linear head correction was applied based on the linear head diagrams presented above. A linear plot of the corrected and uncorrected head versus time is presented in Figure A7-27 in Appendix 7.

Interpreted flow regimes and calculated parameters

During the flow period, a transition to approximate pseudo-radial flow occurred at intermediate times. A change in flow rate occurred after c 19,000 min during the flow period. After the flow rate change, a transition towards a new pseudo-radial flow regime occurred. The recovery period displays a transition period followed by an approximate pseudo-radial flow regime by the end. The responses during the flow and recovery periods are similar. Transient evaluation was based on variable flow rate. The transient evaluation is uncertain due to the disturbance from the pumping in KFM08D.

The agreement in evaluated parameter values between the flow and recovery period is good. The parameter values from the flow period are selected as the most representative.

Transient interpretation of the flow and recovery periods is shown in log-log diagrams in Figures A7-28 and A7-29, Appendix 7. The results from the transient evaluation are summarized in Table 5-5 in the main report.

Observation section KFM05A:6 100.07–114.00 m

In Figure A6-4 an overview of the observed head responses in observation borehole KFM05A is shown. General test data from the observation section KFM05A:6 are presented in Table A6-10.

Comments on the test

A small response is indicated in this section due to pumping in KFM02B. The beginning of the response during the flow period is disturbed by the pumping activities in KFM08D, see above. A corrected drawdown during the flow period of c 0.1 m was registered. A (corrected) drawdown of 0.1 m was reached approximately 55,000 min (c 917 hours) after start of pumping in KFM02B. There was a corrected recovery of c 0.2 m during the recovery period of approximately 19 days. Substantial precipitation around the 29th of May caused a peak in the head values that resulted in higher corrected head values at the stop of recovery than before the start of flow period.

The response is disturbed by the overall decreasing trend in the water level that started before start of pumping in KFM02B and which is not related to the pumping. There was also some precipitation shortly before stop of pumping which may have disturbed the evaluation of the recovery period. The heads in this section were corrected for the natural trend before the transient analysis. A linear head correction was applied based on the linear head diagrams presented above. A linear plot of the corrected and uncorrected head versus time is presented in Figure A7-30 in Appendix 7.

Table A6-10. General test data from observation section KFM05A:6 during pumping in KFM02B.

Pressure data	Nomenclature	Unit	Value	Corrected Value[1)]
Hydraulic head in test section before start of flow period	h_i	m	0.51	0.51
Hydraulic head in test section before stop of flow period	h_p	m	0.27	0.39
Hydraulic head in test section at stop of recovery period	h_F	m	0.49	0.62
Hydraulic head change during flow period (h_i–h_p)	dhp	m	0.25	0.13

[1)] Head corrected for the natural decreasing head trend.

Interpreted flow regimes and calculated parameters

During the flow period, a transition to approximate pseudo-radial flow occurred at intermediate times. A change in flow rate occurred after c 19,000 min during the flow period. After the flow rate change, a transition towards a new pseudo-radial flow regime occurred. The recovery period displays a transition period followed by an approximate pseudo-radial flow regime by the end. Transient evaluation was based on variable flow rate. The transient evaluation is uncertain due to the disturbance from the pumping in KFM08D.

The agreement in evaluated parameter values between the flow and recovery period is good. The parameter values from the flow period are selected as the most representative.

Transient, quantitative interpretation of the flow and recovery period is shown in log-log diagrams in Figures A7-31 and A7-32, Appendix 7. The results from the transient evaluation are summarized in Table 5-5 in the main report.

Observation borehole HFM16

In Figure A6-5 an overview of the observed head responses in observation borehole HFM16 is shown. Clear responses were observed in all sections and these are presented below.
There is an overall decreasing trend in the water levels which is not related to the pumping in KFM02B. The responses are also disturbed by the pumping in borehole KFM08D, see Section 5.3 in the main report.

Observation section HFM16:1 68.00-132.50 m

In Figure A6-5 an overview of the observed head responses in observation borehole HFM16 is shown. General test data from the observation section HFM16:1 is presented in Table A6-11.

Comments on the test

A clear response to the pumping in KFM02B is indicated in this section. The corrected drawdown during the flow period was c 0.4 m. A (corrected) drawdown of 0.1 m was reached approximately 1,000 min (c 17 hours) after start of pumping in KFM02B. There was a corrected recovery of c 0.4 m during the recovery period lasting for approximately 19 days.

The response is disturbed by the overall decreasing trend in the water levels that commences before the start of the pumping in KFM02B and which is not related to the pumping. There were also some events of precipitation shortly before stop of pumping which may have disturbed the evaluation recovery period. The head in this section was corrected for the natural trend before the analysis. A linear correction was applied based on the linear drawdown diagrams presented above. A linear plot of the corrected and uncorrected head versus time is presented in Figure A7-33 in Appendix 7.

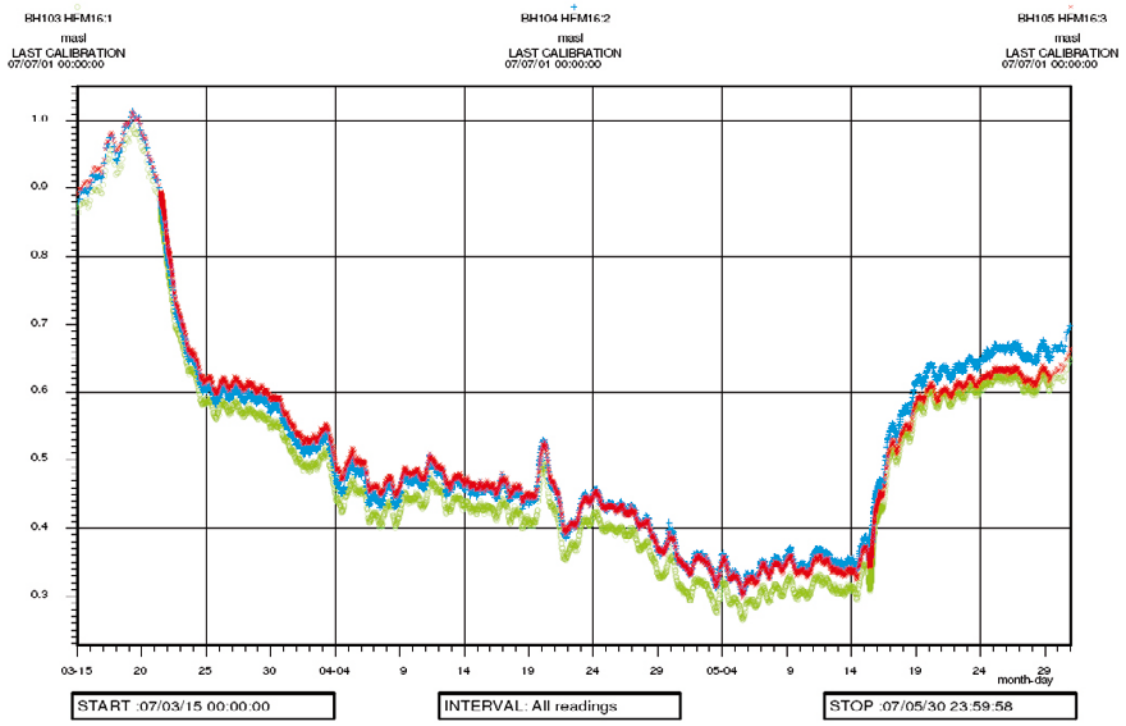

Figure A6-5. *Linear plot of observed head versus time in the observation section HFM16 during pumping in KFM02B.*

Table A6-11. General test data from observation section HFM16:1 during pumping in KFM02B.

Pressure data	Nomenclature	Unit	Value	Corrected Value[1)]
Hydraulic head in test section before start of flow period	h_i	m.a.s.l.	0.86	0.86
Hydraulic head in test section before stop of flow period	h_p	m.a.s.l.	0.31	0.48
Hydraulic head in test section at stop of recovery period	h_F	m.a.s.l.	0.63	0.86
Hydraulic head change during flow period (h_i–h_p)	dh_p	m	0.55	0.38

[1)] Head corrected for the natural decreasing head trend.

Interpreted flow regimes and calculated parameters

During the flow period a short period of pseudo-radial flow occurred followed by a transition to a pseudo-spherical (leaky) flow. A change in flow rate occurred after c 19,000 min during the flow period. During the recovery period dominating pseudo-radial flow occurred followed by a transition to slightly pseudo-spherical (leaky) flow by the end. Transient evaluation was based on variable flow rate.

The agreement in evaluated parameter values between the flow and recovery period is good. The parameter values from the flow period are selected as the most representative.

Transient, quantitative interpretation of the flow and recovery period is shown in log-log diagrams in Figures A7-34 and A7-35, Appendix 7. The results from the transient evaluation are summarized in Table 5-5 in the main report.

Observation section HFM16:2 54.00–67.00 m

In Figure A6-5 an overview of the observed head responses in observation borehole HFM16:2 is shown. General test data from the observation section HFM16:2 are presented in Table A6-12.

Comments on the test

A clear response to the pumping in KFM02B is indicated in this section. The corrected drawdown during the flow period was c 0.4 m. A (corrected) drawdown of 0.1 m was reached approximately 1,000 minutes (c 17 hours) after start of pumping in KFM02B. There was a corrected recovery of c 0.4 m during the recovery period lasting for approximately 19 days.

The response is disturbed by the overall decreasing trend in the water levels that begins before the start of the pumping in KFM02B and which is not related to the pumping. There were also some events of precipitation shortly before stop of pumping which may have disturbed the evaluation recovery period. The head in this section was corrected for the natural trend before the analysis. A linear correction was applied based on the linear drawdown diagrams presented above. A linear plot of the corrected and uncorrected head versus time is presented in Figure A7-36 in Appendix 7.

Interpreted flow regimes and calculated parameters

During the flow period a short period of pseudo-radial flow occurred followed by a transition to a pseudo-spherical (leaky) flow. A change in flow rate occurred after c 19,000 min during the flow period. During the recovery period dominating pseudo-radial flow occurred followed by a transition to slightly pseudo-spherical (leaky) flow by the end. Transient evaluation was based on variable flow rate.

The agreement in evaluated parameter values between the flow and recovery period is good. The parameter values from the flow period are selected as the most representative.

Transient, quantitative interpretation of the flow and recovery period is shown in log-log diagrams in Figures A7-37 and A7-38, Appendix 7. The results from the transient evaluation are summarized in Table 5-5 in the main report.

Table A6-12. General test data from observation section HFM16:2 during pumping in KFM02B.

Pressure data	Nomenclature	Unit	Value	Corrected Value[1)]
Hydraulic head in test section before start of flow period	h_i	m.a.s.l.	0.88	0.88
Hydraulic head in test section before stop of flow period	h_p	m.a.s.l.	0.36	0.51
Hydraulic head in test section at stop of recovery period	h_F	m.a.s.l.	0.68	0.88
Hydraulic head change during flow period (h_i–h_p)	dh_p	m	0.52	0.37

[1)] Head corrected for the natural decreasing head trend.

Observation section HFM16:3 12.02–53.00 m

In Figure A6-5 an overview of the observed head responses in observation borehole HFM16:3 is shown. General test data from the observation section HFM16:3 are presented in Table A6-13.

Comments on the test

A clear response to the pumping in KFM02B is indicated in this section. The corrected drawdown during the flow period was c 0.4 m. A (corrected) drawdown of 0.1 m was reached approximately 1,100 minutes (c 18 hours) after start of pumping in KFM02B. There was a corrected recovery of c 0.4 m during the recovery period lasting for approximately 19 days.

The response is disturbed by the overall decreasing trend in the water levels that starts before the start of the pumping in KFM02B and which is not related to the pumping. There were also some events of precipitation shortly before stop of pumping which may have disturbed the evaluation recovery period. The head in this section was corrected for the natural trend before the analysis. A linear correction was applied based on the linear drawdown diagrams presented above. A linear plot of the corrected and uncorrected head versus time is presented in Figure A7-39 in Appendix 7.

Interpreted flow regimes and calculated parameters

During the flow period a short period of pseudo-radial flow occurred followed by a transition to a pseudo-spherical (leaky) flow. A change in flow rate occurred after c 19,000 min during the flow period. During the recovery period dominating pseudo-radial flow occurred followed by a transition to slightly pseudo-spherical (leaky) flow by the end. Transient evaluation was based on variable flow rate.

The agreement in evaluated parameter values between the flow and recovery period is good. The parameter values from the flow period are selected as the most representative.

Transient, quantitative interpretation of the flow and recovery period is shown in log-log diagrams in Figures A7-40 and A7-41, Appendix 7. The results from the transient evaluation are summarized in Table 5-5 in the main report.

Observation borehole KFM06B

In Figure A6-6 an overview of the observed head responses in observation borehole KFM06B is shown. Clear responses were observed in all sections and these are presented below.
There is an overall decreasing trend in the water levels which is not related to the pumping in KFM02B. The responses are also disturbed by the pumping in borehole KFM08D, see Section 5.3 in the main report.

Table A6-13. General test data from observation section HFM16:3 during pumping in KFM02B.

Pressure data	Nomenclature	Unit	Value	Corrected Value[1)]
Hydraulic head in test section before start of flow period	h_i	m.a.s.l.	0.88	0.88
Hydraulic head in test section before stop of flow period	h_p	m.a.s.l.	0.35	0.50
Hydraulic head in test section at stop of recovery period	h_F	m.a.s.l.	0.65	0.85
Hydraulic head change during flow period (h_i–h_p)	dh_p	m	0.53	0.38

[1)] Head corrected for the natural decreasing head trend.

Observation section KFM06B:1 51.00–100.33 m

In Figure A6-6 an overview of the pressure responses in observation borehole KFM06B is shown. General test data from the observation section KFM06B:1 are presented in Table A6-14.

Comments on the test

A clear response to the pumping in KFM02B is indicated in this section. The corrected drawdown during the flow period was c 0.4 m. A corrected drawdown of 0.1 m was reached approximately 1,000 min (c 17 hours) after start of pumping in KFM02B. There was a corrected recovery of c 0.4 m during the recovery period lasting for approximately 19 days.

The response is disturbed by the overall decreasing trend in the water levels that begins before the start of the pumping in KFM02B and which is not related to the pumping. There were also some precipitations shortly before stop of pumping which may have disturbed the evaluation recovery period. The head in this section was corrected for the natural trend before the analysis. A linear correction was applied based on the linear drawdown diagrams presented above. A linear plot of the corrected and uncorrected head versus time is presented in Figure A7-42 in Appendix 7.

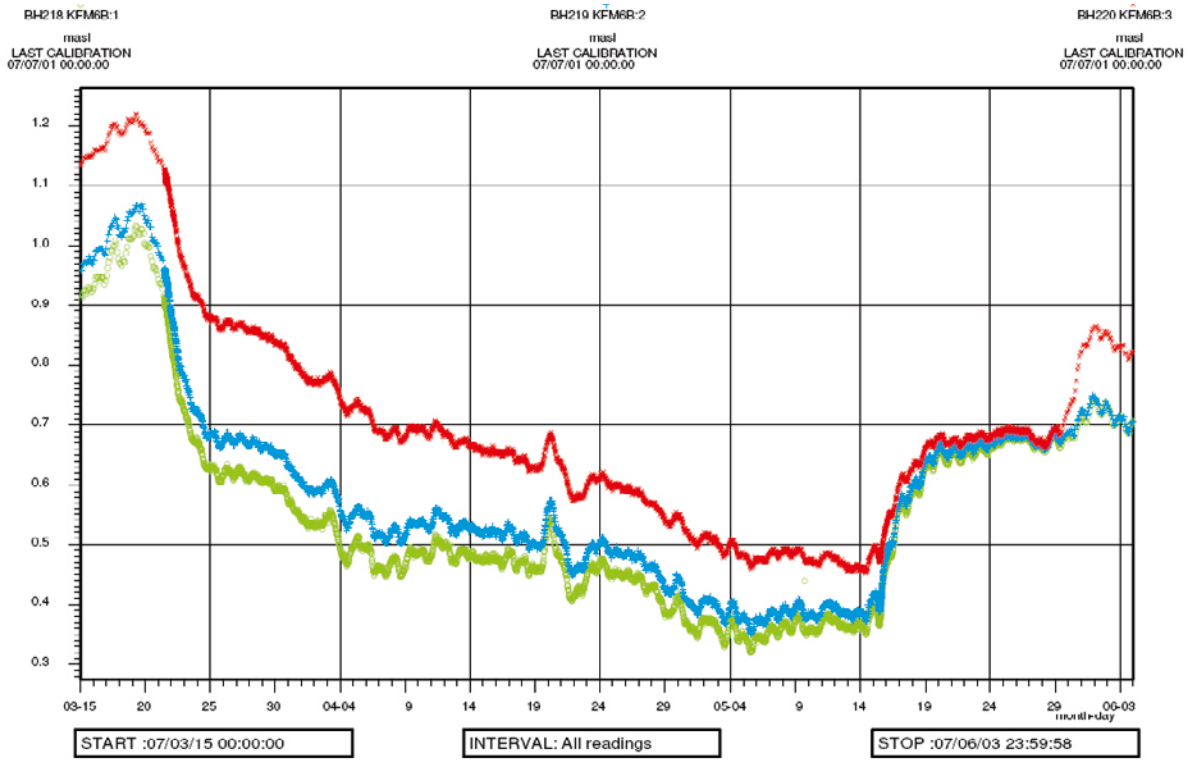

Figure A6-6. *Linear plot of observed head versus time in observation borehole KFM06B during pumping in KFM02B.*

Table A6-14. General test data from observation section KFM06B:1 during pumping in KFM02B.

Pressure data	Nomenclature	Unit	Value	Corrected Value[1)]
Hydraulic head in test section before start of flow period	h_i	m.a.s.l.	0.90	0.90
Hydraulic head in test section before stop of flow period	h_p	m.a.s.l.	0.37	0.50
Hydraulic head in test section at stop of recovery period	h_F	m.a.s.l.	0.70	0.85
Hydraulic head change during flow period (h_i–h_p)	dh_p	m	0.53	0.40

[1)] Head corrected for the natural decreasing head trend.

Interpreted flow regimes and calculated parameters

During both the flow and recovery period pseudo-radial flow occurred transitioning to pseudo-spherical (leaky) flow by the end. A change in flow rate occurred after c 19,000 min during the flow period. The responses during the flow and recovery period are similar. Transient evaluation was based on variable flow rate.

The agreement in evaluated parameter values between the flow and recovery period is good. The parameter values from the flow period are selected as the most representative.

Transient, quantitative interpretation of the flow and recovery period is shown in log-log diagrams in Figures A7-43 and A7-44, Appendix 7. The results from the transient evaluation are summarized in Table 5-5 in the main report.

Observation section KFM06B:2 27.00–50.00 m

In Figure A6-6 an overview of the observed head responses in observation borehole KFM06B is shown. General test data from the observation section KFM06B:2 are presented in Table A6-15.

Comments on the test

A rather clear response to the pumping is indicated in this section. The corrected drawdown during the flow period was c 0.4 m. A (corrected) drawdown of 0.1 m was reached approximately 1,000 minutes (c 17 hours) after start of pumping in KFM02B. There was a corrected recovery of c 0.4 m during the recovery period lasting for approximately 19 days.

The response is disturbed by the overall decreasing trend in the water levels that starts before the start of the pumping in KFM02B and which is not related to the pumping. There were also some events of precipitation shortly before stop of pumping which may have disturbed the evaluation recovery period. The head in this section was corrected for the natural trend before the analysis. A linear correction was applied based on the linear drawdown diagrams presented above. A linear plot of the corrected and uncorrected head versus time is presented in Figure A7-45 in Appendix 7.

Interpreted flow regimes and calculated parameters

During both the flow and recovery period pseudo-radial flow occurred transitioning to pseudo-spherical (leaky) flow by the end. A change in flow rate occurred after c 19,000 min during the flow period. The responses during the flow and recovery period are similar. Transient evaluation was based on variable flow rate.

The agreement in evaluated parameter values between the flow and recovery period is good. The parameter values from the flow period are selected as the most representative.

Transient, quantitative interpretation of the flow and recovery period is shown in log-log diagrams in Figures A7-46 and A7-47, Appendix 7. The results from the transient evaluation are summarized in Table 5-5 in the main report.

Table A6-15. General test data from observation section KFM06B:2 during pumping in KFM02B.

Pressure data	Nomenclature	Unit	Value	Corrected Value[1)]
Hydraulic head in test section before start of flow period	h_i	m.a.s.l.	0.95	0.95
Hydraulic head in test section before stop of flow period	h_p	m.a.s.l.	0.40	0.57
Hydraulic head in test section at stop of recovery period	h_F	m.a.s.l.	0.70	0.93
Hydraulic head change during flow period (h_i–h_p)	dh_p	m	0.55	0.38

[1)] Head corrected for the natural decreasing head trend.

Observation section KFM06B:3 6.33–26.00 m

In Figure A6-6 an overview of the observed head responses in observation borehole KFM06B is shown. General test data from the observation section KFM06B:3 are presented in Table A6-16.

Comments on the test

A rather clear response to the pumping in KFM02B is indicated in this section. The corrected drawdown during the flow period was c 0.4 m. A (corrected) drawdown of 0.1 m was reached approximately 1,250 mins (c 21 hours) after start of pumping in KFM02B. There was a corrected recovery of c 0.4 m during the recovery period lasting for approximately 19 days.

The response is disturbed by the overall decreasing trend in the water levels that started before start of pumping in KFM02B and which is not related to the pumping. There was also some precipitation shortly before stop of pumping which may have disturbed the evaluation of the recovery period. The head in this section was corrected for the natural trend before the analysis. A linear correction was applied based on the linear head diagrams presented above. A linear plot of the corrected and uncorrected head versus time is presented in Figure A7-48 in Appendix 7.

Interpreted flow regimes and calculated parameters

During both the flow and recovery period pseudo-radial flow occurred transitioning to pseudo-spherical (leaky) flow by the end. A change in flow rate occurred after c 19,000 min during the flow period. The responses during the flow and recovery period are similar. Transient evaluation was based on variable flow rate.

The agreement in evaluated parameter values between the flow and recovery period is good. The parameter values from the flow period are selected as the most representative.

Transient, quantitative interpretation of the flow and recovery period is shown in log-log diagrams in Figures A7-49 and A7-50, Appendix 7. The results from the transient evaluation are summarized in Table 5-5 in the main report.

Observation borehole KFM06A

In Figure A6-7 an overview of the observed head responses in observation borehole KFM06A is shown. Clear responses were observed in sections 6, 7 and 8. These sections are presented below. No certain responses from the pumping in KFM02B can be detected in sections 1, 2, 3, 4 or 5 and thus no transient analysis is performed in these sections.

There is an overall decreasing trend in the water levels which is not related to the pumping in KFM02B. The responses are also disturbed by the pumping in borehole KFM08D, see Section 5.3 in the main report

Table A6-16. General test data from observation section KFM06B:3 during pumping in KFM02B.

Pressure data	Nomenclature	Unit	Value	Corrected Value[1)]
Hydraulic head in test section before start of flow period	h_i	m.a.s.l.	1.12	1.12
Hydraulic head in test section before stop of flow period	h_p	m.a.s.l.	0.48	0.68
Hydraulic head in test section at stop of recovery period	h_F	m.a.s.l.	0.82	1.09
Hydraulic head change during flow period (h_i–h_p)	dh_p	m	0.64	0.44

[1)] Head corrected for the natural decreasing head trend.

Observation section KFM06A:6 247.00–340.00 m

In Figure A6-7 an overview of the pressure responses in observation borehole KFM06A is shown. General test data from the observation section KFM06A:6 are presented in Table A6-17.

Comments on the test

A small response is indicated in this section due to pumping in KFM02B. A corrected drawdown during the flow period of c 0.2 m was registered. A (corrected) drawdown of 0.1 m was reached approximately 1,200 min (c 20 hours) after start of pumping in KFM02B. There was a corrected recovery of c 0.2 m during the recovery period of approximately 19 days.

The response is disturbed by the overall decreasing trend in the water levels that began before start of pumping in KFM02B and which is not related to the pumping. There was also some precipitation shortly before stop of pumping which may have disturbed the evaluation of the recovery period. The head in this section was corrected for the natural trend before the transient analysis. A linear head correction was applied based on the linear head diagrams presented above. A linear plot of the corrected and uncorrected head versus time is presented in Figure A7-51 in Appendix 7.

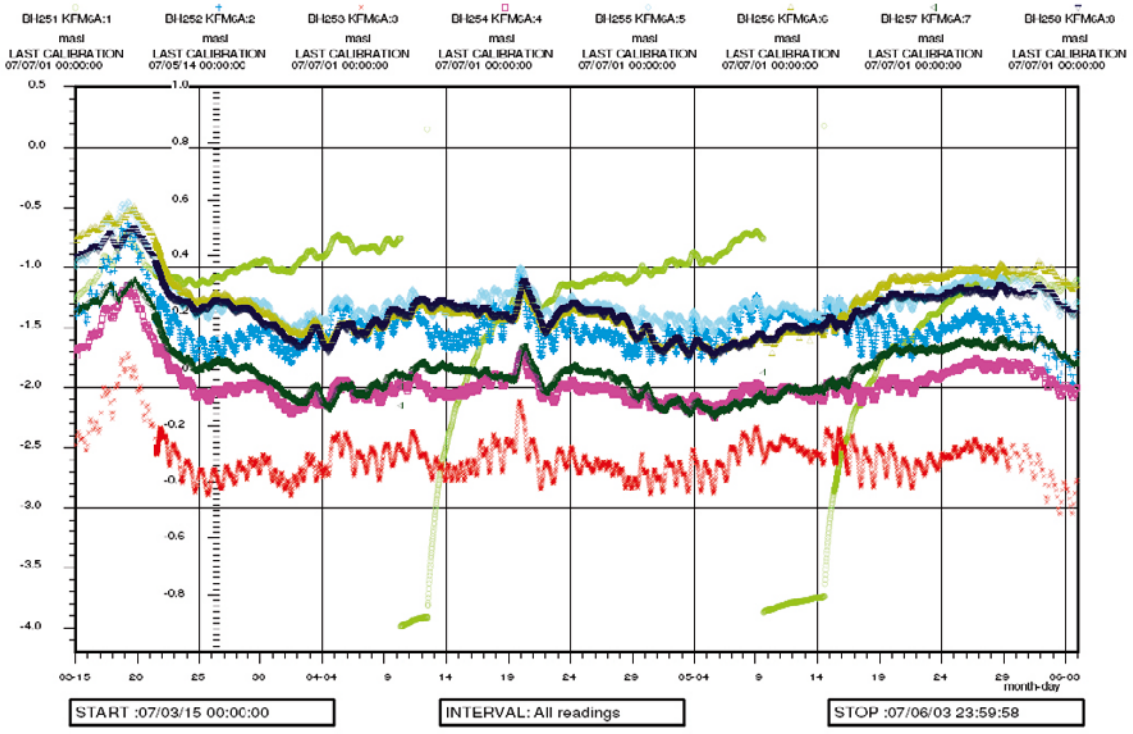

Figure A6-7. *Linear plot of observed head versus time in the observation sections in KFM06A during pumping in KFM02B.*

Table A6-17. General test data from observation section KFM06A:6 during pumping in KFM02B.

Pressure data	Nomenclature	Unit	Value	Corrected Value[1)]
Hydraulic head in test section before start of flow period	h_i	m	0.44	0.44
Hydraulic head in test section before stop of flow period	h_p	m	0.14	0.20
Hydraulic head in test section at stop of recovery period	h_F	m	0.36	0.38
Hydraulic head change during flow period (h_i–h_p)	dh_p	m	0.30	0.24

[1)] Head corrected for the natural decreasing head trend.

Interpreted flow regimes and calculated parameters

During the flow period, a transition to approximate pseudo-spherical flow occurred at intermediate times. A change in flow rate occurred after c 19,000 min during the flow period. After the flow rate change, a transition towards a new pseudo- spherical flow regime occurred. The recovery period displays a transition period followed by an approximate pseudo-spherical flow regime by the end. Transient evaluation was based on variable flow rate.

The agreement in evaluated parameter values between the flow and recovery period is good. The parameter values from the flow period are selected as the most representative.

Transient, quantitative interpretation of the flow and recovery period is shown in log-log diagrams in Figures A7-52 and A7-53, Appendix 7. The results from the transient evaluation are summarized in Table 5-5 in the main report.

Observation section KFM06A:7 151.00–246.00 m

In Figure A6-7 an overview of the observed head responses in observation borehole KFM06A:7 is shown. General test data from the observation section KFM06A:7 are presented in Table A6-18.

Comments on the test

A small response is indicated in this section due to pumping in KFM02B. A corrected drawdown during the flow period of c 0.2 m was registered. A (corrected) drawdown of 0.1 m was reached approximately 1,300 min (c 22 hours) after start of pumping in KFM02B. There was a corrected recovery of c 0.1 m during the recovery period of approximately 19 days.

The response is disturbed by the overall decreasing trend in the water levels that began before start of pumping in KFM02B and not related to the pumping. There was also some precipitation shortly before stop of pumping which may have disturbed the evaluation of the recovery period. The head in this section was corrected for the natural trend before the transient analysis. A linear head correction was applied based on the linear head diagrams presented above. A linear plot of the corrected and uncorrected head versus time is presented in Figure A7-54 in Appendix 7.

Interpreted flow regimes and calculated parameters

During the flow period, a transition to approximate pseudo-spherical flow occurred at intermediate times. A change in flow rate occurred after c 19,000 min during the flow period. After the flow rate change, a transition towards a new pseudo- spherical flow regime occurred. The recovery period displays a transition period followed by an approximate pseudo-spherical flow regime by the end. Transient evaluation was based on variable flow rate.

The agreement in evaluated parameter values between the flow and recovery period is good. The parameter values from the flow period are selected as the most representative.

Transient, quantitative interpretation of the flow and recovery period is shown in log-log diagrams in Figures A7-55 and A7-56, Appendix 7. The results from the transient evaluation are summarized in Table 5-5 in the main report.

Table A6-18. General test data from observation section KFM06A:7 during pumping in KFM02B.

Pressure data	Nomenclature	Unit	Value	Corrected Value[1)]
Hydraulic head in test section before start of flow period	h_i	m	0.18	0.18
Hydraulic head in test section before stop of flow period	h_p	m	-0.06	0.01
Hydraulic head in test section at stop of recovery period	h_F	m	0.10	0.12
Hydraulic head change during flow period (h_i–h_p)	dh_p	m	0.24	0.17

[1)] Head corrected for the natural decreasing head trend.

Observation section KFM06A:8 100.40–150.00 m

In Figure A6-7 an overview of the observed head responses in observation borehole KFM06A is shown. General test data from the observation section KFM06A:8 are presented in Table A6-19.

Comments on the test

A small response is indicated in this section due to pumping in KFM02B. A corrected drawdown during the flow period of c 0.1 m was registered. A (corrected) drawdown of 0.1 m was reached approximately 1,350 min (c 23 hours) after start of pumping in KFM02B. There was a corrected recovery of c 0.1 m during the recovery period of approximately 19 days.

The response is disturbed by the overall decreasing trend in the water levels that began before start of pumping in KFM02B and which is not related to the pumping. There was also some precipitation shortly before stop of pumping which may have disturbed the evaluation of the recovery period. The head in this section was corrected for the natural trend before the transient analysis. A linear head correction was applied based on the linear head diagrams presented above. A linear plot of the corrected and uncorrected head versus time is presented in Figure A7-57 in Appendix 7.

Interpreted flow regimes and calculated parameters

During both the flow and recovery period approximate pseudo-spherical flow occurred by the end. A change in flow rate occurred after c 19,000 min during the flow period. The responses during the flow and recovery period are similar. Transient evaluation was based on variable flow rate.

The agreement in evaluated parameter values between the flow and recovery period is good. The parameter values from the flow period are selected as the most representative.

Transient, quantitative interpretation of the flow and recovery period is shown in log-log diagrams in Figures A7-58 and A7-59, Appendix 7. The results from the transient evaluation are summarized in Table 5-5 in the main report.

Table A6-19. General test data from observation section KFM06A:8 during pumping in KFM02B.

Pressure data	Nomenclature	Unit	Value	Corrected Value[1)]
Hydraulic head in test section before start of flow period	h_i	m.a.s.l.	0.36	0.36
Hydraulic head in test section before stop of flow period	h_p	m.a.s.l.	0.16	0.23
Hydraulic head in test section at stop of recovery period	h_F	m.a.s.l.	0.29	0.29
Hydraulic head change during flow period (h_i–h_p)	dh_p	m	0.21	0.14

[1)] Head corrected for the natural decreasing head trend.

Observation borehole HFM15

In Figure A6-8 an overview of the observed head responses in observation borehole HFM15 is shown. A weak response from the pumping in KFM02B is shown both section 1 and 2. There is an overall decreasing trend in the water levels which is not related to the pumping in KFM02B. The responses are also very disturbed by the pumping in borehole KFM08D, see Section 5-3 in the main report.

Because of the weak response and the disturbance from the pumping in KFM08D no unambiguous transient evaluation is possible in this borehole.

Observation section HFM15:1 85.00–95.00 m

In Figure A6-8 an overview of the observed head responses in observation borehole HFM15 is shown. General test data from the observation section HFM15:1 are presented in Table A6-20.

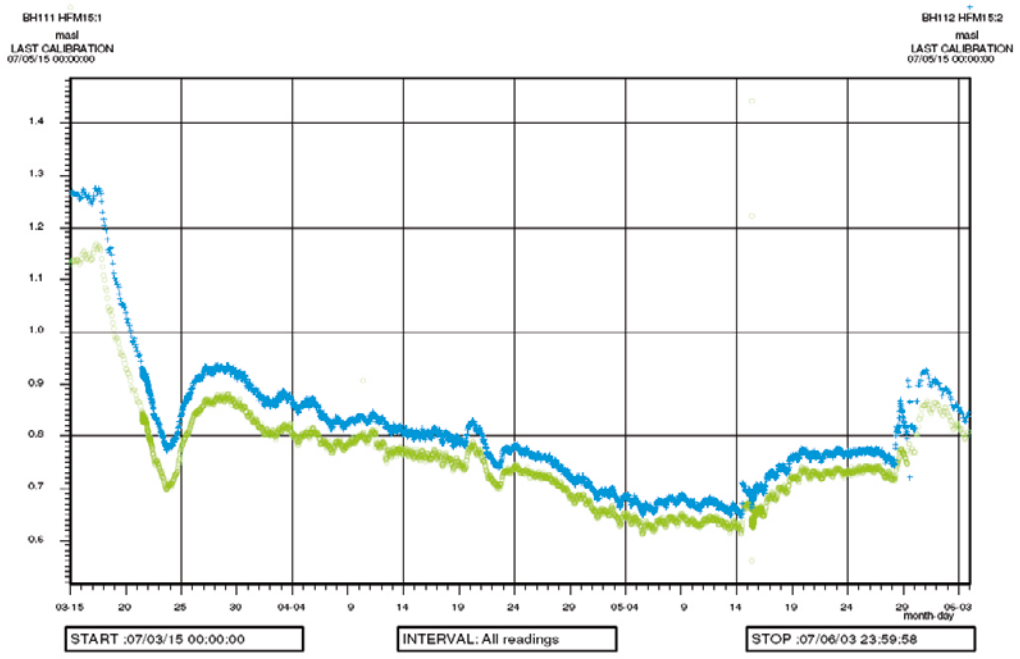

Figure A6-8. *Linear plot of observed head versus time in the observation sections in HFM15 during the pumping in KFM02B.*

Table A6-20. General test data from observation section HFM15:1 during pumping in KFM02B.

Pressure data	Nomenclature	Unit	Value	Corrected Value[1)]
Hydraulic head in test section before start of flow period	h_i	m.a.s.l.	0.83	0.83
Hydraulic head in test section before stop of flow period	h_p	m.a.s.l.	0.63	0.75
Hydraulic head in test section at stop of recovery period	h_F	m.a.s.l.	0.83	0.97
Hydraulic head change during flow period (h_i–h_p)	dh_p	m	0.20	0.08

[1)] Head corrected for the natural decreasing head trend.

Comments on the test

A small response is indicated in this section due to pumping in KFM02B. The beginning of the response during the flow period is significantly disturbed by the pumping activities in KFM08D, see above. A corrected drawdown during the flow period of c 0.1 m was registered. A corrected drawdown of 0.1 m was reached approximately 64,000 min (c 1,067 hours) after start of pumping in KFM02B. There was an apparent corrected recovery of c 0.2 m during the recovery period of approximately 19 days. Substantial precipitation around the 29th of May provides a peak in the head resulting in that the corrected head values are higher at stop of recovery than before start of the flow period.

The response is disturbed by the overall decreasing trend in the water level that commenced before start of pumping in KFM02B and which is not related to the pumping. There was also some precipitation shortly before stop of pumping which may have disturbed the evaluation of the recovery period. The head in this section was corrected for the natural trend before the transient analysis. A linear head correction was applied based on the linear head diagrams presented above. A linear plot of the corrected and uncorrected head versus time is presented in Figure A7-60 in Appendix 7.

Interpreted flow regimes and calculated parameters

No unambiguous transient evaluation is possible due to the disturbance from the pumping in KFM08D. A possible, however not unambiguous, transient, quantitative interpretation of the flow and recovery period is shown in log-log diagrams in Figures A7-61 and A7-62, Appendix 7.

Observation section HFM15:2 6.00–84.00 m

In Figure A6-8 an overview of the observed head responses in observation borehole HFM15 is shown. General test data from the observation section HFM15:2 are presented in Table A6-21.

Comments on the test

A small response is indicated in this section due to pumping in KFM02B. The beginning of the response during the flow period is significantly disturbed by the pumping activities in KFM08D, see above. A corrected drawdown during the flow period of c 0.1 m was registered.
A corrected drawdown of 0.1 m was reached approximately 56,000 min (c 933 hours) after start of pumping in KFM02B. There was a corrected recovery of c 0.2 m during the recovery period of approximately 19 days. Substantial precipitation around the 29th of May provides a peak in the head resulting in that the corrected head values are higher at stop of recovery than before start of the flow period.

The response is disturbed by the overall decreasing trend in the water levels that started before start of pumping in KFM02B and which is not related to the pumping. There was also some precipitation shortly before stop of pumping which may have disturbed the evaluation of the recovery period. The head in this section was corrected for the natural trend before the transient analysis. A linear head correction was applied based on the linear head diagrams presented above. A linear plot of the corrected and uncorrected head versus time is presented in Figure A7-63 in Appendix 7.

Table A6-21. General test data from observation section HFM15:2 during pumping in KFM02B.

Pressure data	Nomenclature	Unit	Value	Corrected Value[1)]
Hydraulic head in test section before start of flow period	h_i	m.a.s.l.	0.92	0.92
Hydraulic head in test section before stop of flow period	h_p	m.a.s.l.	0.68	0.83
Hydraulic head in test section at stop of recovery period	h_F	m.a.s.l.	0.90	1.05
Hydraulic head change during flow period (h_i–h_p)	dh_p	m	0.24	0.09

[1)] Head corrected for the natural decreasing head trend.

Interpreted flow regimes and calculated parameters

No unambiguous transient evaluation is possible due to the disturbance from the pumping in KFM08D. A possible, however not unambiguous, transient, quantitative interpretation of the flow and recovery period is shown in log-log diagrams in Figures A7-64 and A7-65, Appendix 7.

Observation borehole HFM19

In Figure A6-9 an overview of the observed head responses in observation borehole HFM19 is shown. A weak response from the pumping in KFM02B is shown all sections.

There is an overall decreasing trend in the water levels which is not related to the pumping in KFM02B. The borehole is also very disturbed by the pumping in borehole KFM08D, se Section 5-3 in the main report.

Because of the weak response and the disturbance from the pumping in KFM08D no unambiguous transient evaluation is possible in this borehole.

Observation section HFM19:1 168.00–182.00 m

In Figure A6-9 an overview of the pressure responses in observation borehole HFM19 is shown. General test data from the observation section HFM19:1 are presented in Table A6-22.

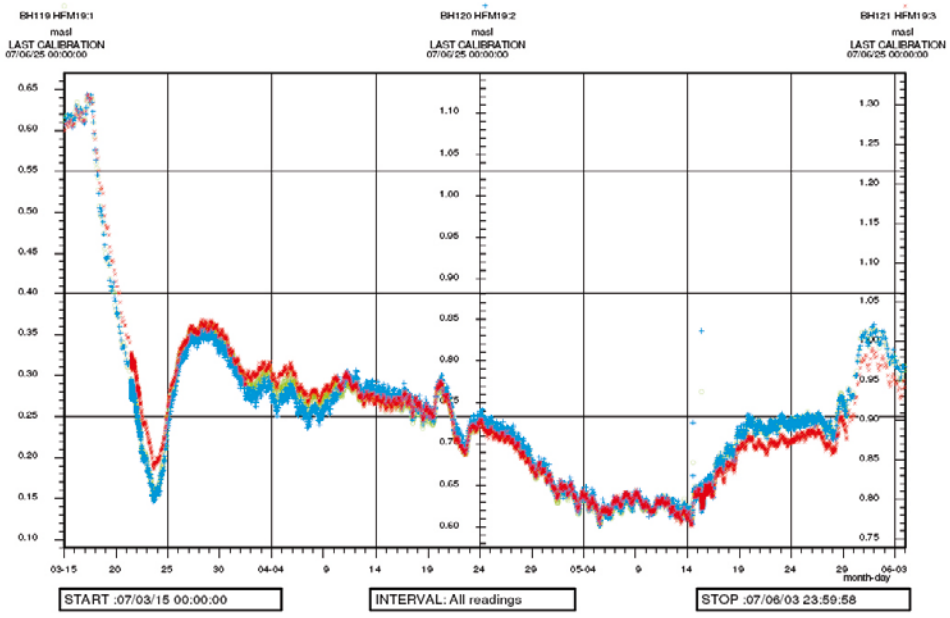

Figure A6-9. *Linear plot of observed head versus time in the observation sections in HFM19 during the pumping in KFM02B.*

Table A6-22. General test data from observation section HFM19:1 during pumping in KFM02B.

Pressure data	Nomenclature	Unit	Value	Corrected Value[1)]
Hydraulic head in test section before start of flow period	h_i	m.a.s.l.	0.28	0.28
Hydraulic head in test section before stop of flow period	h_p	m.a.s.l.	0.14	0.24
Hydraulic head in test section at stop of recovery period	h_F	m.a.s.l.	0.35	0.44
Hydraulic head change during flow period (h_i–h_p)	dh_p	m	0.14	0.04

[1)] Head corrected for the natural decreasing head trend.

Comments on the test

A very small response is indicated in this section due to pumping in KFM02B. The beginning of the response during the flow period is significantly disturbed by the pumping activities in KFM08D, see above. A corrected drawdown during the flow period of c 0.04 m was registered. A corrected drawdown of 0.01 m was reached approximately 54,000 min (c 900 hours) after start of pumping in KFM02B. (A corrected drawdown of 0.1 m was never reached). There was an apparent corrected recovery of c 0.2 m during the recovery period of approximately 19 days. Substantial precipitation around the 29th of May provides a peak in the head resulting in that the corrected head values are higher at stop of recovery than before start of the flow period.

The response is disturbed by the overall decreasing trend in the water levels that began before start of pumping in KFM02B and which is not related to the pumping. There was also some precipitation shortly before stop of pumping which may have disturbed the evaluation of the recovery period. The head in this section was corrected for the natural trend before the transient analysis. A linear head correction was applied based on the linear head diagrams presented above. A linear plot of the corrected and uncorrected head versus time is presented in Figure A7-66 in Appendix 7.

Interpreted flow regimes and calculated parameters

No unambiguous transient evaluation is possible due to the disturbance from the pumping in KFM08D. A possible, however not unambiguous, transient, quantitative interpretation of the flow and recovery period is shown in log-log diagrams in Figures A7-67 and A7-68, Appendix 7.

Observation section HFM19:2 104.00–167.00 m

In Figure A6-9 an overview of the observed head responses in observation borehole HFM19 is shown. General test data from the observation section HFM19:2 are presented in Table A6-23.

Comments on the test

A very small response is indicated in this section due to pumping in KFM02B. The beginning of the response during the flow period is significantly disturbed by the pumping activities in KFM08D, see above. A corrected drawdown during the flow period of c 0.03 m was registered. A corrected drawdown of 0.01 m was reached approximately 50,000 min (c 833 hours) after start of pumping in KFM02B. (A corrected drawdown of 0.1 m was never reached). There was an apparent corrected recovery of c 0.2 m during the recovery period of approximately 19 days. Substantial precipitation around the 29th of May provides a peak in the head resulting in that the corrected head values are higher at stop of recovery than before start of the flow period.

The response is disturbed by the overall decreasing trend in the water levels that begun before start of pumping in KFM02B and which is not related to the pumping. There was also some precipitation shortly before stop of pumping which may have disturbed the evaluation of the recovery period. The head in this section was corrected for the natural trend before the transient analysis. A linear head correction was applied based on the linear head diagrams presented above. A linear plot of the corrected and uncorrected head versus time is presented in Figure A7-69 in Appendix 7.

Table A6-23. General test data from observation section HFM19:2 during pumping in KFM02B.

Pressure data	Nomenclature	Unit	Value	Corrected Value[1)]
Hydraulic head in test section before start of flow period	h_i	m.a.s.l.	0.76	0.76
Hydraulic head in test section before stop of flow period	h_p	m.a.s.l.	0.63	0.73
Hydraulic head in test section at stop of recovery period	h_F	m.a.s.l.	0.79	0.93
Hydraulic head change during flow period (h_i–h_p)	dh_p	m	0.13	0.03

[1)] Head corrected for the natural decreasing head trend.

Interpreted flow regimes and calculated parameters

No unambiguous transient evaluation is possible due to the disturbance from the pumping in KFM08D. A possible, however not unambiguous, transient, quantitative interpretation of the flow and recovery period is shown in log-log diagrams in Figures A7-70 and A7-71, Appendix 7.

Observation section HFM19:3 12.04–103.00 m

In Figure A6-9 an overview of the observed head responses in observation borehole HFM19 is shown. General test data from the observation section HFM19:3 are presented in Table A6-24.

Comments on the test

A very small response is indicated in this section due to pumping in KFM02B. The beginning of the response during the flow period is significantly disturbed by the pumping activities in KFM08D, see above. A corrected drawdown during the flow period of c 0.04 m was registered. A corrected drawdown of 0.01 m was reached approximately 52,000 min (c 867 hours) after start of pumping in KFM02B. (A corrected drawdown of 0.1 m was never reached). There was an apparent corrected recovery of c 0.2 m during the recovery period of approximately 19 days. Substantial precipitation around the 29th of May provides a peak in the head resulting in that the corrected head values are higher at stop of recovery than before start of the flow period.

The response is disturbed by the overall decreasing trend in the water levels that commenced before start of pumping in KFM02B and which is not related to the pumping. There was also some precipitation shortly before stop of pumping which may have disturbed the evaluation of the recovery period. The head in this section was corrected for the natural trend before the transient analysis. A linear head correction was applied based on the linear head diagrams presented above. A linear plot of the corrected and uncorrected head versus time is presented in Figure A7-72 in Appendix 7.

Interpreted flow regimes and calculated parameters

No unambiguous transient evaluation is possible due to the disturbance from the pumping in KFM08D. A possible, however not unambiguous, transient, quantitative interpretation of the flow and recovery period is shown in log-log diagrams in Figures A7-73 and A7-74, Appendix 7.

Table A6-24. General test data from observation section HFM19:3 during pumping in KFM02B.

Pressure data	Nomenclature	Unit	Value	Corrected Value[1)]
Hydraulic head in test section before start of flow period	h_i	m.a.s.l.	0.97	0.97
Hydraulic head in test section before stop of flow period	h_p	m.a.s.l.	0.80	0.93
Hydraulic head in test section at stop of recovery period	h_F	m.a.s.l.	0.97	1.12
Hydraulic head change during flow period (h_i–h_p)	dh_p	m	0.18	0.05

[1)] Head corrected for the natural decreasing head trend.

Observation borehole HFM13

In Figure A6-10 an overview of the observed head responses in observation borehole HFM13 is shown. A weak response from the pumping in KFM02B is shown both section 1 and 2. No responses from the pumping in KFM02B can be detected in section 3.

There is an overall decreasing trend in the water levels which is not related to the pumping in KFM02B. The borehole is also very disturbed by the pumping in borehole KFM08D, see Section 5.3 in the main report. The short period of increased head in section 3 which can be observed in connection to stop of the pumping in KFM02B (2007-05-15) is probably due to precipitation.

Because of the weak response and the disturbance from the pumping in KFM08D no unambiguous transient evaluation is possible in this borehole.

Observation section HFM13:1 159.00–173.00 m

In Figure A6-10 an overview of the observed head responses in observation borehole HFM13 is shown. General test data from the observation section HFM13:1 are presented in Table A6-25.

Comments on the test

A very small response is indicated in this section due to pumping in KFM02B. The beginning of the response during the flow period is significantly disturbed by the pumping activities in KFM08D, see above. A corrected drawdown during the flow period of c 0.04 m was registered.

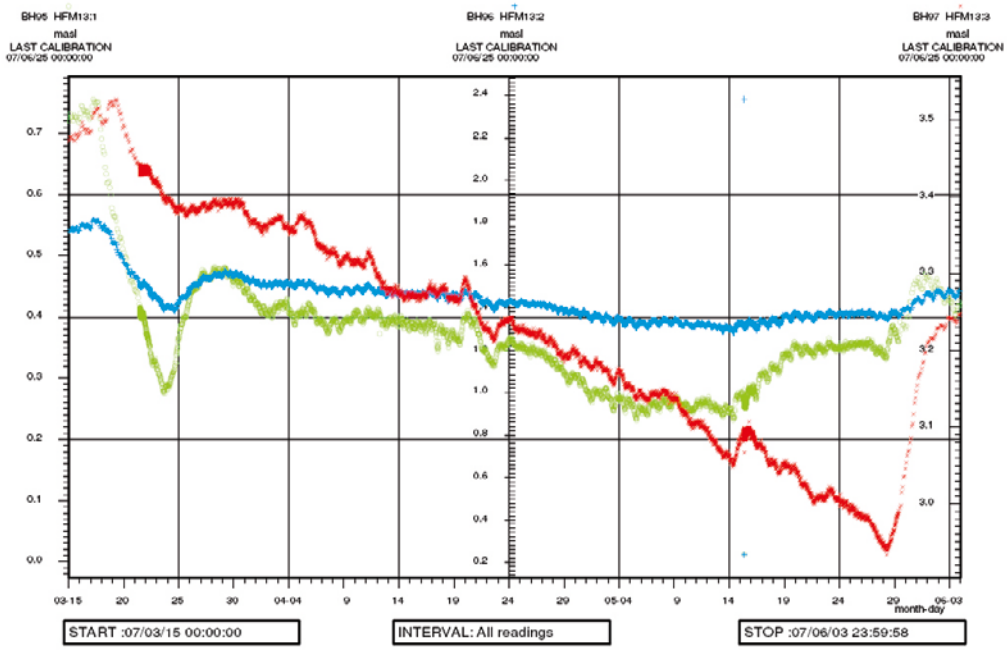

Figure A6-10. *Linear plot of observed head versus time in the observation sections in HFM13 during the pumping in KFM02B.*

Table A6-25. General test data from observation section HFM13:1 during pumping in KFM02B.

Pressure data	Nomenclature	Unit	Value	Corrected Value[1)]
Hydraulic head in test section before start of flow period	h_i	m.a.s.l.	0.41	0.41
Hydraulic head in test section before stop of flow period	h_p	m.a.s.l.	0.26	0.37
Hydraulic head in test section at stop of recovery period	h_F	m.a.s.l.	0.42	0.57
Hydraulic head change during flow period (h_i–h_p)	dh_p	m	0.15	0.04

[1)] Head corrected for the natural decreasing head trend.

A (corrected) drawdown of 0.01 m was reached approximately 50,000 min (c 833 hours) after start of pumping in KFM02B. (A corrected drawdown of 0.1 m was never reached). There was an apparent corrected recovery of c 0.2 m during the recovery period of approximately 19 days. Substantial precipitation around the 29th of May provides a peak in the head resulting in that the corrected head values are higher at stop of recovery than before start of the flow period.

The response is disturbed by the overall decreasing trend in the water level that started before start of pumping in KFM02B and which is not related to the pumping. There was also some precipitation shortly before stop of pumping which may have disturbed the evaluation of the recovery period. The head in this section was corrected for the natural trend before the transient analysis. A linear head correction was applied based on the linear head diagrams presented above. A linear plot of the corrected and uncorrected head versus time is presented in Figure A7-75 in Appendix 7.

Interpreted flow regimes and calculated parameters

No unambiguous transient evaluation is possible due to the disturbance from the pumping in KFM08D. A possible, however not unambiguous, transient, quantitative interpretation of the flow and recovery period is shown in log-log diagrams in Figures A7-76 and A7-77, Appendix 7.

Observation section HFM13:2 101.00–158.00 m

In Figure A6-10 an overview of the observed head responses in observation borehole HFM13 is shown. General test data from the observation section HFM13:2 are presented in Table A6-26.

Comments on the test

A very small response is indicated in this section due to pumping in KFM02B. The beginning of the response during the flow period is significantly disturbed by the pumping activities in KFM08D, see above. A corrected drawdown during the flow period of c 0.02 m was registered. A (corrected) drawdown of 0.01 m was reached approximately 55,000 min (c 917 hours) after start of pumping in KFM02B. (A corrected drawdown of 0.1 m was never reached). There was an apparent corrected recovery of c 0.2 m during the recovery period of approximately 19 days. Substantial precipitation around the 29th of May provides a peak in the head resulting in that the corrected head values are higher at stop of recovery than before start of the flow period.

The response is disturbed by the overall decreasing trend in the water levels that started before start of pumping in KFM02B and which is not related to the pumping. There was also some precipitation shortly before stop of pumping which may have disturbed the evaluation of the recovery period. The head in this section was corrected for the natural trend before the transient analysis. A linear head correction was applied based on the linear head diagrams presented above. A linear plot of the corrected and uncorrected head versus time is presented in Figure A7-78 in Appendix 7.

Interpreted flow regimes and calculated parameters

No unambiguous transient evaluation is possible due to the disturbance from the pumping in KFM08D. A possible, however not unambiguous, transient, quantitative interpretation of the flow and recovery period is shown in log-log diagrams in Figures A7-79 and A7-80, Appendix 7.

Table A6-26. General test data from observation section HFM13:2 during the pumping in KFM02B.

Pressure data	Nomenclature	Unit	Value	Corrected Value[1)]
Hydraulic head in test section before start of flow period	h_i	m.a.s.l.	1.50	1.50
Hydraulic head in test section before stop of flow period	h_p	m.a.s.l.	1.31	1.48
Hydraulic head in test section at stop of recovery period	h_F	m.a.s.l.	1.48	1.70
Hydraulic head change during flow period (h_i–h_p)	dh_p	m	0.19	0.02

[1)] Head corrected for the natural decreasing head trend.

Observation boreholes with uncertain responses

In some borehole sections it is not considered possible to deduce if a response or not occurred due to the pumping in KFM02B due to disturbances as e.g. precipitation, other pumping activities etc These borehole sections are discussed below.

Observation borehole KFM10A

In Figure A6-11 an overview of the observed head responses in observation borehole KFM10A is shown. A possible weak response from the pumping in KFM02B can not be confirmed but nor excluded in sections 1, 2, 3 and 4. No responses from the pumping in KFM02B can be detected in section 5.

New sections are installed in the borehole during the pumping. There is an overall decreasing trend in the water levels which is not related to the pumping in KFM02B. The borehole is also very disturbed by the pumping in borehole KFM08D, see Section 5.3 in the main report. Because of the uncertainty in the response, no unambiguous transient evaluation is possible in this borehole.

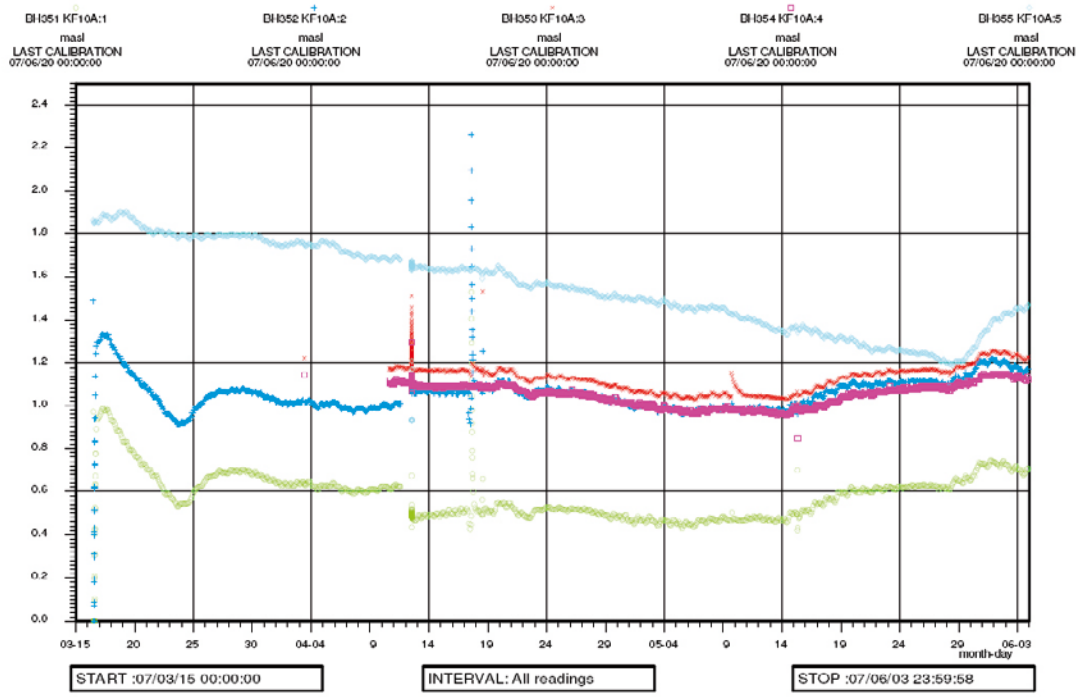

Figure A6-11. *Linear plot of observed head versus time in the observation sections in KFM10A during the pumping in KFM02B.*

Observation borehole KFM01C

In Figure A6-12 an overview of the observed head responses in observation borehole KFM01C is shown. A possible weak response from the pumping in KFM02B can not be confirmed but nor excluded in sections 2 and 3. No responses from the pumping in KFM02B can be detected in section 1.

There is an overall decreasing trend in the water levels which is not related to the pumping in KFM02B. The borehole is also very disturbed by the pumping in borehole KFM08D, see Section 5.3 in the main report.

Because of the uncertainty in the response no unambiguous transient evaluation is possible in this borehole.

Observation borehole HFM01

In Figure A6-13 an overview of the pressure responses in observation borehole HFM01 is shown. A possible weak response from the pumping in KFM02B can not be confirmed but nor excluded in any section in the borehole.
There is an overall decreasing trend in the water levels which is not related to the pumping in KFM02B. The borehole is also very disturbed by the pumping in borehole KFM08D, see Section 5.3 in the main report.

Because of the uncertainty in the response no unambiguous transient evaluation is possible in this borehole.Appendix 7

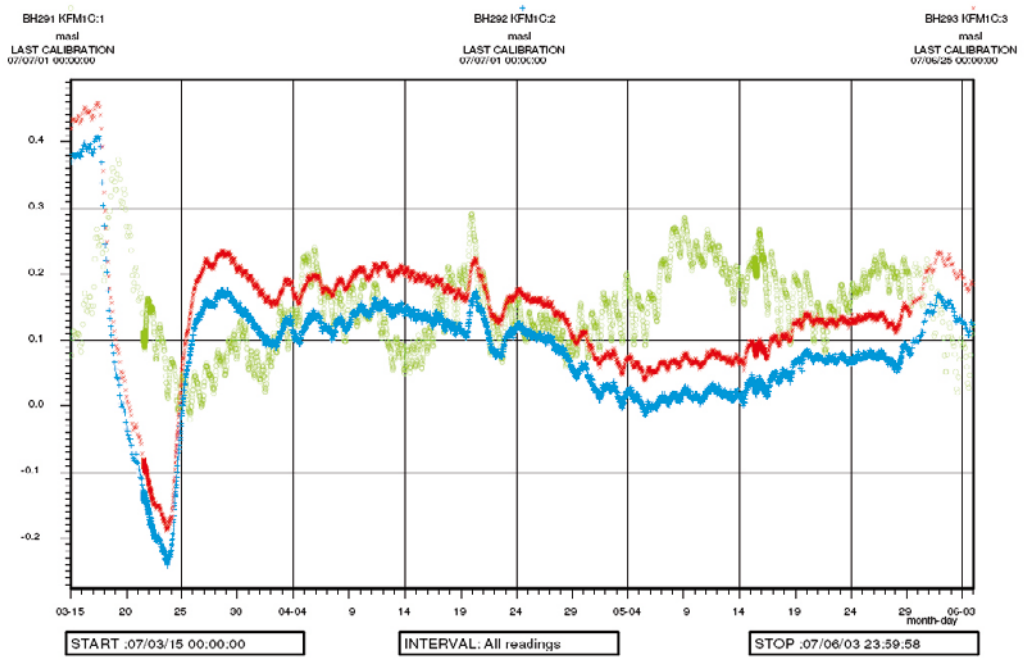

Figure A6-12. *Linear plot of observed head versus time in the observation sections in KFM01C during the pumping in KFM02B.*

Appendix 7

Test diagrams and meteorological data

Nomenclature for AQTESOLV:

T = transmissivity (m^2/s)
S = storativity (-)
K_Z/K_r = ratio of hydraulic conductivities in the vertical and radial direction (set to 1)
Sw = skin factor
r(w) = borehole radius (m)
r(c) = effective casing radius (m)
r/B = leakage coefficient (s^{-1})
b = thickness of formation (m)

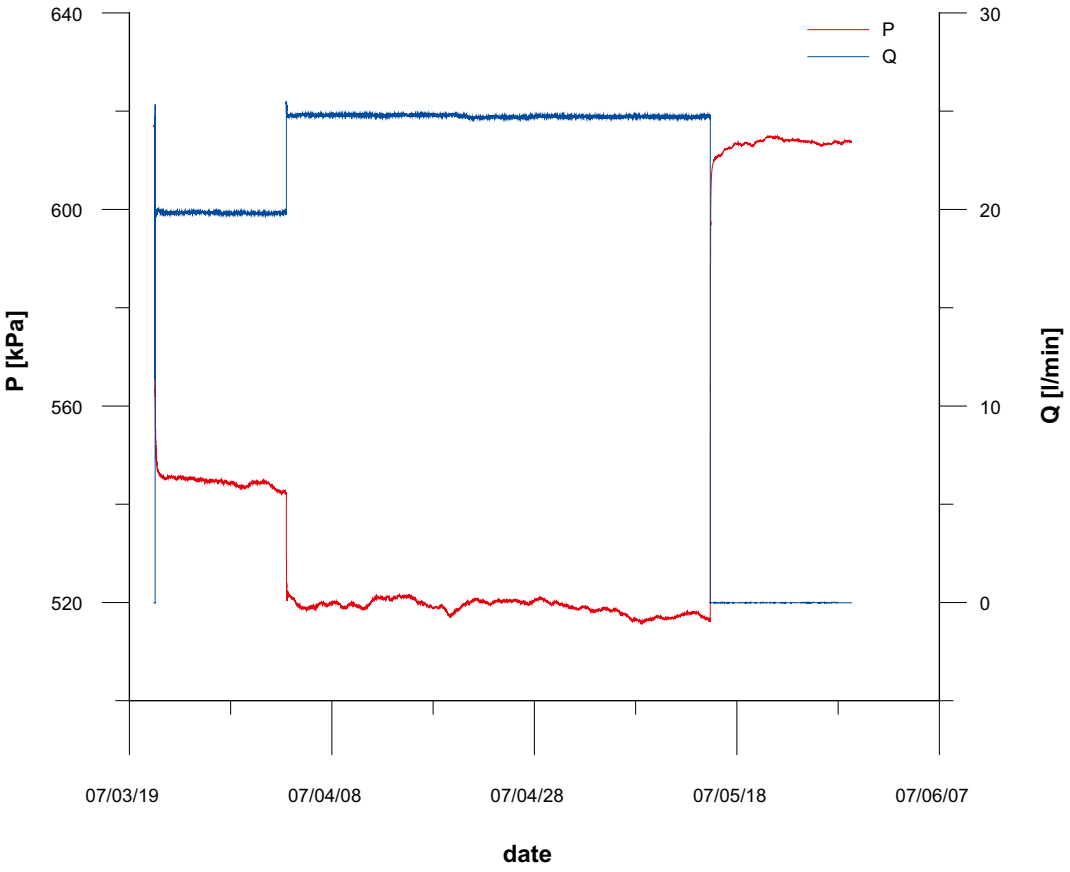

Figure A7-1. *Linear plot of pressure versus time in the pumping borehole KFM02B, 408.5–434.0 m.*

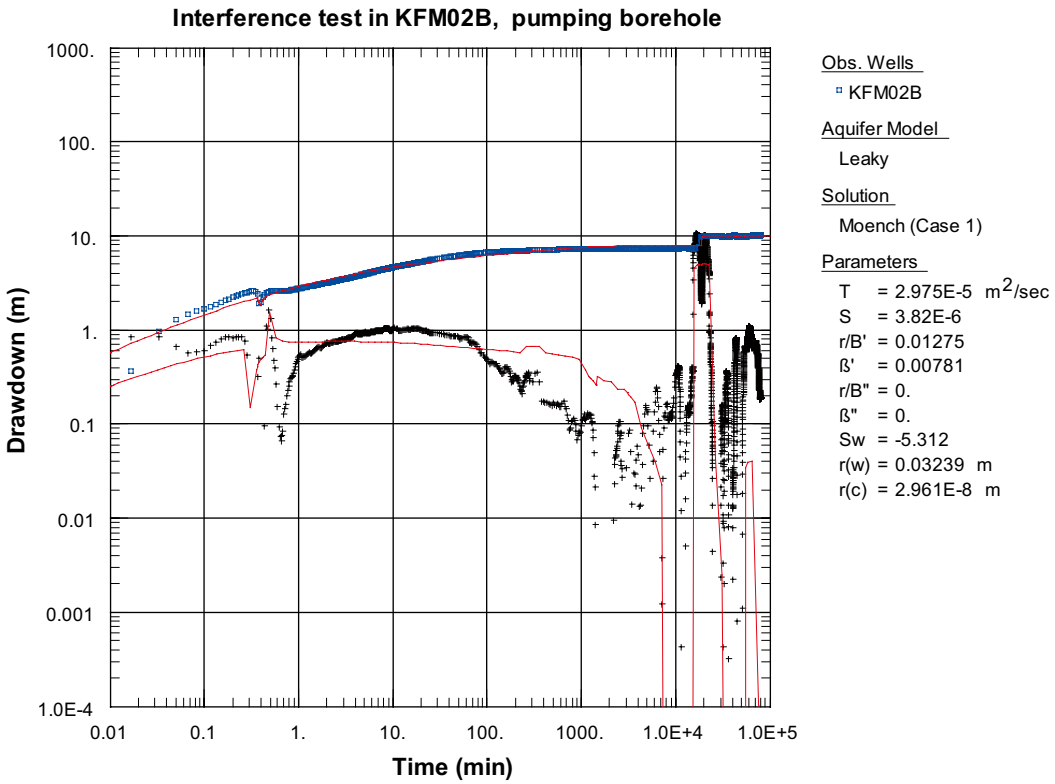

Figure A7-2. *Log-log plot of drawdown (▫) and drawdown derivative, ds/d(ln t) (+), versus time in KFM02B, 408.5–434.0 m, during the interference test in KFM02B.*

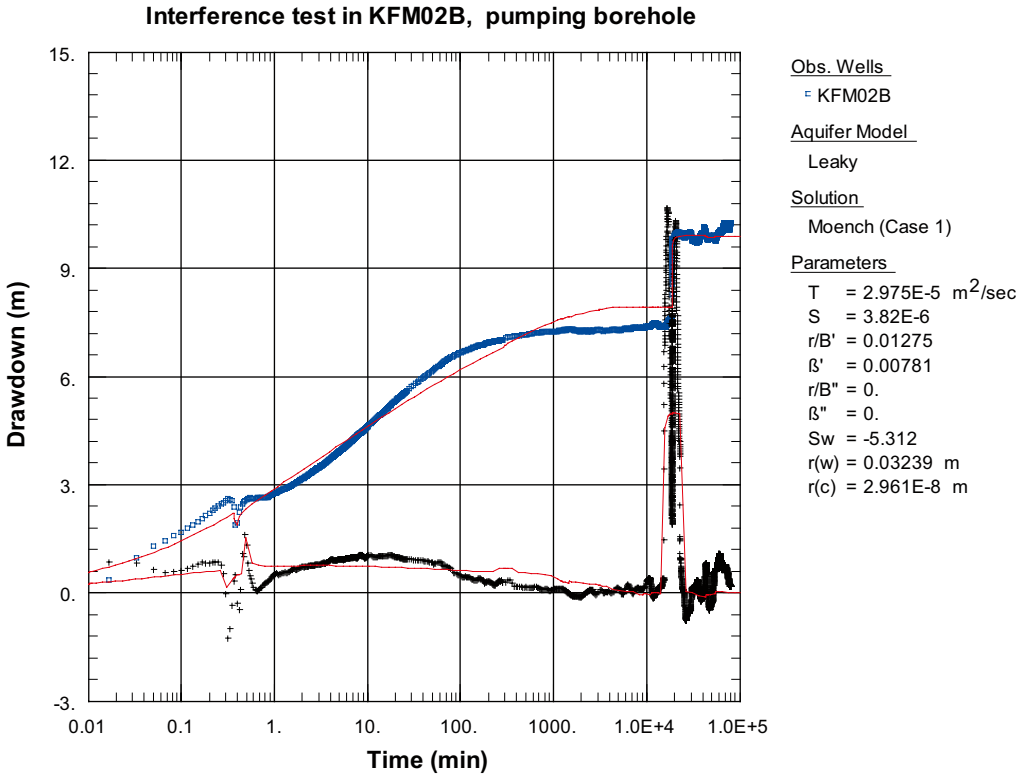

Figure A7-3. *Lin-log plot of drawdown (▫) and drawdown derivative, ds/d(ln t) (+), versus time in KFM02B, 408.5–434.0 m, during the interference test in KFM02B.*

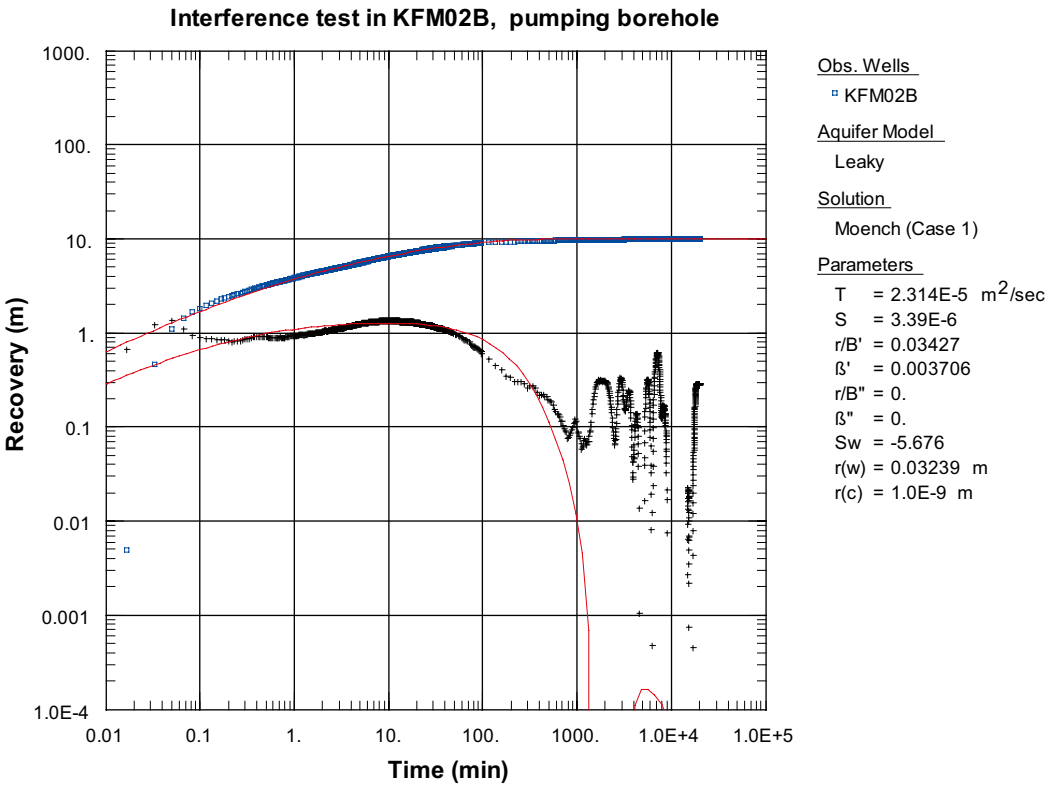

Figure A7-4. *Log-log plot of recovery (▫) and recovery derivative, ds/d(ln t) (+), versus time in KFM02B, 408.5–434.0 m, during the interference test in KFM02B.*

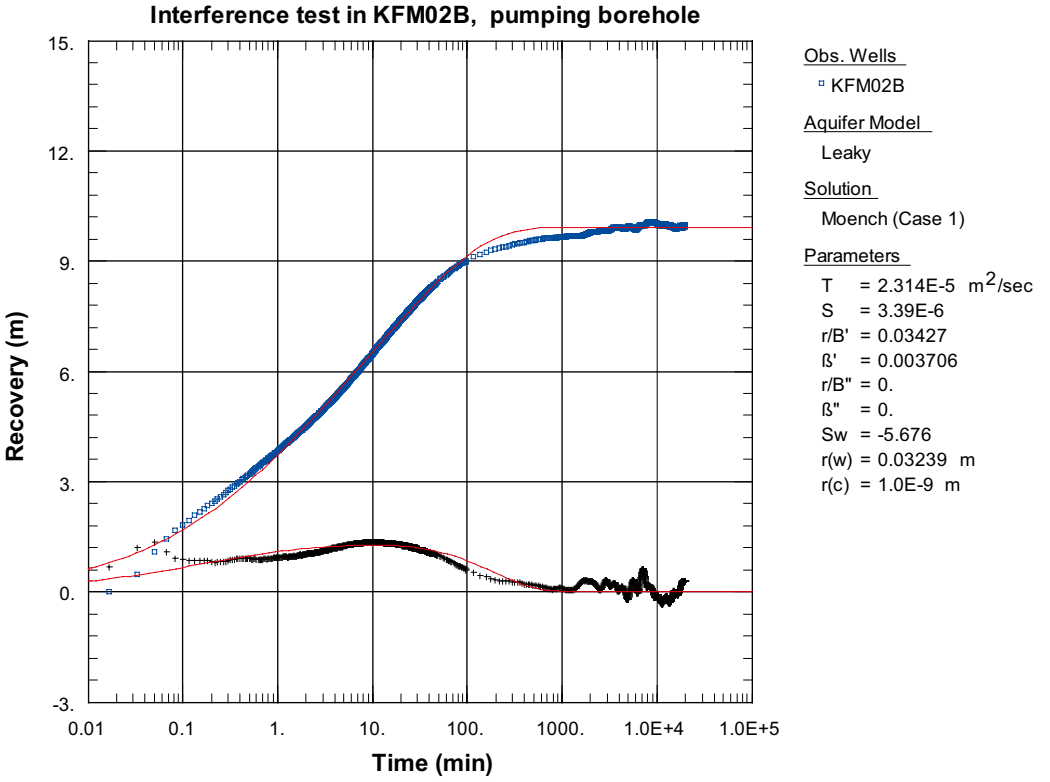

Figure A7-5. *Lin-log plot of recovery (▫) and recovery derivative, ds/d(ln t) (+), versus time in KFM02B, 408.5–434.0 m, during the interference test in KFM02B.*

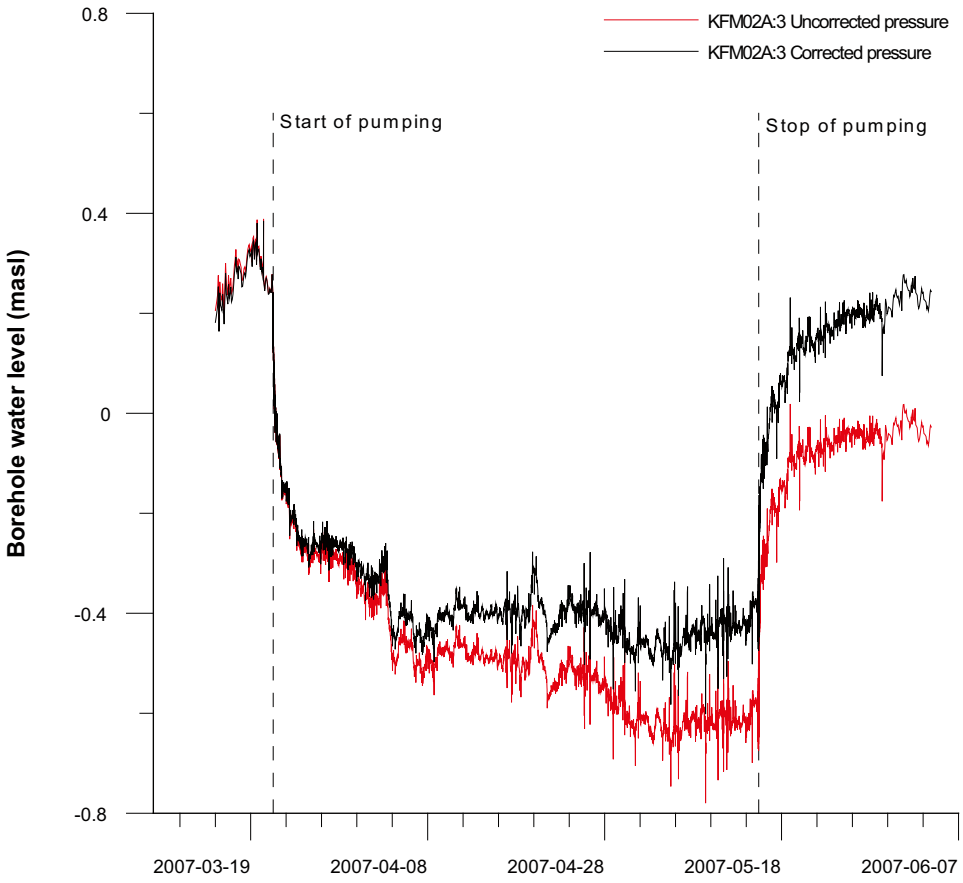

Figure A7-6. *Linear plot of pressure and pressure corrected for the natural decreasing pressure trend versus time in the observation section KFM02A:3 during the pumping in KFM02B.*

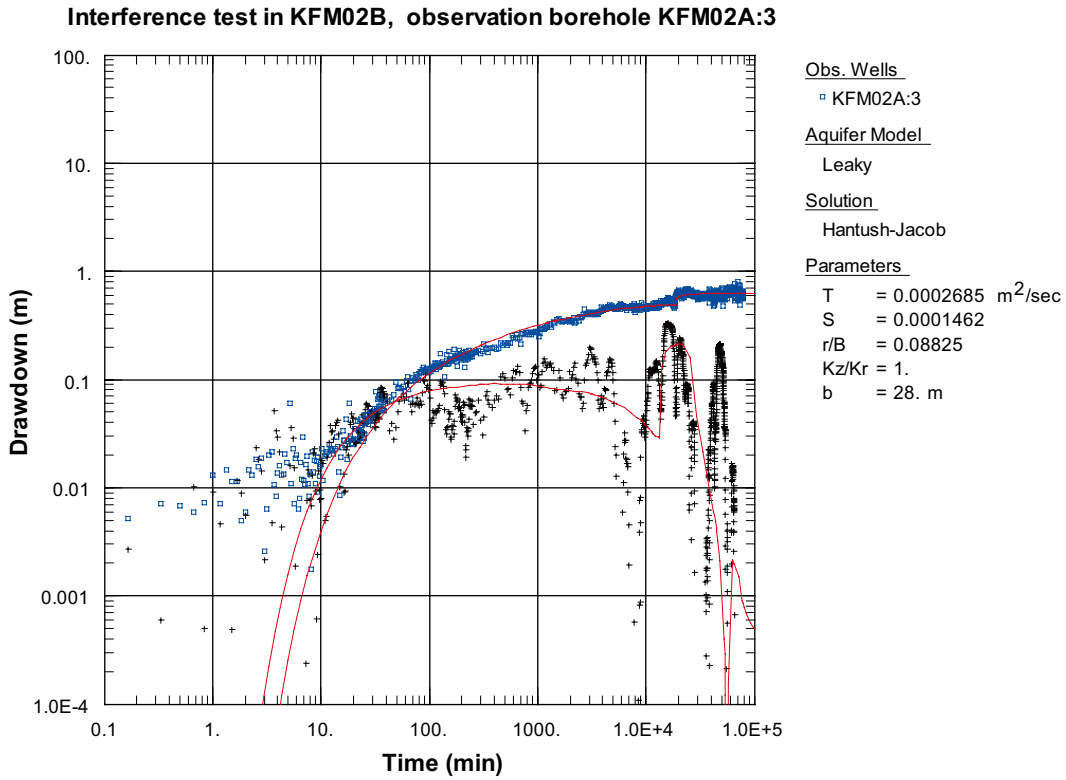

Figure A7-7. *Log-log plot of drawdown (▫) and drawdown derivative, ds/d(ln t) (+), versus time in KFM02A:3 during the interference test in KFM02B.*

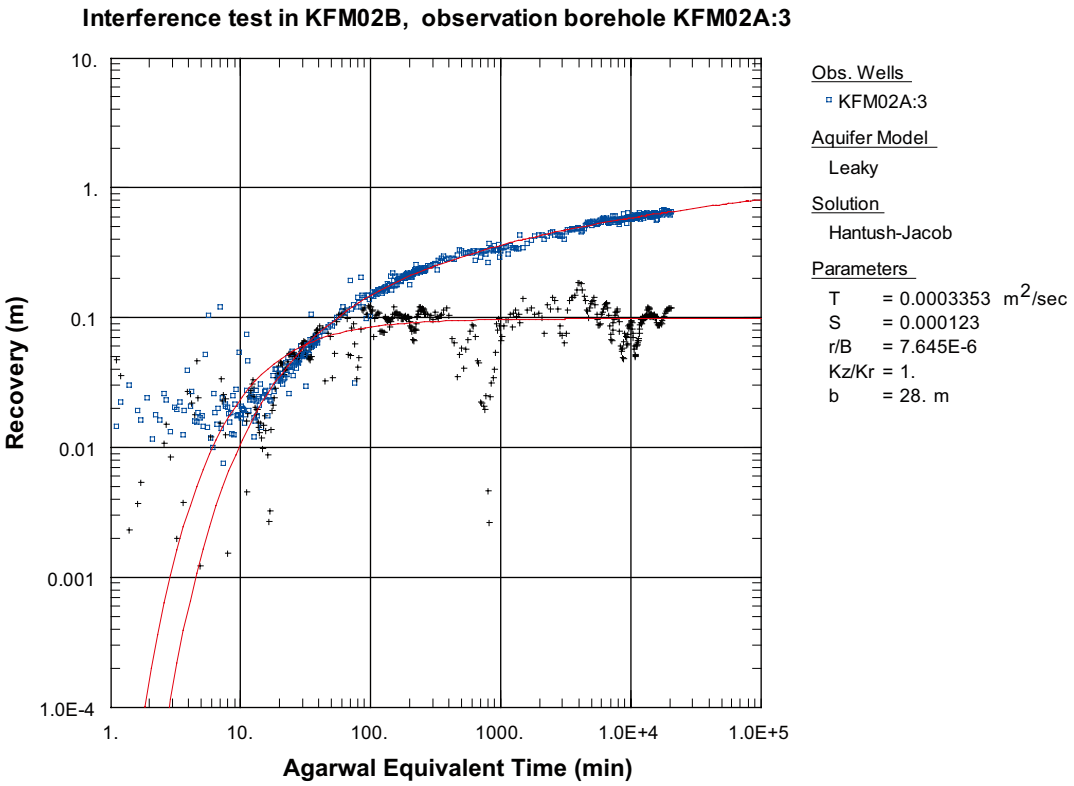

Figure A7-8. *Log-log plot of recovery (▫) and recovery derivative, ds/d(ln t) (+), versus time in KFM02A:3 during the interference test in KFM02B.*

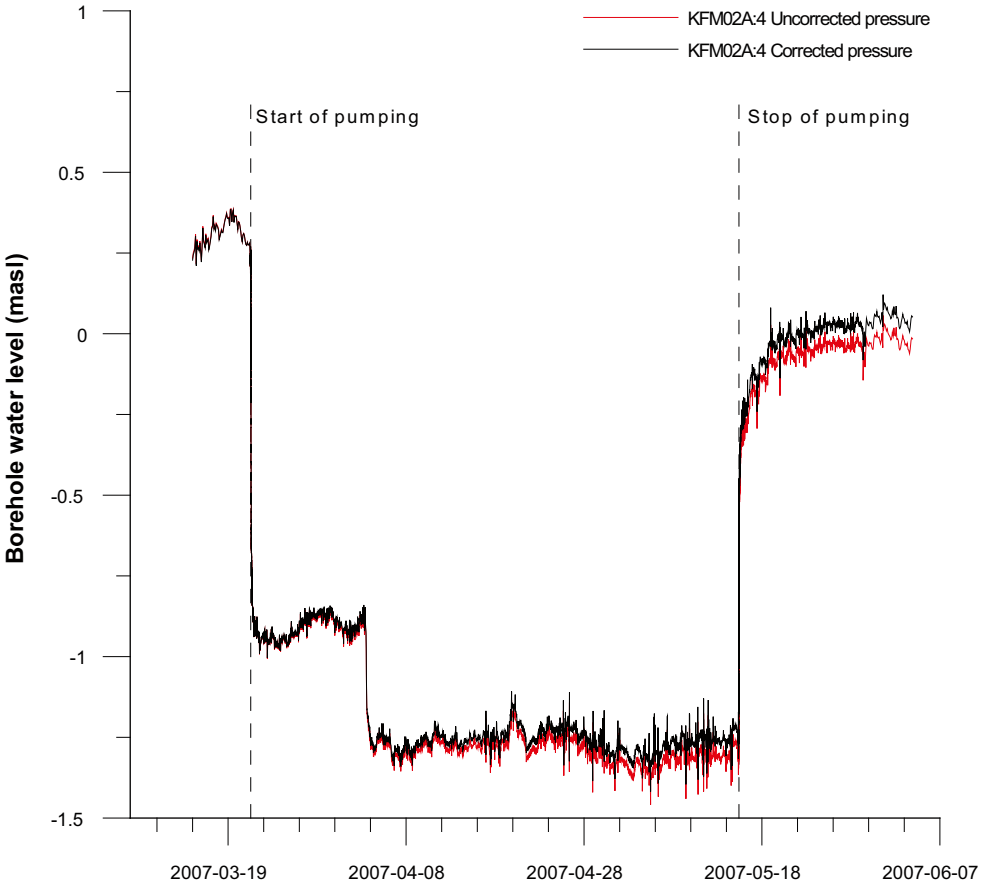

Figure A7-9. *Linear plot of pressure and pressure corrected for the natural decreasing pressure trend versus time in the observation section KFM02A:4 during the pumping in KFM02B.*

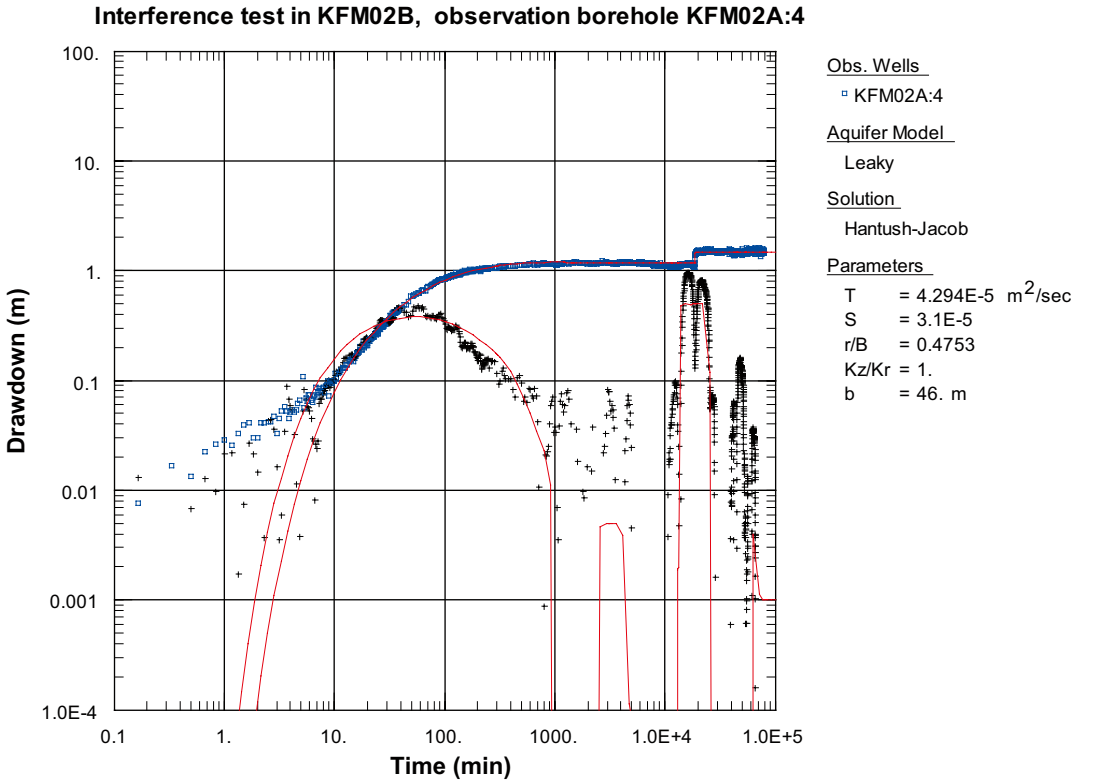

Figure A7-10. *Log-log plot of drawdown (▫) and drawdown derivative, ds/d(ln t) (+), versus time in KFM02A:4 during the interference test in KFM02B.*

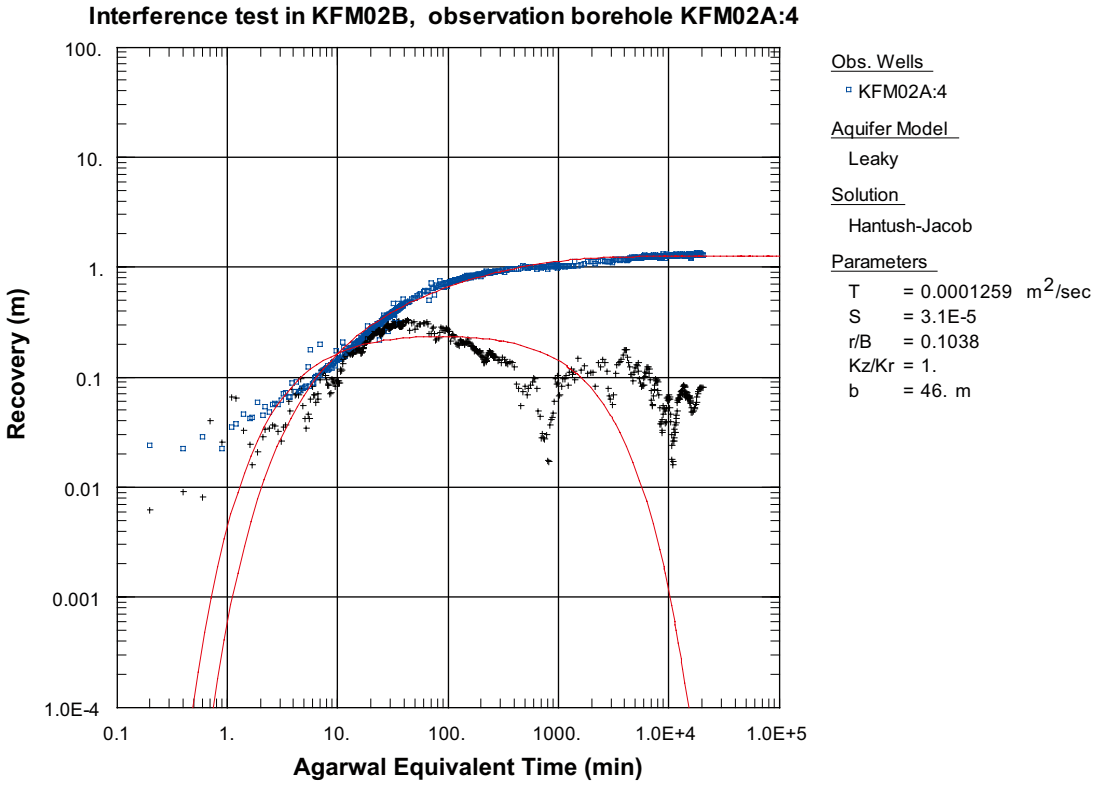

Figure A7-11. *Log-log plot of recovery (▫) and recovery derivative, ds/d(ln t) (+), versus time in KFM02A:4 during the interference test in KFM02B.*

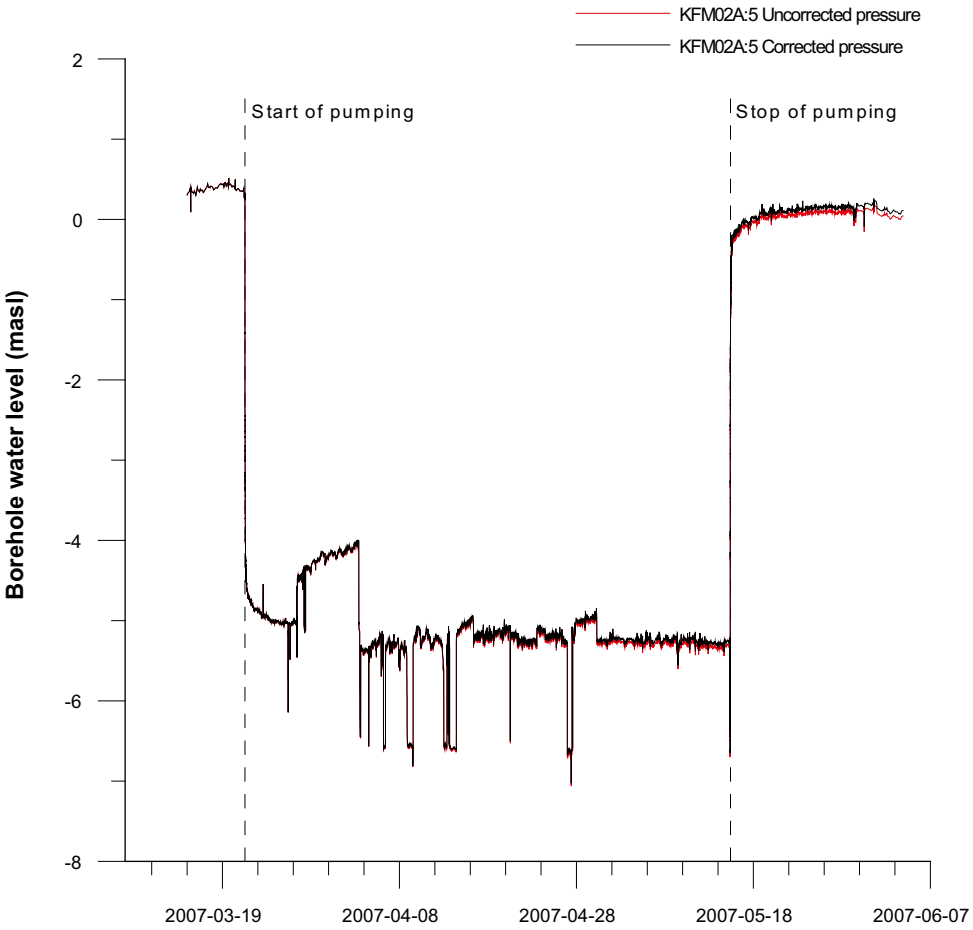

Figure A7-12. *Linear plot of pressure and pressure corrected for the natural decreasing pressure trend versus time in the observation section KFM02A:5 during the pumping in KFM02B.*

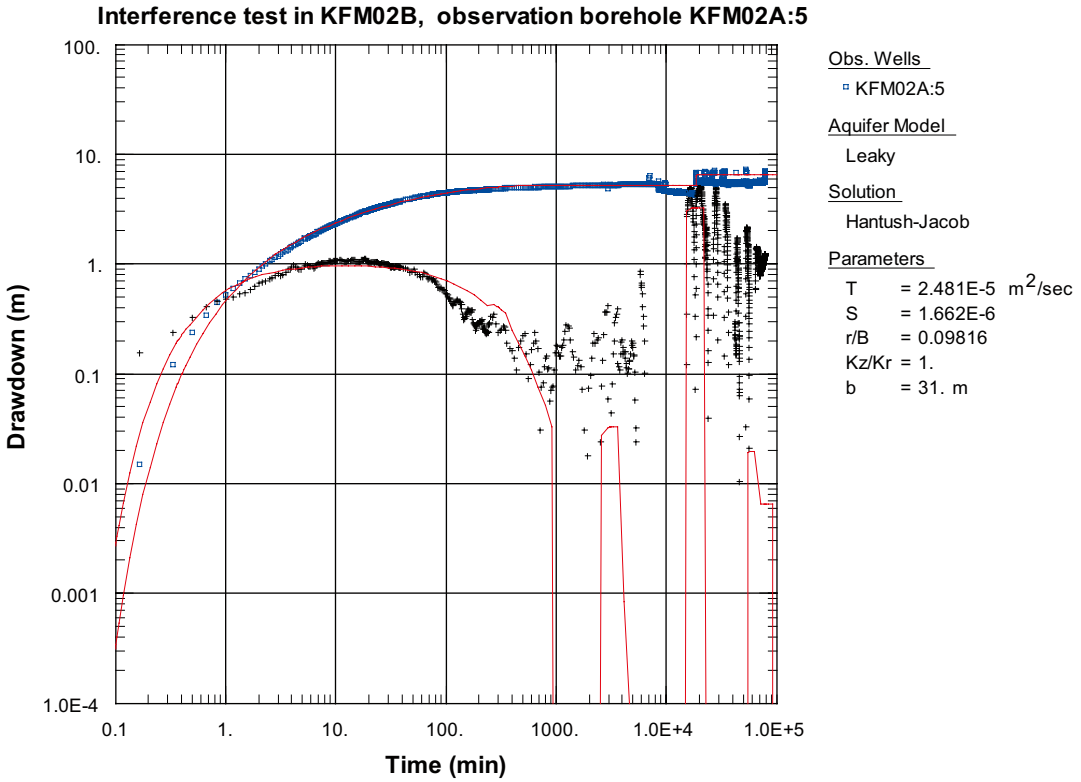

Figure A7-13. *Log-log plot of drawdown (▫) and drawdown derivative, ds/d(ln t) (+), versus time in KFM02A:5 during the interference test in KFM02B.*

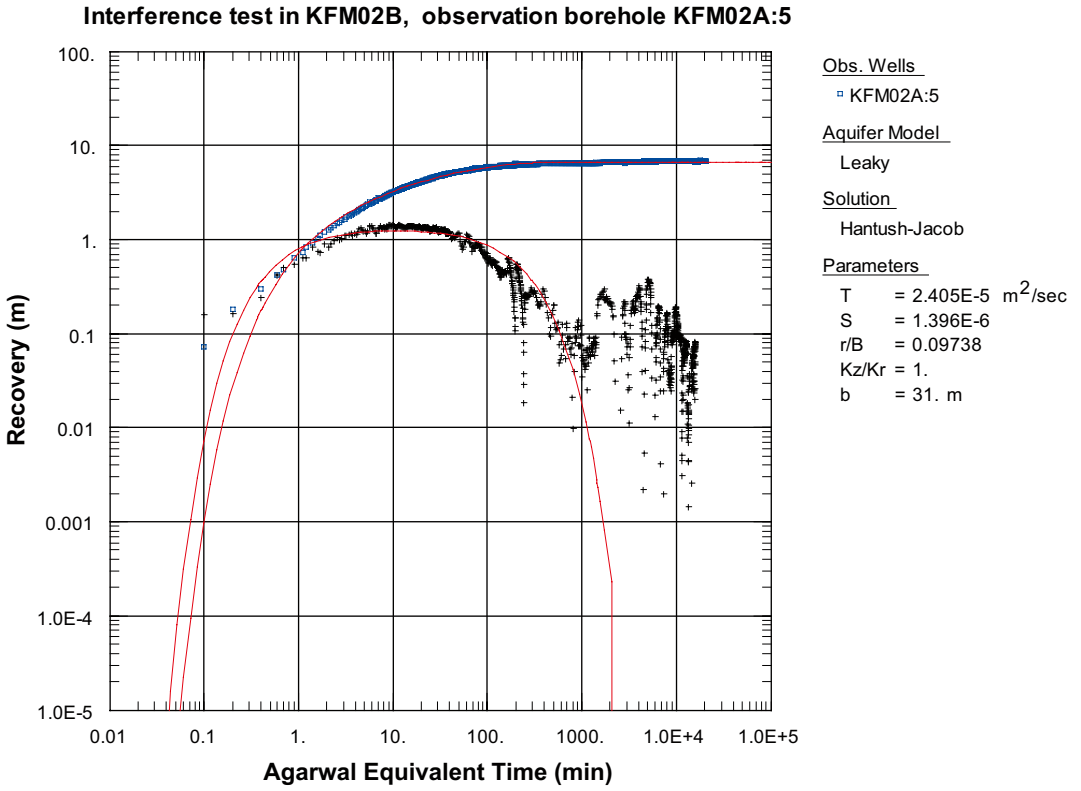

Figure A7-14. *Log-log plot of recovery (▫) and recovery derivative, ds/d(ln t) (+), versus time in KFM02A:5 during the interference test in KFM02B.*

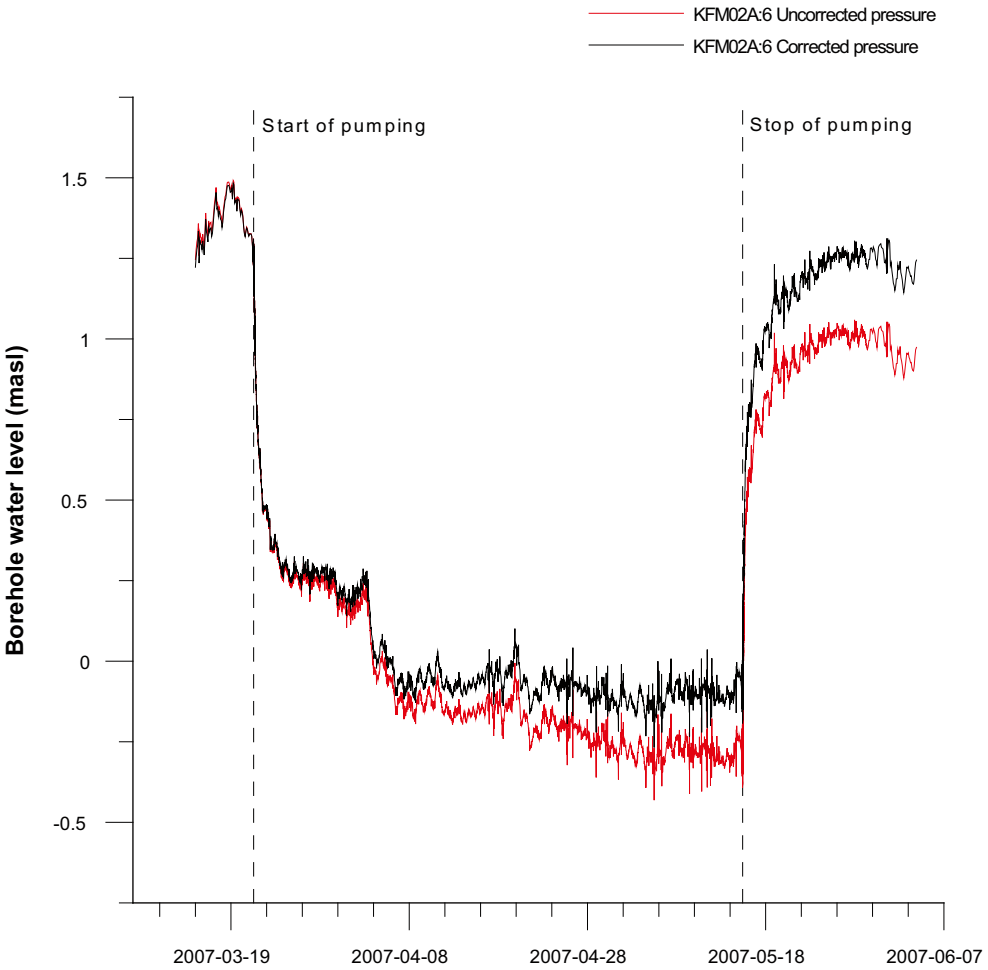

Figure A7-15. *Linear plot of pressure and pressure corrected for the natural decreasing pressure trend versus time in the observation section KFM02A:6 during the pumping in KFM02B.*

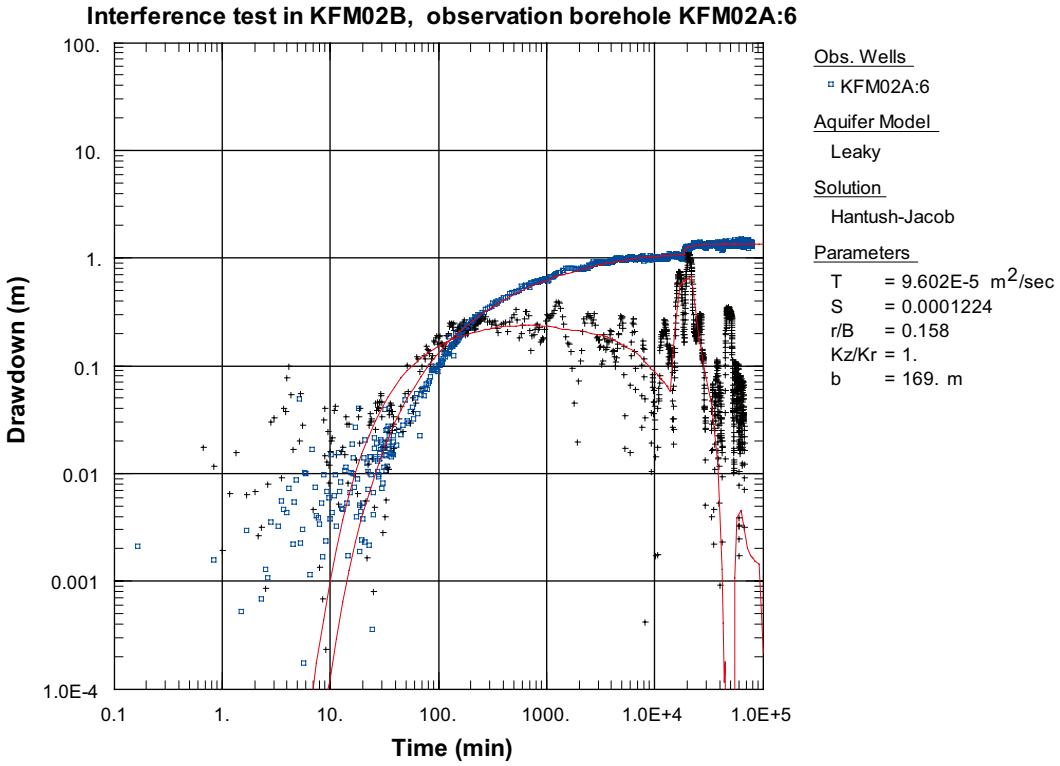

Figure A7-16. *Log-log plot of drawdown (▫) and drawdown derivative, ds/d(ln t) (+), versus time in KFM02A:6 during the interference test in KFM02B.*

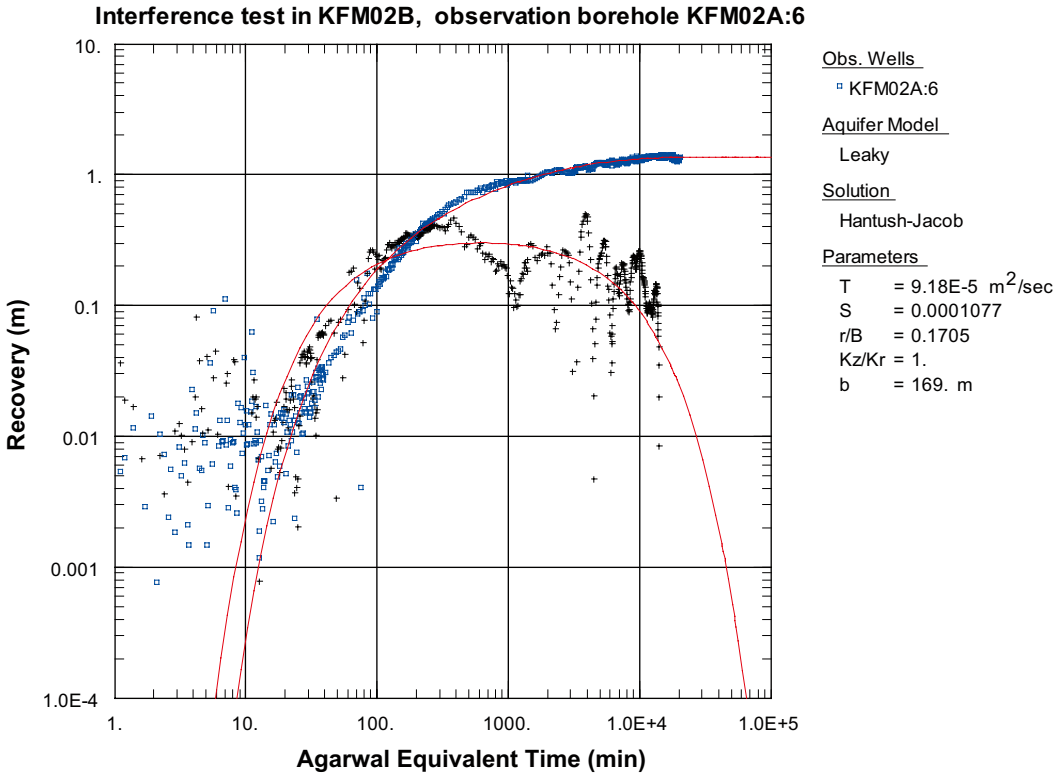

Figure A7-17. *Log-log plot of recovery (▫) and recovery derivative, ds/d(ln t) (+), versus time in KFM02A:6 during the interference test in KFM02B*

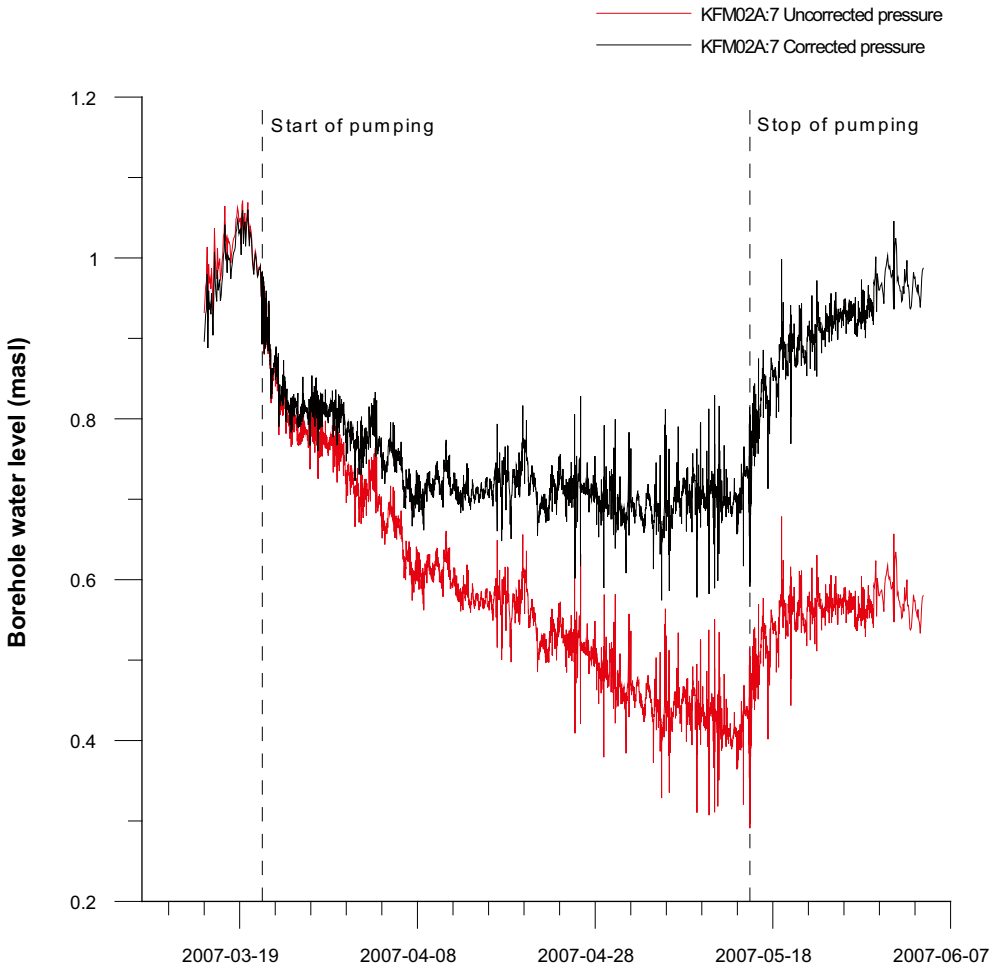

Figure A7-18. *Linear plot of pressure and pressure corrected for the natural decreasing pressure trend versus time in the observation section KFM02A:7 during the pumping in KFM02B.*

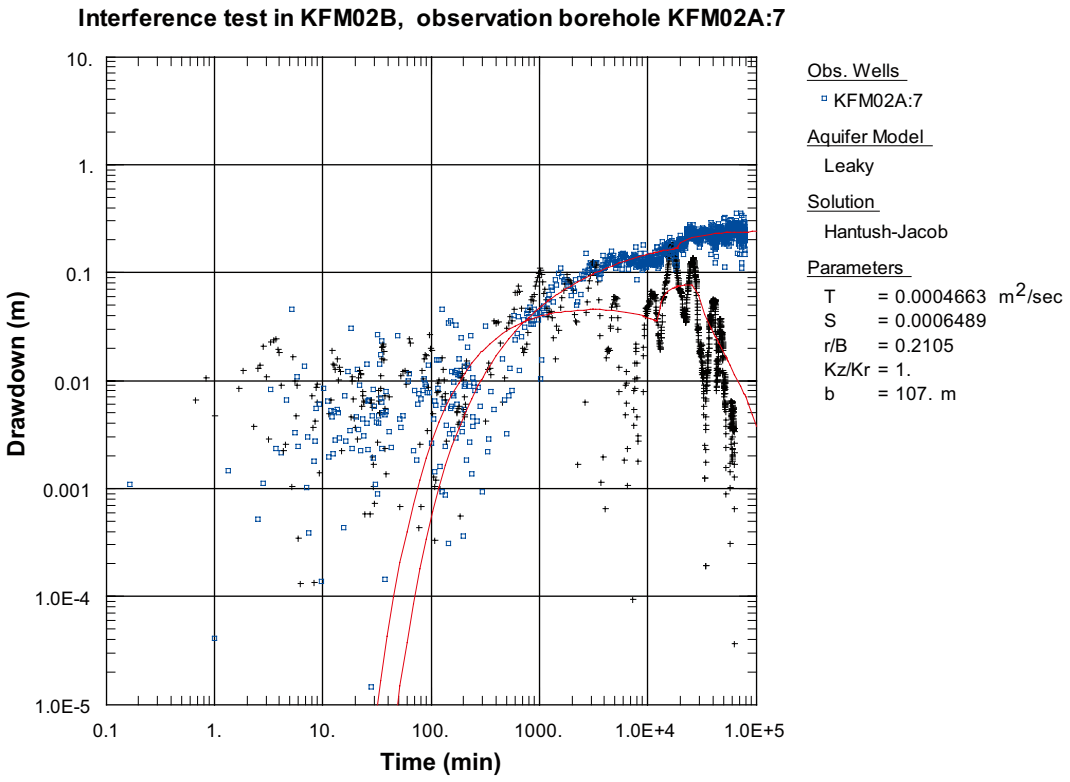

Figure A7-19. *Log-log plot of drawdown (▫) and drawdown derivative, ds/d(ln t) (+), versus time in KFM02A:7 during the interference test in KFM02B.*

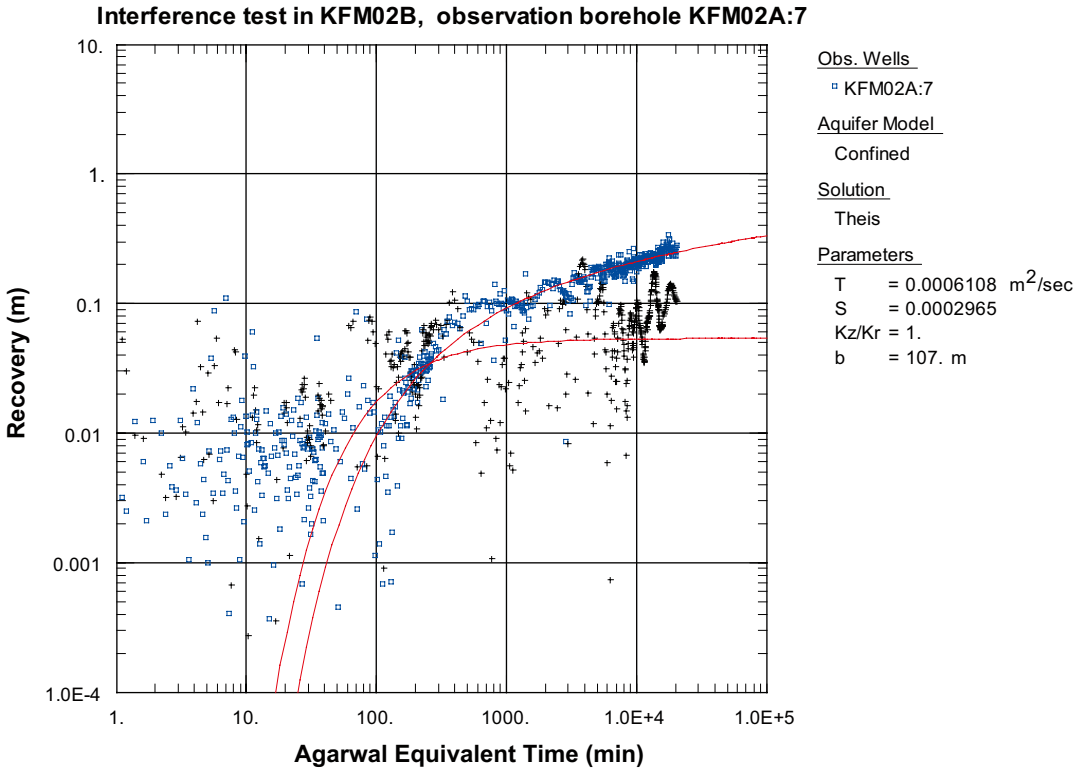

Figure A7-20. *Log-log plot of recovery (▫) and recovery derivative, ds/d(ln t) (+), versus time in KFM02A:7 during the interference test in KFM02B.*

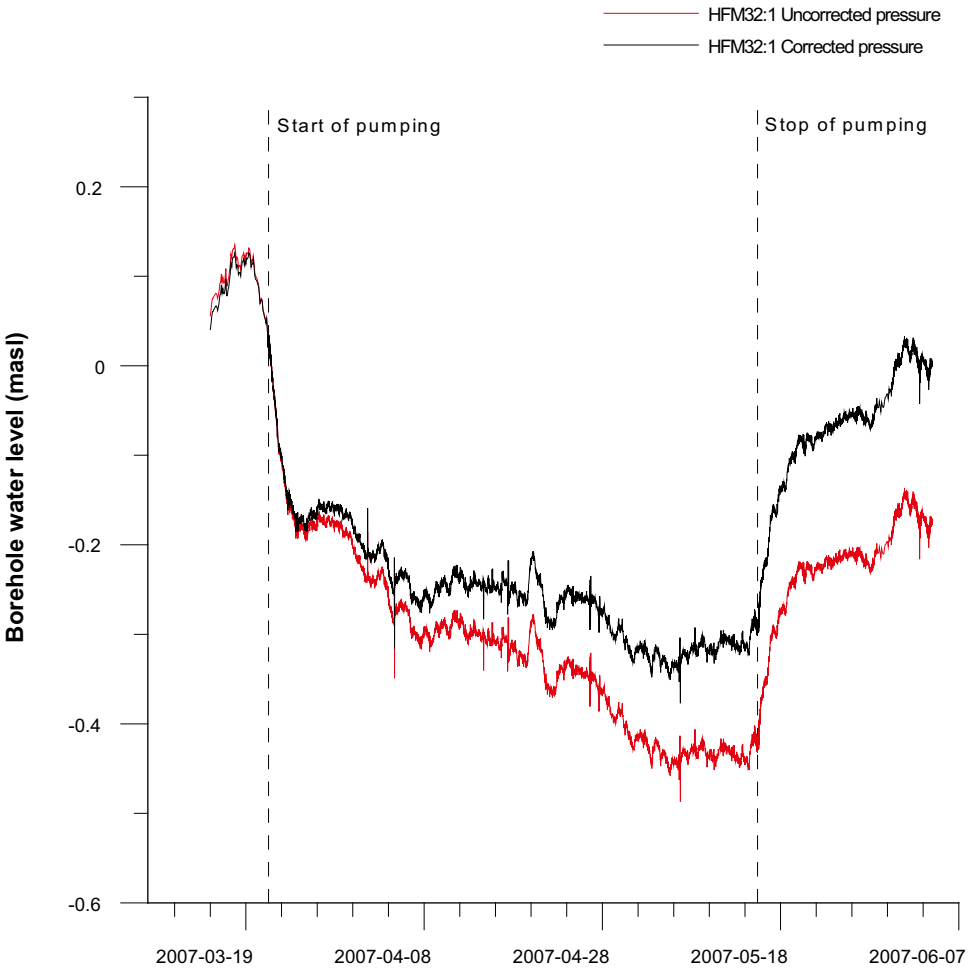

Figure A7-21. *Linear plot of pressure and pressure corrected for the natural decreasing pressure trend versus time in the observation section HFM32:1 during the pumping in KFM02B.*

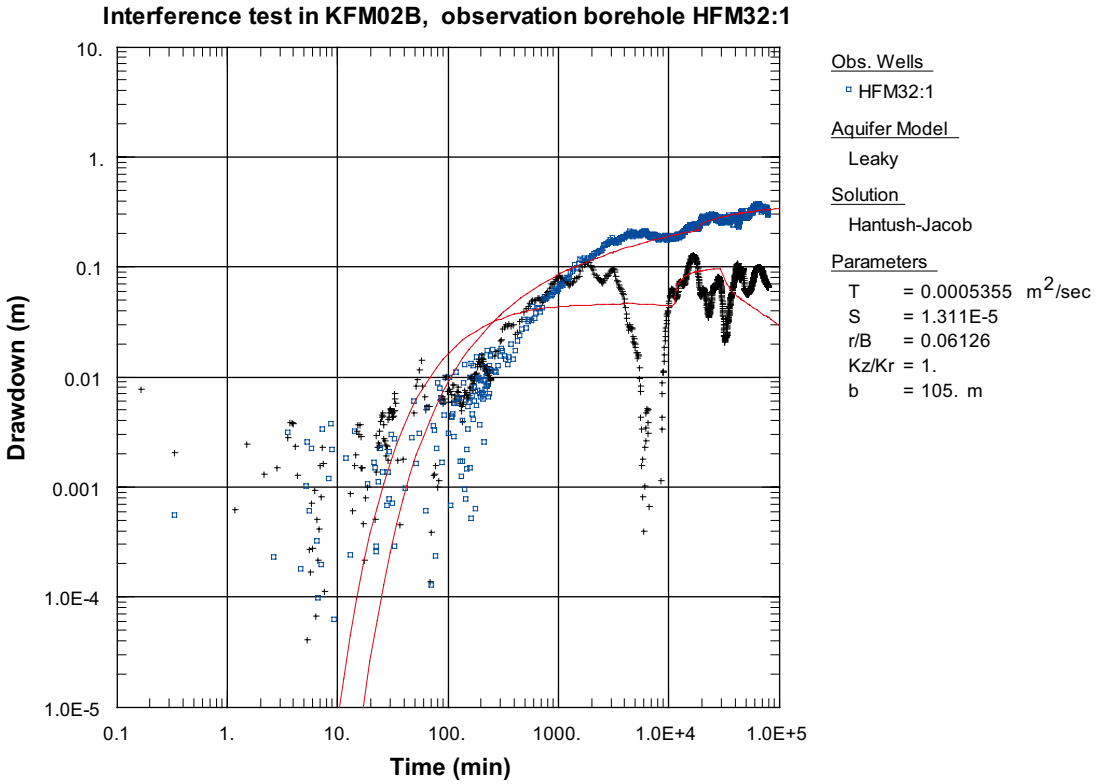

Figure A7-22. *Log-log plot of drawdown (▫) and drawdown derivative, ds/d(ln t) (+), versus time in HFM32:1 during the interference test in KFM02B.*

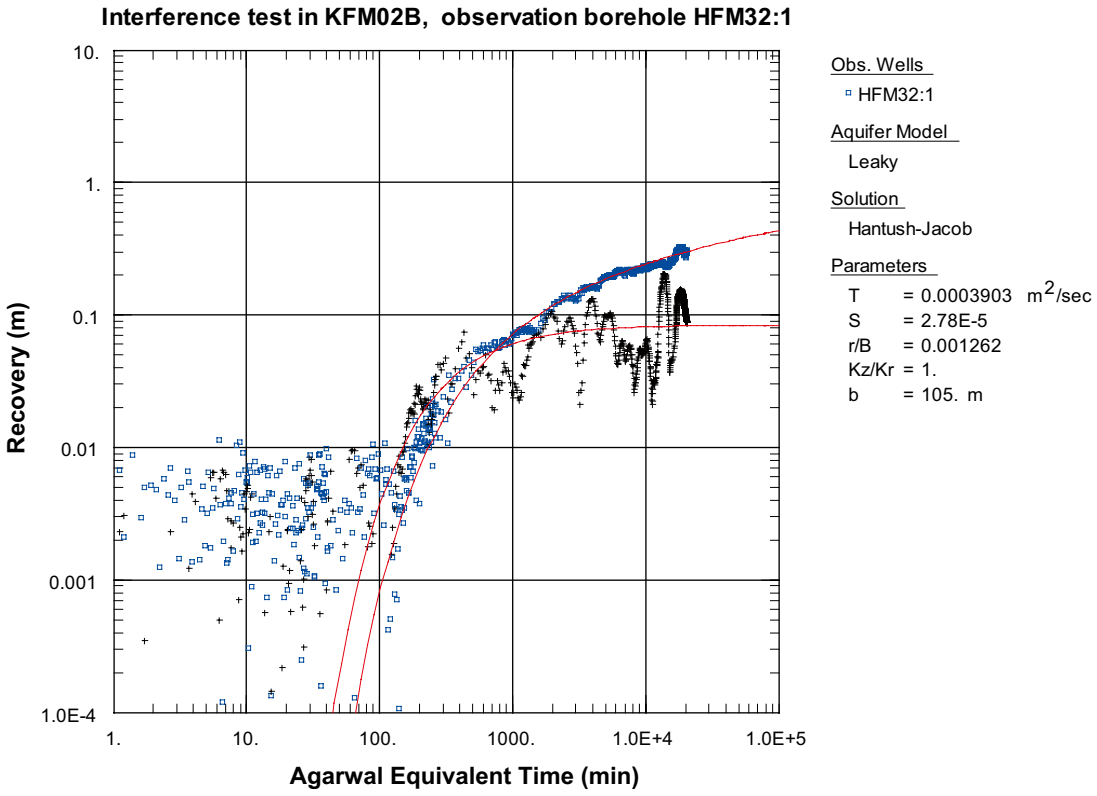

Figure A7-23. *Log-log plot of recovery (▫) and recovery derivative, ds/d(ln t) (+), versus time in HFM32:1 during the interference test in KFM02B.*

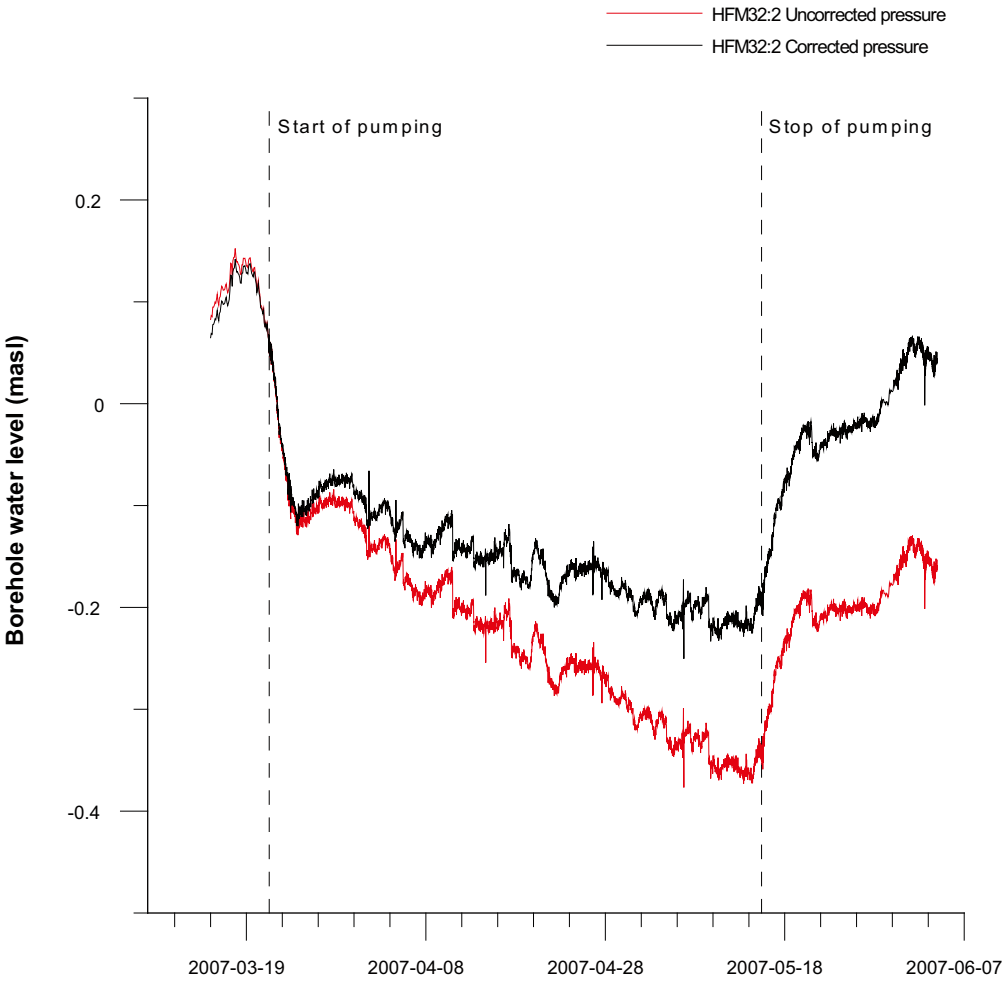

Figure A7-24. *Linear plot of pressure and pressure corrected for the natural decreasing pressure trend versus time in the observation section HFM32:2 during the pumping in KFM02B.*

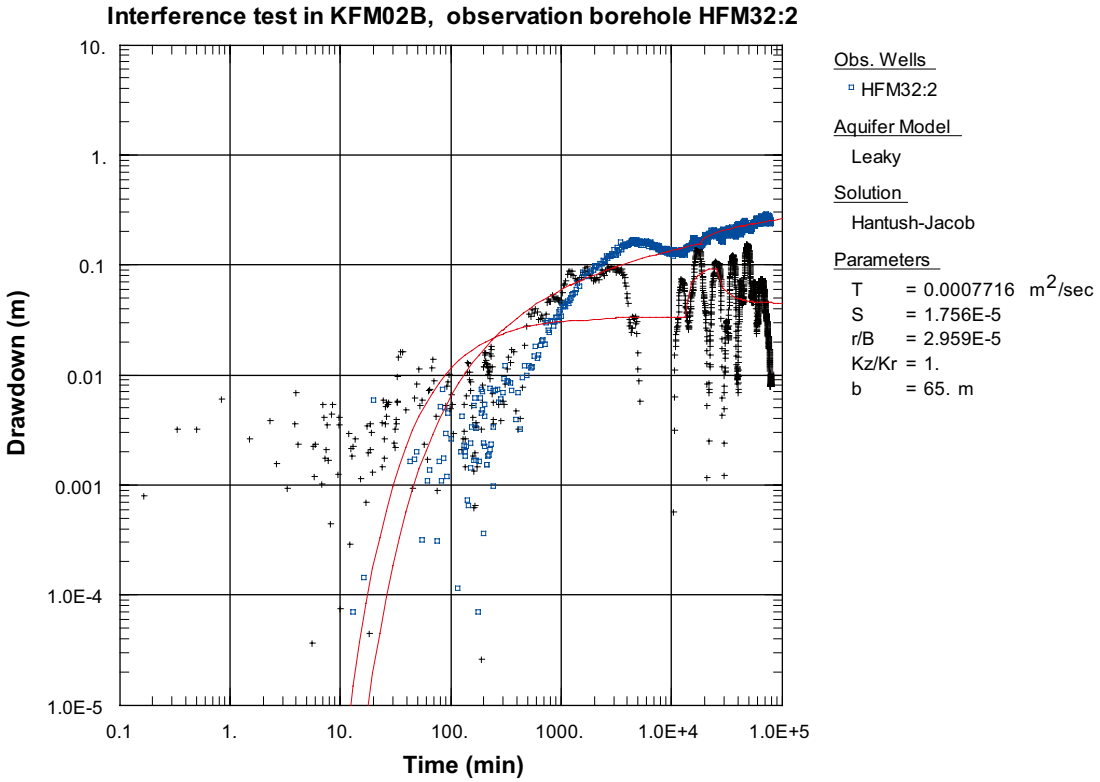

Figure A7-25. *Log-log plot of drawdown (▫) and drawdown derivative, ds/d(ln t) (+), versus time in HFM32:2 during the interference test in KFM02B.*

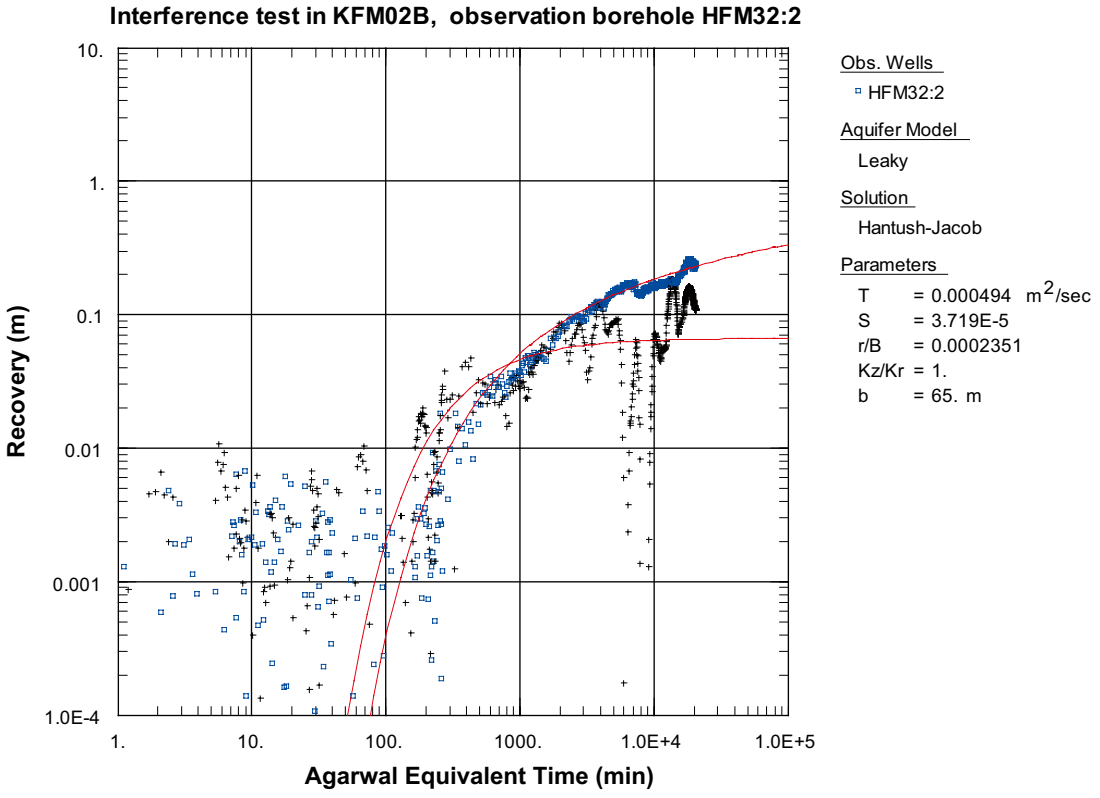

Figure A7-26. *Log-log plot of recovery (▫) and recovery derivative, ds/d(ln t) (+), versus time in HFM32:2 during the interference test in KFM02B.*

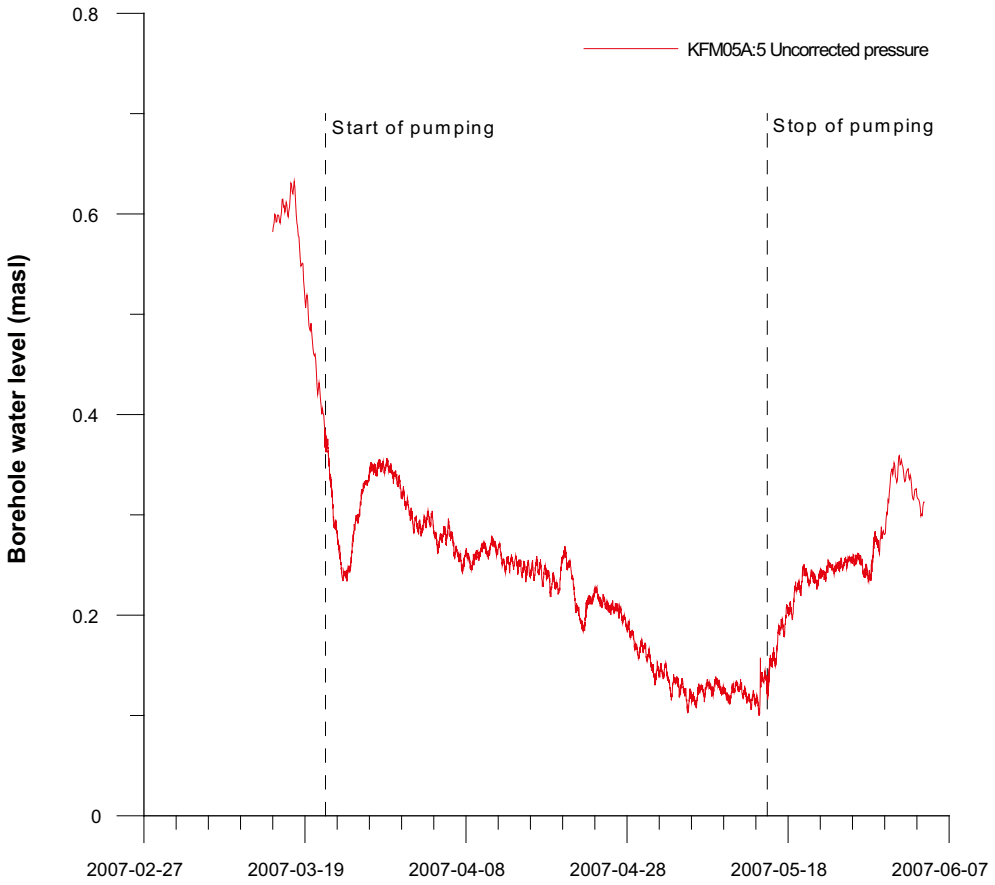

Figure A7-27. *Linear plot of pressure versus time in the observation sections in KFM05A:5 during the pumping in KFM02B.*

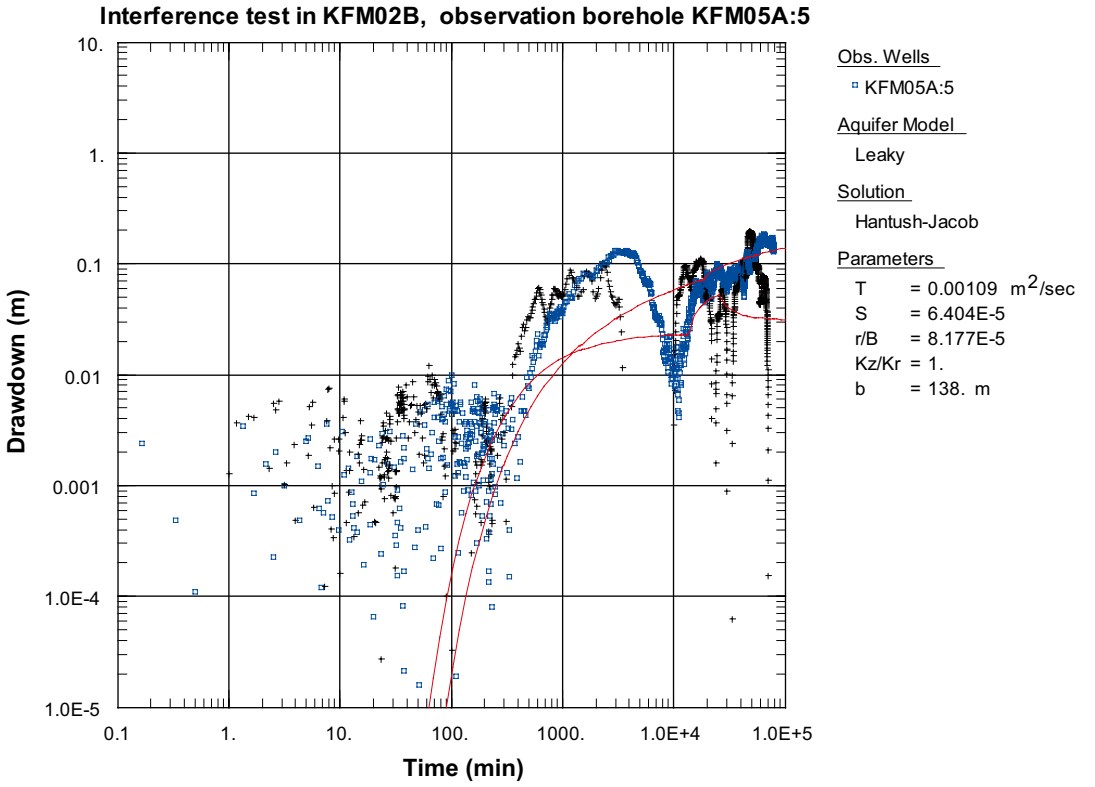

Figure A7-28. *Log-log plot of drawdown (▫) and drawdown derivative, ds/d(ln t) (+), versus time in KFM05A:5 during the interference test in KFM02B.*

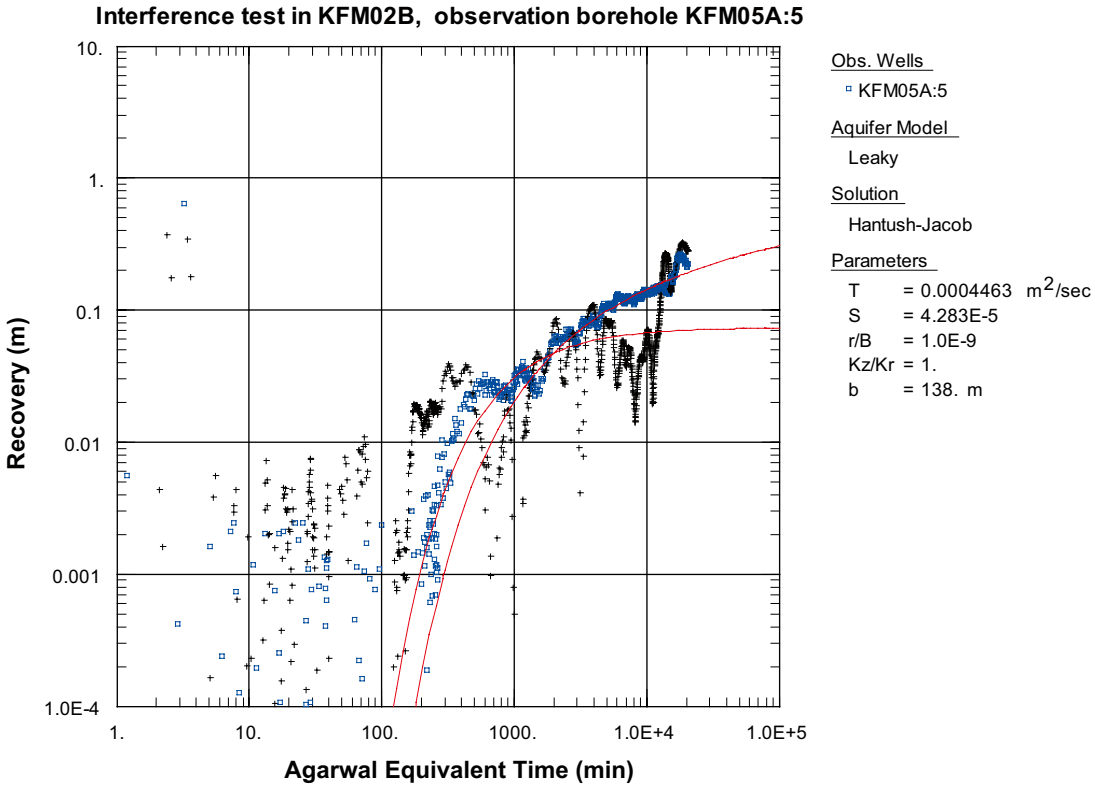

Figure A7-29. *Log-log plot of recovery (▫) and recovery derivative, ds/d(ln t) (+), versus time in KFM05A:5 during the interference test in KFM02B.*

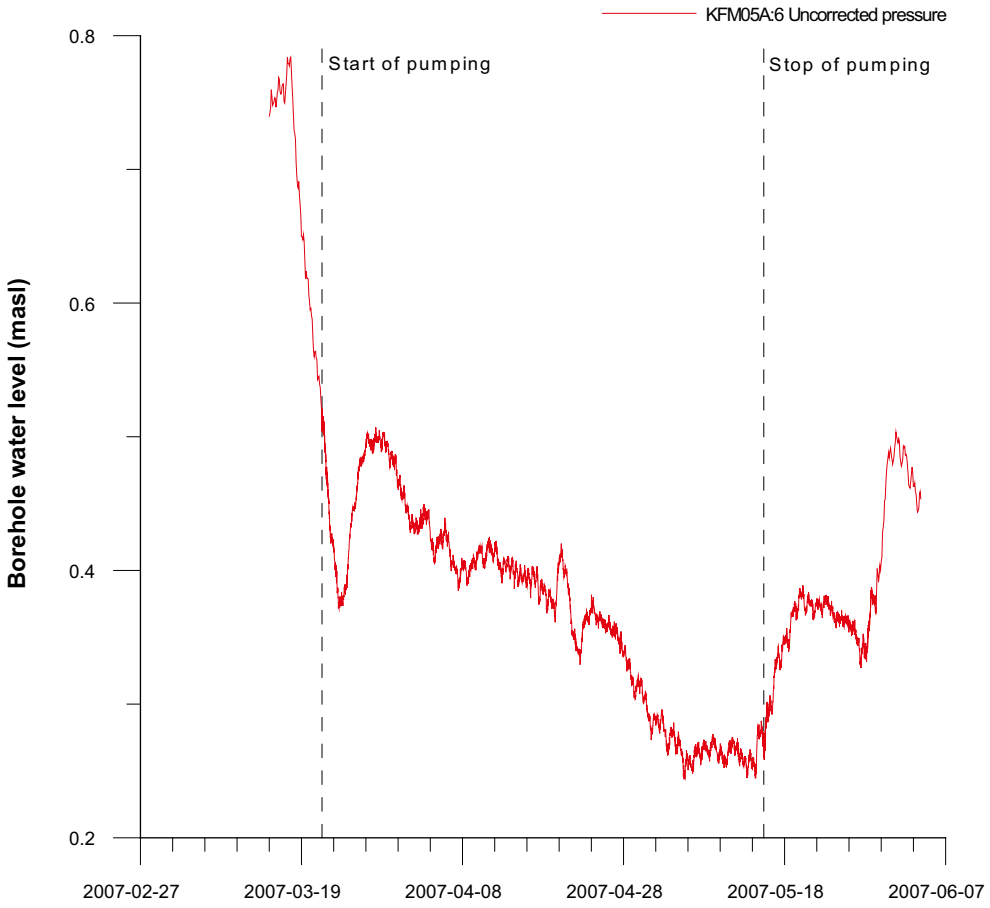

Figure A7-30. *Linear plot of pressure versus time in the observation sections in KFM05A:6 during the pumping in KFM02B.*

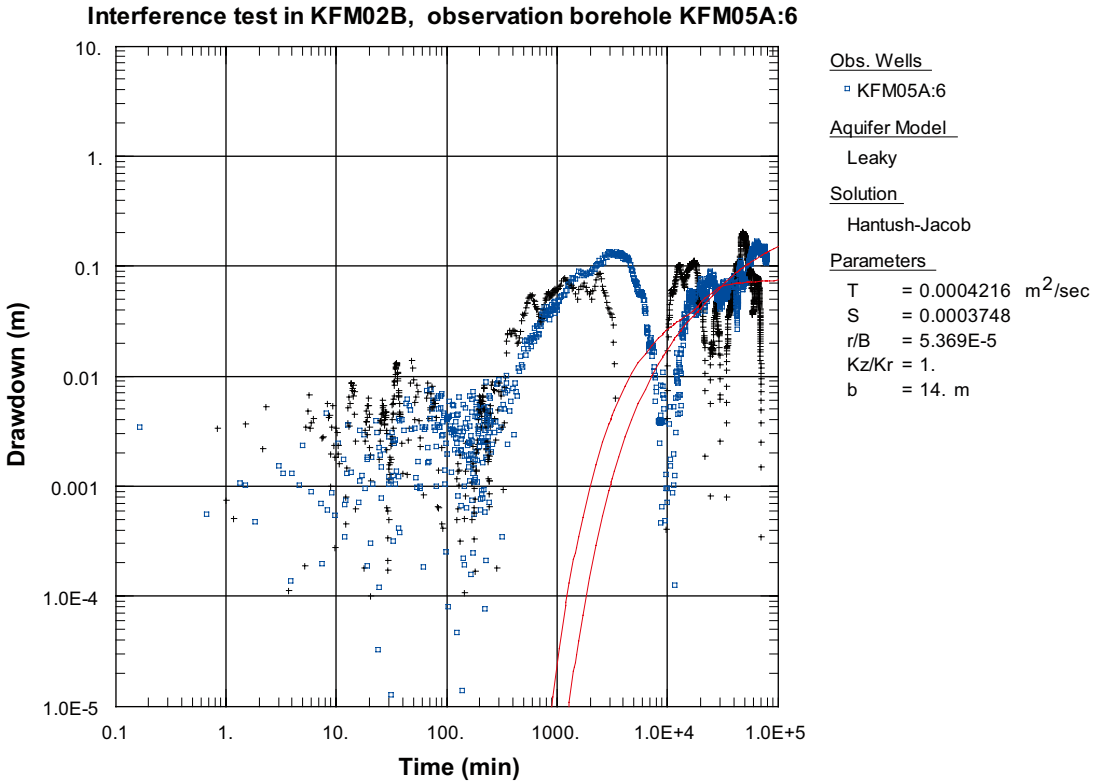

Figure A7-31. *Log-log plot of drawdown (▫) and drawdown derivative, ds/d(ln t) (+), versus time in KFM05A:6 during the interference test in KFM02B.*

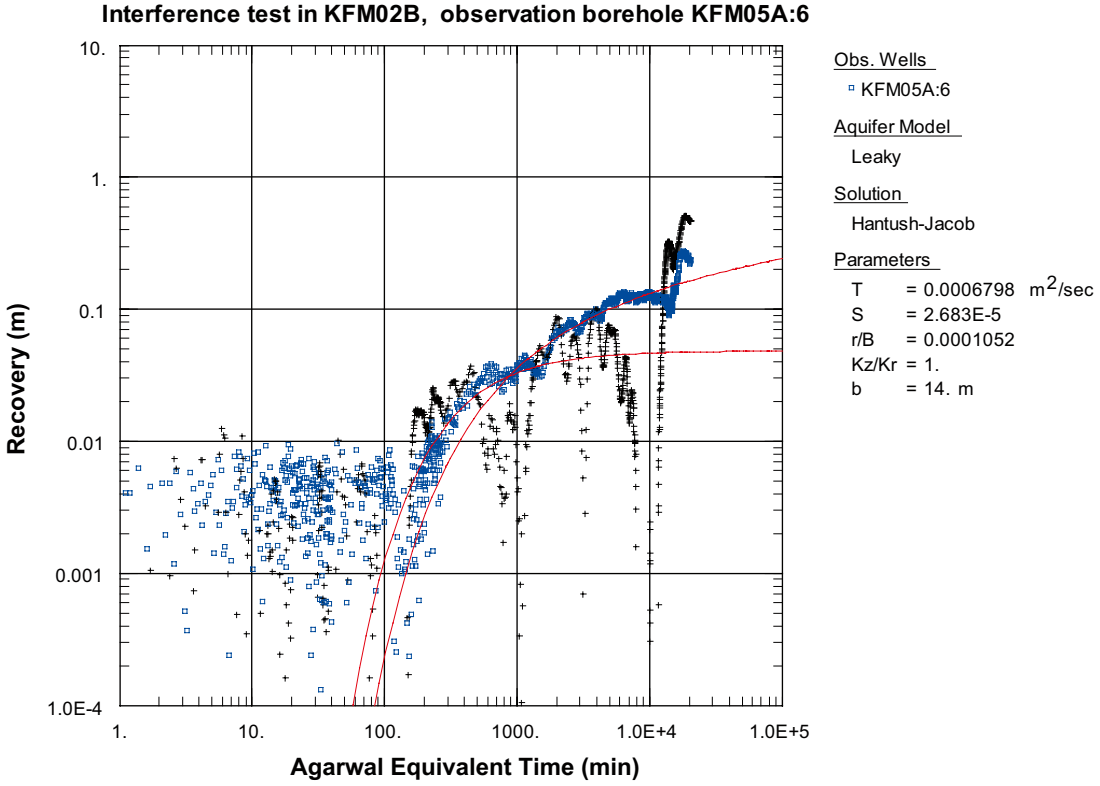

Figure A7-32. *Log-log plot of recovery (▫) and recovery derivative, ds/d(ln t) (+), versus time in KFM05A:6 during the interference test in KFM02B.*

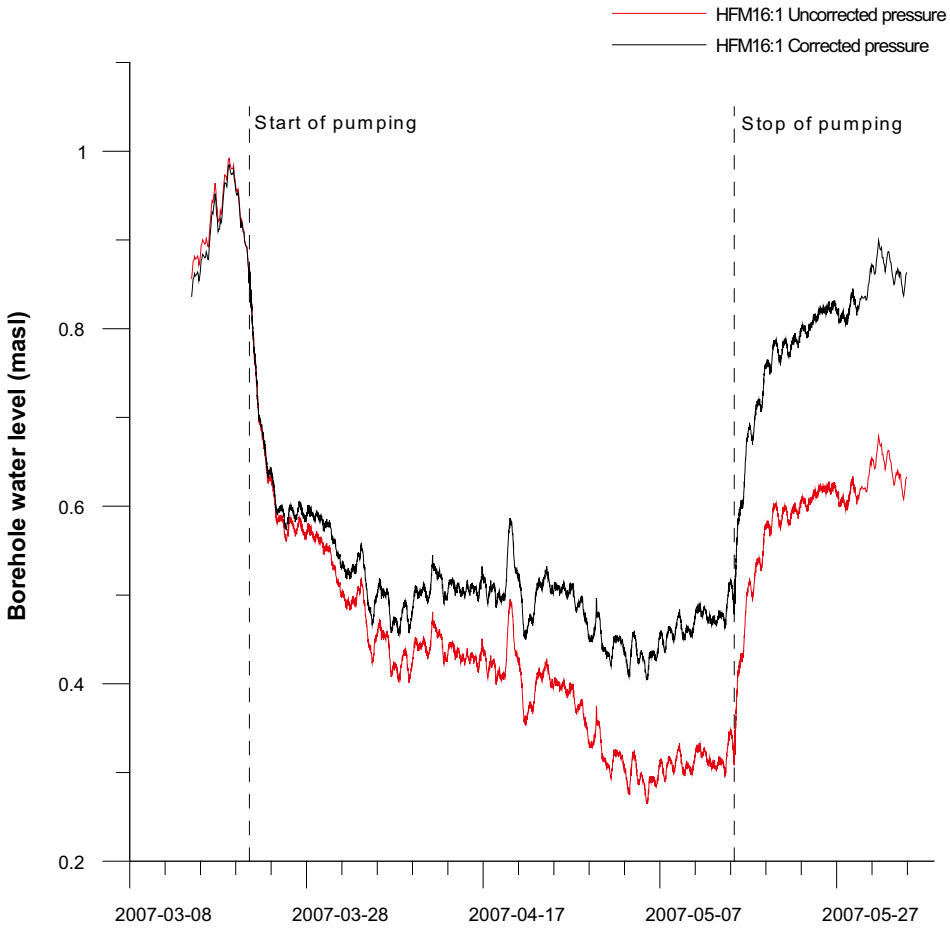

Figure A7-33. *Linear plot of pressure versus time in the observation section HFM16:1 during the pumping in KFM02B.*

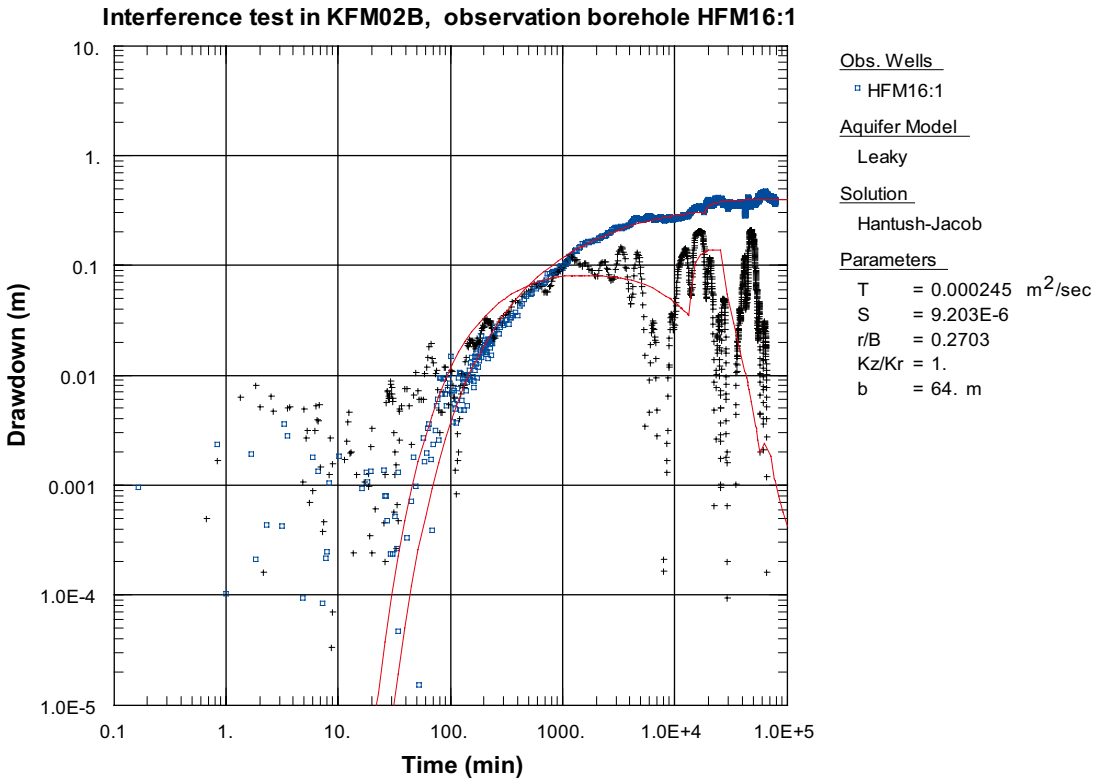

Figure A7-34. *Log-log plot of drawdown (▫) and drawdown derivative, ds/d(ln t) (+), versus time in HFM16:1 during the interference test in KFM02B.*

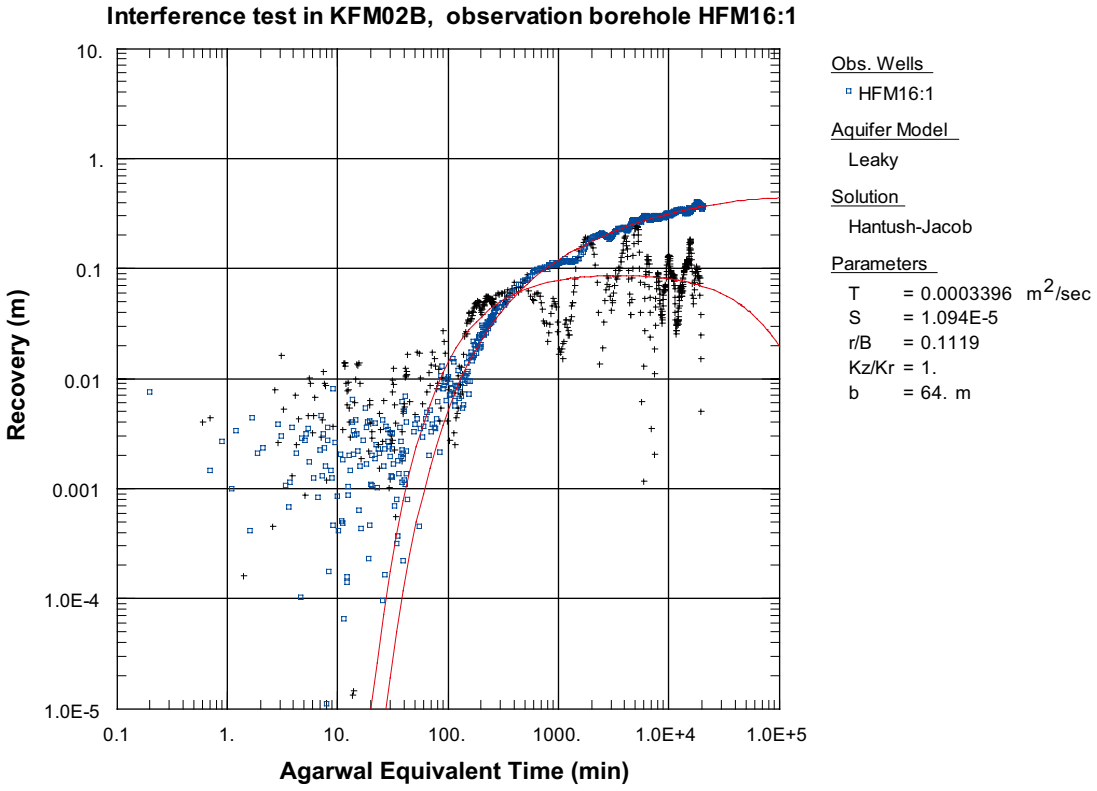

Figure A7-35. *Log-log plot of recovery (▫) and recovery derivative, ds/d(ln t) (+), versus time in HFM16:1 during the interference test in KFM02B.*

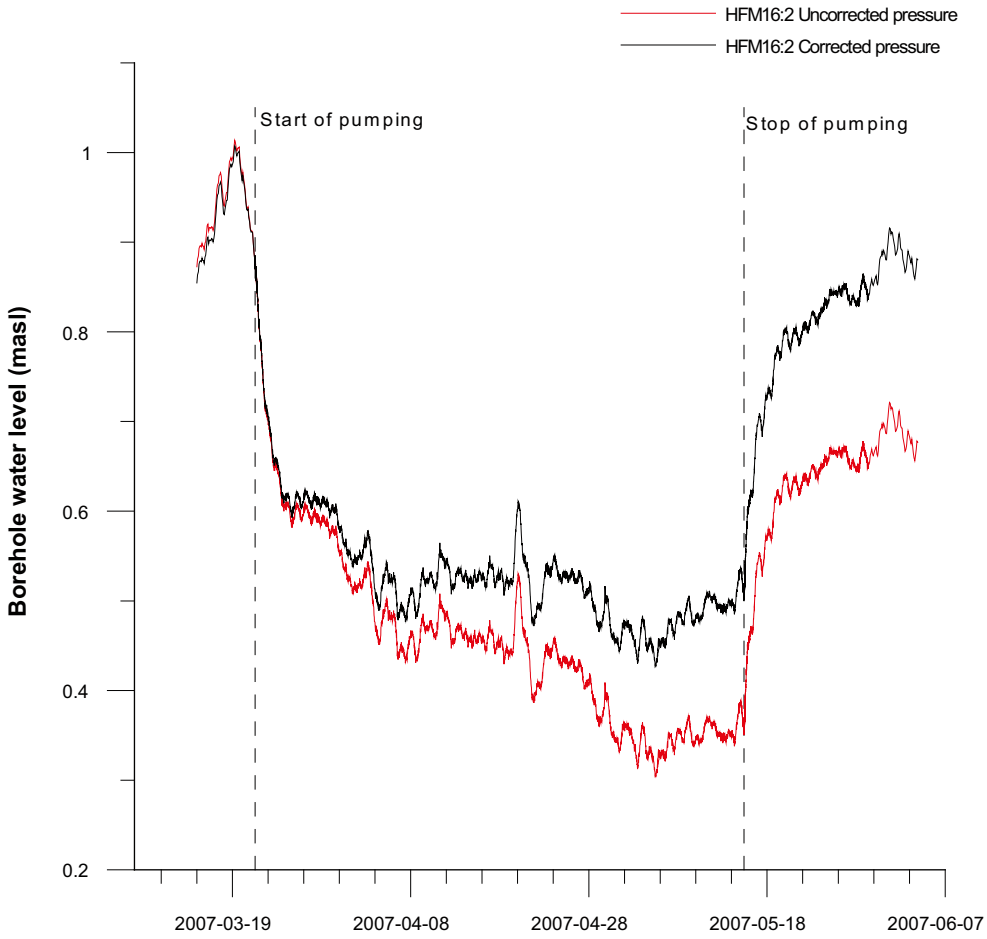

Figure A7-36. *Linear plot of pressure versus time in the observation sections in HFM16:2 during the pumping in KFM02B.*

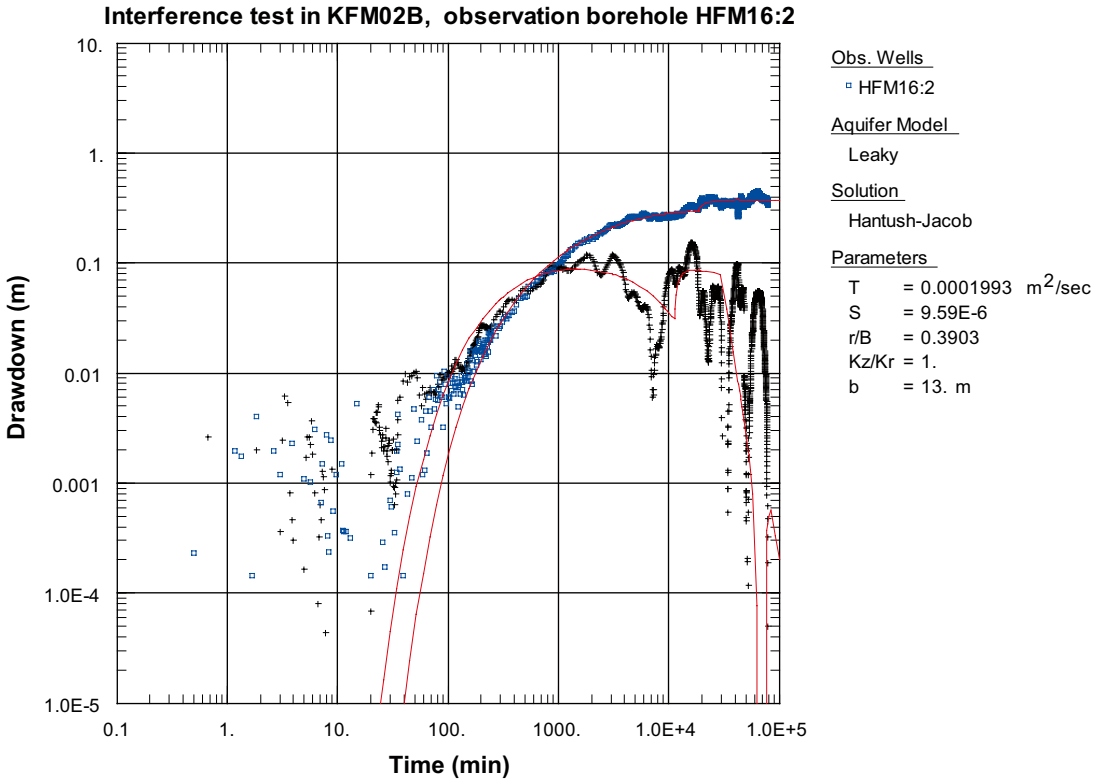

Figure A7-37. *Log-log plot of drawdown (▫) and drawdown derivative, ds/d(ln t) (+), versus time in HFM16:2 during the interference test in KFM02B*

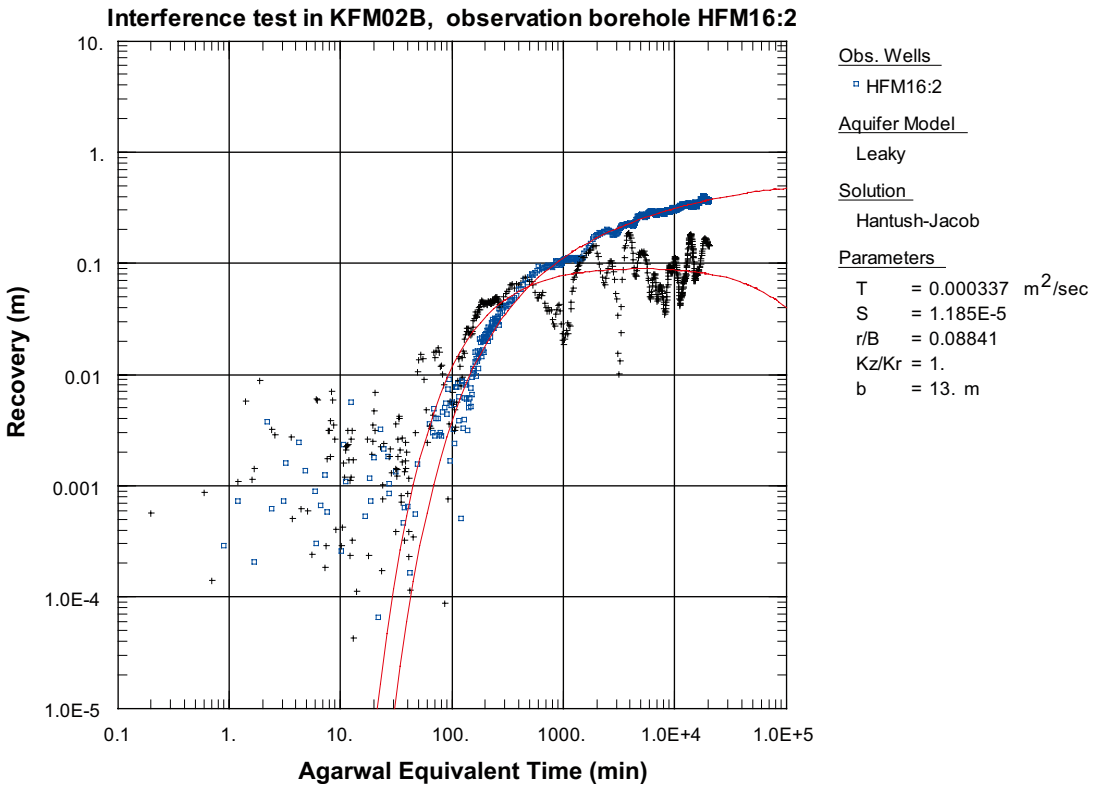

Figure A7-38. *Log-log plot of recovery (▫) and recovery derivative, ds/d(ln t) (+), versus time in HFM16:2 during the interference test in KFM02B.*

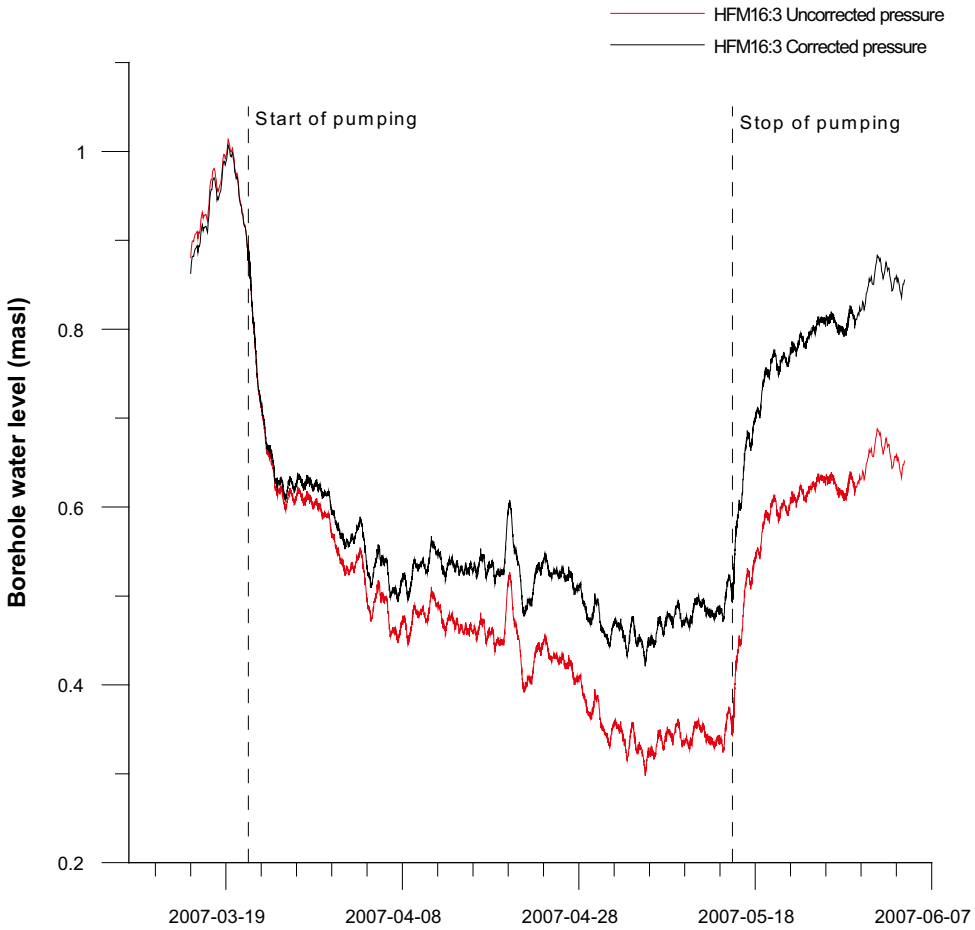

Figure A7-39. *Linear plot of pressure versus time in the observation sections in HFM16:3 during the pumping in KFM02B.*

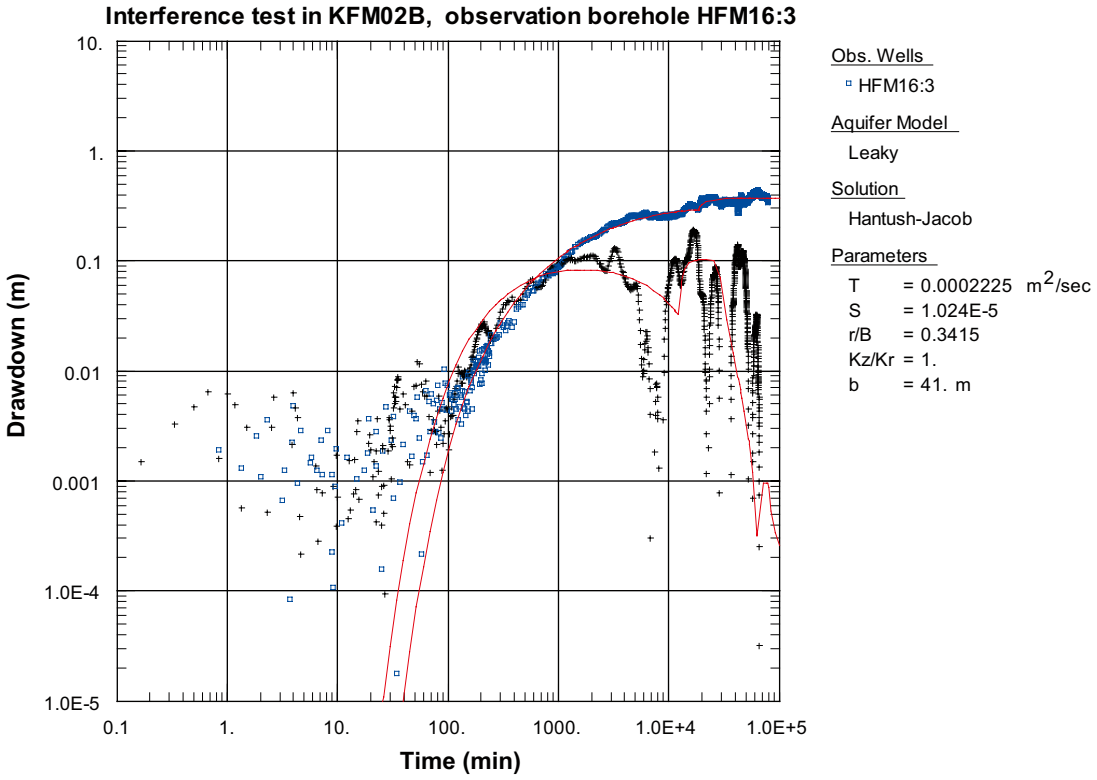

Figure A7-40. *Log-log plot of drawdown (▫) and drawdown derivative, ds/d(ln t) (+), versus time in HFM16:3 during the interference test in KFM02B.*

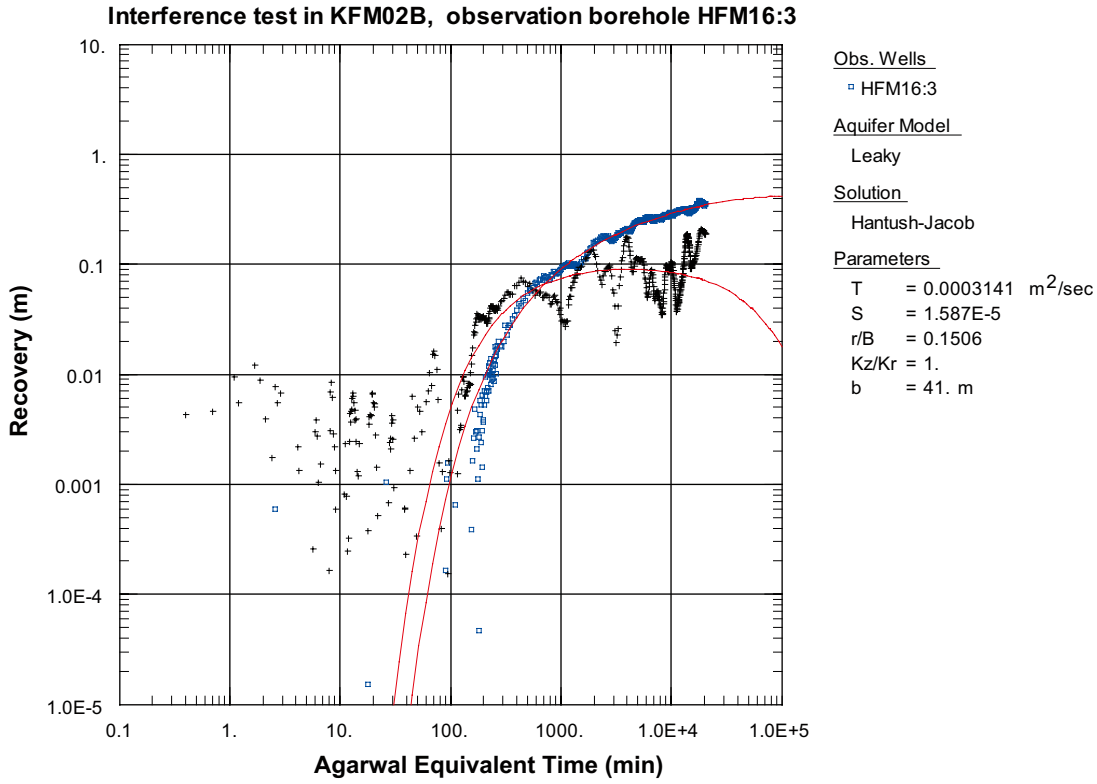

Figure A7-41. *Log-log plot of recovery (▫) and recovery derivative, ds/d(ln t) (+), versus time in HFM16:3 during the interference test in KFM02B.*

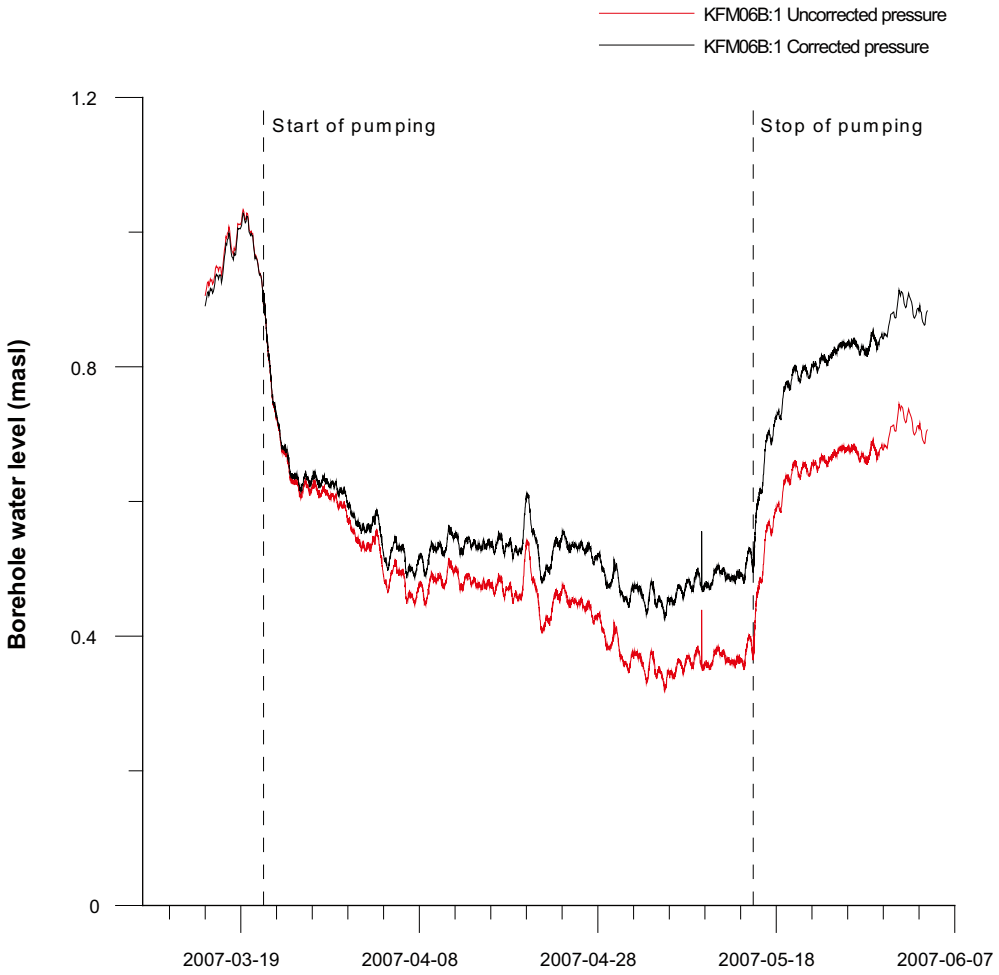

Figure A7-42. *Linear plot of pressure and pressure corrected for the natural decreasing pressure trend versus time in the observation section KFM06B:1 during the pumping in KFM02B.*

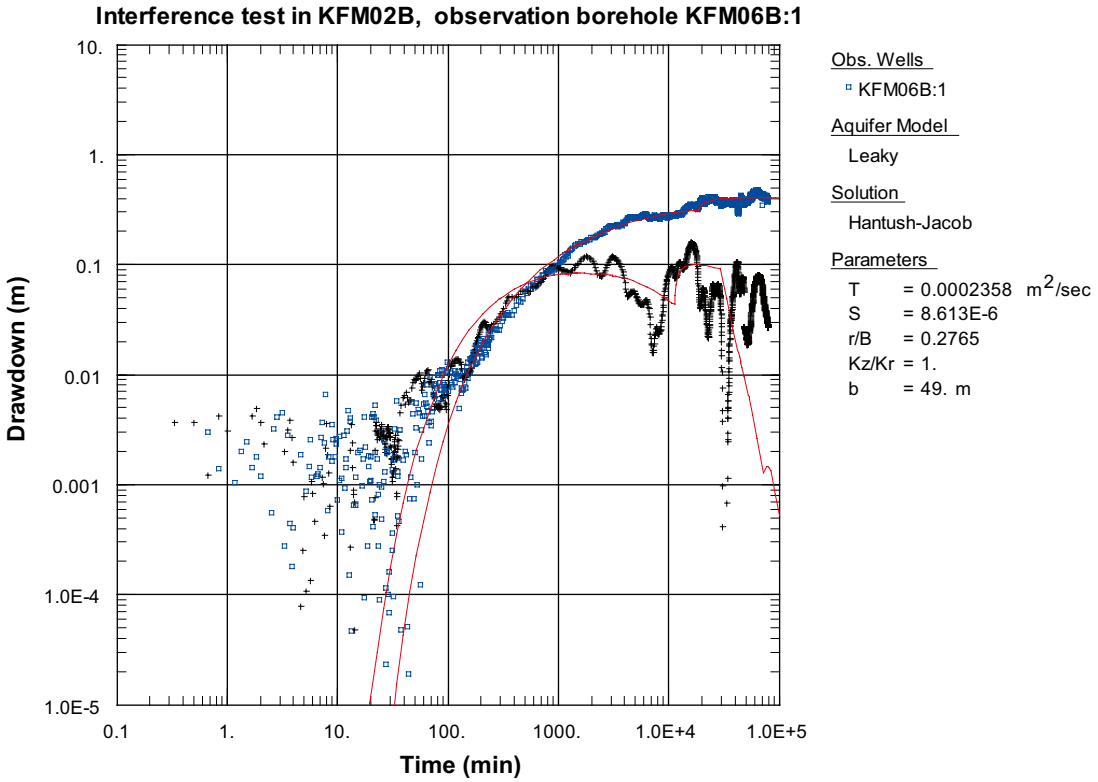

Figure A7-43. *Log-log plot of drawdown (▫) and drawdown derivative, ds/d(ln t) (+), versus time in KFM06B:1 during the interference test in KFM02B.*

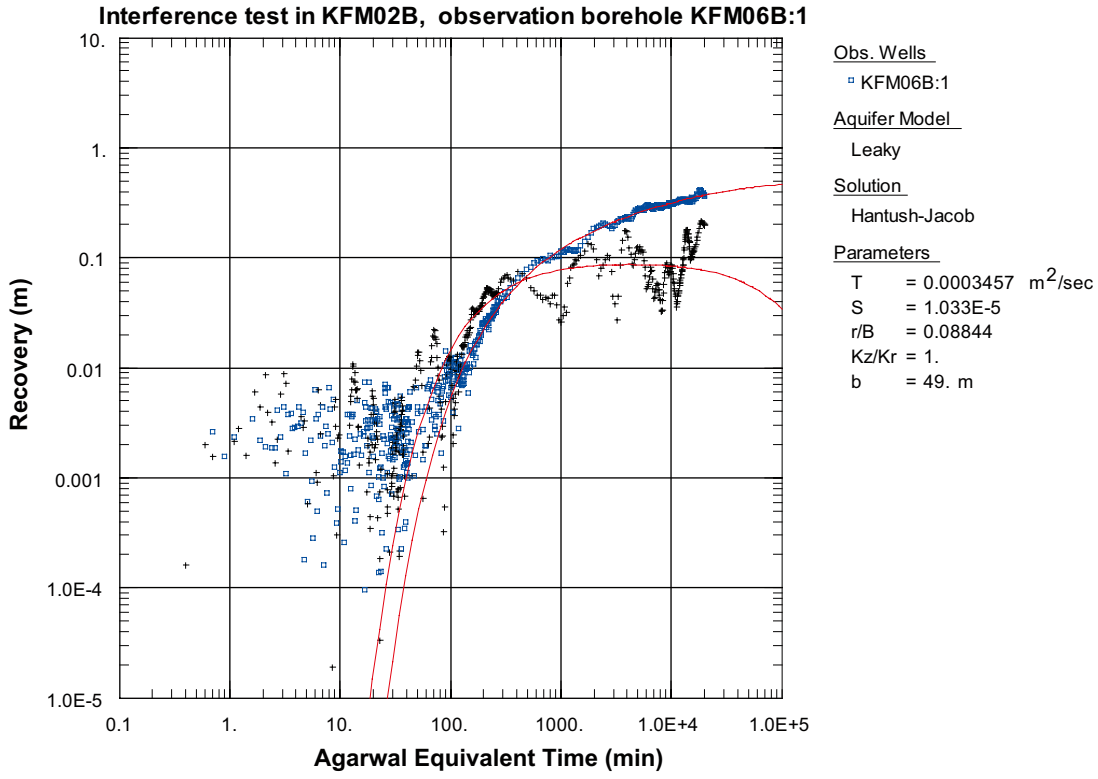

Figure A7-44. *Log-log plot of recovery (▫) and recovery derivative, ds/d(ln t) (+), versus time in KFM06B:1 during the interference test in KFM02B.*

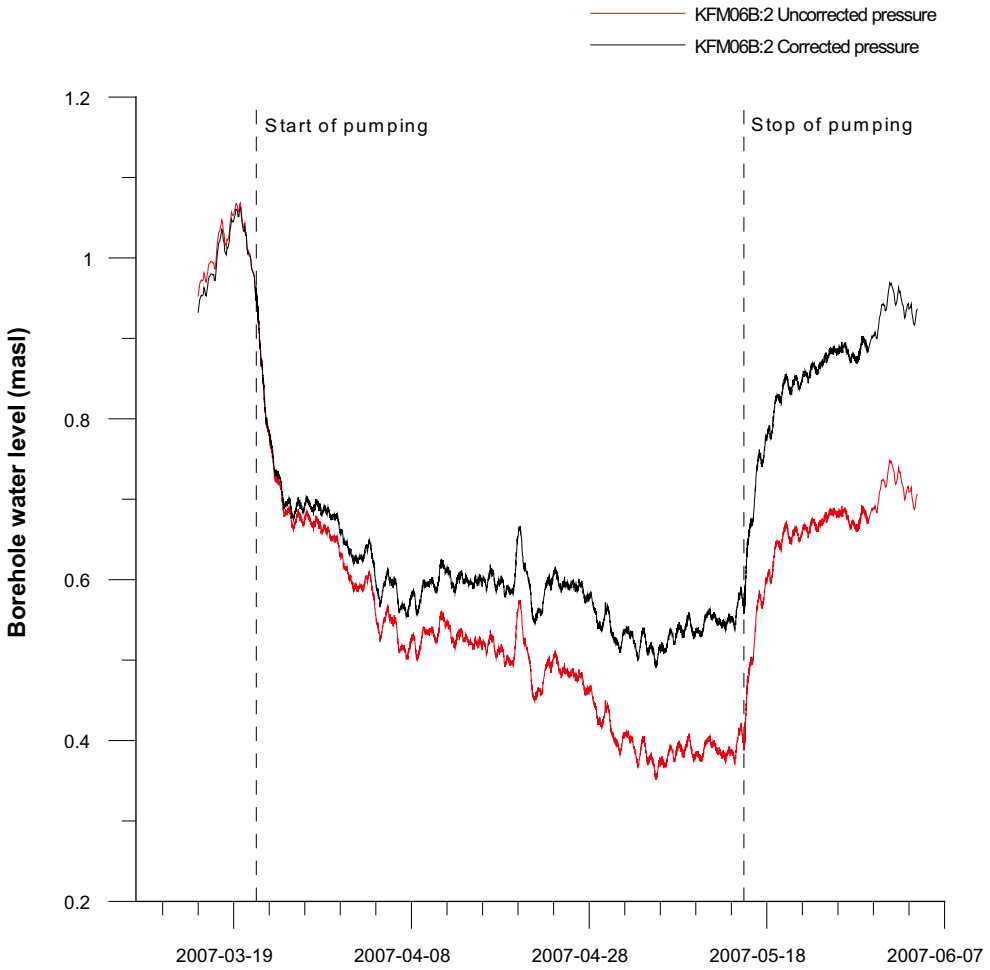

Figure A7-45. *Linear plot of pressure and pressure corrected for the natural decreasing pressure trend versus time in the observation section KFM06B:2 during the pumping in KFM02B.*

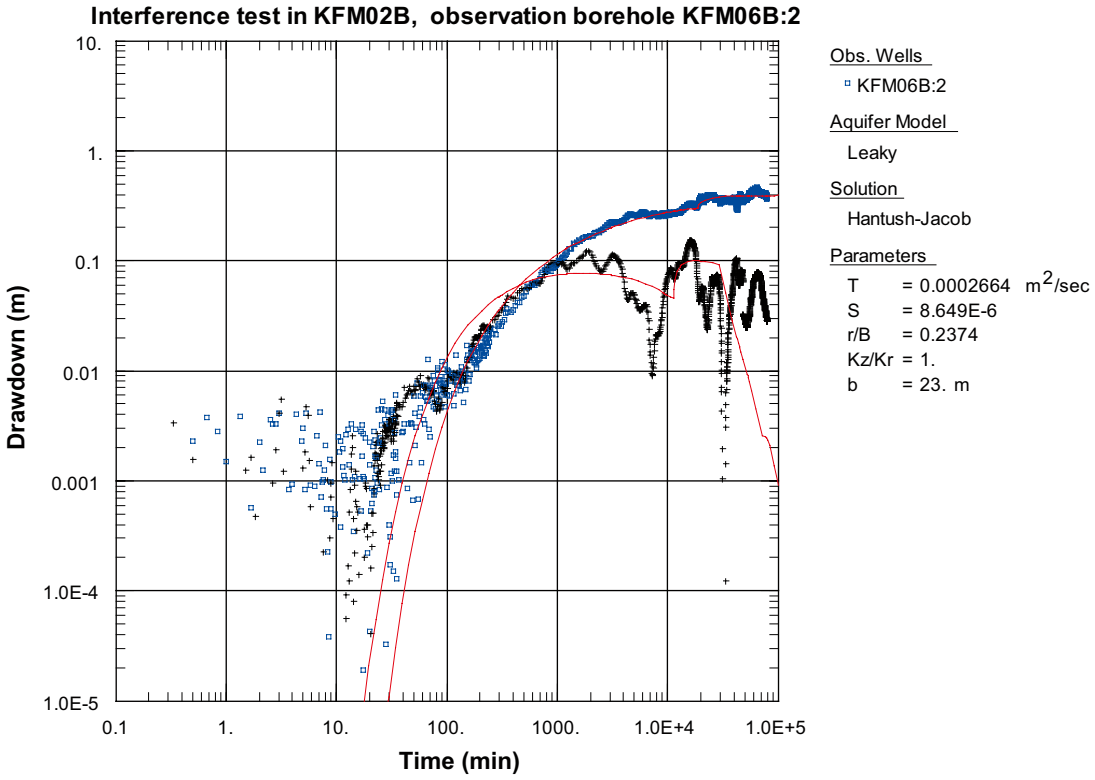

Figure A7-46. *Log-log plot of drawdown (▫) and drawdown derivative, ds/d(ln t) (+), versus time in KFM06B:2 during the interference test in KFM02B.*

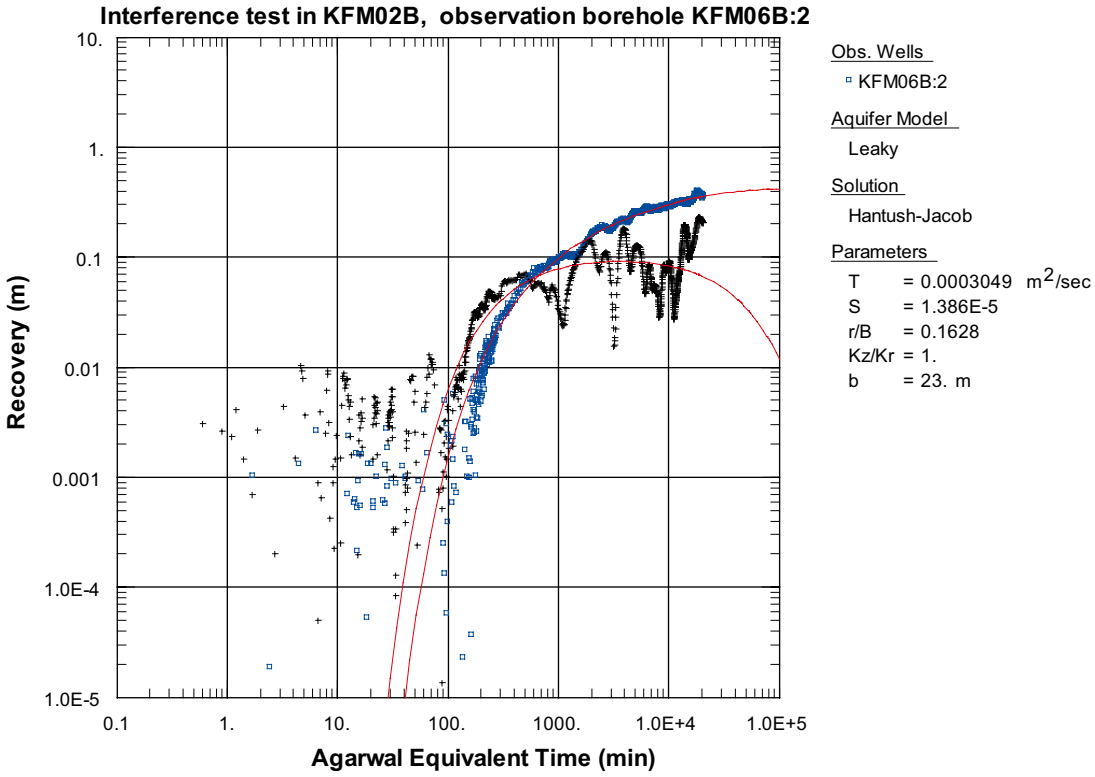

Figure A7-47. *Log-log plot of recovery (▫) and recovery derivative, ds/d(ln t) (+), versus time in KFM06B:2 during the interference test in KFM02B.*

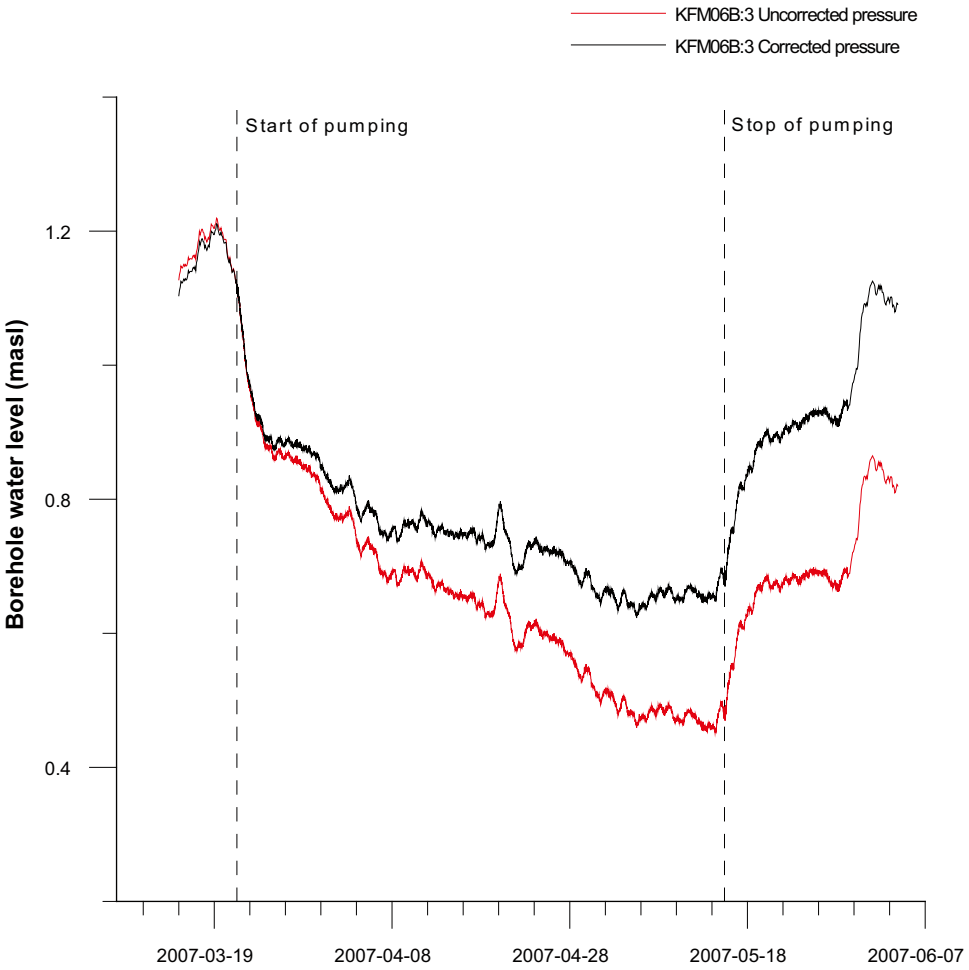

Figure A7-48. *Linear plot of pressure and pressure corrected for the natural decreasing pressure trend versus time in the observation section KFM06B:3 during the pumping in KFM02B.*

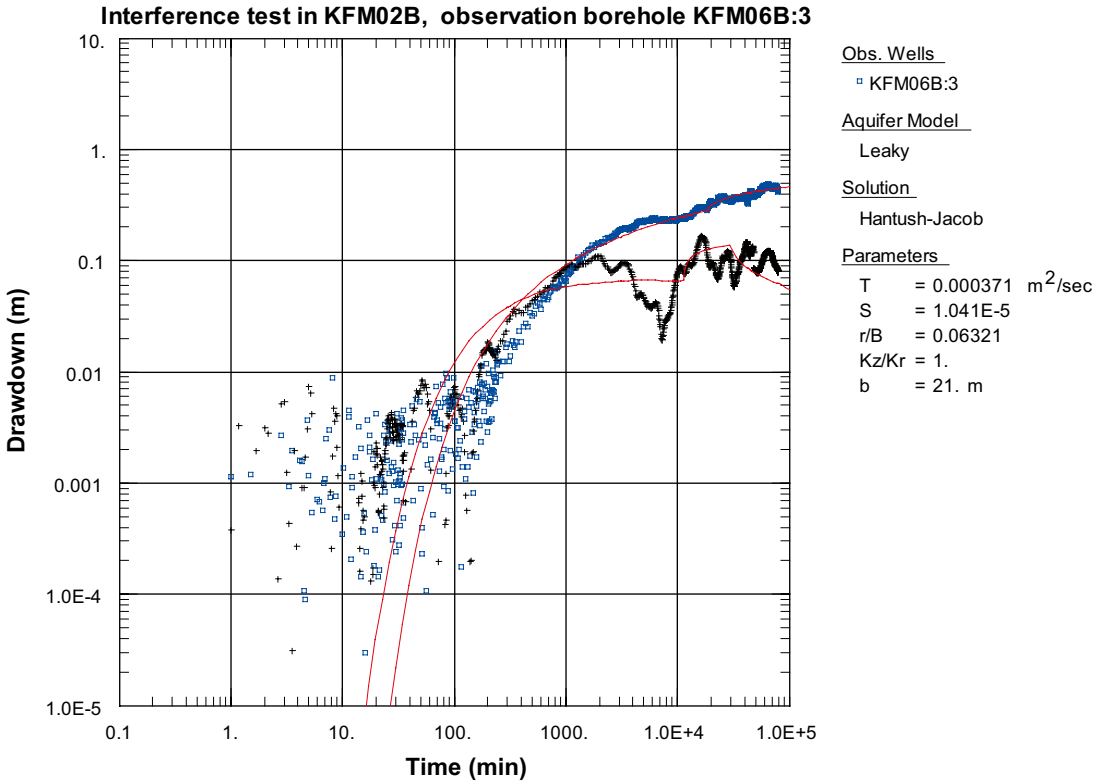

Figure A7-49. *Log-log plot of drawdown (▫) and drawdown derivative, ds/d(ln t) (+), versus time in KFM06B:3 during the interference test in KFM02B.*

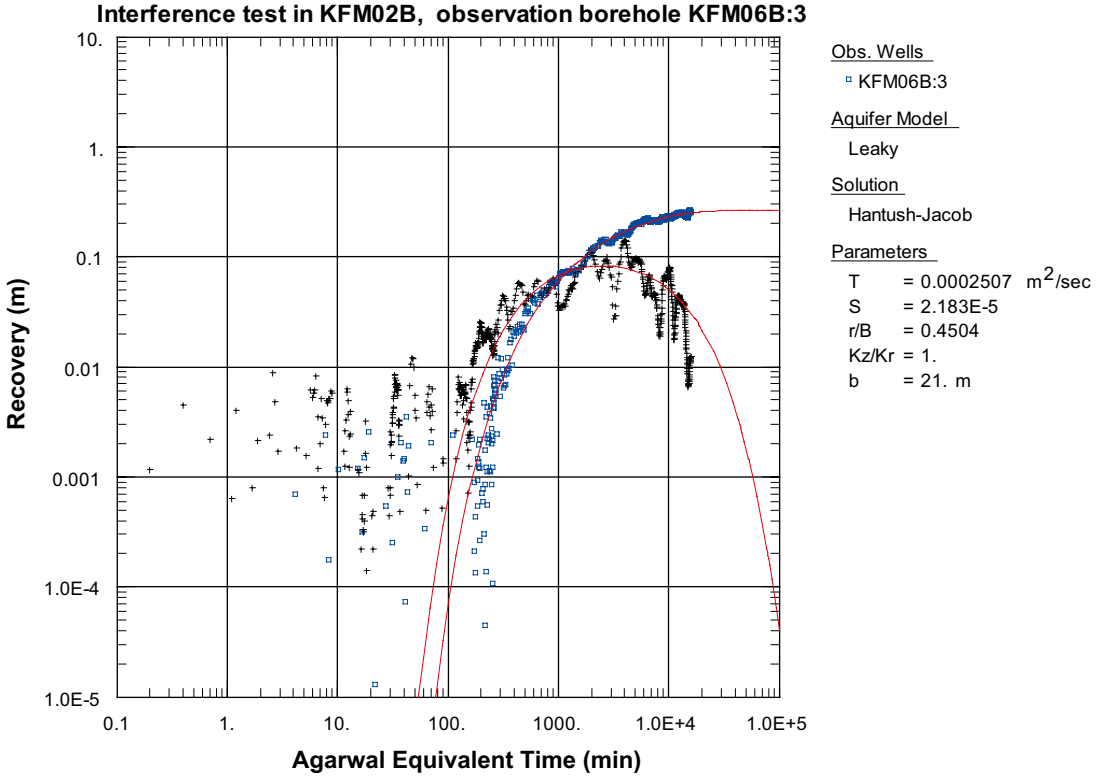

Figure A7-50. *Log-log plot of recovery (▫) and recovery derivative, ds/d(ln t) (+), versus time in KFM06B:3 during the interference test in KFM02B.*

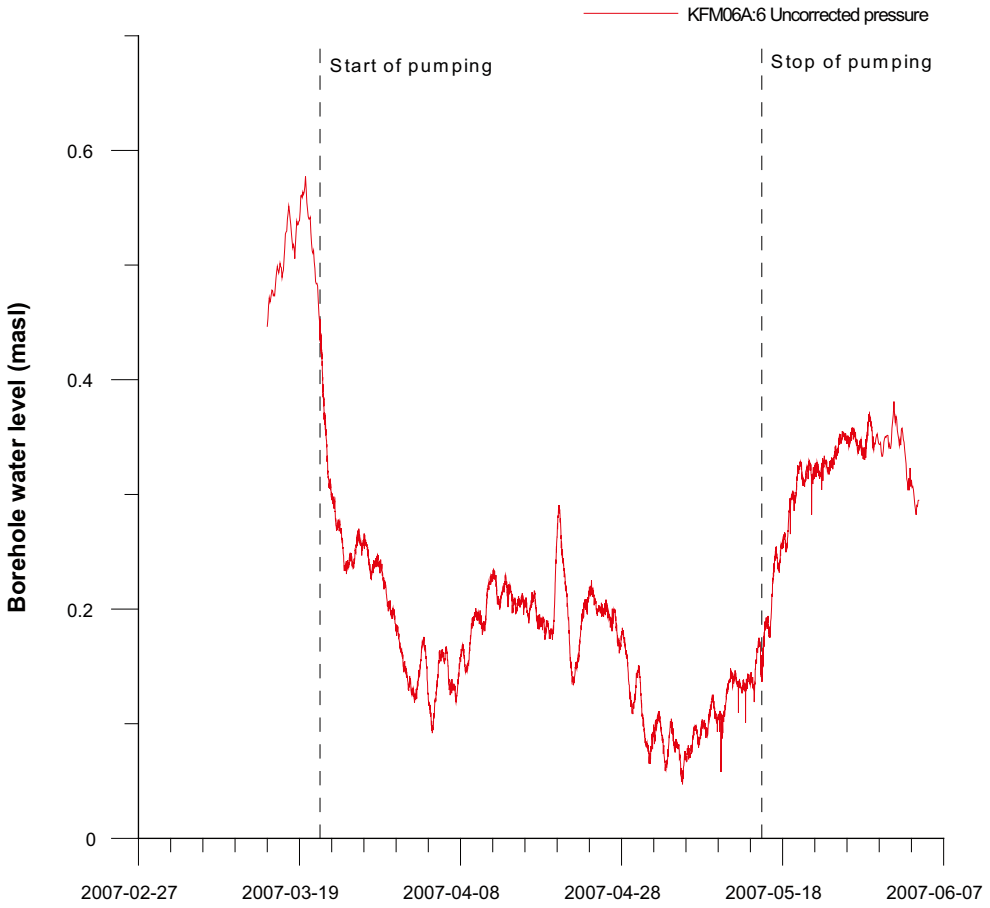

Figure A7-51. *Linear plot of pressure versus time in the observation sections in KFM06A:6 during the pumping in KFM02B.*

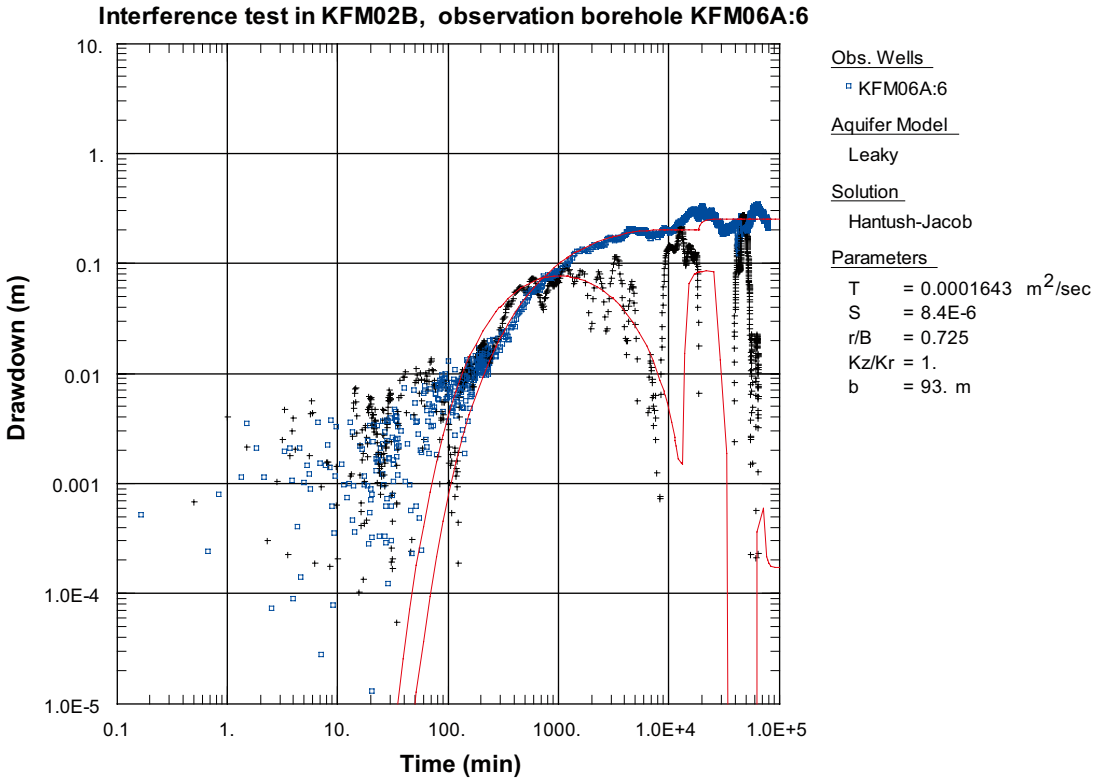

Figure A7-52. *Log-log plot of drawdown (▫) and drawdown derivative, ds/d(ln t) (+), versus time in KFM06A:6 during the interference test in KFM02B.*

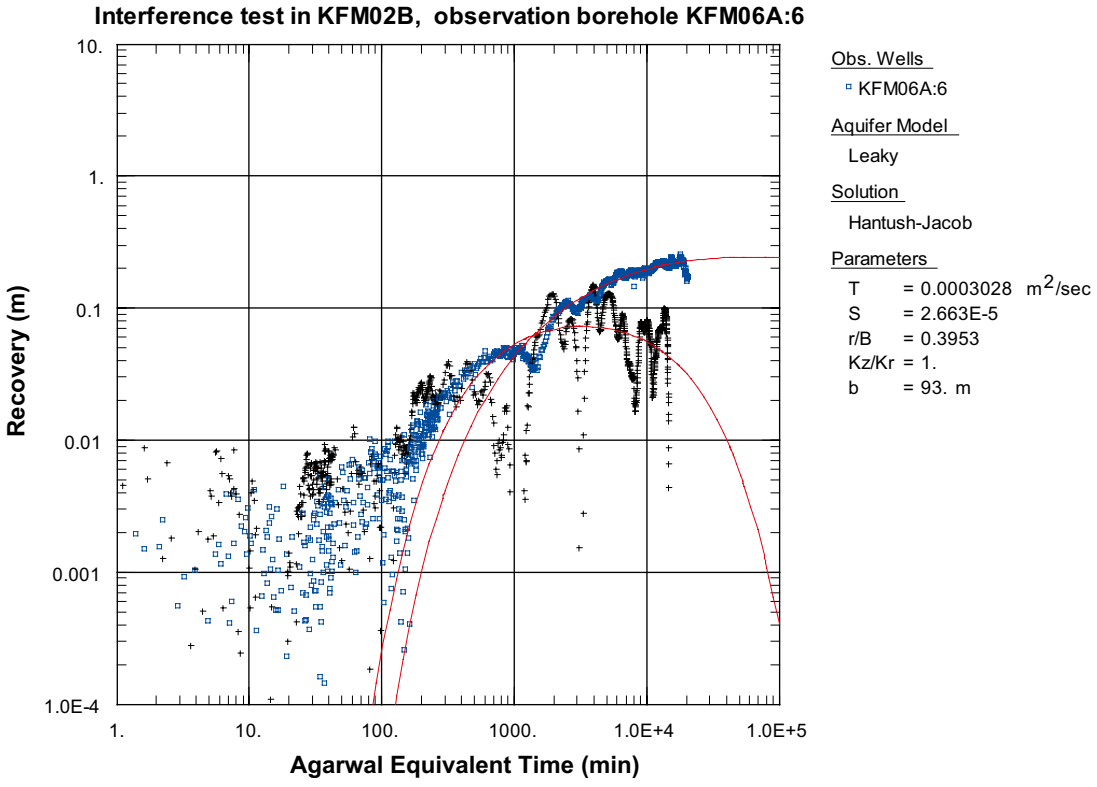

Figure A7-53. *Log-log plot of recovery (▫) and recovery derivative, ds/d(ln t) (+), versus time in KFM06A:6 during the interference test in KFM02B.*

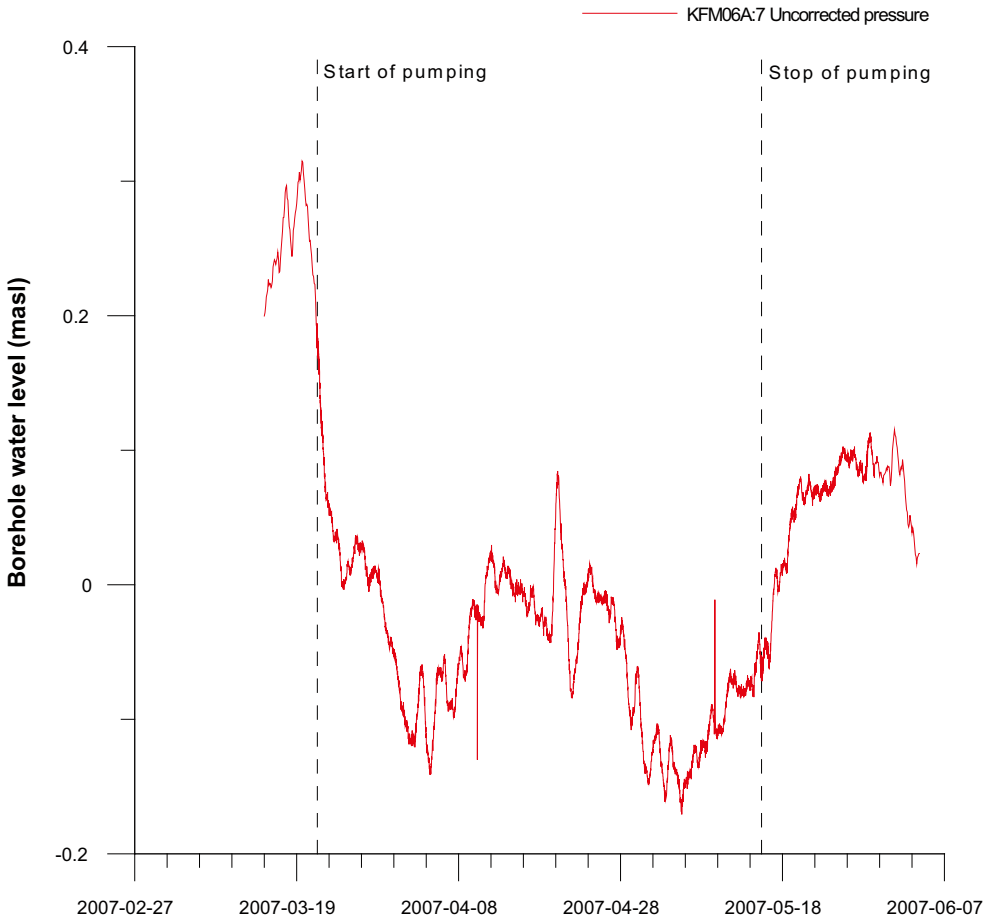

Figure A7-54. *Linear plot of pressure versus time in the observation sections in KFM06A:7 during the pumping in KFM02B.*

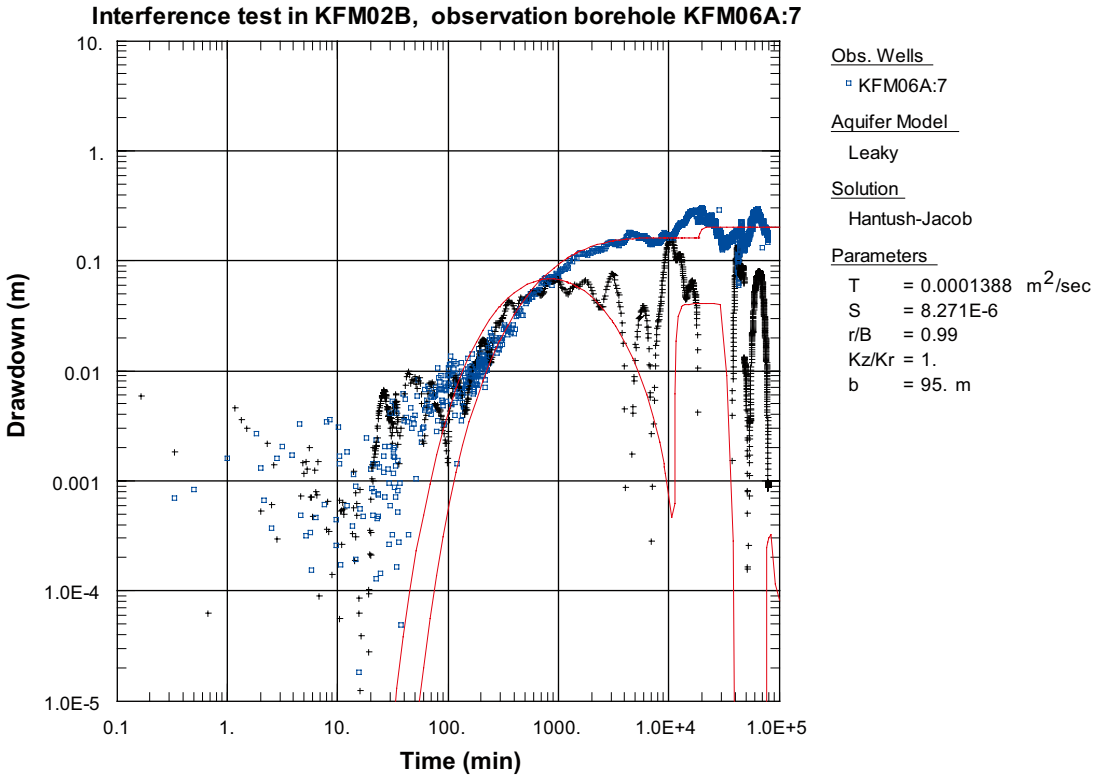

Figure A7-55. *Log-log plot of drawdown (▫) and drawdown derivative, ds/d(ln t) (+), versus time in KFM06A:7 during the interference test in KFM02B.*

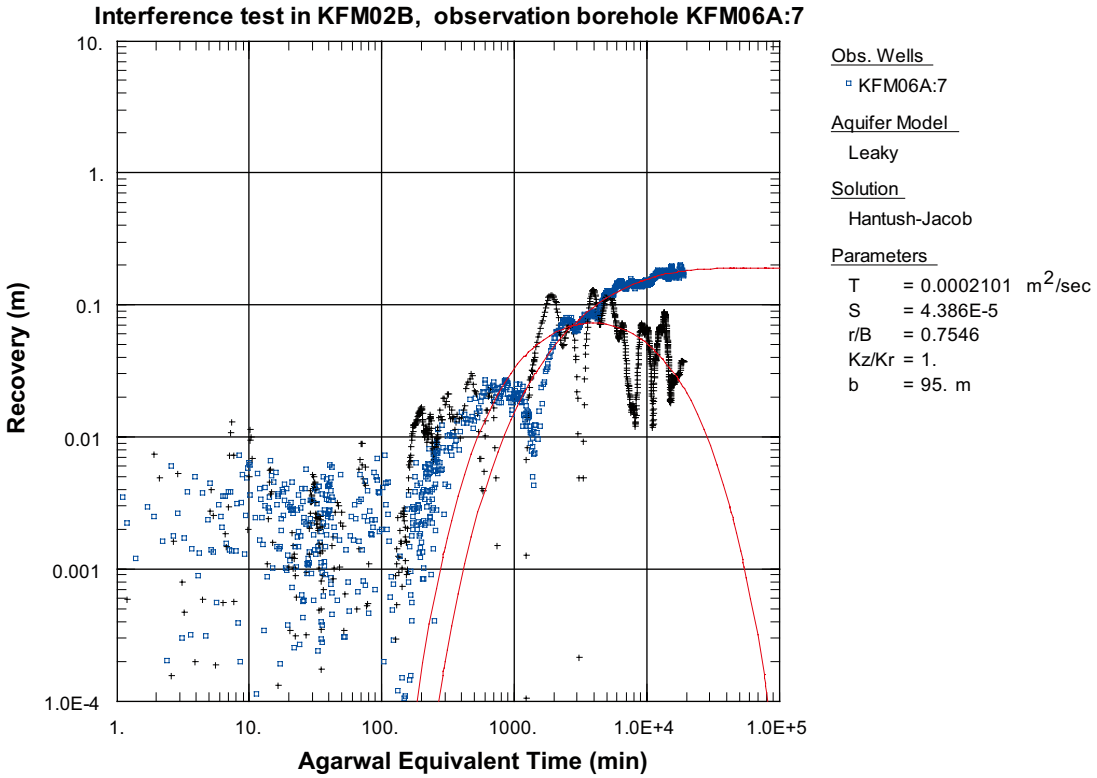

Figure A7-56. *Log-log plot of recovery (▫) and recovery derivative, ds/d(ln t) (+), versus time in KFM06A:7 during the interference test in KFM02B.*

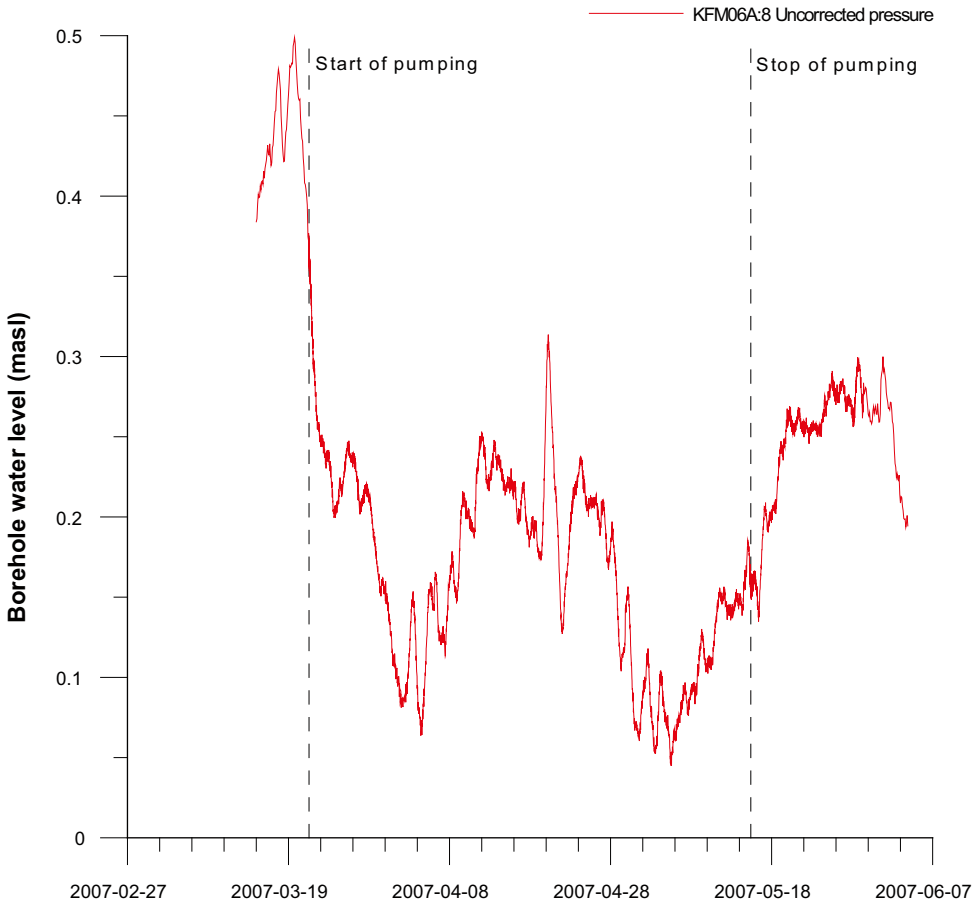

Figure A7-57. *Linear plot of pressure versus time in the observation sections in KFM06A:8 during the pumping in KFM02B.*

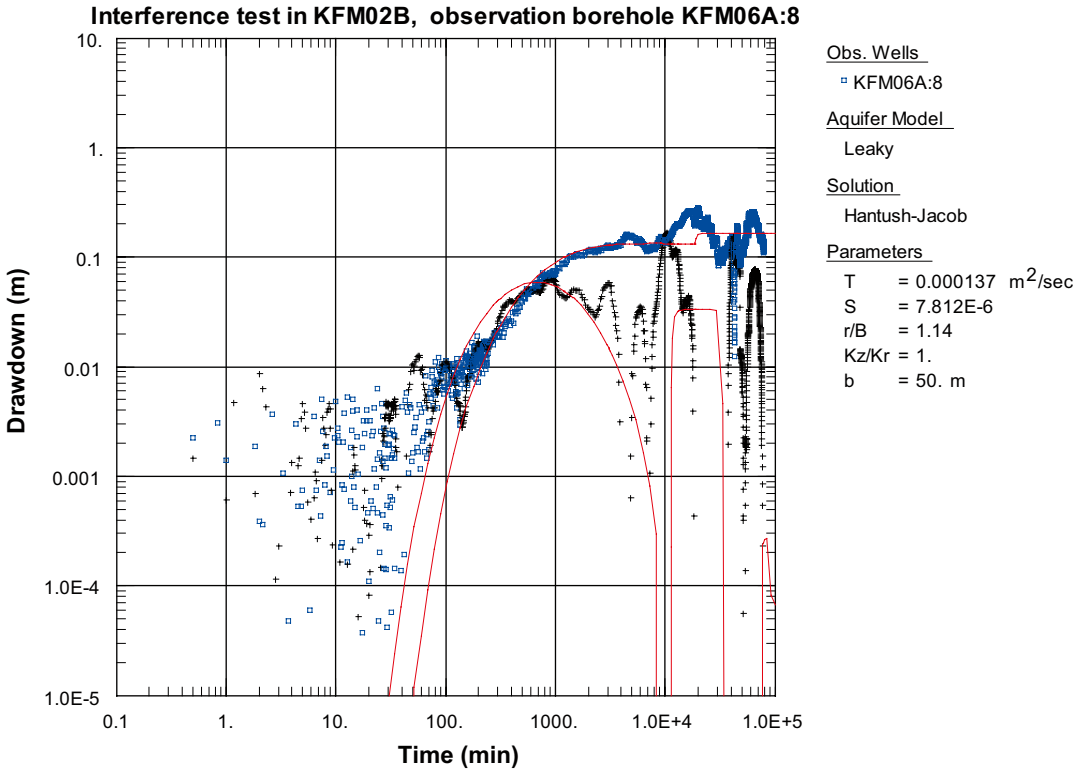

Figure A7-58. *Log-log plot of drawdown (▫) and drawdown derivative, ds/d(ln t) (+), versus time in KFM06A:8 during the interference test in KFM02B.*

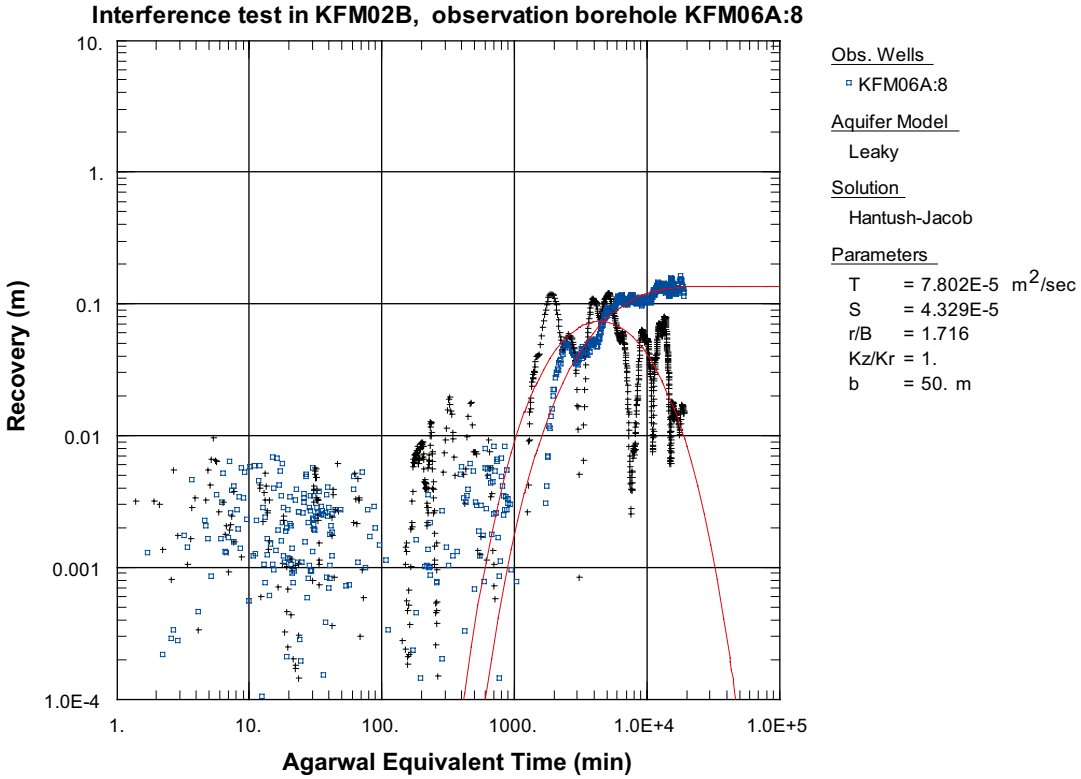

Figure A7-59. *Log-log plot of recovery (▫) and recovery derivative, ds/d(ln t) (+), versus time in KFM06A:8 during the interference test in KFM02B.*

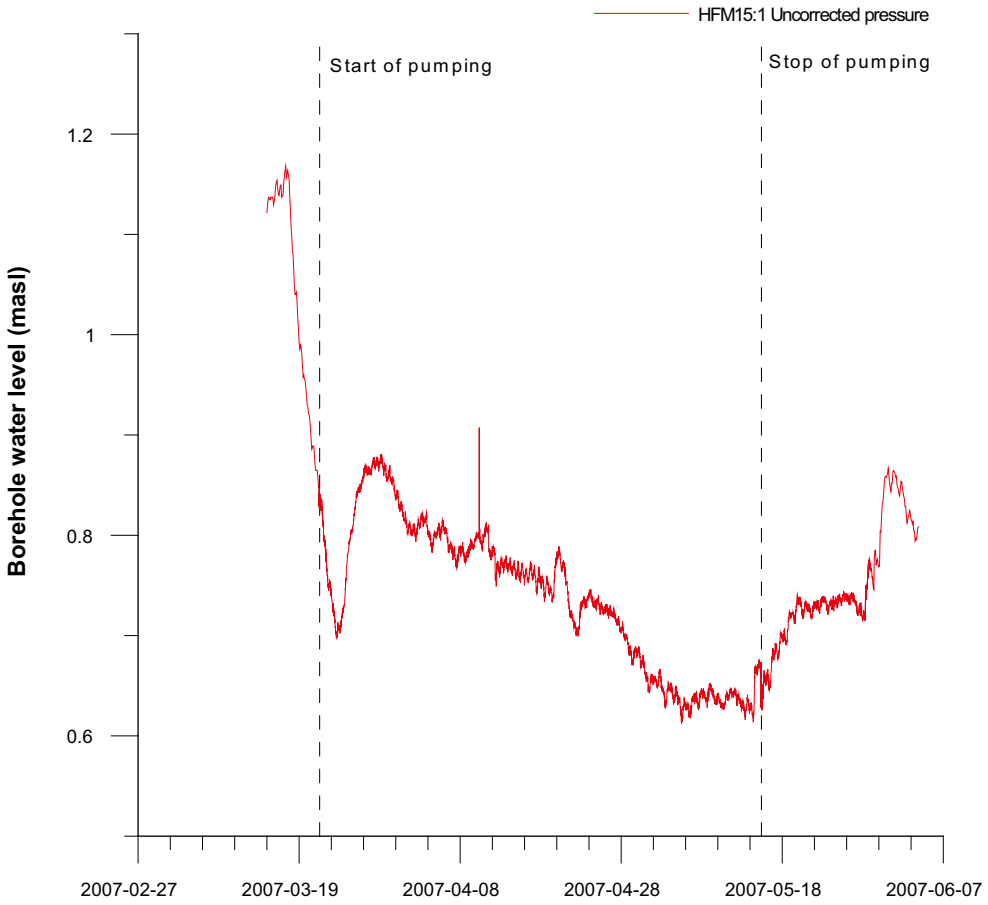

Figure A7-60. *Linear plot of pressure versus time in the observation sections in HFM15:1 during the pumping in KFM02B.*

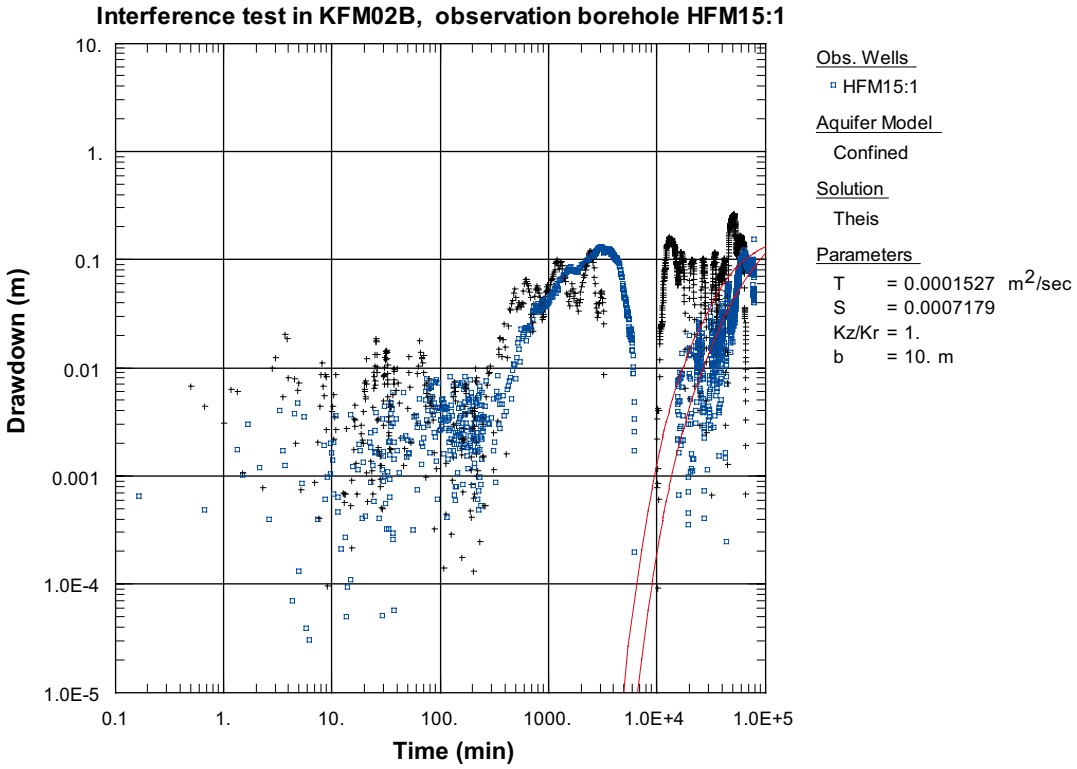

Figure A7-61. *Log-log plot of drawdown (▫) and drawdown derivative, ds/d(ln t) (+), versus time in HFM15:1 during the interference test in KFM02B. The type curve fit is showing a possible, however not unambiguous, evaluation.*

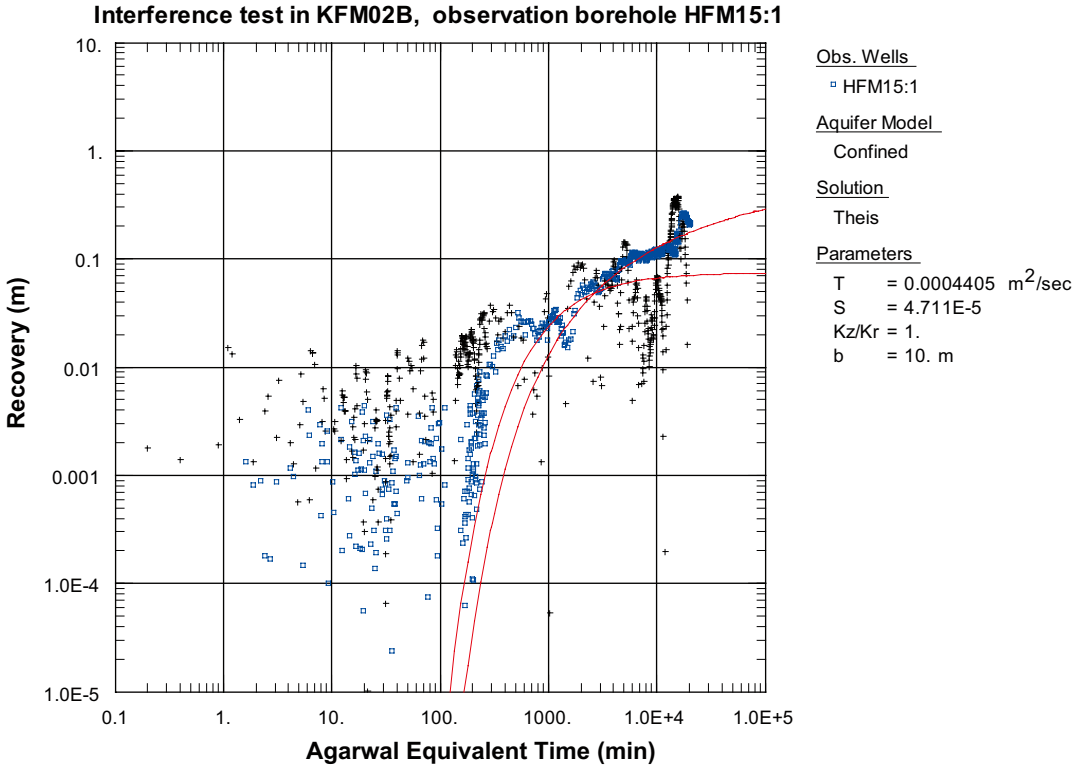

Figure A7-62. *Log-log plot of recovery (▫) and recovery derivative, ds/d(ln t) (+), versus time in HFM15:1 during the interference test in KFM02B. The type curve fit is showing a possible, however not unambiguous, evaluation.*

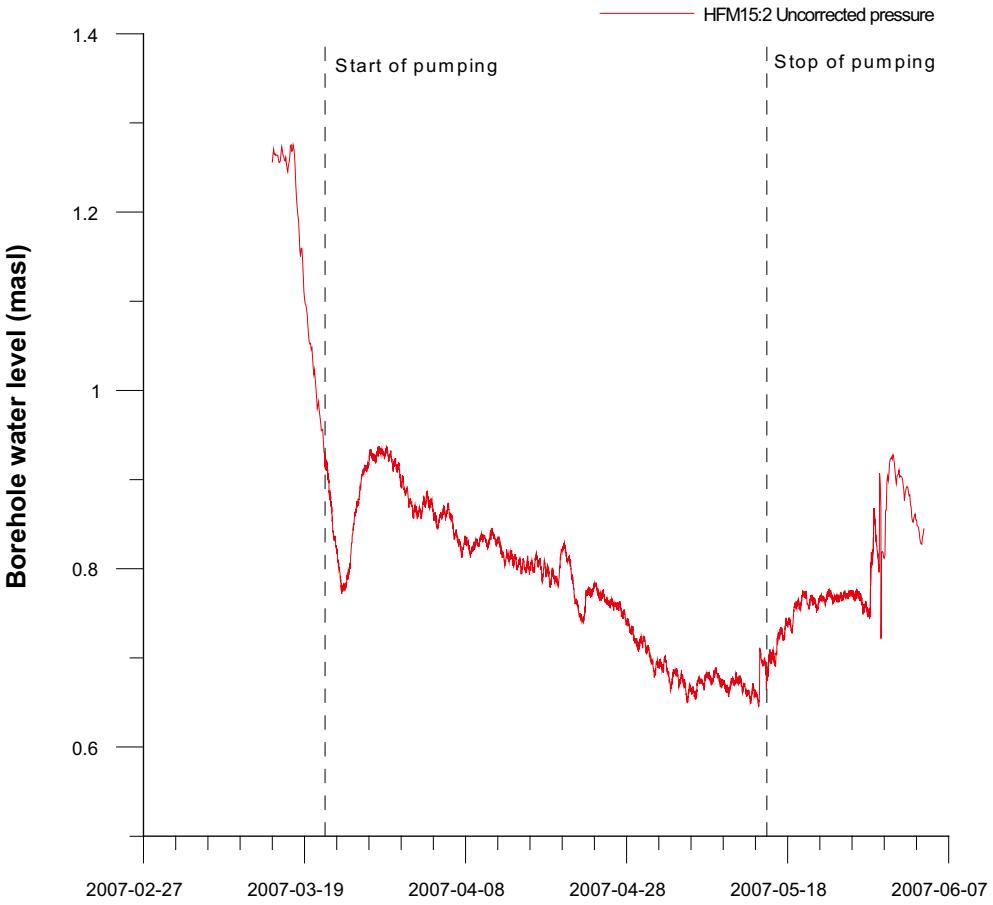

Figure A7-63. *Linear plot of pressure versus time in the observation sections in HFM15:2 during the pumping in KFM02B.*

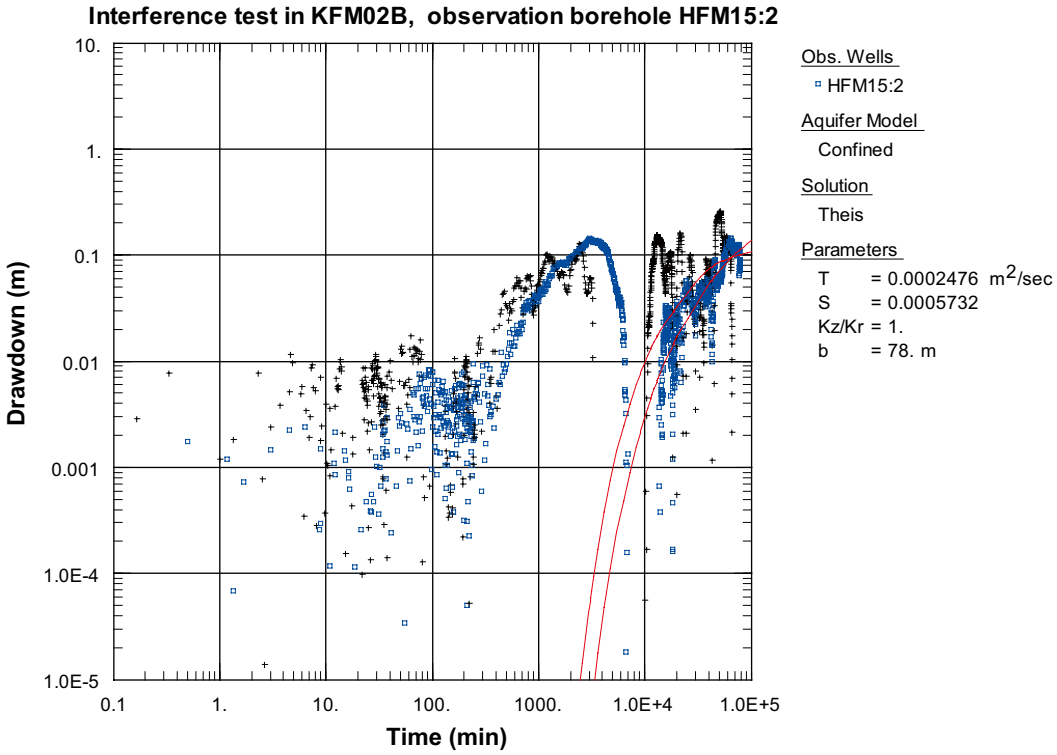

Figure A7-64. *Log-log plot of drawdown (▫) and drawdown derivative, ds/d(ln t) (+), versus time in HFM15:2 during the interference test in KFM02B. The type curve fit is showing a possible, however not unambiguous, evaluation.*

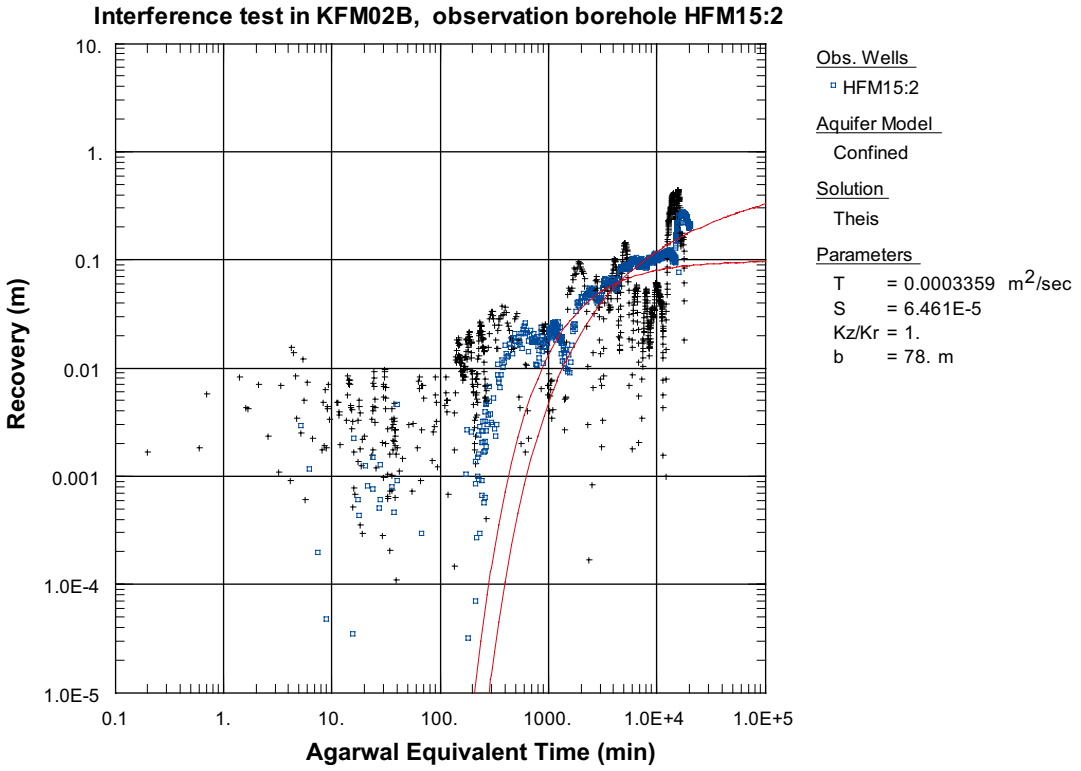

Figure A7-65. *Log-log plot of recovery (▫) and recovery derivative, ds/d(ln t) (+), versus time in HFM15:2 during the interference test in KFM02B. The type curve fit is showing a possible, however not unambiguous, evaluation.*

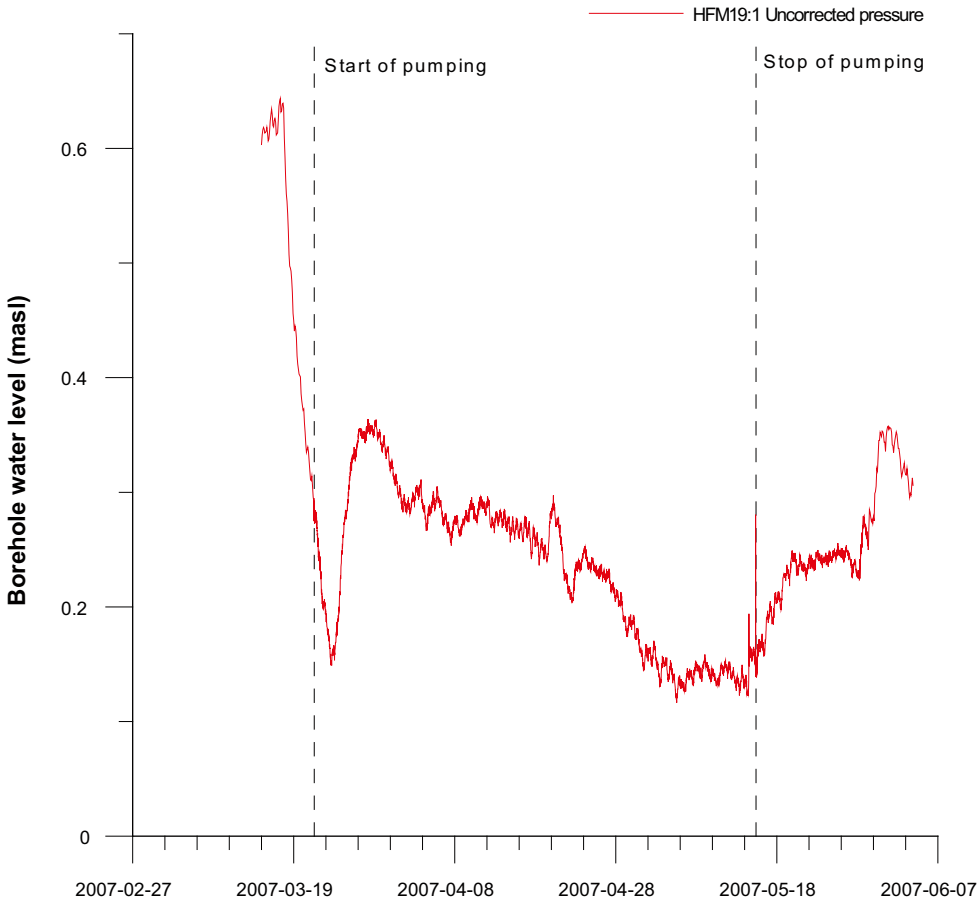

Figure A7-66. *Linear plot of pressure versus time in the observation sections in HFM19:1 during the pumping in KFM02B.*

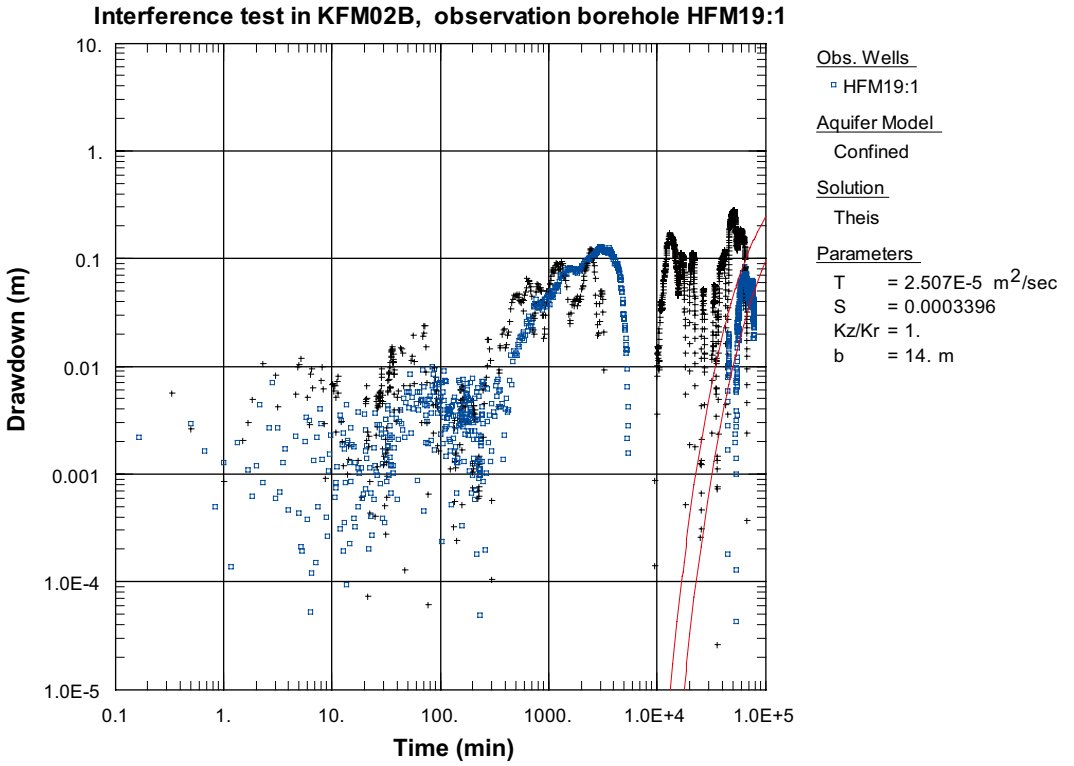

Figure A7-67. *Log-log plot of drawdown (▫) and drawdown derivative, ds/d(ln t) (+), versus time in HFM19:1 during the interference test in KFM02B. The type curve fit is showing a possible, however not unambiguous, evaluation.*

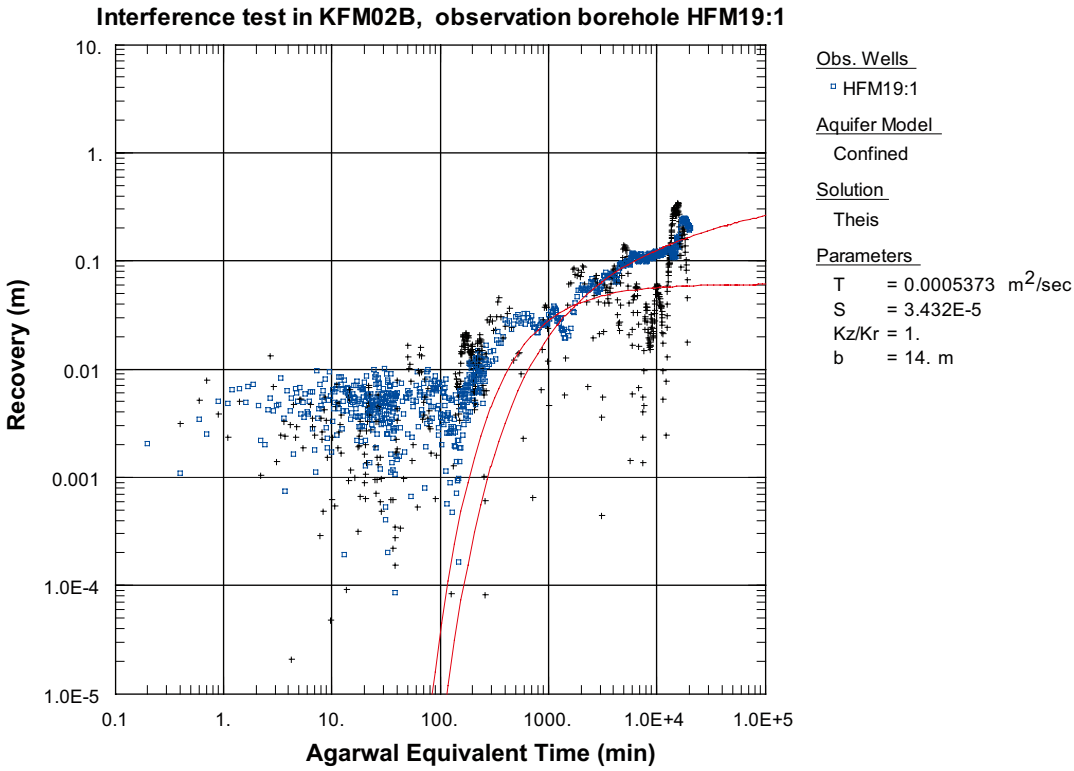

Figure A7-68. *Log-log plot of recovery (▫) and recovery derivative, ds/d(ln t) (+), versus time in HFM19:1 during the interference test in KFM02B. The type curve fit is showing a possible, however not unambiguous, evaluation.*

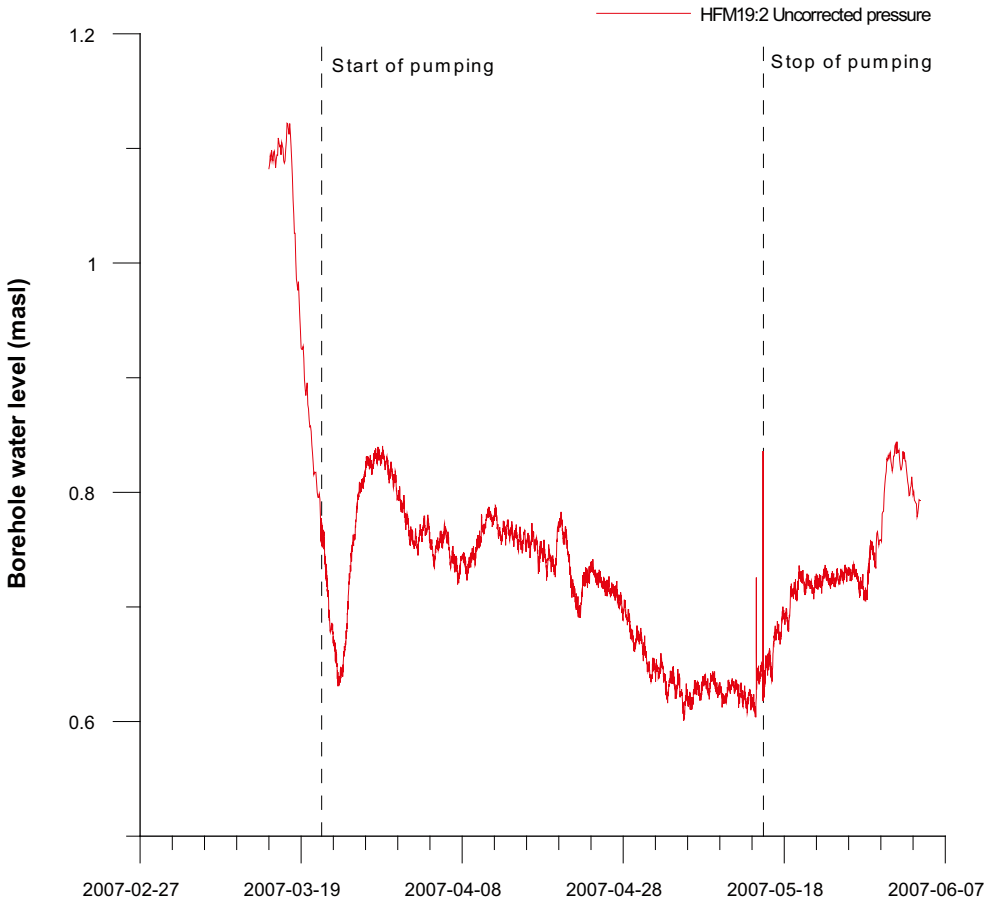

Figure A7-69. *Linear plot of pressure versus time in the observation sections in HFM19:2 during the pumping in KFM02B.*

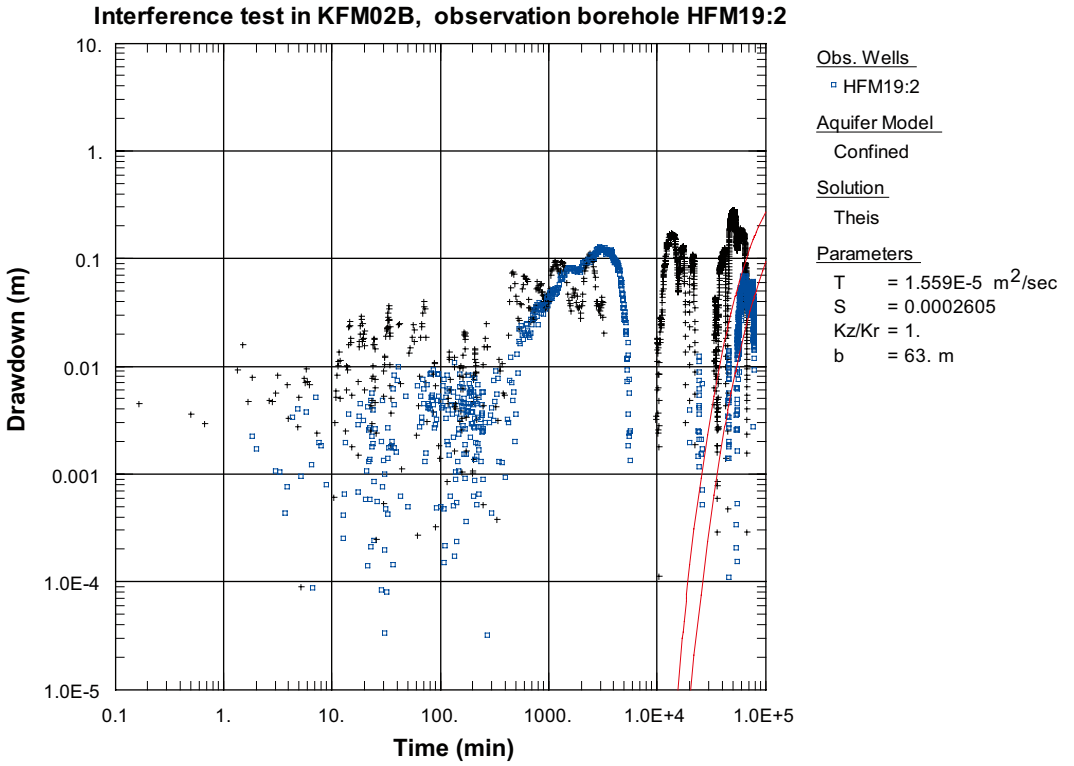

Figure A7-70. *Log-log plot of drawdown (▫) and drawdown derivative, ds/d(ln t) (+), versus time in HFM19:2 during the interference test in KFM02B. The type curve fit is showing a possible, however not unambiguous, evaluation.*

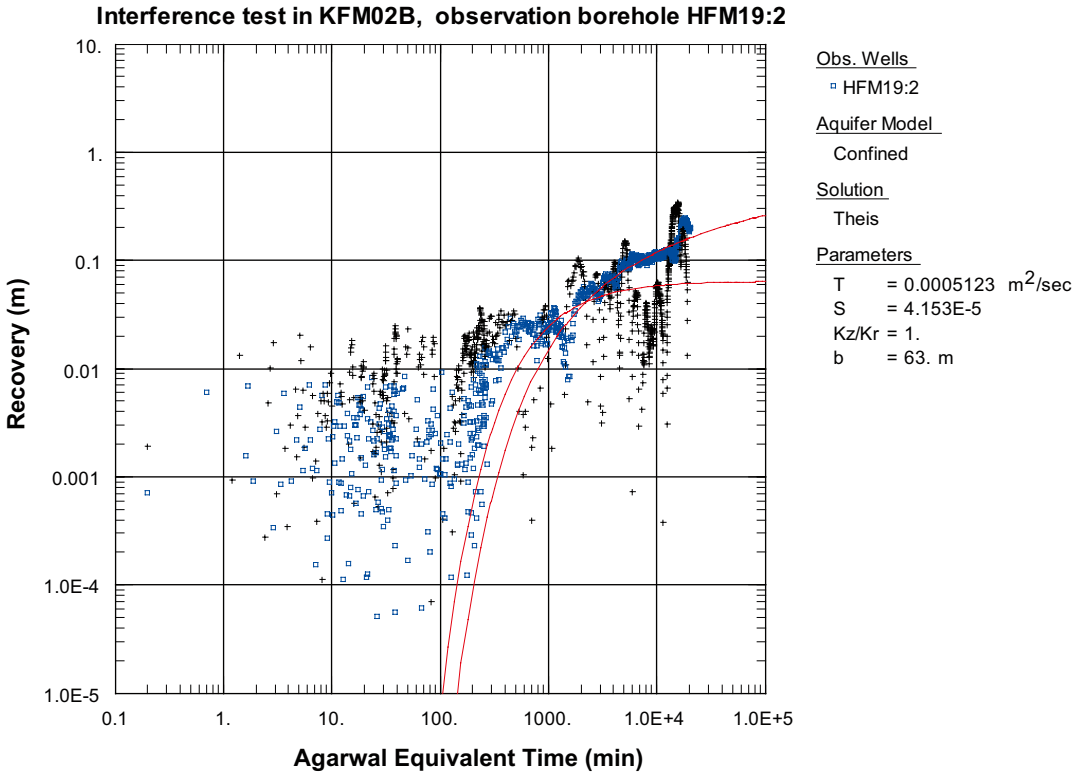

Figure A7-71. *Log-log plot of recovery (▫) and recovery derivative, ds/d(ln t) (+), versus time in HFM19:2 during the interference test in KFM02B. The type curve fit is showing a possible, however not unambiguous, evaluation.*

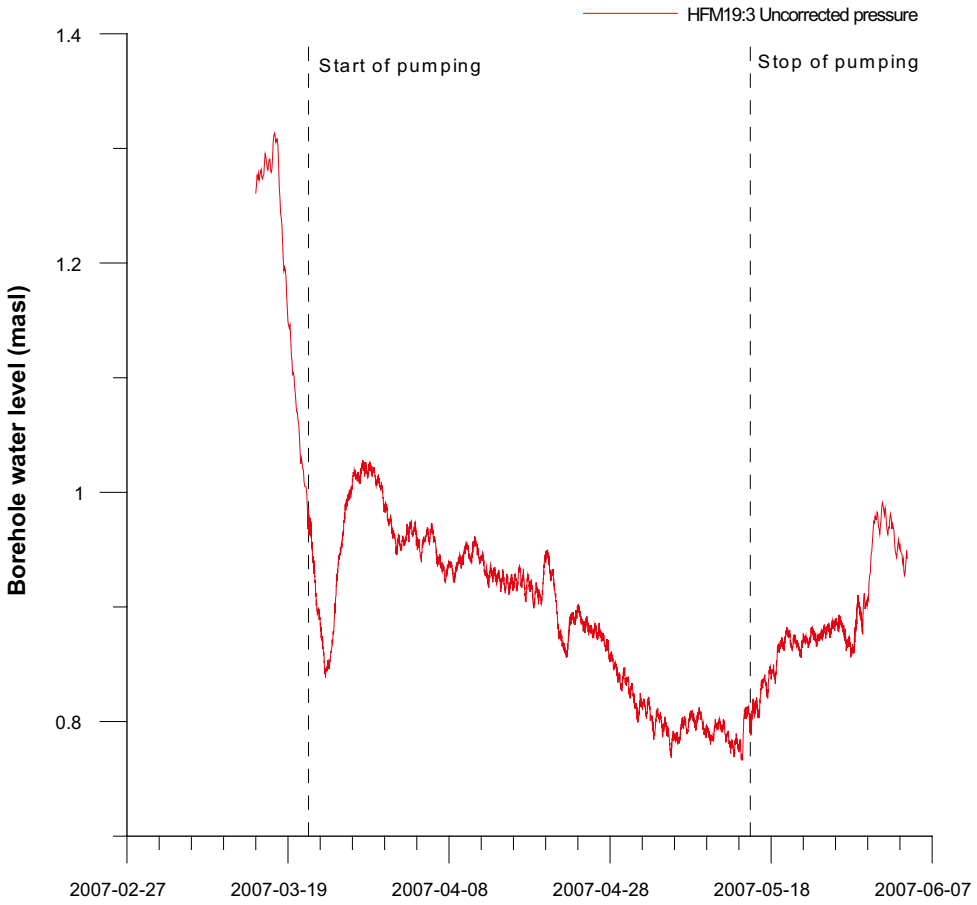

Figure A7-72. *Linear plot of pressure versus time in the observation sections in HFM19:3 during the pumping in KFM02B.*

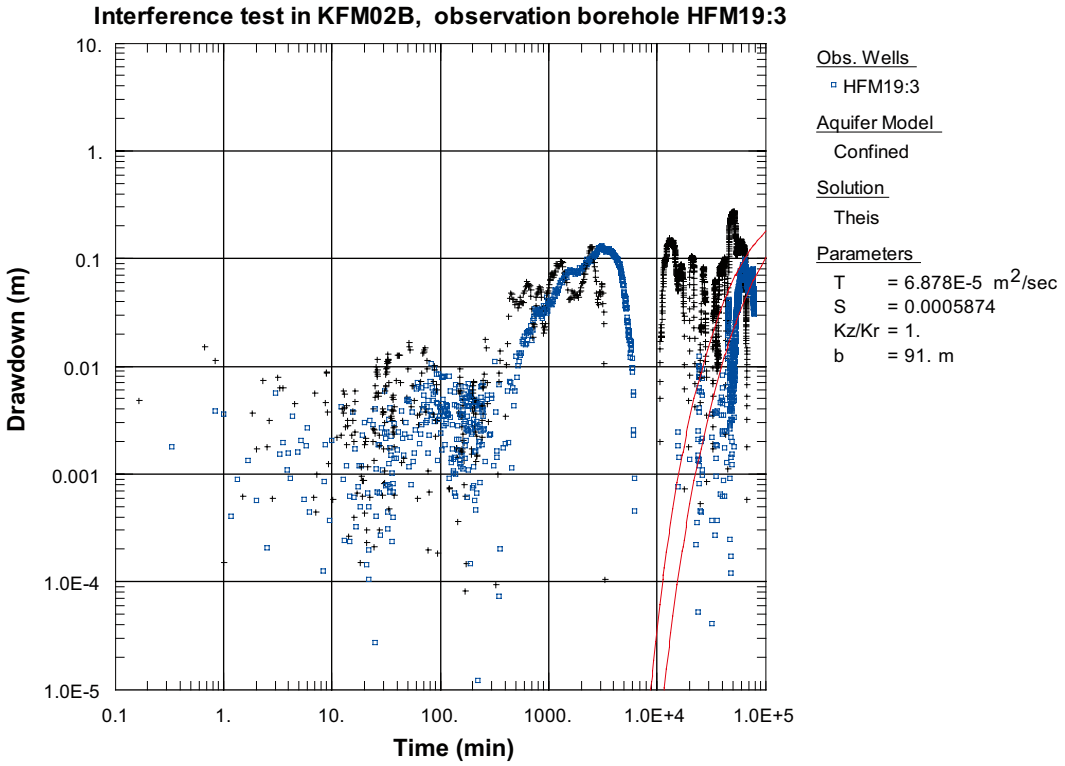

Figure A7-73. *Log-log plot of drawdown (▫) and drawdown derivative, ds/d(ln t) (+), versus time in HFM19:3 during the interference test in KFM02B. The type curve fit is showing a possible, however not unambiguous, evaluation.*

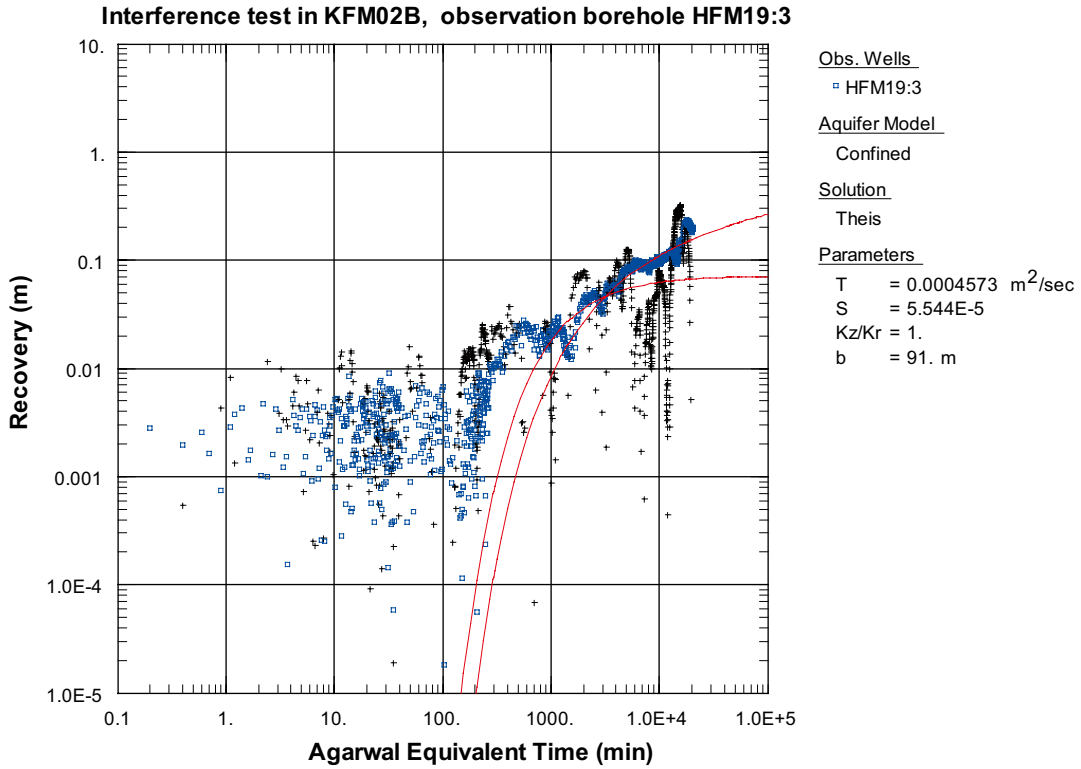

Figure A7-74. *Log-log plot of recovery (▫) and recovery derivative, ds/d(ln t) (+), versus time in HFM19:3 during the interference test in KFM02B. The type curve fit is showing a possible, however not unambiguous, evaluation.*

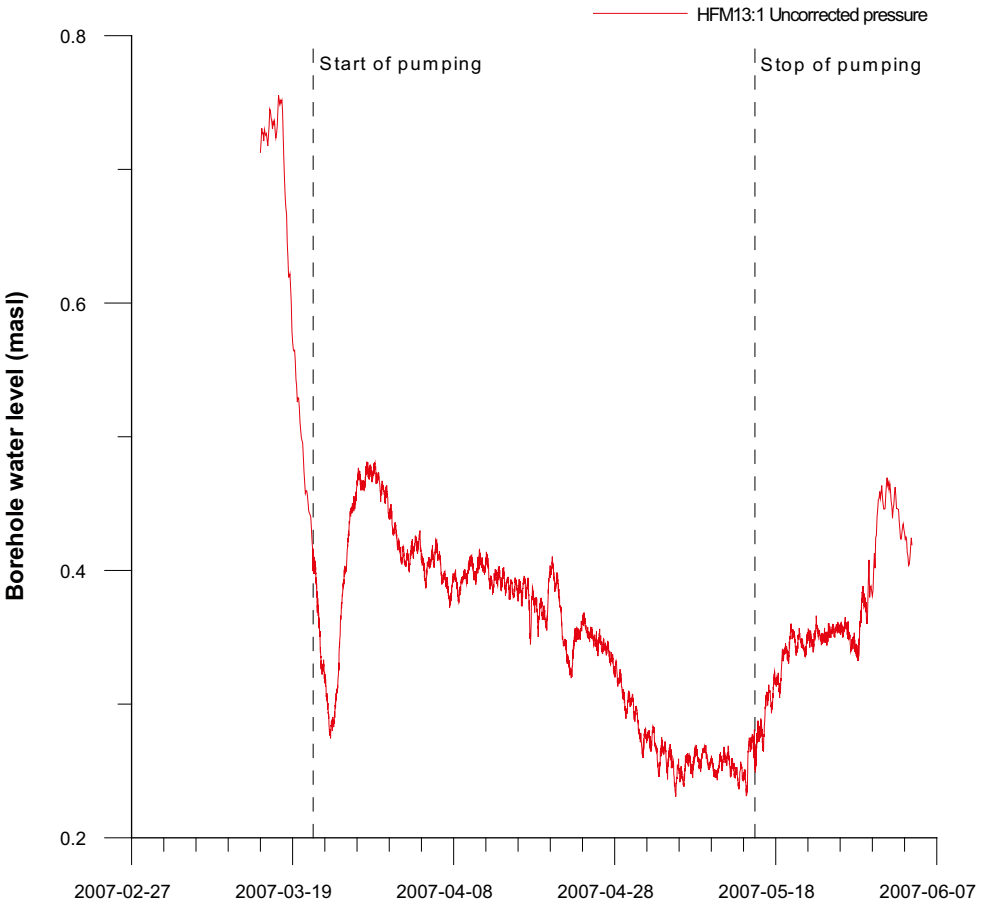

Figure A7-75. *Linear plot of pressure versus time in the observation sections in HFM13:1 during the pumping in KFM02B.*

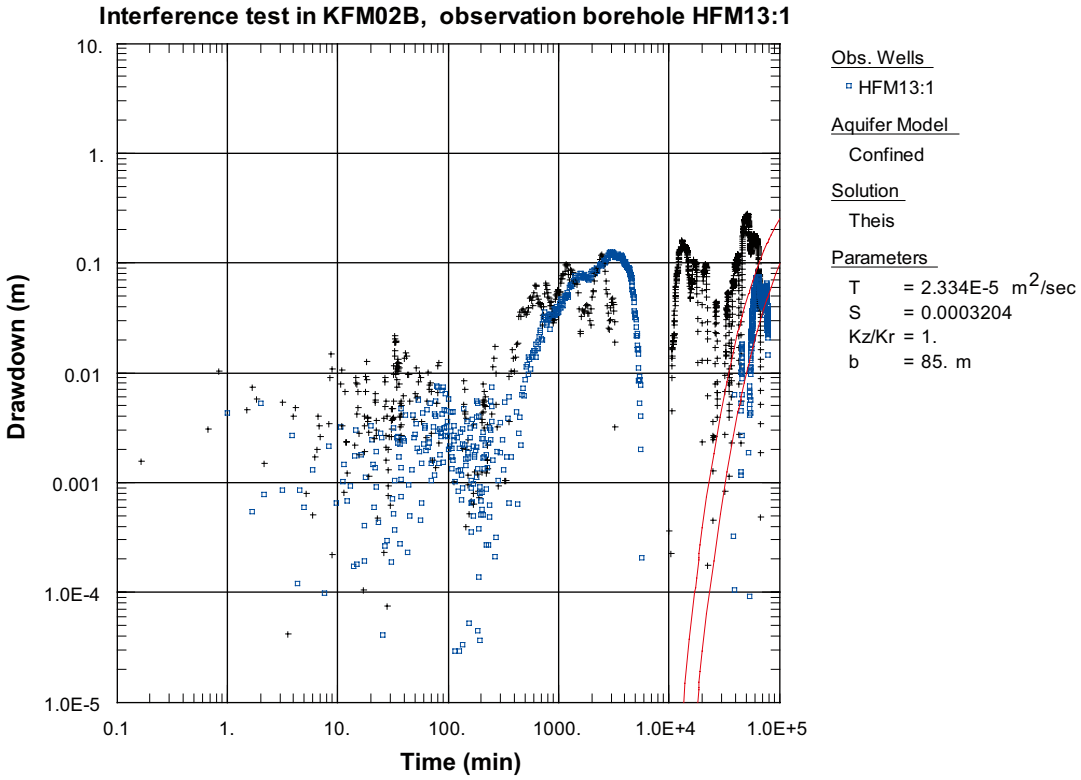

Figure A7-76. *Log-log plot of drawdown (□) and drawdown derivative, ds/d(ln t) (+) versus time in HFM13:1 during the interference test in KFM02B. The type curve fit is showing a possible, however not unambiguous, evaluation.*

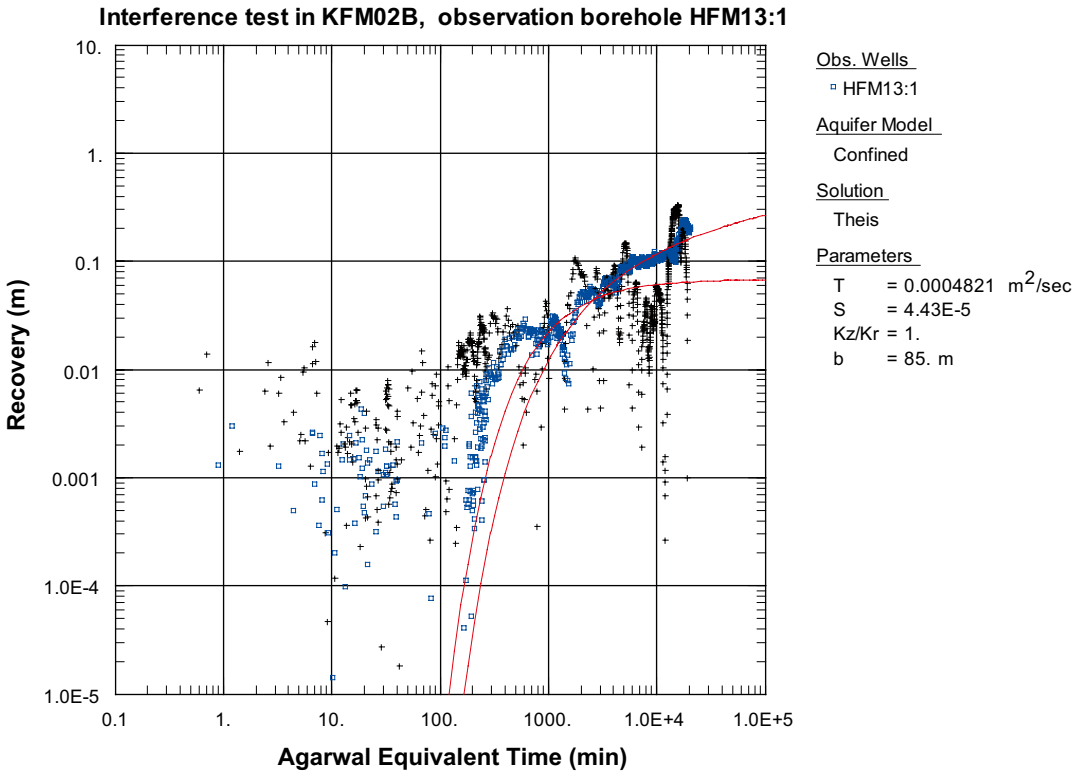

Figure A7-77. *Log-log plot of recovery (▫) and recovery derivative, ds/d(ln t) (+), versus time in HFM13:1 during the interference test in KFM02B. The type curve fit is showing a possible, however not unambiguous, evaluation.*

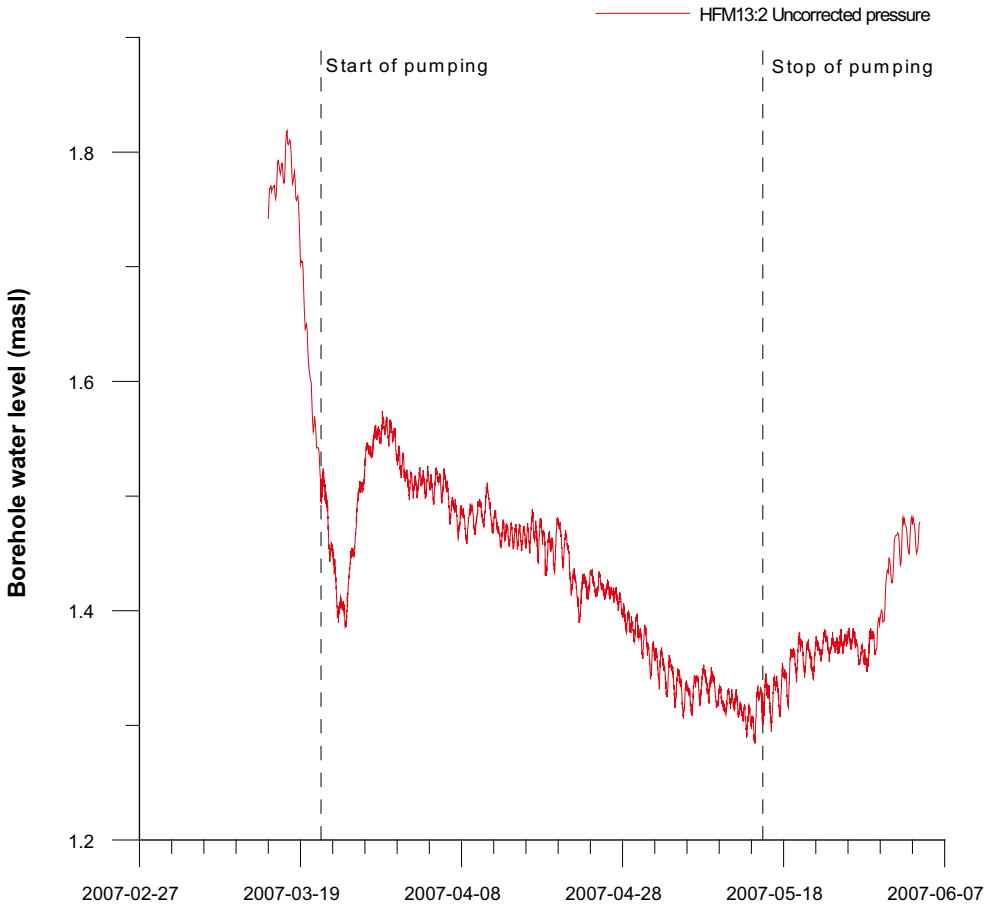

Figure A7-78. *Linear plot of pressure versus time in the observation sections in HFM13:2 during the pumping in KFM02B.*

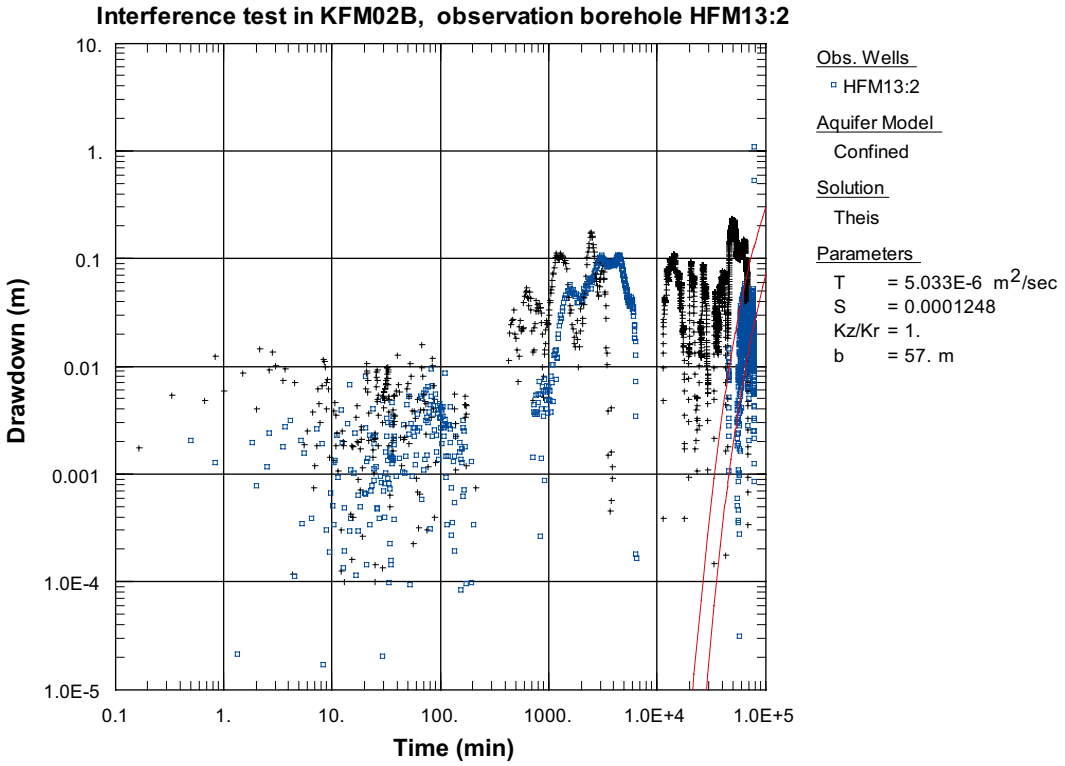

Figure A7-79. *Log-log plot of drawdown (▫) and drawdown derivative, ds/d(ln t) (+), versus time in HFM13:2 during the interference test in KFM02B. The type curve fit is showing a possible, however not unambiguous, evaluation.*

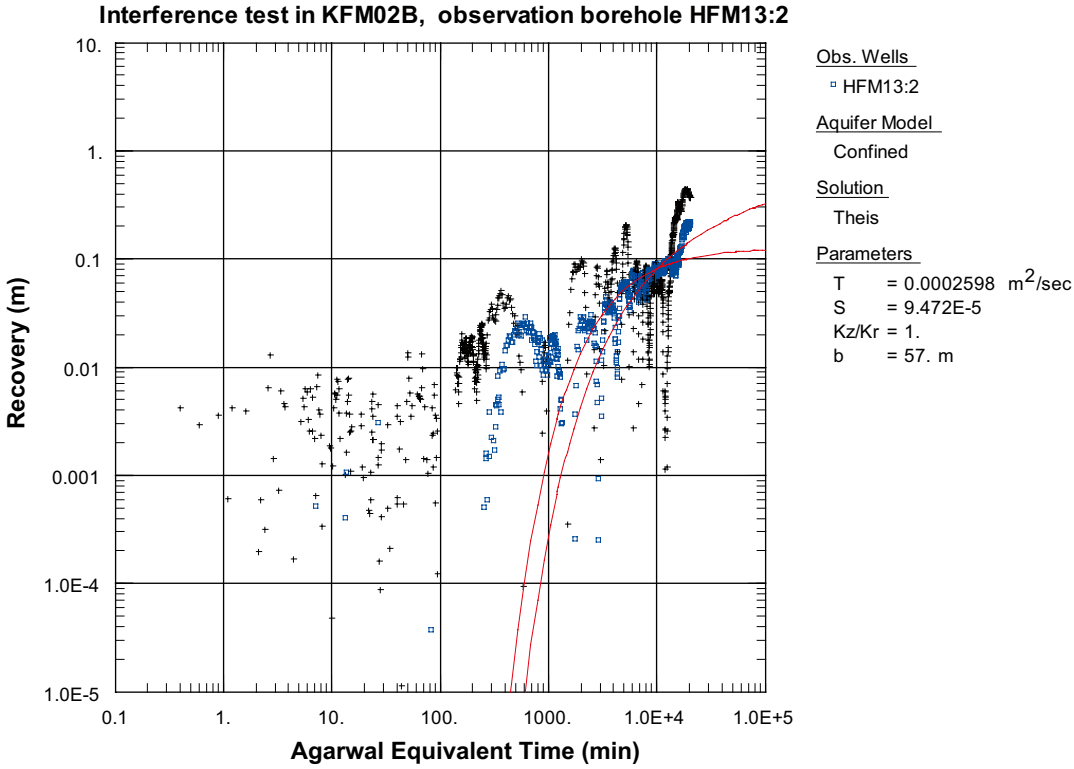

Figure A7-80. *Log-log plot of recovery (▫) and recovery derivative, ds/d(ln t) (+), versus time in HFM13:2 during the interference test in KFM02B. The type curve fit is showing a possible, however not unambiguous, evaluation.*

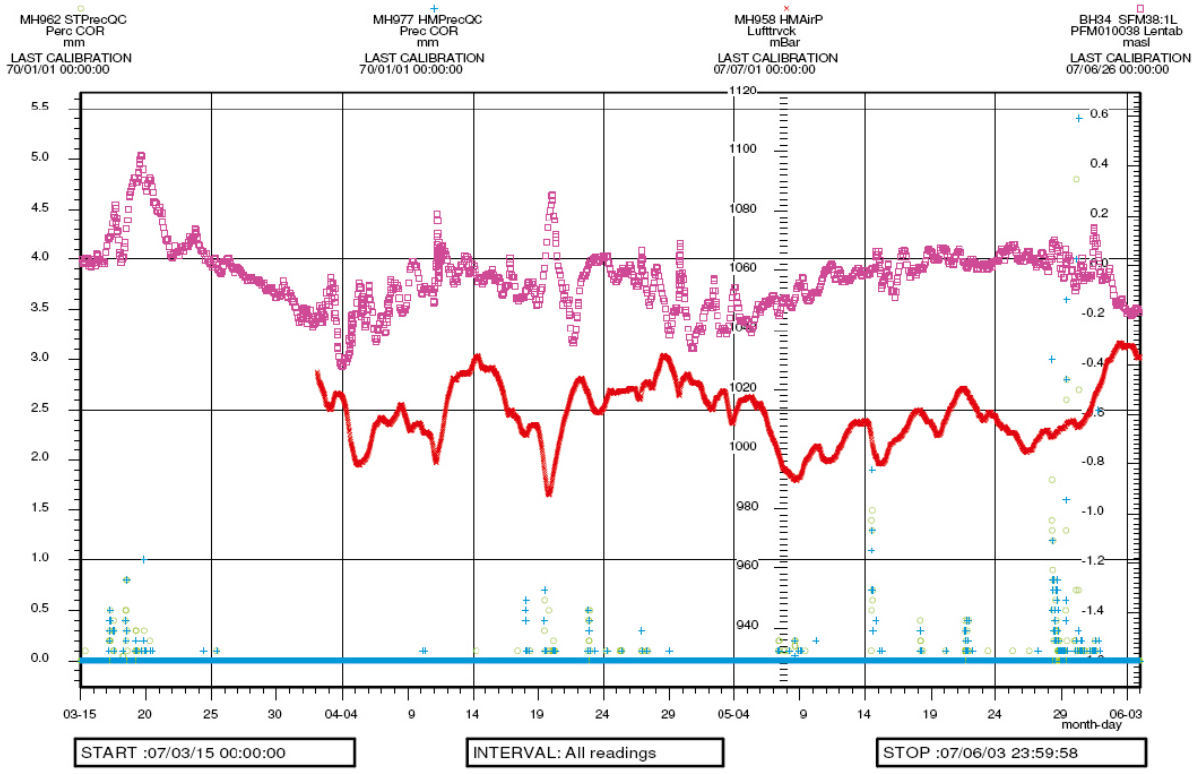

Figure A7-81. *Precipitation [mm] (blue and green), air pressure [mBar] (red) and sea water level [m.a.s.l] (purple) recorded at a station near the experimental site during the measurement period.*

Appendix 8

Correction of head and drawdown for natural decreasing trend

As can be seen from Figure A8-1, a natural, decreasing head trend was ongoing during the entire period of the interference test in KFM02B. The data from the test period were corrected for the natural trend using the graphical technique described in Figure A8-2. The difference between the head at start of pumping and the head at maximal pressure recovery after stop of pumping was assumed to represent the existing natural head trend during the entire test period. A linear trend correction with time was determined individually for all responding observation sections according to Eqn. (A8-1) and applied to the drawdown and recovery period. The total correction at stop of pumping is denoted corr(tp). The corrected drawdown s(t)corr at time t is calculated according to Eqn. (A8-2).

$$corr(t)=[corr(t_p) / t_p] \cdot t \qquad \text{(A8-1)}$$

$$s(t)_{corr} = s(t) - corr(t) \qquad \text{(A8-2)}$$

$s(t)_{corr}$=corrected drawdown at time t after start of pumping (m)

s(t)= measured drawdown at time t after start of pumping (m)

corr(t)=applied correction at time t after start of pumping (m)

$corr(t_p)$=applied correction at time tp at stop of pumping (m)

t_p = duration of drawdown period (s)

Data files with time and corrected head and drawdown for all responding observation sections were prepared and stored in Sicada.

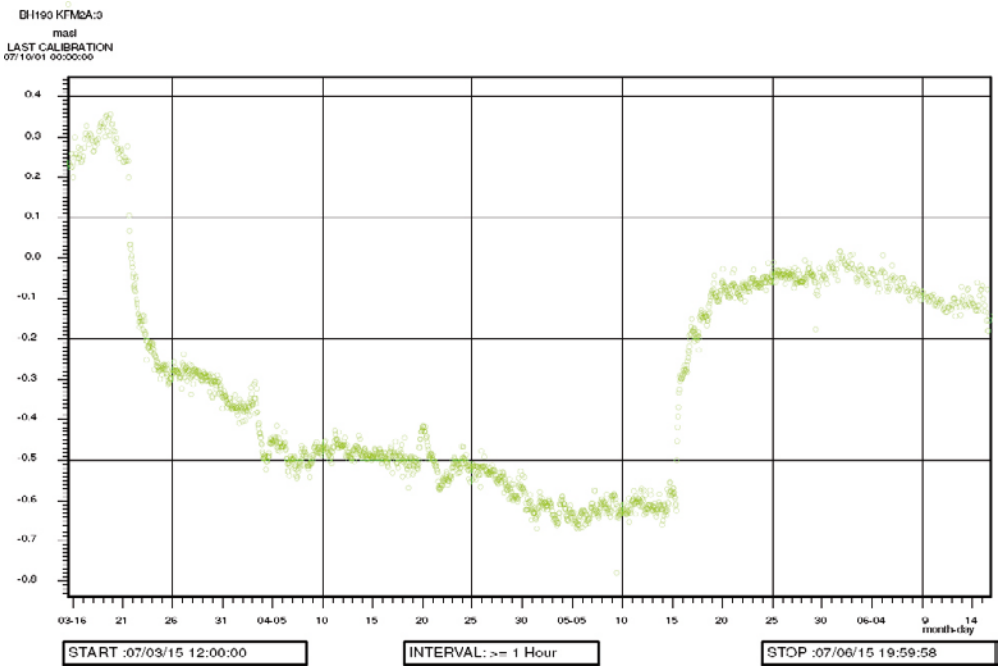

Figure A8-1. *Linear plot of head versus time in observation section KFM02A:3 during the interference test in KFM02B.*

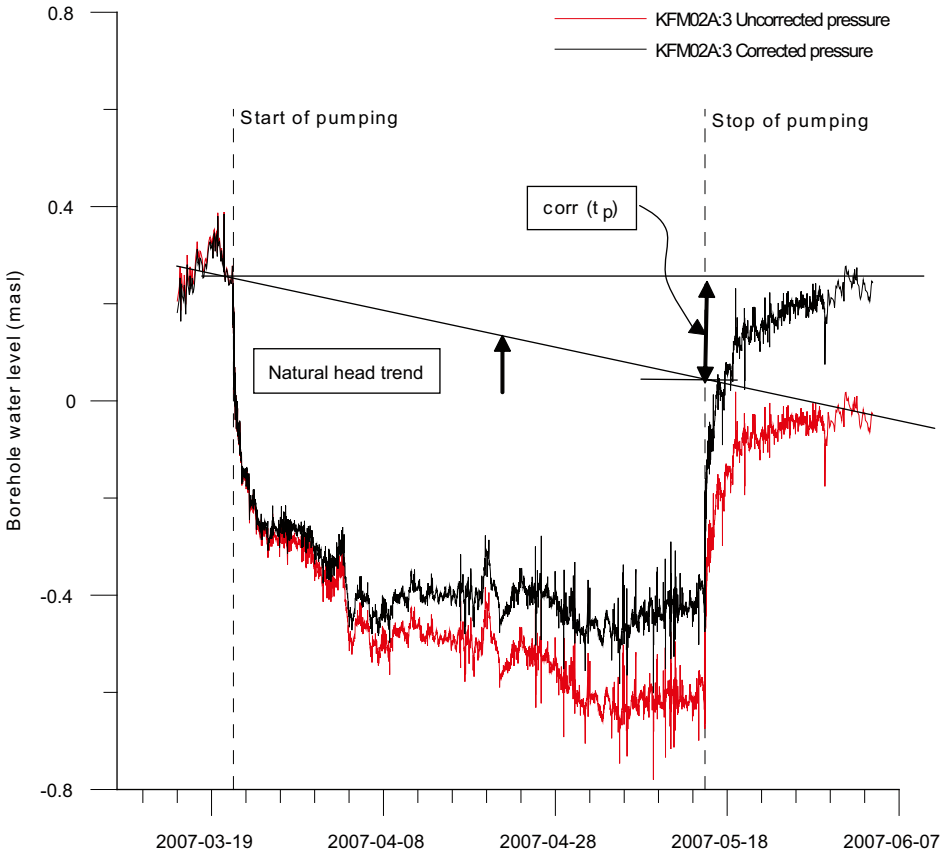

Figure A8-2. *Example of the applied correction technique for the natural decreasing head trend in observation section KFM02A:3 during the interference test in KFM02B. The final drawdown correction at stop of pumping is denoted corr(t_p).*

Appendix 9

Injection functions and breakthrough curves

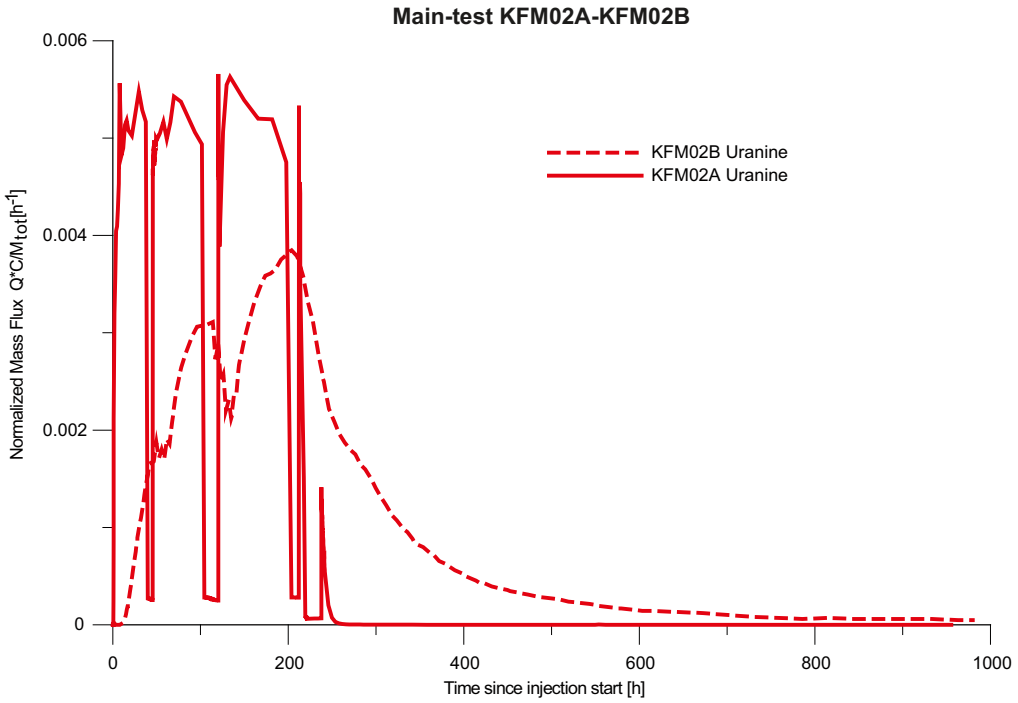

Figure A9-1. *Uranine in injection section in KFM02A and breakthrough curve in KFM02B from the main tracer test. Normalized mass flux against elapsed time.*

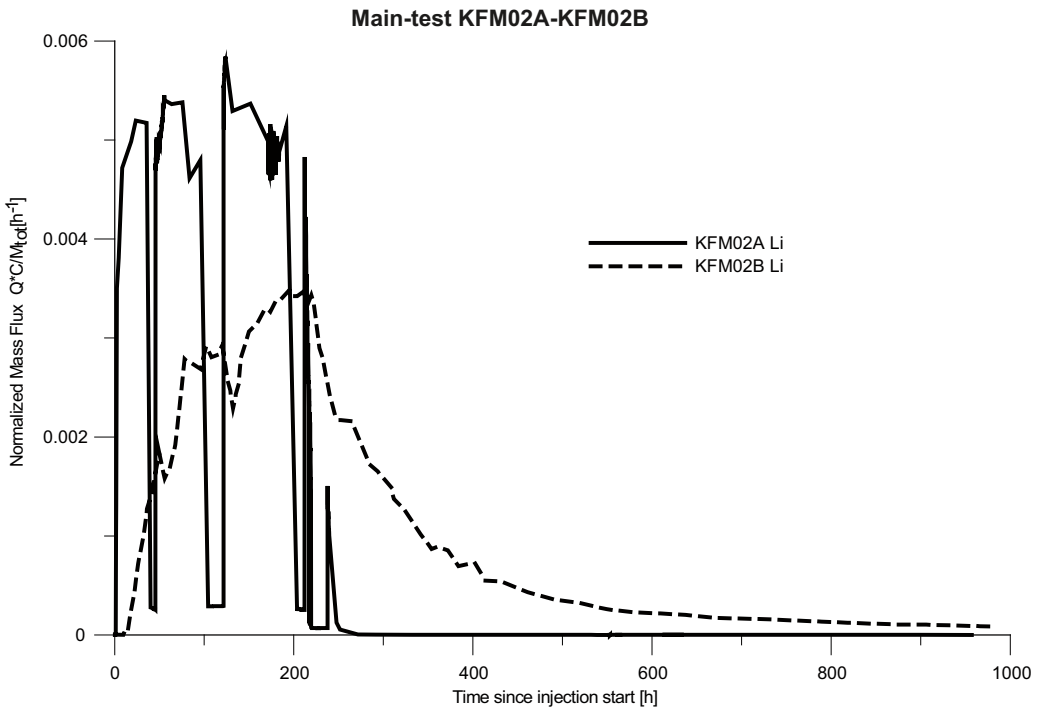

Figure A9-2. *Lithium in injection section in KFM02A and breakthrough curve in KFM02B from the main tracer test. Normalized mass flux against elapsed time.*

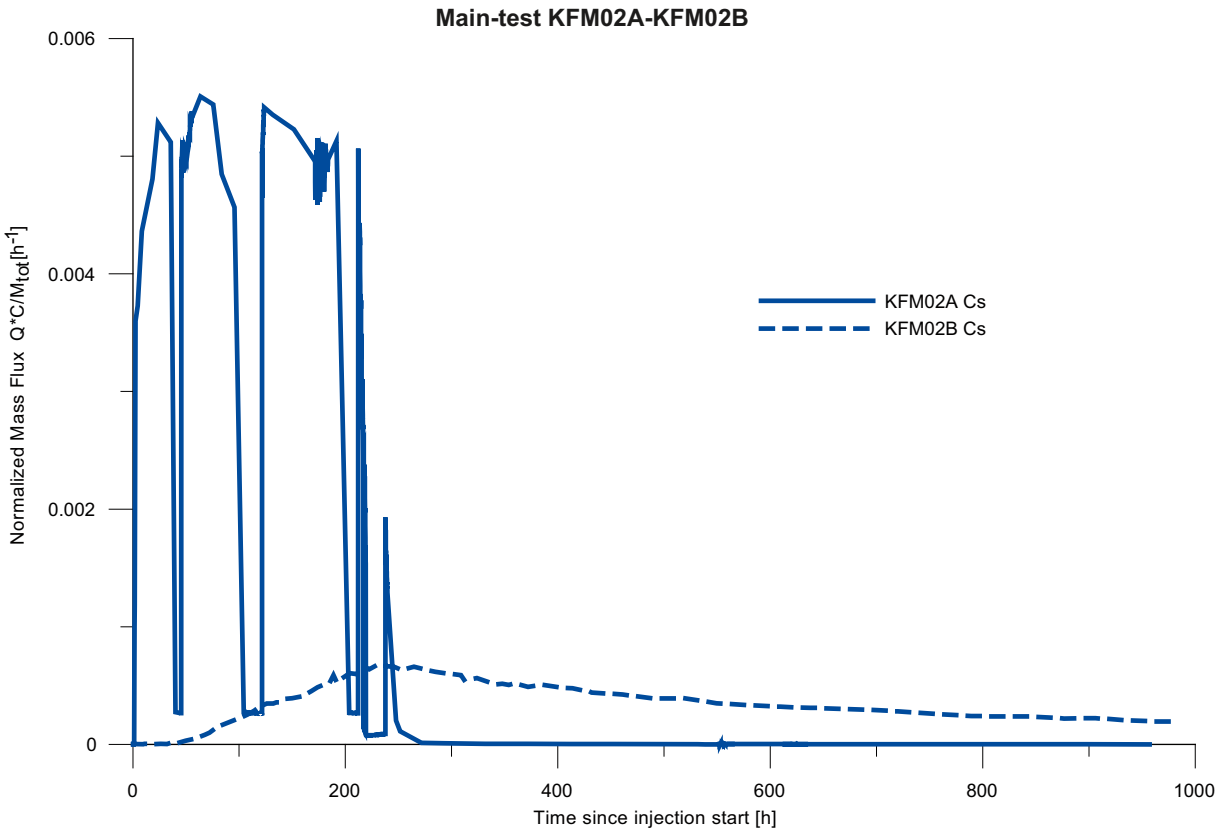

Figure A9-3. *Caesium in injection section in KFM02A and breakthrough curve in KFM02B from the main tracer test. Normalized mass flux against elapsed time.*

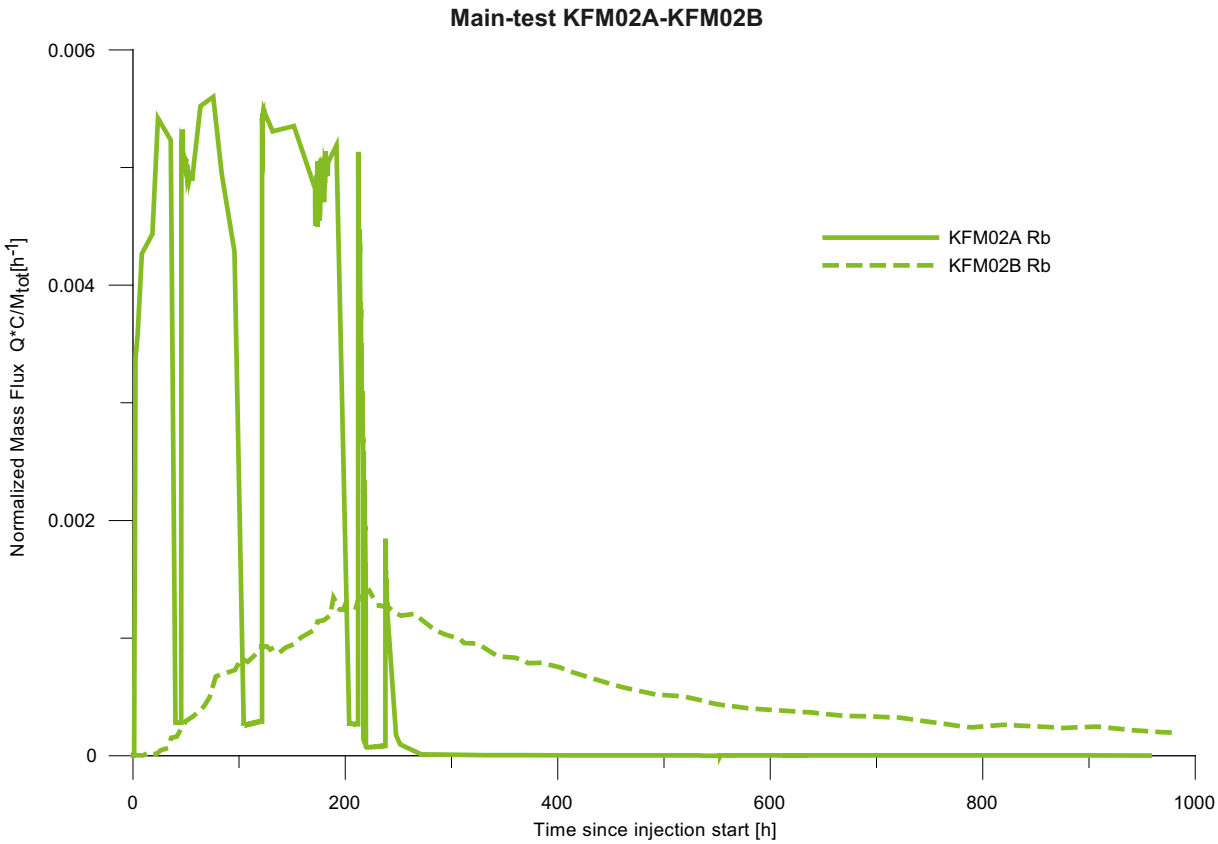

Figure A9-4. *Rubidium in injection section in KFM02A and breakthrough curve in KFM02B from the main tracer test. Normalized mass flux against elapsed time.*

Appendix 10

Calculation of radius of influence

The radius of influence at a certain time may be estimated from Jacob's approximation of the Theis' well function, /Cooper and Jacob, 1946/:

$$r_i = \sqrt{\frac{2.25Tt}{S}} \qquad \text{(A10-1)}$$

T = representative transmissivity from the test (m^2/s)

S = storativity estimated from Equation 5-3

r_i = radius of influence (m)

t = time after start of injection (s)

If a certain time interval of pseudo-radial flow (PRF) from t_1 to t_2 can be identified during the test, the radius of influence is estimated using time t_2 in Equation 5-7. If no interval of PRF can be identified, the actual total flow time t_p is used. The radius of influence can be used to deduce the length of the hydraulic feature(s) tested.

Furthermore, an r_i-index (–1, 0 or 1) is defined to characterize the hydraulic conditions by the end of the test. The r_i-index is defined as shown below. It is assumed that a certain time interval of PRF can be identified between t_1 and t_2 during the test.

- r_i-index = 0: The transient response indicates that the size of the hydraulic feature tested is greater than the radius of influence based on the actual test time ($t_2=t_p$), i.e. the PRF is continuing at stop of the test. This fact is reflected by a flat derivative at this time.
- r_i-index = 1: The transient response indicates that the hydraulic feature tested is connected to a hydraulic feature with lower transmissivity or an apparent barrier boundary (NFB). This fact is reflected by an increase of the derivative. The size of the hydraulic feature tested is estimated as the radius of influence based on t_2.
- r_i-index = –1: The transient response indicates that the hydraulic feature tested is connected to a hydraulic feature with higher transmissivity or an apparent constant head boundary (CHB). This fact is reflected by a decrease of the derivative. The size of the hydraulic feature tested is estimated as the radius of influence based on t_2.

If a certain time interval of PRF cannot be identified during the test, the r_i-indices –1 and 1 are defined as above. In such cases the radius of influence is estimated using the flow time t_p in Equation A10-1.